https://theses.gla.ac.uk/

Theses Digitisation:

https://www.gla.ac.uk/myglasgow/research/enlighten/theses/digitisation/

This is a digitised version of the original print thesis.

Copyright and moral rights for this work are retained by the author

A copy can be downloaded for personal non-commercial research or study, without prior permission or charge

This work cannot be reproduced or quoted extensively from without first obtaining permission in writing from the author

The content must not be changed in any way or sold commercially in any format or medium without the formal permission of the author

When referring to this work, full bibliographic details including the author, title, awarding institution and date of the thesis must be given

Enlighten: Theses
https://theses.gla.ac.uk/
research-enlighten@glasgow.ac.uk

Symbols p. 16
p. 103
p 173.

© C.G. Black B.Sc., 1988

A METHODOLOGY FOR THE IDENTIFICATION OF HELICOPTER MATHEMATICAL MODELS FROM FLIGHT DATA BASED ON THE FREQUENCY DOMAIN.

Colin Gordon Black

Submitted for the Degree of Ph.D. in the

Dept. Aeronautics and Fluid Mechanics
University of Glasgow

ProQuest Number: 10970806

All rights reserved

INFORMATION TO ALL USERS
The quality of this reproduction is dependent upon the quality of the copy submitted.

In the unlikely event that the author did not send a complete manuscript
and there are missing pages, these will be noted. Also, if material had to be removed,
a note will indicate the deletion.

ProQuest 10970806

Published by ProQuest LLC (2018). Copyright of the Dissertation is held by the Author.

All rights reserved.
This work is protected against unauthorized copying under Title 17, United States Code
Microform Edition © ProQuest LLC.

ProQuest LLC.
789 East Eisenhower Parkway
P.O. Box 1346
Ann Arbor, MI 48106 – 1346

CONTENTS

		Page:
Contents		i
Acknowledgements		viii
Abstract		x
1.	Introduction: The Helicopter System Identification Problem.	1
(1.1)	Introduction.	1
1.1.1	The Nature of System Identification.	1
1.1.2	The Need for System Identification in Helicopter Applications.	3
(1.2)	The Helicopter Model.	3
1.2.1	The Nature of a Model	3
1.2.2	Adequate Models.	6
1.2.3	Model Structure.	9
1.2.4	The Helicopter Model.	14
1.2.5	A Suitable Model for the Identification of Quasi-Static Derivatives.	20
1.2.6	The Theoretical Model (HELISTAB).	24

(1.3) Difficulties Associated with Helicopter System Identification. 25

1.3.1 General Discussion of Identification Difficulties. 25

1.3.2 Kinematic Consistency Checking. 31

1.3.3 The Role of Extended Kalman Filtering Techniques. 33

(1.4) Obtaining an Adequate Response for Helicopter System Identification. 35

1.4.1 The Design of Suitable Test Inputs. 35

1.4.2 The Problem of Identifying a Linear Model from Non-Linear Data. 41

Summary. 44

2. Some Preliminaries on the Use of the Frequency Domain. 47

(2.1) Introduction: 47

2.1.1 An Outline of the Previous Use of the Frequency Domain in Aircraft System Identification Work. 47

(2.2) The Use of Frequency Domain Data. 50

2.2.1 The Spectral-Analysis Approach. 50

2.2.2 An Alternative Use of Fourier Transforms. 51

2.2.3 An Expression for the Discrete Fourier Transform of a Time Derivative. 61

2.2.4 A Frequency-Domain Representation of the Model. 67

2.2.5 The Modelling of Noise in the Frequency Domain. 73

(2.3) The Inclusion of Time Delays in the Model. 77

2.3.1 Representation of Delays in the Model. 77

2.3.2 Effect of Sampling Interval on the Estimates of the Delay. 83

2.3.3 A Demonstration of the Use of a Time Delay Using Real Flight Data. 88

Summary. 94

3 Initial Stages in the Identification Methodology, and a Consideration of Some Relevant Identification Techniques. 98

(3.1) Introduction and Overview of the Methodology. 98

(3.2) The Frequency-Domain Equation-Error Stage in the Identification Methodology. 98

3.2.1 The Basic Method and Some Comments on the Frequency-Domain Formulation. 100

3.2.2 Subset Regression. 115

3.2.3 The Method of Successive Residuals. 120

3.2.4 Parameter Significance Values. 125

3.2.5 Implementation of the Equation-Error Method Using Singular-Value Decomposition. 127

3.2.6 Practical Application of the Singular-Value-Decomposition Approach to Frequency-Domain System Identification. 138

3.2.7 Some Comments on the Use of Zero Pads in Frequency Domain Indentification. 141

3.2.8 Summary of Section 3.2. 145

(3.3) Applications of the Singular-Value-Decomposition Frequency-Domain Equation-Error Method to Flight Data. 146

3.3.1 Flight Data Sets and Basic Model Equations Used. 146

3.3.2 Selection of Frequency Range. 150

3.3.3 Length of Time-Domain Record Used. 153

3.3.4 Selection of an Appropriate Number of Orthogonal Components. 154

3.3.5 Implementation of Estimates with Theoretical Values. 160

3.3.6 An Equation-Error Multirun Example. 166

3.3.7 Consideration of the Predictive Qualities of a Model. 167

4. The Frequency-Domain Output-Error Stage in the Identification Methodology. 169

(4.1) Introduction. 169

4.1.1 Background to the Use of the Output-Error Technique. 169

4.1.2 Previous Applications of the Technique. 170

(4.2) Development of the Frequency-Domain Output-Error Algorithm. 172

4.2.1 Formulation of the Frequency-Domian Cost Function. 172

4.2.2 Implementation of the Gauss-Newton Minimisation Algorithm. 180

4.2.3 Constrained Optimization. 197

4.2.4 Controlling Convergence of the Algorithm. 203

4.2.5 Some Further Comments on Neglecting Process-Noise Terms. 204

4.2.6 Summary of Section 4.2. 209

(4.3) Application of the Frequency-Domain Output-Error Method to Flight Data. 210

4.3.1 Applications Involving Longitudinal Test Inputs. 210

4.3.2 Applications Involving Lateral Test Inputs with a Consideration of Trends in the Estimates for Different Flight Conditions. 227

5. Final Stage of the Identification Methodology and a Summary of the Complete Identification Approach. 241

(5.1) Estimation of Zero Offsets and Initial Conditions. 241

5.1.1 Introduction. 241

5.1.2 Minimisation of Time-Domain Cost Function. 241

5.1.3 Correlations Between the Sets of Parameters. 245

(5.2) Summary of the Complete Identification Methodolgy. 247

5.2.1 Stage 1: Frequency-Domain Singular-Value-Decomposition Equation-Error Identification 248

5.2.2 Stage 2: Frequency-Domain Output-Error Identification (with options for the inclusion of constraints) 249

5.2.3 Stage 3: Time-Domain Output-Error Identification (with options for the inclusion of constraints). 251

6. Conclusions and Recommendations for Future Work. 253

Tables 260

Figures 296

Nomenclature 347

7. Appendices 354

Appendix 1: Linearised Equations of Aircraft Motion. 354

Appendix 2: Conditions for Unbiased Estimates from the Frequency-Domain Output-Error Method. 359

Appendix 3: The Line-Search Algorithm. 363

Appendix 4: The Kalman-Filter Algorithm. 367

References/Bibliography. 371

Acknowledgements.

I should first like to express my sincere thanks to Professor David Murray-Smith, of the Department of Electronics and Electrical Engineering, for the encouragement, help, and perceptive guidance given to me over the course of the research. His sharp intellect and clearness of thought has been a great source of inspiration.

I am also greatly indebted to Mr Roy Bradley of the Department of Aeronautics and Fluid Mechanics for the help and advice, often outside the call of duty, given to me. His insightfulness into many aspects of the work has been invaluable.

Thanks are also due to my external supervisor Doctor Gareth Padfield, of the Royal Aircraft Establishment, Bedford, who, in effect, set me on my present course many years ago. His enthusiasm and wide-ranging knowledge must be acknowledged as an essential contribution to the research.

I should also like to acknowledge Professor Brian Richards, of the Department of Aeronautics and Fluid Mechanics, for his efforts in supporting the research project.

Thanks are also due to the computing staff: Mrs Linda McCormick and Mrs Carol Carmichael, for their cheerful helpfulness over the years.

Finally I wish to thank Mr Frank Lombos and his

assistants for typing this document.

This research was supported by the U.K. Ministry of Defence (Procurement Executive) through Agreement No. 2048/028 XR/STR.

This thesis is dedicated to my parents.

ABSTRACT

There is considerable need for the application of system identification techniques to helicopters. These include their use in the validation and improvement of existing theoretical flight-mechanics models, and for development flight testing. In both cases, estimates of stability and control parameters are sought. Most applications of system identification techniques to helicopters have involved time-domain methods which use reduced-order mathematical models representing six-degrees-of-freedom rigid-body motion. In this document, an identification methodology which uses the frequency-domain to obtain estimates of the stability and control parameters is advocated.

For applications to helicopters, the use of the frequency domain has some considerable advantages for the identification. For example, in the identification of six-degrees-of-freedom rigid-body models, where an adequate description of the fuselage motion is required, the ability to use a restricted frequency range (i.e. one which excludes the higher-order frequencies associated with faster rotor dynamics) is advantageous. In addition to providing a basis for establishing reduced-order models valid over a defined range of frequencies, the use of the frequency domain also results in a significant data reduction in comparison with time-domain methods, thus resulting in a speedier identification. The fact

that the model is represented in terms of Fourier transformed quantities is advantageous for the development of expressions required for the minimisation algorithm, and also facilitates the incorporation of time delays into the model. A suitable means of symbolically representing the model equations in the frequency-domain is presented. Models valid for small perturbations about a nominal trim state are used in the identification.

The identification methodology is based upon the use of three distinct identification stages similar to those advocated by Fu and Marchand in their paper presented at the Ninth European Rotocraft Forum at Stresa, Italy, in 1983. Firstly, a frequency-domain equation-error type identification is used to provide initial parameter estimates. Secondly, a frequency-domain output-error type estimation is used to provide under ideal conditions unbiased estimates of the stability and control derivatives. And finally, a time-domain output-error type estimation is used to obtain initial state conditions and zero offsets, and to provide a time-domain verification of the identified model.

For the identification methodology developed in this document, additional features to the basic identification methods are advocated. In broad terms these relate to the form of the model used, to the determination of a suitable model structure, and to the implementation of the identification algorithms. An important and original feature of the identification methodology developed here

is the incorporation and estimation of time delays in some of the controls. This is seen primarily as a means of accounting for the effect of rotor-transient effects which are ignored in the quasi-static formulation of the rigid-body motion. It is known from previous studies that unmodelled rotor effects can have a corrupting influence on some important parameters when a simplified form of model is used in the identification; the improvement in the identification resulting from this new approach is demonstrated using real flight-data from a Puma helicopter.

The use of techniques (singular-value decomposition for the equation-error method and rank deficiency for the output-error method) that enable the analyst to explore the effects, and likely improvements, as a result of effectively changing the model structure through the introduction of constrained relationships between parameters within the model, is an approach advocated here. It is believed that these techniques have not previously found an application in helicopter system identification. Results demonstrating the usefulness of these techniques are presented, and are obtained using real flight data. For the frequency-domain output-error method, additional means of introducing constraints into the identification are considered.

The identification results are discussed in terms of a comparison between the estimated values and those suggested by theory, as well as through the frequency-

domain fits obtained and the time-domain verifications of the identified model. Results are presented for real flight-data, corresponding to the application of test-input signals on both longitudinal and lateral controls.

Some recommendations that can assist in overcoming some of the practical difficulties traditionally associated with helicopter system identification are made. In addition, some new theoretical results and observations relating to the frequency-domain formulation of the identification are made.

CHAPTER 1

1.0 INTRODUCTION: THE HELICOPTER SYSTEM IDENTIFICATION PROBLEM.

1.1 Introduction.

1.1.1 The Nature of System Identification.

In a large number of branches of science, the requirement for a mathematical formulation of the behaviour of a system based on measurements of the response to various inputs, has led to the development of system identification. System identification is commonly referred to as an inverse problem, because instead of computing the response of a system with known characteristics, an attempt is made to solve the opposite problem: that of obtaining the system characteristics from measured responses. In the reference MAIN002, it is suggested that the inverse problem might be phrased as: "Given the answer, what was the question?"

In successfully applying the techniques of system identification, the analyst must be able to draw upon results and analytical tools from a wide range of different fields of mathematics (categorized under such titles as probability, statistics, optimization, numerical analysis, linear algebra, mechanics etc.). In addition, the analyst needs to be familiar with the

details of the data collection, such as: the characteristics of the instrumentation; the level of noise on the measurements; the limitation of information content as a result of the sampling rate, or record length, etc. Even in the case of familiarity with all these aspects, much more is still required if the analyst is to be successful in applying the techniques of system identification. Insight into the system under consideration is important, and subjective judgements (i.e. engineering judgement) have an important role to play in the work.

System identification, it could be said, is as much an art as a science - that is, knowledge acquired through experience and intuitive insight is important, and is complimentary to the more exact aspects of this applied subject. In this context, the following sentence taken from MAIN002, relating to the justification for the application of a particular algorithm (axial iteration, discussed infact in Chapter 4) is relevant: "...Often with little more justification than it seems to work well. This is, of course, the final and most important justification."

The term: system identification, is the most general description of the inverse modelling procedure, involving both the determination of an appropriate model structure, and the estimation of the coefficients (i.e. parameters) within that model structure; the latter process is known more commonly as parameter estimation, though the terms

are often used to mean the same thing. The term, parameter identification may also be used, but this has come to imply a situation where the form of the system model is assumed to be known.

1.1.2 The Need for System Identification in Helicopter Applications.

In the context of helicopters, system identification techniques have considerable potential for the validation, or improvement, of theoretical flight mechanics models; this in turn leads to its usage as an aid to the testing of new designs. In addition, during development flight-testing using clinical flight qualities tests, measurements made can be used to estimate stability and control parameters of interest, in order to demonstrate compliance with requirement specifications. A further application involves the use of an on-line identification procedure in an adaptive flight-control system; this however, has yet to be fully exploited.

1.2 The Helicopter Model.

1.2.1 The Nature of a Model.

Since the purpose of system identification is to obtain models of a particular system (in the current

context, the system is a helicopter), it would be useful to define what is meant by a model. In the reference KRAM001, the following words are said on the subject of models: "The essence of using models is that a material, or formal image of a system is made which is easier to study than the system itself. This image is then used as a model of the system. The model must then obviously contain information about the system. Hence there must be a **certain resemblance** [emphasis added by the current author] between the model and the system." The same reference gives the following formal definition of a model: "If a system M, independent of a system S, is used to obtain information about system S, we say that M is a model of S."

The last definition begs the question as to what is a system. The same reference gives the definition of a system (actually before defining a model): "A system is a set of interrelated entities, of which no subset is unrelated to any other subset." The system M - that is the model shall in the case of the current investigation be an abstract model, consisting of constant-coeffecient, coupled, ordinary differential equations. Although the form of the equations used arise from linearisations of the equations of motion, use of the adjective linear is avoided to allow for time delays in some of the terms, rendering the description as linear, inexact. The models identified, however, are based on the requirement of small-scale perturbations in the states,

and so it would be equally inexact to talk of non-linear models; instead I shall henceforth refer to them as state-space models (e.g. GELB001) with delays.

Model Simplifications.

In the reference MAIN002, it is pointed out that a system is never described exactly by the simplified models used for analysis, and unexplained sources of modelling will always be present, since there is no unique correct model. The models used for the helicopter system identification in this document, for example, are based on the rigid-body motion (with six degrees of freedom: three of body translation, and three of body rotation). The most important aspect of the helicopter apparently excluded from this type of model, is that involving the behaviour of the main and tail rotors, and their interaction or influence on the rigid-body motion. However, by using rigid-body models, in conjunction with a new modelling technique developed in this document (viz the use of time delays in some of the controls), an attempt can be made to model the influence of the rotor(s) on the rigid-body motion. The dynamics of the states associated with the rotor(s) (i.e. flap, lag, torsion etc.) are excluded from the state-space representation of the model. This approach is consistent with another feature of the rigid-body models used in the identification work presented in this document: that of

using some state variables as "pseudo-controls" in a reduced-order model. For example, in the identification of the longitudinal subset of the six-degrees-of-freedom model, important lateral states may be included as forcing terms along with the controls and this facilitates the formulation of the identification problem in a manageable form. Examples showing the use of this form of model reduction are presented in Sections 2.3.3 and 4.3.2.

Most models require simplifying assumptions, and the analyst is forced by practical constraints to define the system boundary at some point, that is, where the relations between entities are "less concentrated" (KRAM001); in the present context, we might say: "almost decoupled."

1.2.2 Adequate Models.

As a result of the practical constraints imposed on the model (e.g. its size), it can be appreciated that there is no such thing as a "true" model. Consequently, the emphasis should be on the estimation of an "adequate" model (i.e. one that is suitable for the purpose required) and not on the estimation of the "true" model. The myth of the "true" model is very strong, and in MAIN002, the authors quote the comments made by someone on this matter: "A favourite form of lunacy among aeronautical engineers produces countless attempts to

decide what differential equation governs the motion of some physical object, such as a helicopter rotor... But arguments about which differential equation represents truth, together with their fitting calculations, are wasted time."

In the context of the work carried out in this document, some degree of validation of a theoretical model is the primary motivation for the identification work. The theoretical model concerned is HELISTAB (SMIT001). This has six degrees-of-freedom, and assumes that the rotor-disc tilts instantaneously for a given stick input (and similarly for the tail-rotor following a pedal input). Consequently, the most adequate model for the purpose of the identification (and validation) will have six degrees-of freedom (with the same states as the theoretical model, so that direct comparisons can be made easily between parameters). However, since the real system, i.e. the helicopter, has a rotor-disc which does not respond instantaneously to pilot stick inputs, but has a finite transient response (which is, in fact, very quick in comparison to the transient behaviour of the rigid-body), it suggests some further modifications to the basic model are required in order to have an adequate representation of the system for identification. In fact, results have indicated that by ignoring the short term transient effects of the rotor on the rigid-body states, the unmodelled "contaminating" effects will result in physically unrealistic (biased, or wrong, call them what

you may) estimates of some parameters; the most striking example of which, is in the case of the primary-rate pitch-damping parameter M_q (this is considered, in detail, in Section 2.3.4).

Accuracy of Estimates

To make effective use of parameter estimates we must be able to gauge their accuracy, and in order to define accuracy, it is necessary to have an assumed model structure. Once we have decided upon an adequate model structure to use in the identification, then several measures of accuracy can be found. A commonly used statistical measure is the estimated standard deviations of the parameter estimates, also known as the Cramer-Roo bound (MAIN001). As pointed out in the reference, this measure combines two commonly used indicators of parameter accuracy, that of sensitivity of a parameter, and correlation between any two parameters. The estimated deviation is the measure of parameter accuracy used for the work covered in this document. It should be stressed that the derivation of these error bounds is based on assumptions regarding the noise characteristics on the model; these assumptions will be pointed out in due course for the equation-error and output-error techniques used here.

1.2.3 Model Structure.

It is said in the reference MAIN002, that the real model-structure determination problem is not to determine some non-existent "correct" model structure, but to determine an adequate model structure. If too detailed a model structure is demanded for a data set containing insufficient information, then the result will be a model which appears to fit the given data set closely, but which may be, in reality, a poor and inadequate model, with poor predictive qualities when extrapolated to data different from that used in the estimation. The inclusion of more and more parameters to get a better fit to the observed data, with the additional parameters not really reflecting any physical effect, is known in identification parlance as "over parameterization."

Sometimes it is wiser to use a simple, rather than detailed, model; this is known as the "principle of parsimony." In the reference KLEI003, the authors speak of a "parsimonious model", and seek to obtain, using the equation-error approach, a model (i.e. an equation) that has good predictive qualities, and is not over-parameterized. They define a criterion for testing the predictive quality of a model (the prediction sum of squares), and use it in conjunction with an automatic model structure determination process known as optimal subset regression.

In the optimal subset regression procedure, the

"best" model is selected from a pool of possible candidate models. On the basis of statistical tests performed on the model fit and individual parameter estimates, variables can be incorporated into, or removed from, a model structure. Hence the "optimal" model will consist of a subset of the available variables. In most implementations of the method, it is usually possible to force variables into the model (sometimes called modified stepwise regression; e.g. KLEI002) regardless of whether or not they would be included by the statistical tests, thus introducing a subjective element into the model selection procedure. The subset regression procedure is discussed in more detail in Section 3.2.2.

There are many other methods for determining the adequacy of a model structure (e.g. SODE001). One such method is the testing of residuals; this has been used successfully by the current author in studies using simulated data, to show the superiority of one model structure over another. Plots of the residuals and their autocorrelation function (which should be impulsive in appearance for uncorrelated stationary Guassian noise) are used (BLAC003).

With the frequency-domain identification methodology developed in this document, one important means for determining an adequate model structure, both for the equation-error and output-error techniques, is based on the "degree of singularity" (i.e. the condition number-

see Section 3.2.5) of the information matrix. In the case of the equation-error method, use is made of the singular-value-decomposition technique to enable solutions to be found, that correspond to a fit obtained using, in effect, a parameter sub-space; this is discussed in detail in Section 3.2.5. There is a direct analogy with the method of subset-regression mentioned earlier (and discussed in Section 3.2.2) in the sense that the "best" model is arrived at using only a subset (or subspace) of available variables. However, in the case of the singular-value-decomposition approach, orthogonal variables - constructed as linear combinations of the original model variables - are used, and it is combinations of variables rather than individual variables, which in general, are excluded from the model. An interpretation that the exclusion of insignificant orthogonal variables from the model, corresponds to the introduction of relational constraints between the parameters in the original model, is offered by the current author in Section 3.2.5. For the equation-error identification technique, using singular-value decomposition, the decision as to what constitutes the "best" model can be based (as with most practical applications of the subset-regression procedure), on both objective and subjective criteria.

Both the subset-regression and the singular-value-decomposition approaches, ultimately use the correlations that exist between the responses of the variables

considered, in the selection of a suitable model structure, and any attempt to say that one method is more correct than another would be inappropriate. The most striking difference between the two approaches, however, is that estimates are provided for all the parameters stipulated to be in the model in the case of the singular-value-decomposition approach (regardless of the dimension of the parameter sub-space used in the estimation), whilst in the case of the subset-regression approach estimates are only provided for those parameters incorporated into the model on completion of the algorithm. For example, for the pitching-moment equation we know from the physics of the system that an appropriate equation has the form:

$$\dot{q} = M_u u + M_w w + M_q q + M_v v + M_p p + M_{\eta_{1s}} \eta_{1s} \qquad (1.2\text{-}1)$$

For the singular-value-decomposition approach, we will obtain estimates of Mu, Mw, Mq, Mv, Mp and $M_{\eta_{1s}}$, regardless of the model structure (defined by the constraints relating dependent sets of parameters, and determined on the basis of the data used in the identification).

Applying the subset-regression procedure to the same set of data, we may find that the proposed adequate model structure is:

$$\dot{q} = M_u u + M_w w + M_q q + M_{\eta_{1s}} \eta_{1s} \qquad (1.2\text{-}2)$$

Thus providing estimates of the parameters Mu, Mw, Mq, and $M_{\Lambda_{1S}}$, but not of Mv and Mp (except that is it implied that they can be considered to be zero for the data used in identification).

The equation-error method is seen, for the identification methodology developed in this document, as a means of providing initial guesses for the more advanced output-error method. The singular-value-decomposition approach provides a full set of parameter values for use in the output-error method, whereas the subset-regression procedure, in general, does not. It is also of interest to point out that the speed of application of the singular-value decompostion procedure to the problem of helicopter system identification, is greatly facilitated by the use of the frequency domain, because of the small number of data used.

The equation-error approach, in addition to providing initial estimates for the output-error method, can also assist in the determination of a suitable model structure through the use of some measures of parameter significance, as defined and described in Section 3.2.4. In addition, some investigation into the use of different model structures for the output-error identification stage can be performed using rank deficiency. This is described in Section 4.2.3, where the method is implemented using a singular-value decomposition of the information matrix. Here, it is found that it may be appropriate to reduce the effective dimension of the

parameter space used in the iterative estimation technique. This amounts to introducing relational constraints on the update increments.

The preferred techniques for obtaining a suitable model structure for both the equation-error and output-error methods (referred to by the current author thorughout this document as singular-value-decomposition and rank-deficiency respectively, for the purpose of distinction) are demonstrated in Sections 3.3.4 and 4.3.2 using real flight data.

1.2.4 the Helicopter Model.

The helicopter equations of motion used for the work in this document, correspond to the form of model defined in the reference PADF009. Here the applied forces and moments acting on the vehicle are incorporated into equations, with a right-hand set of body-fixed axes X,Y,Z defining the rigid body, having vehicle translational velocity components u,v,w, and vehicle rotational componenets p,q,r, along and about the X,Y and Z axes respectively. The Euler angles Ψ, Θ, ϕ represent the transformation from earth to rigid-body axes.

The six-degrees-of-freedom rigid-body equations of motion are used in linearised form for the identification work carried out in this document. Here, the equations of motion are linearised about a given trimmed flight condition, and small perturbations about this nominal

level are assumed. The linearisation is presented in Appendix 1, and allows a suitable state-space form of the helicopter model to be written as:

$$\dot{\underset{\sim}{X}} = A\underset{\sim}{X} + B\underset{\sim}{U} \tag{1.2-3}$$

$$\underset{\sim}{X} \triangleq (u, w, q, \theta, v, p, \phi, r)^T \quad ; \quad \underset{\sim}{U} \triangleq (\eta_c, \eta_{1s}, \eta_{1c}, \eta_p)^T$$

(The states $\underset{\sim}{X}$ in the model, and the measured quantities $\underset{\sim}{Z}$ are in general, related in a non-linear manner; this is discussed in Section 2.2.4).

A more general representation of the helicopter, will also include equations with states representing the behaviour of the rotor, and its coupling with the rigid-body motion of the helicopter. It is convenient to represent the rotor by means of the attitude and shape of the tip-path plane, with respect to the shaft, instead of considering individual blade motions (whose description requires a system of coordinates rotating with the rotor). This is achieved using a multi-blade coordinate transformation (e.g. PADF009) and corresponds to the representation of the rotor as a continuous and periodic function of azimuth position. For a four-bladed rotor, the three terms of a Fourier series representation, corresponding to the average, and first harmonic sine and cosine terms, and a fourth term corresponding to the average of the second harmonic sine and cosine terms, can be obtained. In the case of blade flap, these correspond to β_0 (coning angle); β_{1c} (tip-path plane tilt in pitch);

β_{1s} (tip-path plane tilt in roll); and β_d (differential coning). They are obtained using (PADF009):

$$\beta_0 = 1/4 \sum_{i=1}^{4} \beta_i$$

$$\beta_{1s} = 2/4 \sum_{i=1}^{4} \beta_i \sin \psi_i \qquad (1.2\text{-}4)$$

$$\beta_{1c} = 2/4 \sum_{i=1}^{4} \beta_i \cos \psi_i$$

$$\beta_d = 1/4 \sum_{i=1}^{4} \beta_i (-1)^i$$

for a four-bladed rotor, with individual blade flapping measurements β_i, and rotor azimuth position ψ_i. Identical expressions can be defined for the lagging motion of the rotors.

If we define the rigid-body states to be $\underset{\sim}{X}_F$, and the rotor states to be $\underset{\sim}{X}_R$, then we can write the following linear constant coefficent model (KALE001):

$$\dot{\underset{\sim}{X}}_F = A_{FF} \underset{\sim}{X}_F + A_{FR} \underset{\sim}{X}_R + B_F \underset{\sim}{U} \qquad (1.2\text{-}5)$$

$$\dot{\underset{\sim}{X}}_R = A_{RF} \underset{\sim}{X}_F + A_{RR} \underset{\sim}{X}_R + B_R \underset{\sim}{U} \qquad (1.2\text{-}6)$$

Where the matrices A_{FF} and A_{RR} represent the uncoupled systems for the fuselage and rotor. The matrices A_{FR} and A_{RF} represent the coupling between the fuselage and the rotor; B_F and B_R are the fuselage and rotor control dispersion matrices.

It is pointed out in the reference KALE001 for a model with 14 degrees of freedom (i.e. 6 rigid-body, 4

rotor flap, and 4 rotor lag), with the rotor modelled as a second-order system, that there are 326 state matrix coefficients (of which, about 300 have to be identified). And this is after two approximations have been made: namely the small perturbation assumption, and the averaging of periodic terms in (1.2-5) and (1.2-6) to give constant coefficients. This is obviously an unrealistic number of parameters to even consider attempting to estimate. The comments made in Section 1.2.1 about the practical constraints which force the analyst to make necessary simplifications, are relevant in this context. The simplifications which can be carried out here include neglecting lead-lag states (on the basis that the frequencies associated with them are well separated from those associated with the rigid-body states), thus representing the rotor dynamics in terms of flapping motion only. In turn, the rotor flap motion can undergo a series of simplifications, whereby the second-order system can be simplified to a first-order system, and ultimately to a zeroth order system. The final simplification (i.e. zeroth order system) is a form of quasi-static model. It assumes an instantaneous response of the rotor following a pilot control input, and is a form of model which has found applications in real time helicopter simulations (e.g. PADF009). Again, this assumption is justified on the basis that the frequency seperation between the rotor modes and the fuselage rigid-body modes is high: for the time scales typical of

the rigid-body motion, the behaviour of the rotor states appears to be instantaneous.

The Quasi-Static Assumption.

Using the assumption that the rotor disc tilts instantaneously following the application of a pilot control input, a form of the model given in (1.2-5) and (1.2-6) can be written which considers fuselage states only. Setting $\dot{\underset{\sim}{X}}_R$ in (1.2-6) to zero gives (KALE001):

$$\underset{\sim}{X}_R = -A_{RR}^{-1} \cdot A_{RF} \underset{\sim}{X}_F - A_{RR}^{-1} \cdot B_R \underset{\sim}{U} \qquad (1.2\text{-}7)$$

And substituting for $\underset{\sim}{X}_R$ in (1.2-5) we have:

$$\dot{\underset{\sim}{X}}_F = (A_{FF} - A_{FR} \cdot A_{RR}^{-1} \cdot A_{RF}) \underset{\sim}{X}_F + (B_F - A_{FR} \cdot A_{RR}^{-1} \cdot B_R) \underset{\sim}{U} \qquad (1.2\text{-}8)$$

$$= A_{FF}^{*} \underset{\sim}{X}_F + B_F^{*} \underset{\sim}{U} \qquad (1.2\text{-}9)$$

The contribution to the rotorcraft motion made by the rotor is lumped into the fuselage coefficients. The point can be made that the derivatives, identified for a model of the form given in (1.2.9), but with data which is not quasi-static, will in general be different to the theoretical quasi-static values.

The effects of rotor/fuselage coupling on derivative estimation was demonstrated in MOLU003, by attempting an

identification of a six-degrees-of-freedom model from simulation data that included rotor flapping modes. Substantial differences existed between the predictions and the quasi-static values. However by including the multiblade flapping coordinates β_o, β_{1c}, and β_{1s}, in the assumed model, and performing the identification, and then reducing to a six-degrees-of-freedom form (as in 1.2-8), the values obtained agreed very well with the calculated quasi-static values. The conclusion was that the quasi-static mode was quite adequate in representing the long-term helicopter motion, but that profound difficulties could be expected in trying to estimate quasi-static model parameters using fuselage states only, in the estimation. The most serious discrepancy was the underestimation of primary-rate damping derivatives such as Mq.

The inclusion of rotor states in the estimation is one possibility suggested by the above conclusion. However, this would require a fairly large increase in the number of parameters to be estimated. The technique developed by the current author in the following section, requires only the inclusion of one extra parameter, namely a time delay, for an improved estimation of quasi-static derivatives.

1.2.5 A Suitable Model for the Identification of Quasi-Static Derivatives.

The quasi-static model containing fuselage states only is given in (1.2-8), and is written compactly in (1.2-9). To be exact, an additional term is required in (1.2-9) to represent the transient rotor effects. We may rearrange (1.2-6), to obtain (c.f. 1.2-7):

$$\underset{\sim}{X}_R = - A_{RR}^{-1} \cdot A_{RF} \underset{\sim}{X}_F - A_{RR}^{-1} \cdot B_R \underset{\sim}{U} + A_{RR}^{-1} \dot{\underset{\sim}{X}}_R \qquad (1.2\text{-}10)$$

Substituting for $\underset{\sim}{X}_R$ in (1.2-5), and rearranging as in (1.2-8), we have:

$$\dot{\underset{\sim}{X}}_F = A_{FF}^{*} \underset{\sim}{X}_F + B_F^{*} \underset{\sim}{U} + A_{FR} \cdot A_{RR}^{-1} \dot{\underset{\sim}{X}}_R \qquad (1.2\text{-}11)$$

Hence it is the unmodelled input $- A_{FR} \cdot A_{RR}^{-1} \dot{\underset{\sim}{X}}_R$ representing the rotor transient effects, which is responsible for the poor estimates of some quasi-static parameters in the matrices A_{FF}^{*} and B_F^{*}. It can be appreciated that the unmodelled input $A_{FR} \cdot A_{RR}^{-1} \dot{\underset{\sim}{X}}_R$ will become significant for a small time following a movement of the stick (or pedal) by the pilot: the time span of this transient term will be characterized by the time-constants of the corresponding important main rotor (or tail rotor) modes. There is clearly a requirement for a remodelling of the effective control input. We require the estimates of the quasi-state derivatives: A_{FF}^{*} and

B_F^* for direct comparison with theory, and we shall seek a model for the identification with the following form:

$$\dot{\underset{\sim}{X}}_F = A_{FF}^* \underset{\sim}{X}_F + B_F^* \underset{\sim}{U}_{ef} \tag{1.2-12}$$

where $\underset{\sim}{U}_{ef}$ is the effective control input to the model. A comparison of (1.2-11) and (1.2-12) implies that:

$$B_F^* \underset{\sim}{U} + A_{FR} A_{RR}^{-1} \dot{\underset{\sim}{X}}_R = B_F^* \underset{\sim}{U}_{ef} \tag{1.2-13}$$

When $\dot{\underset{\sim}{X}}_R = 0$ (or near enough) then we have the effective control input $\underset{\sim}{U}_{ef}$ equals the measured pilot input U; this will be the case for a step input after a time-span of the order of the time constants of the important main rotor (or tail rotor) modes has elapsed. When $\dot{\underset{\sim}{X}}_R \neq 0$, the only meaningful interpretation of (1.2-13) is a least-squares solution for $\underset{\sim}{U}_{ef}$. The dimensions of B_F^* are n x m (for n fuselage states and m controls). Since n > m, we have an overdetermined system of equations which may be solved for $\underset{\sim}{U}_{ef}$ using the following pseudo inverse (e.g GELB001);

$$[B_F^*]^{\#} = (B_F^{*T} B_F)^{-1} B_F^{*T} \tag{1.2-14}$$

Hence using (1.2-14) in (1.2-13), we have:

$$\underset{\sim}{U}_{ef} = \underset{\sim}{U} + (B_F^{*T} B_F^*)^{-1} B_F^{*T} A_{FR} A_{RR}^{-1} \dot{\underset{\sim}{X}}_R \tag{1.2-15}$$

An improvement on the assumption of an instantaneous response of the rotor states $\underset{\sim}{X}_R$, following a pilot control input, is to use a first-order model. If we ignore all but the most important element in $\underset{\sim}{X}_R$ (assuming $\underset{\sim}{X}_R$ represents rotor flapping states), this will leave, for example, β_{1c} for a longitudinal cyclic input η_{1s} . Hence (1.2-15) can be written as a scalar equation.
The effective input is composed of the pilot input and an additional transient term related to the rotor states.

$$U_{ef} = U + b X_R \tag{1.2-16}$$

An approximate approach adopted here, incorporating transient and steady-state behaviour, involved modelling the effective control input U_{ef} as a first-order lag, driven by the applied or measured pilot input U. The time constant would be expected to have a value characteristic of the important main rotor (or tail rotor) modes. We can thus write:

$$\dot{U}_{ef} + 1/\tau\, U_{ef} = 1/\tau\, U \tag{1.2-17}$$

Transforming (1.2-17) into the frequency domain (see Section 2.2.2) and for a periodic measurement window of length T (U(o) = U(T) = 0) we have

$$\hat{U}_{ef}(\omega) = (1 + j\omega\tau)^{-1}\hat{U}(\omega) \tag{1.2-18}$$

where $U_{ef}(0) = 0$, since U(0) = 0 and using (1.2-16).

Now for $|\omega\tau| << 1$, (i.e. for small frequencies and small time constants) we can write (1.2-18) as:

$$\hat{U}_{ef}(\omega) \simeq (1 - j\omega\tau + O(\omega^2\tau^2))\,\hat{U}(\omega) \tag{1.2-19}$$

Since for $|\omega\tau| << 1$ it is true that

$$e^{-j\omega\tau} \simeq 1 - j\omega\tau + O(\omega^2\tau^2) \tag{1.2-20}$$

we have:

$$\hat{U}_{ef}(\omega) \simeq e^{-j\omega\tau}\,\hat{U}(\omega) \tag{1.2-21}$$

In the reference ISER001, and in the context of transfer-function representations, the replacement of small time constants in the denominator by delays in the numerator, is a suggested simplification; this corresponds to the approximation given by (1.2-20). Converting (1.2-21) back into the time domain we have.

$$U_{ef}(t) = U(t-\tau) \tag{1.2-22}$$

Hence a more suitable model for the identification of quasi-static derivatives (A^*_{FF} and B^*_F) using fuselage states and the measured or applied pilot control input, is given by:

$$\dot{\underset{\sim}{X}}_F = A^*_{FF}\,\underset{\sim}{X}_F + B^*_F\,\underset{\sim}{U}(t-\tau) \tag{1.2-23}$$

where τ is an unknown parameter to be estimated alongside

elements of A^*_{FF} and B^*_F. The estimated time delay τ may also contain a "transport" component in the control.

1.2.6 The Theoretical Model (HELISTAB).

The helicopter flight-mechanics software package-HELISTAB, developed at the Royal Aircraft Establishment, Bedford (SMIT001), is used to provide the theoretical quasi-static parameter values for comparison with estimates obtained from flight data. In addition, the package can be used to generate simulated non-linear or linear time responses, which is useful both for the validation of estimation techniques and software. It has options for a range of different degrees of freedom (DOF) in the model: 6DOF (quasi-static model); 9 DOF (with first order modelling of main rotor flap); 12 DOF (with second order modelling of rotor flap).

The theoretical non-linear model (PADF009) - for a specified helicopter configuration - is linearised for a given flight condition in order to provide the theoretical quasi-static linear model values. A trim routine calculates the control settings for the given flight condition, and then the force and moment derivatives are calculated numerically using forward and backward differencing about the trim point. These are then combined with the linearised kinematic and gravitational effects to produce the complete linear model.

1.3 Difficulties Associated with Helicopter System Identification.

1.3.1 General Discussion of Identification Difficulties.

The application of system-identification techniques, especially in the time domain, has a relatively long history of success in the context of fixed-wing aircraft (e.g. ROSS001, KLEI007, FOST002, FOST003). The pioneering work of Molusis in helicopter system identification (MOLU001, MOLU002, MOLU003), and work published by subsequent authors (e.g. PADF002, PADF005, BLAC007, DUVA001), highlighted some of the difficulties of applying identification techniques to helicopters. These difficulties, including those encountered for the frequency-domain methodology developed in this document, will be considered now:

1. System Complexity: As was discussed in Section 1.2.4, the helicopter represents a complex, and highly coupled system. Strong coupling exists between the longitudinal and lateral fuselage dynamics. Consequently a large number of parameters are required for a model approaching something of a global representation of the helicopter. It is pointed out in KALE001 that such "global" models may be very inefficient for use in problems such as control system design, stability and control analysis,

and direct correlation with flight test data for validation purposes. There is therefore a need for simplifications in the model representation.

The justification for the assumed form of model used in the identification work covered in this document, has been given in the previous sections. It was also mentioned that a further reduction in the model complexity can be obtained by excluding lateral dynamics, but incorporating lateral states in an extended control vector for a longitudinal input (and vice versa). This reduces the identification problem to a manageable size for the output-error method, and is an approach advocated in the helicopter system identification methodology developed in this document.

Identification problems resulting from fuselage-rotor interaction were discussed in Section 1.2.4, and a new feature of the assumed model structure, namely the use of a time delay, was presented as a means of overcoming to some extent these problems; this circumvents the need for introducing the additional complexity in the estimation model that would occur with the inclusion of rotor states.

2. High-Vibration Environment: Helicopter vibration is caused mainly by the higher harmonic components of the blade flapping and lagging motion, in addition to blade bending modes. The high-vibration environment reduces the signal-to-noise ratio. A high degree of uncertainty

or noise in the measurements results in a greater degree of uncertainty in the parameter estimates finally obtained.

3. Instabilities: The inherent instability of the helicopter restricts the length of the data records available for estimation. Data records which are short in comparison to long-period modes, may result in identification problems; the convergence of parameter estimates with record length is discussed and demonstrated in Section 3.3.3. The smallest frequency which can be used in the identification is determined solely by the length of the data record; an artificial means of reducing the spacing between frequencies, namely by the use of zero pads, is shown in Section 3.2.7 to be worthless for identification purposes.

Because of the instability of the helicopter, difficulties can be experienced in the practical application by the pilot, of test input signals which may have desirable spectral properties for system identification work, but which may result in an unacceptable response of the aircraft.

The use of stability augmentation systems can enable longer data records to be obtained. However a decreased accuracy in the estimates of the parameters can be expected because of the likely existence of strong correlations between the states and the controls, when feedback loops are used. The identification of a highly

augmented airplane is considered in the reference BATT001, where time-domain stepwise regression and maximum-likelihood procedures are used; it was concluded for the identified model, that some degree of correlation between the parameters must be accepted. The use of rank-deficiency as a means of establishing a suitable model structure when strong correlations or nearly perfectly defined relationships exist between groups of parameters, is one aspect of the identification methodology used by the current author. The use of rank-deficiency, together with the longer data records that would be possible as a result of using a stability augmentation system, may well offer some new possibilities for improved helicopter system identification.

The use of a stability and control augmentation system in obtaining response data for system identification work, is also mentioned in TISC001, where it is stated as a key requirement that the total surface deflection (i.e. the control input signal) must contain a significant component from the pilot which is uncorrelated with the output.

4. Non Linearities: One of the drawbacks of the frequency-domain identification methodology is that it is restricted to linearised state-space models with time delays. As a result there is a need to avoid large excursions of the helicopter from the trim, in order not

to violate the small-perturbation assumptions on which the model is based. Consequently there is a requirement at the data-collection stage to use control input signals which will induce a favourable type of response in the helicopter. The effect of control input shape and the effect of non-linearities is considered in more detail in Sections 1.4.1 and 1.4.2.

5. Errors Associated with Measurement Devices: Some measurement devices (e.g vanes measuring sideslip and incidence angles, and the speed probe) are susceptible to rotor wake and fuselage flow-field effects. Dynamic lags may also be present in some measurement devices, such as accelerometers, and as such, should be taken into consideration when the measurement system is modelled. If measurement channels with lags were to be used in an identification, then for the frequency-domain output-error program: OUTMOD, developed by the current author, the corresponding measurement channel could be modelled with a time delay, for both small frequencies and small accelerometer time constants (See Equations 1.2-17 to 1.2-22 in Section 1.2.5 for some justification of this).

It may be the case that scale factor or bias errors are present in the data; these are considered in more detail in Section 2.2.4. For the use of frequency-domain data, constant biases have no effect on the estimation, when the $\omega = 0$ frequency is excluded from the stipulated range. In addition, it is possible to estimate

measurement scale factors occurring in the linearised measurement transition matrix (relating measured responses to states in the model) using the frequency-domain output-error program: OUTMOD.

The locations of measurement devices, relative to the centre of gravity, have to be taken into consideration when modelling the measurement system, although these can also be estimated as unknown parameters. Offsets relative to the centre of gravity are discussed in Section 2.2.4.

6. Correlations in the Data: A specific difficulty resulting from highly correlated lateral response variables, associated with a "Dutch-Roll" type mode, is considered in Section 4.3.2. This is thought to be largely responsible for the physically unrealistic estimates obtained for some lateral parameters in previous studies (PADF002). The use of rank-deficiency in the output-error method is demonstrated in Section 4.3.2, as a technique, which through the establishment of a more appropriate model structure, leads to improved estimates.

Some Further Remarks: A list of further, and possibly insidious, sources of error in the identification would be endless. However, some additional problems encountered by the current author include: errors in the calibration (introduced at the data preparation stage); the use of incorrect measurement units (i.e. a scale- factor type

error) the use of an inappropriate data window for the identification (e.g. the inclusion of a portion of data, usually at the end of a measurement data file, corresponding to the pilot recovery period, and which is not adequately modelled using only one control input in the identification model).

1.3.2 Kinematic Consistency Checking.

Errors in the flight due to instrumentation failure, or errors introduced at the pre-estimation processing stage (i.e. conversion into standard measurement units using calibration values) can cause a lot of wasted hours at the estimation stage. However, the presence of such errors can be revealed by performing a Kinematic consistency check (REID001, FEIK002) on the data. A Kinematic-consistency check program was developed by the current author (KINECON) for use in such cases.

The Kinematic equations of translational motion and associated Euler equations of rotational motion, shown below, from the basis of the computer program - KINECON.

$$
\begin{aligned}
\dot{U} &= -Wq + Vr + a_x \\
\dot{V} &= -Ur + Wp + a_y \\
\dot{W} &= -Vp + Uq + a_z \qquad (1.3\text{-}1) \\
\dot{\phi} &= p + q\sin\phi\tan\theta + r\cos\phi\tan\theta \\
\dot{\theta} &= q\cos\phi - r\sin\phi \\
\dot{\psi} &= q\sin\phi\sec\theta + r\cos\phi\sec\theta
\end{aligned}
$$

The above set of equations may be integrated (using Euler's method or a Runge-Kutta method) to obtain time histories of the velocity components: U,V,W, and Euler angles: ϕ, θ, ψ . The integration is driven by measurements of the accelerations: ax, ay, az, and rotational velocities: p, q, r. A comparison is made with estimates of U, V, W, obtained independently of ax, ay, and az, by solving iteratively the following non-linear set of coupled equations (shown in a form that includes the offsets relative to the centre of gravity in Section 2.2.5, and implemented in the program in such a form).

$$
\begin{aligned}
V_{sp} &= (U^2 + V^2 + W^2)^{1/2} \\
\beta &= \tan^{-1}(V/U) \\
\alpha &= \tan^{-1}(W/U)
\end{aligned}
\qquad (1.3\text{-}2)
$$

Measurements of speed, flank angle and incidence angle: V_{sp}, β, α, are obtained for use in the above procedure.

A graphical comparison of "measured" time histories of: U, V, W, ϕ, θ, V_{sp}, β, α and the corresponding quantities obtained by integration of (1.3-1) can then be made. This can highlight bias errors which show up as drifts in the computed time history (see Figure 1-1).

A procedure for estimation of accelerometer biases is also a feature of the program KINECON. The biases are estimated by an iterative regressive procedure which attempts at each stage to fit a least squares regression

line through the residuals obtained for the U, V and W comparisons. Using the slopes obtained, estimates for the biases are found, and the corresponding accelerometer measurements are corrected. Integration of Equations (1. 3-1) is then repeated, and a new comparison of the observed and estimated quantities U, V and W is made. The procedure is repeated until a satisfactory match between the observations and the estimates is obtained. The use of the technique is illustrated in Figure 1-1, and has proven its worth in application to a large number of flight test records. A more general facility for handling bias and scale factor errors is given by the identification methodology developed in this document.

1.3.3 The Role of Extended Kalman Filtering Techniques.

A problem encountered in the application of system identification techniques to helicopters, is the presence on some measurement channels of large amounts of noise. State estimation, or Kalman filtering techniques seek to reduce the amount of uncertainty associated with a given signal. A computer program specifically for rotorcraft state estimation was developed by NASA, called DEFKIS (HALL002). The program represents the implementation of an Extended Kalman filter and smoother (e.g. GELB001), where the non-linear model is based on the Kinematic equations of motion, similar to those given in (1.3-1), but supplemented by further equations incorporating

additional states. The program can also be seen to play the role of a Kinematic consistency checker, and in addition, allows for the reconstruction of unmeasured states and state time derivatives. The DEFKIS program is an integral part of the time-domain helicopter system identification package PEP, currently implemented at the Royal Aircraft Establishment Bedford, and outlined in the reference PADF005.

A significant disadvantage in the use of DEFKIS is the sheer complexity of the input data required for successful operation of the program. The user is required to specify certain noise statistics (measurement and process) which may not be known apriori with confidence. Execution time of the program may also be considerable.

The frequency-domain methodology developed here is capable of using the untreated measured flight data, where it is transformed directly into the frequency domain. For the frequency-domain equation-error method, it is shown in Section 3.2.1 that measurements of time derivatives need not be available for the estimation to proceed; in addition, the Fourier transforms of states to be included in the model, are easily obtained from the transformed measurements.

The possible need for the use of an Extended Kalman Filter/Smoother Program, such as DEFKIS, within the frequency-domain identification methodology, is discussed in Section 4.2.5 in the context of noisily observed

inputs to the output-error method.

1.4 Obtaining an Adequate Response for Helicopter System Identification.

1.4.1 The Design of Suitable Test Inputs.

Mode Participation

In order to be able to perform a satisfactory identification, it is necessary for the measured responses to contain sufficient information about the system. For a linear system of the form given in 1.2-3, with n states, the following expression can be written for the free response (PADF003):

$$\underset{\sim}{X}(t) = \sum_{i=1}^{n} (V_i^T \cdot \underset{\sim}{X}(0)) e^{\lambda_i} \underset{\sim}{U}_i \qquad (1.4\text{-}1)$$

where $\underset{\sim}{X}(0)$ is the value of the state vector following the application of the test-input signal; $\underset{\sim}{U}_i$ are the eigenvectors of the system matrix A; V_i is the ith row of U^{-1}, where U is the n x n matrix formed by closing together in ordered form the n eigenvectors of A.

The terms in (1.4-1), in parenthesis, are scalars known as mode participation factors. If $\underset{\sim}{X}(0)$ is proportional to one of the $\underset{\sim}{U}_i$, then only that mode will respond. For the free response, the relative degree to which each mode participates in the motion is determined

by the participation factor.

It is because of the fact that the application of a test input signal, on a given control, may not adequately excite all the required rigid body modes, that the combination of several data sets for the identification is advocated, and even stated as necessary, by some authors (e.g. KALE001). This is not, however, a universally held belief: a methodology based on single run equation-error evaluation in the time domain is described in the reference (DUVA001), and is considered in Section 3.2.3. The use of multirun data for the equation-error method is demonstrated in Section 3.3.6 using real flight data.

Multi Step Inputs

The design of suitable control inputs for aircraft system identification studies is an area which has received considerable attention (e.g. GUPT002, STEP001, AGAR001). The object of these test inputs is to excite the system so that the modes of interest are participating significantly in the response. In the context of helicopter system identification, the use of pseudo-stochastic multistep inputs has been proposed (e.g. MURR002). Originally developed for fixed-wing applications, these signals can be tailored so that the frequency components of the signals span the passband of the system under test. However, it should also be pointed

out that sharp-edged inputs might excessively excite the higher-order rotor modes, which is an undesirable feature for the identification of rigid-body models (DUVA001).

A commonly used signal of this type is the "3211"; this is shown in Figure 1-2, together with its auto spectrum, for clock periods of 1.0 and 0.5 seconds. The "3211" input is often favoured as a test input because it has an auto spectrum which closely approximates that of a band-limited white noise source, which has an equal power distribution over a certain frequency range, and so excites all modes within the band equally.

For the flight data sets analysed by the current author, the "3211" inputs occurred with a 1.0 second clock period. It can be appreciated that as the clock period of a multi-step is increased, there will be an increase in the overall power content of the signal; this is shown in Figure 1-2 for a "3211" input. The problem with applying a signal which has a relatively high power level throughout the range of frequencies associated with the rigid-body modes (0-3 rads/s), is that it will induce large excursions of the aircraft, invalidating the small-perturbation assumptions of the model. This is likely to be a significant reason why better results were obtained for doublet inputs (shown in Figure 1-3, together with auto spectrum), of shorter duration, by the current author, for the flight data sets considered.

The above findings have been supported by some additional research, subsequently carried out at Glasgow

University (LEIT001), in which it was shown that the "3211" input, with a 1.0 second clock period had a lower coherence function (BEND001) than the 1.0 second clock period doublet, over the range of frequencies associated with the rigid-body motion. A lowering of the coherency at particular frequencies can be caused by insufficient excitiation and non linearities; both of which are undesirable features from the point of view of identification.

An identification carried out by the current author (BLAC003) using simulated data generated by the HELISTAB program, sought to compare the 0.5 second "3211" input and a doublet of similar duration. For the regression fits obtained, it was concluded by examination of the residuals (and their auto-correlation functions, where for uncorrelated Guassian residuals it is an impulse function) that the 0.5 second "3211" was the better of the two. This conclusion was also backed up by consideration of the coherency functions of the two inputs, shown in (LEIT001).

Another factor which has to be taken into account, for a given multistep shape, is the amplitude of the signal; increasing the amplitude, for a given clock period, has the effect of scaling the autospectrum. A large-amplitude input will thus also induce an undesirably large response of the helicopter. Some results of an investigation carried out by the current author (BLAC003) into the effect of amplitude and clock

period on estimates of lateral derivatives, using non-linear simulation data generated by HELISTAB, are shown in Figure 1-4. The deteriorating effect of both increasing clock-period and increasing amplitude for "3211" input is demonstrated, where normalised lateral derivative estimates (normalised with respect to the corresponding linear model values) are shown. In reality, of course, very small amplitude inputs will be unrealistic in that they need to be large enough to overcome the dead zone of the control; in addition, a very small response would be overwhelmed by measurement noise.

It is clear from the aforegoing discussion, that in the design of suitable test inputs for helicopter system identification, more consideration than has been given in the past is needed of the factors likely to induce severe non-linearities in the response. Previously, frequency characteristics based on the general shape of the input have been given primary consideration. Recently, however, a procedure for the design of multi- step inputs that are suitable for helicopter system identification, has been developed, which takes into consideration such factors, and some new input types have been designed (LEIT001)

Other Test Inputs Used

In addition to multistep inputs, some other types of test input signals have been used in the past. In

(TISC001) the authors use frequency sweeps (or swept sine waves) in the identification of single-input single-output transfer functions for the XV-15 tilt rotor aircraft; these inputs are cited as ideal because they result in bounded and reasonable excursions of the aircraft, and suitably excite the important rigid-body modes over the entire frequency range of interest.

However it is believed that fatigue problems may arise with frequency-sweep inputs when applied manually through the pilot's controls. With manual inputs it is difficult to limit the magnitude of the perturbation at the resonant frequencies of the aircraft. With an appropriate control input device, these problems can be overcome by limiting the amplitude of the test signal at critical parts of the frequency range.

In the context of time-domain helicopter system identification, the authors in the reference DUVA001 consider a "3211", a doublet, and a low frequency sinusoid as test-input signals. Simulated data representing the Rotor Systems Research Aircraft, with rotor degrees of freedom was used. The simulations included cases with a stability augmentation system (SAS) switched on. It was found that the use of a "3211" and doublet, both of which have significant high frequency components capable of excessive excitation of rotor modes, resulted in considerable SAS activity. (The detrimental effect of the use of stablility augmentation systems on an identification was discussed in Section

1.3.1). In contrast, the sinusoid input provided only low frequency excitation, reducing the SAS activity, which in turn lead to better regression estimates of longitudinal parameters. However, it was also concluded in DUVA001, that in the event that the SAS can be left off for lateral excitation, it may prove more effective to use inputs with higher frequency components (i.e. a "3211").

1.4.2 The Problem of Identifying a Linear Model from Non-Linear Data.

The extent to which the response of a helicopter in flight-test conditions is non-linear is determined, to a large extent, by the test input signal used; this was considered in the last section. A disadvantage of the frequency-domain methodology advocated here, is that it is limited to the identification of small-perturbation models. However, for the state-space formulation assumed for the identification, it is possible in theory to include specific non-linear terms in the model by including non-linear states in an extended control input vector. The state-space model would have the form:

$$\dot{\underset{\sim}{X}}(t) = A\,\underset{\sim}{X}(t) + [B : B^{x}]\begin{bmatrix}\underset{\sim}{U}(t)\\ \underset{\sim}{\delta}^{n}(t)\end{bmatrix} \qquad (1.4\text{-}2)$$

where $\underset{\sim}{\delta}^{n}(t)$ is the non-linear input vector (corresponding to higher-order terms in the Taylor Expansion of the non-linear model); and B^{x} is the

corr esponding partition of the enlarged control dispersion matrix. The use of higher-order aerodynamic terms in time-domain fixed-wing system identification is discussed in KLEI002 using stepwise regression and in ROSS001 for the output-error approach where a formulation of the model identical to that given in Equation (1.4-2) is considered. The inclusion of such non-linear terms in the model will mean an increase in the number of parameters to be estimated. In the case of helicopter system identification, an increase in the number of parameters should be avoided at all costs, and it is thus better to reduce non-linear effects at the outset than to introduce additional complexity into the estimation.

Non linearities corresponding to the known kinematic terms (see Equations 1.3-1) and gravitational effects (known components of the accelerations ax,ay and az given in Equations 1.3-1) could also be included as non-linear inputs (assumed to be noise-free). This would mean that linearisations of the aerodynamic force and moment terms only are considered in the identification.

An investigation was carried out by the current author using non-linear simulation data from the HELISTAB package, in order to gain an appreciation of any difficulties that can be expected in the estimation of a linearised version of a non-linear system. The results are presented in detail in the reference BLAC003. The general conclusions were although the linearised reponse (when added to the trim values) may be very

similar in appearance to the non-linear response, for a given control input, the estimates obtained, using the equation-error approach, can be quite different for some of the weakly-defined parameters. Differences were observed in both sign and order of magnitude.

The time-domain residuals from model-fits when there was a substantial amount of non-linearity were quite deterministic in form. The presence of deterministic unmodelled non-linear effects is effectively the same as having a correlated equation-error term, and as shown in Section 3.2.1, will lead to biased parameter estimates. It was demonstrated in the simulation study, that small non-linear effects have a much more detrimental effect on the estimates of parameters, than a 'larger' amount of white measurement noise on the variables. When estimates obtained either from non-linear simulation studies or from actual flight data are compared with the theoretical HELISTAB linear model values, it should be noted that the HELISTAB values are obtained by numerical differencing of the non-linear model and as such, are dependent on the prescribed perturbation values used in the differencing. The perturbation values used in the linearisation can be varied.

One observation which is encouraging for the identification of small-perturbation models, was that for the longitudinal derivatives considered for the investigation, important derivatives such as the pitching moment derivatives: M_u, M_w, M_q, M_v, M_p, $M_{\Delta_{1s}}$, and the

normal force derivative Zw, gave estimates which were close to the calculated linear model values. A reduction in the amplitude of the control input used, brought about an even closer match between the two sets of values. Estimates of the aforementioned parameters obtained from flight data, using the frequency-domain estimation techniques developed in this document, are presented in Chapters 2 and 3.

Summary of Chapter 1.

The general concept of system identification was discussed for the specific application considered here, namely the identification of quasi-static helicopter models involving fuselage states only. System identification was presented as a means of verifying, and updating, a theoretical helicopter simulation model.

A form of model was proposed for use in the identification which was considered to be more appropriate than those used hitherto for the identification of quasi-static derivatives from real flight-data. For the model, which involves fuselage states only, justification was given for the incorporation and estimation of a time delay in some of the controls as a means of accounting for contaminating rotor-transient effects.

The role of the helicopter flight-mechanics package HELISTAB in the identification methodology as a source of

theoretical values for comparison with those obtained from flight-data, and its facility for the generation of simulated responses corresponding to known models which can be then used to test identification techniques and their software implementations, was pointed out.

Some of the difficulties which are associated with the application of system identification techniques to helicopter flight data were enumerated, and some means of alleviating them were suggested. For example, it is possible to derive very comprehensive and high-order linear models for a helicopter; however, their complexity precludes the use of such models for system identification purposes. It was stated that modifications, such as the use of a subsystem in the identification (e.g. longitudinal motion states only) driven by, in addition to the pilot control, pseudo control terms (e.g. lateral states), could allow the identification problem to be cast in a manageable form for an output-error identification. The removal of rotor states from explicit representation in the model, and the use of time delays to model the influence of rotor-transient effects, represents a simplification to the model which is suggested here.

Some means of checking the flight data, prior to identification, were outlined. The role of an Extended Kalman Filter Procedure in the context of helicopter system identification was discussed, particularly as a means of constructing unmeasured states and removing

noise levels prior to a time-domain identification. It was stated that the frequency-domain approach advocated here, also has the facility to effectively construct unmeasured states, and that the ability to successfully apply the identification techniques using raw flight-data, thus avoiding the complexities of an Extended Kalman Filter, is advantageous.

Finally, the problem of obtaining a response from the helicopter which would facilitate a successful identification, were discussed. These included the need for adequate model excitation in addition to the requirement that the small-perturbation assumptions, underlying the form if model used, were not to be violated. Some commonly used test-input signals were described, and it was argued that more attention should be paid to the undesirable effects on the motion of the helicopter of large amplitude and large clock periods for multistep inputs, such as the commonly used '3211'.

CHAPTER 2

2.0 Some Preliminaries on the use of the Frequency Domain

2.1 Introduction

2.1.1 An Outline of the Previous Use of the Frequency Domain in Aircraft System Identification Work.

Most published accounts of applications of system identification techniques to helicopters have been concerned with time-domain methods using a reduced-order mathematical model representing six degrees-of-freedom rigid-body motion (e.g. MOLU001, HALL001, DUVA001, PADF005). However, interest in the use of the frequency domain for aircraft and helicopter system identification has increased recently as evidenced by published work (e.g. KLEI005, FUKH001, TISC001, BLAC007).

In the reference TISC001, transfer function models are used for the modelling of XV-15 tilt-rotor aircraft dynamics, and the identification in the frequency domain is approached using spectral-analysis techniques which are considered briefly in Section 2.2.1. For the identification work carried out in this document, the problem was formulated in terms of a state-space model with stability and control derivatives explicitly represented; it can be shown that an equivalent state-space representation can also be found for a transfer-function model.

A frequency-domain maximum-likelihood method of

system identification, based on a state-space model representation is developed in KLEI005, with a view to application to aircraft system identification problems. The frequency-domain output-error method developed in this document in Chapter 4 is similar, in many respects to the method developed in KLEI005, in that the same form of cost-function is used, whose frequency-domain residual terms are calculated using a state-space type model. Also, a quasi-Newton method is used in the minimisation of the cost-function in both cases, though some additional useful features for introducing various types of constraints into the identification are available for the software implementation written by the current author. The main differences between the method developed in KLEI005 and the method developed in this document, are asociated with both the form of the frequency-domain state-space model used and the way in which it is represented symbolically.

In FUKH001, the authors apply the frequency-domain output-error method, developed in KLEI005, to some helicopter flight data. A modification term for non-periodic measurement windows, to be included in the state equation, is presented as a means of improving the basic method (this modification term is discussed in Section 2.2.3). The results for the application reported in FUKH001, are presented only in terms of the final frequency-domain fits obtained, without any discussion of the parameter values found. Nevertheless, the work

presented by the authors in FUKH001 (and in a similar paper: MARC002) was very important for the development of the frequency-domain methodology presented in this document. To the knowledge of the current author, no applications of a frequency-domain output-error method to helicopter flight data have been reported, with an accompanying assessment of the estimated stability and control derivatives, other than those given in this document (and by the current author in the referencs BLAC005 and BLAC007).

The authors in the paper FUKH001 advocate an identification methdology which uses both an equation-error and a frequency-domain output-error method, with the former used to provide initial estimates to the latter. A final stage involving a time-domain output-error identification of biases and zero-offsets leading on to a time-domain verification of the identified model is also part of the methodology.

The three identification stages given above also form the basis of the identification methodology developed in this document. However, it is believed that the additional features described in this document relating to model representation, model-structure determination, computer-implementation and the software facilities developed, constitute a significantly improved methodology for helicopter system identification.

2.2 The Use of Frequency-Domain Data.

2.2.1 The Spectral-Analysis Approach.

Some of the early approaches to the extraction of airplane stablility and control parameters were carried out using frequency-domain data, (a brief outline of the earlier work is provided in the reference KLEI005). Frequency-response functions, formulated as rational polynomials of $j\omega$, were estimated by least-square minimisation of the equation-errors, (e.g. MARC001). The frequency-response values for the measured data were obtained through the use of auto and cross spectral densities. The equation-error term can be written as:

$$F_{est}(\omega) - F(\omega) = S_{xy}(\omega)/S_{xx}(\omega) - \frac{\sum N_i (j\omega)^i}{\sum D_k (j\omega)^k} \qquad (2.2\text{-}1)$$

$$F_{est}(\omega) = S_{xy}(\omega)/S_{xx}(\omega) \qquad (2.2\text{-}2)$$

N_i and D_k are the coefficients in the numerator and denominator polynomials, and $Sxx(\omega)$ and $Sxy(\omega)$ are the calculated auto and cross spectral density functions. Windowing techniques can be used to help reduce the errors introduced as a result of using finite-length records - i.e. leakage of power from different frequencies, or smearing (loss of resolution) (e.g. PAPO001, BEND001).

The frequency-response errors are:

$$\Delta F(\omega) = F_{est}(\omega) - F(\omega) \tag{2.2-3}$$

$$\Delta F(\omega) = R_e\,[\Delta F(\omega)] + j\,I_m\,[\Delta F(\omega)] \tag{2.2-4}$$

The least-squares criterion is defined as the minimisation of:

$$J = \sum_{\omega} |\Delta F(\omega)|^2 \tag{2.2-5}$$

Frequency-dependent weights can also be incorporated into the above equation.

The majority of texts, when defining frequency-domain estimation, use approaches like the one outlined above (e.g. BENN001), where there is a requirement for the accurate estimation of power-spectral-density functions. The estimated models are in the form of frequency-response functions, characterised by the identified poles and zeros.

2.2.2 An Alternative Use of Fourier Transforms.

There is an alternative way of using the Fourier Transform, and frequency-domain data, to that given in Section 2.2.1. Fourier's thereom (e.g. PAPO001) states that any periodic function f(t), with period T, consists

of a sequence of impulses, separated from each other in the frequency domain by $\omega_0 = 2\pi/T$. The Fourier-series expansion of f(t) is given by:

$$f(t) = \sum_{n=-\infty}^{\infty} a_n \exp(jn\omega_0 t) \tag{2.2-6}$$

where the coefficients a_n are given by:

$$a_n = 1/T \int_{-T/2}^{T/2} f(t) \exp(-jn\omega_0 t)\, dt \tag{2.2-7}$$

This is a common example of a more general result for expansions using orthogonal functions (e.g. WYLI001), where the length of the interval is T seconds, and defines the fundamental frequency $f_0 = \omega_0/2\pi = 1/T$.

For a periodic function f(t), it can easily be shown that for $\Delta t = T/N$ (e.g. PAPO001):

$$f(m\Delta t) = \sum_{n=0}^{N-1} \bar{a}_n \exp(j2\pi mn/N) \tag{2.2-8}$$

where $\bar{a}_n$ are known as the aliased coefficients, and are related to the a_n in (2.2-6), which is defined in (2.2-7), by

$$\bar{a}_n = \sum_{r=-\infty}^{\infty} a_{n+rN} \tag{2.2-9}$$

The finite Fourier-series expansion is a name often given to Equation (2.2-8). From (2.2-8) we see that determining the Fourier series is reduced to the solution of system

of N equations; this corresponds to the well known result (PAPO001):

$$\bar{a}_n = 1/N \sum_{m=0}^{N-1} f(m\Delta t) \exp(-j2\pi mn/N) \qquad (2.2\text{-}10)$$

Taken together, Equations (2.2-8) and (2.2-10) correspond to the well-known finite Fourier-transform pair.

It is perhaps more enlightening to rewrite (2.2-8) in a form which explicitly includes the frequencies ω_n, defined below.

$$f(m\Delta t) = \sum_{n=0}^{N-1} \bar{a}_n \exp(j\omega_n m\Delta t) \qquad (2.2\text{-}11)$$

$$\omega_n \triangleq n2\pi/N\Delta t \qquad (2.2\text{-}12)$$

<u>Folding Frequency</u>

From Shannon's sampling thereom, the highest frequency which can be uniquely distinguished is given by half the sampling frequency $1/\Delta t$ (e.g. OTNE001); this corresponds to the frequency $\omega_{N/2}$ defined in (2.2-12), and frequencies above this are aliased into a lower value. It can also be shown that:

$$R_e[\bar{a}_r] = R_e[\bar{a}_{N-r}] \qquad (2.2\text{-}13)$$

$$I_m[\bar{a}_r] = -I_m[\bar{a}_{N-r}]$$

Average Value

The $\omega = o$ (i.e. ω_o) value represents the estimated average, or D.C. level, of the data. From (2.2-10) we have:

$$\bar{a}_o = 1/N \sum_{m=o}^{N-1} f(m\Delta t) \qquad (2.2\text{-}14)$$

For the current application, these represent approximate values of the trim levels of the measured variables transformed into the frequency domain; that is, the points about which the small perturbation model is being considered. In addition, constant biases or zero off-sets in the measurements, will manifest themselves in this term. The $\omega = o$ value is excluded from the range of frequencies used in the identification; this reduces the number of parameters that have to be identified using frequency-domain data.

Application of Fourier Transforms to State-Space Model

For a state-space model given by:

$$\dot{\underset{\sim}{X}}(t) = A\underset{\sim}{X}(t) + B\underset{\sim}{U}(t) \qquad (2.2\text{-}15)$$

we can apply the discrete Fourier transformation to obtain a frequency-domain representation of the model:

$$\hat{\dot{\underset{\sim}{X}}}(\omega_n) = A\hat{\underset{\sim}{X}}(\omega_n) + B\hat{\underset{\sim}{U}}(\omega_n) \qquad (2.2\text{-}16)$$

where the notation $\hat{\cdot}$ signifies the transform of a time derivative. The model given in (2.2-16) is defined for discrete values of frequency given by (2.2-12).

The frequency-domain estimation techniques subsequently developed, and used in the work covered in this document, use complex-valued frequency-domain quantities, such as those given in (2.1-16) in the estimation algorithms.

<u>Errors Due to Finite Measurement Window Length and Non-Periodicity</u>

Within the limits of machine accuracy, a set of measured data transformed into the frequency domain using Equation (2.2-10), can be obtained once again in its original time-domain form using Equation (2.2-8) (i.e. inverse Fourier transformation). It can be seen, however, using Equation (2.2-8) and the expressions in (2.2-13), that we could perform some sort of filtering operation by setting to zero those calculated Fourier coefficients which correspond to a particular frequency range. For the removal of frequencies in the range ω_q to $\omega_{N/2}$, we have for the "filtered" signal fq:

$$f_q(m\Delta t) = \sum_{n=0}^{N-1} \bar{a}_n \exp(j2\pi nm/N) - \sum_{q}^{N-q} \bar{a}_n \exp(j2\pi qm/N) \qquad (2.2\text{-}17)$$

By performing an estimation with a restricted frequency range, the effective time-domain response, with which the model is being fitted to in the identification, is given by (2.2-17).

In representing a function in the form of a Fourier-series expansion such as Equation (2.2-6) with an infinite number of terms, or as Equation (2.2-8) for a finite number of terms (with aliased coefficients) it was assumed that the function was periodic. However, in the present context we have to note that helicopter responses are transient, and can be considered to be periodic functions with an infinite period. If the transient response of a state has decayed to a value near zero (assuming the response to be that of a stable system) at the end of the record, then we can consider it to be approximately a periodic function within the measurement window. For the test-input signal, we can ensure that it is zero (i.e. its perturbed value above the trim setting is zero) prior to the application of the input, and at the end of the record; thus it is periodic within the measurement window.

For a finite measurement window, the Fourier series approximation assumes that the function duplicates itself at regular intervals, for all times outside the measurement window (i.e. assumes a periodic function). In order to overcome this problem, we would require records of infinite length for the responses and the test-input signal, corresponding to the limiting case of functions

with infinite period. In reality, we can only use finite-length data records. This is equivalent to multiplying the "true infinite" signal by a box-car function, amounting to a convolution of the true Fourier coefficients with the transform of the box-car function (e.g. BEND001). Moreover, the use of a series representation is an approximation, since an infinite-period function can only be described using a continuous range of frequencies (i.e. an integral expression).

The effect of using a finite window - and by implication the assumption of periodicity in the analysis - is apparent when "filtering" operations, as defined by Equation (2.2-17) are performed. This is shown in Figure 2-1 using real flight-data, where the original signal and the "filtered" signal are superimposed for a test-input signal and some measured responses. Uncharacteristic oscillations are present at the beginning and the end of the "filtered" signals in cases where the original unfiltered signals are not periodic within the measurement window. This corresponds to the discrete equivalent of Gibb's phenomenon (e.g. PAPO001) which occurs in analytical work using continuous Fourier integrals, when a restricted low frequency range is used in describing a piecewise continuous function in the vicinity of a discontinuity: the function begins to oscillate rapidly as the discontinuity is approached from both directions, and the concentration of the ripple increases as the frequency range used increases.

The above effects represent the second main disadvantage of the indicated use of the frequency domain in helicopter system identification: namely, the effective approximation of the response using a Fourier-series representation, whose coefficients are calculated using a finite-length record. (The other disadvantage was the restriction of the technique to small perturbation systems represented by a state-space model with delays).

Hence, for the identification, it is desirable to have - for a stable system - long data records, and periodicity in the measurement window, resulting in a representation more characteristic of the real system. However, as was pointed out in Section 1.3.1, obtaining sufficiently long records, without the use of a stability augmentation system, is a major problem for helicopter system identification.

Least-Squares Sense of Orthogonal-Function Approximation

It is a property of the discrete Fourier-series expansion obtained for a given data set, that it represents uniquely the "best" - in the least-squares sense - trigonometric (and hence periodic) approximation for a specified order (ISAA001). The maximum order is determined by the number of data points available, and all other orders of approximation, which are also best in the least-squares sense, correspond to Equation (2.2-17).

This is a consequence of the well known, and more general result for orthogonal series approximations, whereby increasing the order of the approximation does not require the re-calculation of any coefficients, only the inclusion of an additional term. Hence, for the use of a given data set in an identification, carried out over a stipulated frequency-range, the effective time-domain response, to which the model is being fitted, is the "best" periodic approximation in the least-squares sense.

(NAG) Library Routines Used to Obtain Fast Fourier Transforms

The identification software developed by the current author, uses the NAG (FFT) routine C06FAF (NAG001) to obtain the discrete transforms. The Fourier-transform pair so defined are similar to (2.2-8) and (2.2-10) except for multiplicative factor of $1/\sqrt{N}$; they are:

$$f(m\Delta t) = 1/\sqrt{N} \sum_{n=0}^{N-1} a_n \exp(j2\pi mn/N) \quad m = 0,1 \ldots N-1 \quad (2.2\text{-}18)$$

$$a_n = 1/\sqrt{N} \sum_{m=0}^{N-1} f(m\Delta t) \exp(-j2\pi mn/N) \quad n = 0,1 \ldots N-1 \quad (2.2\text{-}19)$$

Equivalence of Time and Frequency-Domain Approaches

Using all the available frequency-domain points in an identification is equivalent to using the original

time- domain sequence. The cost functions which are minimised for the identification techniques (i.e. equation error or output error) can be represented as functions involving sums of squares. Parseval's theorem (PAP0001) states that the following relationship exists between the squared frequency-domain and squared time-domain quantities (it is written in terms of the fourier transform pairs defined in 2.2-8 and 2.2-10):

$$\sum_{n=0}^{N-1} |\bar{a}_n|^2 = 1/N \sum_{m=0}^{N-1} |f(m\Delta t)|^2 \qquad (2.2\text{-}20)$$

The equivalence between the time and frequency domain approaches no longer holds if a restricted frequency range is used. This is, however, one advantage in using the frequency-domain: the frequency range over which the cost function is minimised can be varied as required, within the estimation algorithm, and there is only the requirement for the storage of the original data set. Time-domain estimation for a variety of different frequency ranges would require the production and storage of at least one additional data set.

Some Further Advantages of Using the Frequency Domain

The ease with which the frequency range used in the identification can be restricted was cited above as one

advantage in using the frequency-domain; this is particularly advantageous for helicopter system identification when models for rigid-body dynamics, valid for low frequencies, are to be obtained. The exclusion of high frequencies, representing unmodelled effects, is also beneficial from the point of view of data reduction.

Another advantage is that transformation of the model equations into the frequency-domain has some important implications for the estimation algorithms themselves: operations in the time-domain such as differentiation are replaced by multiplication; and equations, which in the time domain require numerical integrations over the entire time record for each iteration (such as the equations for the partial derivatives of the cost function with respect to the unknown parameters), are replaced by expressions which can be solved by algebraic manipulation. This is brought out in Section 4.2.2, where the expressions are developed.

In addition, by formulating the estimation problem in the frequency-domain, it is easy to include time delays in the set of parameters to be estimated; this is also brought out in Section 4.2.2.

2.2.3 An Expression for the Discrete Fourier Transform of a Time Derivative

From the state-space model given in Equation

(2.2-15), we can write the equation shown in (2.2-21) involving the finite Fourier integral, for an interval of T seconds. The reason for displacing the integration limits from their usual values by half a sampling increment, will be indicated shortly

$$\int_{-\frac{\Delta t}{2}}^{T-\frac{\Delta t}{2}} \dot{\underset{\sim}{X}}(t)\exp(-j\omega t)\,dt = A\int_{-\frac{\Delta t}{2}}^{T-\frac{\Delta t}{2}} \underset{\sim}{X}(t)\exp(-j\omega t)\,dt + B\int_{-\frac{\Delta t}{2}}^{T-\frac{\Delta t}{2}} \underset{\sim}{U}(t)\exp(-j\omega t)\,dt \qquad (2.2\text{-}21)$$

The integral expressions in Equation (2.2-21) are known as finite Fourier integrals (BEND001), and can be defined for a continuous range of frequency values ω.

By integrating the left-hand side of Equation (2.2-21) by parts we can obtain an expression for the finite Fourier integral of a quantity differentiated with respect to time, in terms of the integral of the original quantity. For periodic functions, the result is well known. In the references FUKH001 and MARC002, the authors present an expression for the discrete Fourier transform of a quantity that is differentiated with respect to time which involves both the discrete Fourier transform of the original quantity and some additional points not used in the transformation. An important feature of the result is that it does not assume the measurement data window to be periodic (which is the usual case for helicopter flight data).

The justification for the non-periodic measurement -

window result given in the references FUKH001 and MARC002 relies on using an approximation between a discrete Fourier transform and a Fourier integral defined between the limits $(-\Delta t/2, T-\Delta t/2)$ as its starting point. No mention is made of the numerical integration technique implied in making the approximation (given in 2.2-24), or why the integration limits are so defined. A justification for the approximation, which is the starting point of the derivation, will be provided by the current author in due course. Firstly, however, let us consider the derivation of the result itself. For the discrete Fourier transform defined by (2.2-10) we have:

$$\hat{\dot{X}}(\omega_n) = 1/N \sum_{m=0}^{N-1} \dot{X}(m\Delta t) \exp(-j\omega_n m\Delta t) \qquad (2.2\text{-}22)$$

we will write:

$$\hat{X}(\omega_n) = 1/T \int_{-\frac{\Delta t}{2}}^{T-\frac{\Delta t}{2}} X(t) \exp(-j\omega_n t)\, dt \qquad (2.2\text{-}23)$$

and similarly we can write:

$$\hat{\dot{X}}(\omega_n) = 1/T \int_{-\frac{\Delta t}{2}}^{T-\frac{\Delta t}{2}} \dot{X}(t) \exp(-j\omega_n t)\, dt \qquad (2.2\text{-}24)$$

Integrating the right-hand side of (2.2-24) by parts, and using the fact that we are considering only discrete values of frequency: ω_n, (defined in 2.2-12) we thus have:

$$\hat{\dot{X}}(\omega_n) = j\omega_n \hat{X}(\omega_n) + \Delta X e^{\frac{j\omega_n \Delta t}{2}} \qquad (2.2\text{-}25)$$

$$\Delta X \triangleq [X(T-\Delta t/2) - X(-\Delta t/2)]/T \qquad (2.2\text{-}26)$$

Taken together, (2.2-25) and (2.2-26) represent the result for the transform of a quantity which is differentiated with respect to time, where the measurement window is non-periodic (i.e. $X(T-\Delta t/2)$ $X(-\Delta t/2)$).

Returning now to equations (2.2-23) and (2.2-24), which represent the starting point of the derivation, and which were not justified in the original references; if the Fourier integrals are closely approximated by the discrete Fourier transforms as shown, then the frequency-domain model representation given in (2.2-21) is equivalent to the discrete formulation given in (2.2-16). Now for the mid-point quadrature method (e.g. ISAA001), it turns out that the appropriate formula for a Fourier integral is the same as the discrete Fourier transform summation. Hence equation (2.2-23) strictly speaking, represents an approximation to the integral on the right-hand side, using the mid-point method. The interval of integration is defined as $(-\Delta t/2, T-\Delta t/2)$ to enable the mid-point values to coincide with the discrete measured values at times $t=0, \Delta t, 2\Delta t....N-1\Delta t$, for an interval of length $T=N\Delta t$ seconds. This idea is illustrated in Figure 2.2.

The rectangular method for the numerical evaluation

of the integrals on both sides of the equation (2.2-21) is less accurate than the midpoint method. However, the trapeziodal method is of comparable accuracy to the mid-point method, and it can be formulated so that the interval of integration is (O,T). It can be shown easily (e.g. ISAA001) that for an integral of time-span T, that the errors incurred are proportional to Δt^2 for both methods. However, the quadrature formula for the evaluation of a Fourier integral using the trapeziodal method no longer coincides with the discrete Fourier transform summation, but would require an additional correction term ($\Delta t/2\ (X(N) - X(O))$) to be written on the left-hand side of (2.2-23). Hence the result given in (2.2-25) and (2.2-26) is justified using mid-point integration to evaluate the Fourier integral defined over the interval $(-\Delta t/2,\ T-\Delta t/2)$.

The result given in (2.2-25) and (2.2-26) immediately extends to vector quantities. The model representation given in (2.2-16) for discrete Fourier-transformed quantities can be re-written as:

$$j\omega_n \hat{\underset{\sim}{X}}(\omega_n) = A\hat{\underset{\sim}{X}}(\omega_n) + B\hat{\underset{\sim}{U}}(\omega_n) - \hat{\underset{\sim}{G}}(\omega_n) \qquad (2.2\text{-}27)$$

where $\hat{\underset{\sim}{G}}(\omega_n)$ is the correction term given in (2.2-25) and (2.2-26).

$$\hat{\underset{\sim}{G}}(\omega_n) \triangleq \left[\underset{\sim}{X}(T-\tfrac{\Delta t}{2}) - \underset{\sim}{X}(-\tfrac{\Delta t}{2})\right] e^{\frac{j\omega_n \Delta t}{2}} / T = \qquad (2.2\text{-}28)$$

$$\Delta \underset{\sim}{X}\, e^{\frac{j\omega_n \Delta t}{2}}$$

It can be seen that the term $e^{\frac{j\omega_n \Delta t}{2}}$ could be considered to be a frequency-domain control, with the vector $\Delta \underset{\sim}{X}$ incorporated as an additional column of the control dispersion matrix B. Thus, $\Delta \underset{\sim}{X}$ could be estimated as an unknown set of parameters. The authors in the original references cited earlier advocated the use of a linear interpolation scheme, based on the use of measured values not included in the transformation. To avoid the requirement for the estimation of additional parameters, the same approach was used here. The approximate formulation given in (2.2-29) is thus used for $\Delta \underset{\sim}{X}$:

$$\Delta \underset{\sim}{X} \doteq \left[\underset{\sim}{X}(N-1\,\Delta t) + \underset{\sim}{X}(N\Delta t) - \underset{\sim}{X}(-\Delta t) - \underset{\sim}{X}(0) \right] / 2T \tag{2.2-29}$$

where $\underset{\sim}{X}(N\Delta t)$ and $\underset{\sim}{X}(-\Delta t)$ are the two additional points not used in the original transformation.

<u>Formulation of the Modification Term</u>

Using the discrete Fourier transform pair defined in equations (2.2-18) and (2.2-19) for the NAG mathematical library, it immediately follows that the appropriate formulation of the correction term for software implementation, differs from (2.2-29) by a factor of $\sqrt{N}$.

$$\Delta \underset{\sim}{X}_{NAG} \doteq \sqrt{N} \left[\underset{\sim}{X}(N-1\,\Delta t) + \underset{\sim}{X}(N\Delta t) - \underset{\sim}{X}(-\Delta t) - \underset{\sim}{X}(0) \right] / 2T \tag{2.2-30}$$

This form of the modification term is therefore used in

all subsequent work.

2.2.4 A Frequency-Domain Representation of the Model

A Frequency-Domain Representation of the State Equation

By equating the real and imaginary parts of both sides of the frequency-domain state equation given in (2.2-27), we can write the frequency-domain representation of the state equation in detail (after rearrangement) as:

$$\begin{pmatrix} -A & -\omega I \\ \omega I & -A \end{pmatrix} \begin{pmatrix} \mathrm{Re}\,[\hat{\underset{\sim}{X}}(\omega)] \\ \mathrm{Im}\,[\hat{\underset{\sim}{X}}(\omega)] \end{pmatrix} = \begin{pmatrix} B & 0 \\ 0 & B \end{pmatrix} \begin{pmatrix} \mathrm{Re}\,[\hat{\underset{\sim}{U}}(\omega)] \\ \mathrm{Im}\,[\hat{\underset{\sim}{U}}(\omega)] \end{pmatrix}$$

$$-\sqrt{N}/T \begin{pmatrix} \Delta \underset{\sim}{X} \cos \omega \Delta t/2 \\ \Delta \underset{\sim}{X} \sin \omega \Delta t/2 \end{pmatrix} \qquad (2.2\text{-}31)$$

Given the state matrix A, the control dispersion matrix B, the known transforms of the inputs: $\hat{\underset{\sim}{U}}(\omega)$, and the modification term for non-periodic measurement windows (last term on the right-hand side), the above linear matrix equation can be solved at each of the stipulated (discrete) frequency values to obtain the frequency-domain state-equation vector:

$$\begin{pmatrix} \mathrm{Re}\,[\hat{\underset{\sim}{X}}(\omega)] \\ \mathrm{Im}\,[\hat{\underset{\sim}{X}}(\omega)] \end{pmatrix}$$

A Frequency-Domain Representation of the Measurement System

As has already been stated, the frequency-domain approach is basically limited to linear models, though some non- linearities - notably time delays, can be incorporated. This is because practical difficulties are encountered in applying linear transformations, such as the Fourier transform, to equations which are generally non-linear. Because the measured quantities and states in the model, are in general, non-linearly related, there is a requirement for some linearisations to be carried out. The point about which the linearisation is carried out corresponds to the aircraft trim state. The fact that the measurement devices may be displaced relative to the centre of gravity, has to be taken into consideration in this context. Consider for example, the measurements of speed, flank angle, and incidence angle (V_m, β_m, α_m). These quantities are related to the states (u,v,w,p,q,r) in the model by the following set of non-linear equations:

$$V_m = [(u+U_e+ql_z^v-rl_y^v)^2+(v+V_e+rl_x^v-pl_z^v)^2 + (w+W_e+pl_y^v-ql_x^v)^2]^{1/2}$$

$$\beta_m = \tan^{-1}[(v+V_e+rl_x^\beta-pl_z^\beta)/(u+U_e+ql_z^\beta-rl_y^\beta)] \quad (2.2\text{-}32)$$

$$\alpha_m = \tan^{-1}[(w+W_e+pl_y^\alpha-ql_x^\alpha)/(u+U_e+ql_z^\beta-rl_y^\beta)]$$

where $l_x^v, l_y^v, l_z^v, l_x^\beta, l_y^\beta, l_z^\beta, l_x^\alpha, l_y^\alpha, l_z^\alpha$ are the offsets from the centre of gravity of the speed, flank and incidence measurement devices respectively, and where U_e, V_e,

We represent the trim values of the velocity components in the body-fixed axes along the X, Y, Z directions respectively

The (time-domain) linearised measurement equations, obtained using a first-order Taylor expansion about the trim, are as follows for a typical set of flight measurements, where measurement bias terms: (b_v, b_β, b_α, b_q, b_θ, b_p, b_ϕ, b_r), and measurement noise terms (n_v, n_β, n_α, n_q, n_θ, n_p, n_ϕ, n_r), are included.

$$
\begin{bmatrix} V_m \\ \beta_m \\ \alpha_m \\ q_m \\ \theta_m \\ p_m \\ \phi_m \\ r_m \end{bmatrix}
=
\begin{bmatrix}
1 & 0 & l_z^v & 0 & 0 & 0 & 0 & -l_y^v \\
0 & 0 & 0 & 0 & 1/U_e & -l_z^\beta/U_e & 0 & l_y^\beta/U_e \\
0 & 1/U_e & -l_x^\alpha/U_e & 0 & 0 & l_y^\alpha/U_e & 0 & 0 \\
0 & 0 & 1 & 0 & 0 & 0 & 0 & 0 \\
0 & 0 & 0 & 1 & 0 & 0 & 0 & 0 \\
0 & 0 & 0 & 0 & 0 & 1 & 0 & 0 \\
0 & 0 & 0 & 0 & 0 & 0 & 1 & 0 \\
0 & 0 & 0 & 0 & 0 & 0 & 0 & 1
\end{bmatrix}
\begin{bmatrix} u \\ w \\ q \\ \theta \\ v \\ p \\ \phi \\ r \end{bmatrix}
+
\begin{bmatrix} U_e + b_v \\ V_e/U_e + b_\beta \\ W_e/U_e + b_\alpha \\ b_q \\ \theta_e + b_\theta \\ b_p \\ \phi_e + b_\phi \\ b_r \end{bmatrix}
+
\begin{bmatrix} n_v \\ n_\beta \\ n_\alpha \\ n_q \\ n_\theta \\ n_p \\ n_\phi \\ n_r \end{bmatrix}
\qquad (2.2\text{-}33)
$$

It should be pointed out that the vector, corresponding to the second-last term on the right-hand side of equation (2.2-33) includes constant terms that arise from the linearisation (i.e. trim constants); these terms add to any constant measurement biases present, and it is only the resultant sum which can be identified. The resultant sum is referred to in this document as a zero-offset. By excluding $\omega=0$ from the range of frequencies used, the zero-offset vector is uncoupled from the frequency-domain identification, and can be identified at a later stage in the time-domain; this is explained in detail in chapter 5.

Measurement scale factors can also be incorporated into (2.2-33) by multiplying the left-hand side by a diagonal matrix consisting of these quantities; a change of measurement units could also be represented here. Additional measurement sets could also be used to obtain quantities in the state equation: for example, the accelerations a_x, a_y, a_z could be used to obtain u, v, w. In general, the number of measured variables and states need not be equal.

The time-domain measurement system can be written in vector form as:

$$\underset{\sim}{Z}(t) = H\underset{\sim}{X}(t) + \underset{\sim}{K} + \underset{\sim}{b} + \underset{\sim}{V}(t) \qquad (2.2\text{-}34)$$

where $\underset{\sim}{K}$ is a vector of trim constants, $\underset{\sim}{b}$ is a constant vector of measurement biases, and $\underset{\sim}{V}(t)$ is the measurement

noise. We can consider the measurement scale-factors to have been incorporated into the H matrix.

Transforming (2.2-34) into the frequency domain, and excluding $\omega = 0$ from the allowable discrete values of frequency, we have:

$$\hat{\underset{\sim}{Z}}(\omega) = H\,\hat{\underset{\sim}{X}}(\omega) + \hat{\underset{\sim}{V}}(\omega) \quad ; \quad \omega \neq 0 \tag{2.2-35}$$

The set of unknown parameters for which estimates can be sought, can be extended to include elements of the measurement transition matrix H. The measurement system can be written as:

$$\begin{pmatrix} R_e[\hat{\underset{\sim}{Z}}(\omega)] \\ I_m[\hat{\underset{\sim}{Z}}(\omega)] \end{pmatrix} = \begin{pmatrix} H & 0 \\ 0 & H \end{pmatrix} \begin{pmatrix} R_e[\hat{\underset{\sim}{X}}(\omega)] \\ I_m[\hat{\underset{\sim}{X}}(\omega)] \end{pmatrix} + \begin{pmatrix} R_e[\hat{\underset{\sim}{V}}(\omega)] \\ I_m[\hat{\underset{\sim}{V}}(\omega)] \end{pmatrix} \tag{2.2-36}$$

<u>Representation of the Full Model</u>

We now have the following system of equations representing the full model in the frequency-domain:

$$\hat{\dot{\underset{\sim}{X}}}(\omega) = A\,\hat{\underset{\sim}{X}}(\omega) + B\,\hat{\underset{\sim}{U}}(\omega) \tag{2.2-37}$$

$$\hat{\underset{\sim}{Z}}(\omega) = H\,\hat{\underset{\sim}{X}}(\omega) + \hat{\underset{\sim}{V}}(\omega) \tag{2.2-38}$$

where we have

$$\hat{\dot{\underset{\sim}{X}}}(\omega) = j\omega \hat{\underset{\sim}{X}}(\omega) + \hat{\underset{\sim}{G}}(\omega)$$
$$\omega = K2\pi/N\Delta t \quad , \quad K = 1,2,3 \ldots N/2 \qquad (2.2\text{-}39)$$

If there are any unmodelled effects present in the real system, then an additional process noise term can be included in equation (2.2-37); more consideration is given to this matter in sections 4.2.1 and 4.2.5.

<u>The Use of Measurement Data to Obtain the Modification Term</u>

It was explained in Section 2.2.3 that the modification term for the discrete Fourier transform of a quantity which is differentiated with respect to time can be written in the form $\Delta \underset{\sim}{X}_{NAG} e^{\frac{j\omega\Delta t}{2}}$. The originators of this expression in the references (FUKH001, MARC002) suggested that $\Delta \underset{\sim}{X}$ be obtained formally by interpolation, using values of the state vector as in 2.2-29 (or 2.2-30 for NAG FFT'S). However, $\underset{\sim}{X}$ is not directly measured, and the approach used by the current author is to solve the following set of linear equations for $\Delta \underset{\sim}{X}_{NAG}$ given the analogous expression $\Delta \underset{\sim}{Z}_{NAG}$ obtained from the measurements and a measurement transition matrix H.

$$\Delta \underset{\sim}{Z}_{NAG} = H \, \Delta \underset{\sim}{X}_{NAG} \qquad (2.2\text{-}40)$$

$$\Delta \underset{\sim}{Z}_{NAG} \triangleq \sqrt{N}\,[\underset{\sim}{Z}(N-1\Delta t) + \underset{\sim}{Z}(N\Delta t) - \underset{\sim}{Z}(-\Delta t) - Z(0)]\,/\,2T$$

(2.2-41)

Equation (2.2-40) follows from (2.2-34). It should also be pointed out that for the computer implementation of the frequency-domain output-error method developed by the current author, the most up-to-date estimate of H, for the iterative procedure, is used to solve equation (2.2-40).

2.2.5 The Modelling of Noise in the Frequency Domain

In equation (2.2-34) the measurement system is modelled with additive noise terms associated with the measured response variables; these are represented in the time domain as $\underset{\sim}{V}(t)$. When transformed into the frequency domain this term is represented as $\hat{\underset{\sim}{V}}(\omega)$, as in equation (2.2-38).

A recent paper (SCH0001) analysed the noise influence on the Fourier coefficients obtained from a discrete Fourier transform. For a given quantity subject to a random noise source the following equation was derived, where a_{im} represents a Fourier coefficient of the measured quantity subject to random noisé source in the time domain with mean μ, and a_i represents the true value of the corresponding Fourier coefficient:

$$E[a_{i_m}] = a_i + \mu \sum_{K=0}^{N-1} e^{\frac{-j2\pi Ki}{N}} \qquad (2.2\text{-}42)$$

This shows that the expected values of the Fourier coefficients go to the exact values, except for the zero frequency component which is subject to a systematic error. It is also shown in SCHO001 that the discrete Fourier transform of an uncorrelated Gaussian white noise variable in the time domain produces an uncorrelated Gaussian random variable in the frequency domain; in addition, if the original noise source is not uncorrelated-Gaussian in the time domain, then through the central-limit theorem of statistics (e.g. MOOD001) it tends to an uncorrelated Gaussian distribution as the sample size N tends to infinity. In the paper: SCHO001 it is concluded that:

"the distribution of the discrete Fourier transform components of additive noise is Gaussian regardless of the distribution of the noise".

However, if this conclusion is accepted superficially, then it could lead to some misleading conclusions about the likely benefits gained, as a result of transforming the data into the frequency domain, for estimation purposes. An important point to appreciate is that the uncorrelated Gaussian nature is asymptotic - i.e. tending to, but never reaching - for a large sample size N. For a finite sample, a correlated time-domain source will thus be transformed into a frequency-domain variable which is correlated, or whose expected value is

non-zero, over at least some of the frequency values. As will be shown in Section 3.2.1 for the frequency-domain equation-error method (and in Appendix 2 for the frequency-domain output-error method) this leads to biased parameter estimates, if over the frequency range selected (assuming it is appropriate for the model) the expected value of the noise is not zero.

The implications of the above for the practical implementation of the frequency-domain identification techniques is that for the stipulated frequency range used in the estimation, the frequency-domain noise terms should be closely modelled as uncorrelated Gaussian variables, with a zero mean, whose expected mean-square value is a constant, independent of frequency (i.e. white noise - GELB001): this is an assumption on which the frequency-domain estimation techniques are based.

An advantage of working in the frequency domain, is that the analyst has available transformed residuals with which the validity of the bandlimited white noise assumption can be readily examined, and the extent to which the whiteness assumption is true, appreciated. If the band limit of the white noise lies within the range of frequencies used in the estimation, then the noise will have been modelled incorrectly. This error was first appreciated in the context of time-domain aircraft parameter estimation (MAIN001), where it was observed that the calculated Cramer-Rao error bounds on parameter estimates turned out to be smaller than the observed

scatter of results. The explanation for this discrepancy went undetected for some time (some analysts used 10σ error bounds to increase the range of uncertainty to match the scatter of results) until it was observed by the authors in the reference MAIN001, that the assumption of the band limit being equal to the Nyquist folding Frequency ($1/2\Delta t$ Hz) was implicit, and had passed unnoticed in the theoretical derivation of the maximum likelihood method and in obtaining the errors bounds as the inverse of the information matrix. For time-domain estimation, a solution to the problem was shown in MAIN001 to be given by multiplying the estimated error bounds by $\sqrt{1/2\, B_w \Delta t}$, where B_w is the approximate bandwidth (in Hertz). This correction requires an estimate of B_w to be made.

Equidistribution of Power in a Transformed Variable

There is an equidistribution of power between the real and imaginary parts of the transform of an uncorrelated stationary random variable. Consider the element $V_i(K)$ of the random real-valued vector $\underset{\sim}{V}(L)$ which is transformed into the frequency-domain. It is assumed that the covariance matrix $E[\underset{\sim}{V}(K)^T \underset{\sim}{V}(K)]$ is diagonal (i.e. no correlation between measurement channels, if the vector $\underset{\sim}{V}(K)$ is measurement noise). For the diagonal elements we have (using the definition of the discrete Fourier transform given by 2.2-19):

$$E[R_e[\hat{V}_i(K)]^2] = E[\,1/\sqrt{N}\sum_{L=0}^{N-1} V_i(L)\cos 2\pi KL/N \cdot 1/\sqrt{N}\sum_{J=0}^{N-1} V_i(J)\cos 2\pi KJ/N]$$

$$= 1/N \sum_{J=0}^{N-1} E[V_i(J)]^2 \cos^2 2\pi KJ/N]$$

$$= \sigma_N^2/N \sum_{J=0}^{N-1} \cos^2 2\pi KJ/N = \sigma_N^2/N \cdot N/2$$

$$= \sigma_N^2/2 \qquad (2.2\text{-}43)$$

where $E[V_i(p)V_i(q)] = \sigma_N^2 \quad p=q$

$= 0 \quad p \neq q$

Hence $E[R_e[\hat{V}_i(K)]^2] = \sigma_N^2/2$; similarly it can be shown that $E[I_m[\hat{V}_i(K)]^2] = \sigma_N^2/2$, and $E[R_e[\hat{V}_i(K)]I_m[\hat{V}_i(K)]] = 0$

This equidistribution of power between the real and imaginary parts is of consequence to the calculation of the frequency-domain error-covariance matrix discussed in Section 4.2.2.

2.3 The Inclusion of Time Delays in the Model

2.3.1 Representation of Delays in the Model

The result for the Fourier transform of a time-shifted quantity in terms of the transform of an unshifted quantity is well known (e.g. BEND001):

$$F[X(t+\tau)] = F[X(t)] \cdot \exp(\tau\omega j) \qquad (2.3\text{-}1)$$

where F[] is the Fourier transform operator, and τ is the

time delay in seconds. This result is easily derivable for the classical Fourier transform, defined in terms of an integral between infinite limits:

$$F[X(t+\tau)] \triangleq \int_{-\infty}^{\infty} X(t+\tau)e^{-j\omega t}dt = e^{\tau\omega j}\int_{-\infty}^{\infty} X(t)e^{-j\omega t}dt \qquad (2.3\text{-}2)$$

However, as was shown in the case of the transform of a time derivative, results from classical analysis may need some modification when the discrete Fourier transform (defined for a finite range of data) is used. The following justification for using the same type of result when the discrete Fourier transform is used, as that given by (2.3-1), is proposed by the current author. It makes use of the result given by (2.2-25) and (2.2-26) for the transform of a quantity which is differentiated with respect to time, developed by the authors in the references (FUKH001, MARC002). For a Taylor expansion of $X(i\Delta t+\tau)$ we have:

$$X(i\Delta t+\tau) = X(i\Delta t) + \dot{X}(i\Delta t)\tau + \ddot{X}(i\Delta t)\tau^2/2! + \dddot{X}(i\Delta t)\tau^3/3! + \ldots \qquad (2.3\text{-}3)$$

Using the definition of the discrete Fourier transform, and (2.3-3) we have that:

$$1/N\sum_{i=0}^{N-1} X(i\Delta t+\tau)e^{-j\omega_n i\Delta t} = 1/N\left\{\sum_{i=0}^{N-1} X(i\Delta t)e^{-j\omega_n i\Delta t} + \tau\sum_{i=0}^{N-1}\dot{X}(i\Delta t)e^{-j\omega_n i\Delta t} + \tau^2/2!\sum_{i=0}^{N-1}\ddot{X}(i\Delta t)e^{-j\omega_n i\Delta t} + \tau^3/3!\sum_{i=0}^{N-1}\dddot{X}(i\Delta t)e^{-j\omega_n i\Delta t} + \ldots\right\} \qquad (2.3\text{-}4)$$

From (2.2-25) and (2.2-26) we have the result for $\hat{\dot{X}}(\omega_n)$, and by repeated application for $\hat{\ddot{X}}(\omega_n)$, etc. we have:

$$\hat{\ddot{X}}(\omega_n) = j^2\omega_n^2\,\hat{X}(\omega_n) + j\omega_n\,\hat{G}(\omega_n) + \hat{\dot{G}}(\omega_n) \qquad (2.3\text{-}5)$$

where $\hat{\ddot{X}}(\omega_n)$ is the discrete Fourier transform of the second time derivative of $X(t)$, and $\hat{\dot{G}}(\omega_n)$ is analogous to $\hat{G}(\omega_n)$ given by (2.2-8) but evaluated at the corresponding time derivatives. Hence we may write the right-hand side of (2.3-4) as:

$$\hat{X}(\omega_n) + \tau\left(j\omega_n\,\hat{X}(\omega_n) + \hat{G}(\omega_n)\right) + \tau^2/2!\left(j^2\omega_n^2\,\hat{X}(\omega_n) + j\omega_n\,\hat{G}(\omega_n) + \hat{\dot{G}}(\omega_n)\right) + \dots =$$

$$\left(1 + \tau j\omega_n + \tau^2 j^2\omega_n^2/2! + \dots\right)\hat{X}(\omega_n) + \left(\tau + \tau^2 j\omega_n/2! + \dots\right)\hat{G}(\omega_n) + \left(\tau^2/2! + \dots\right)\hat{\dot{G}}(\omega_n) + O(\tau^3)$$

(2.3-6)

Hence we have that

$$1/N\sum_{i=0}^{N-1} X(i\Delta t+\tau)\,e^{-j\omega_n i\Delta t} = e^{\tau\omega_n}\cdot 1/N\sum_{i=0}^{N-1} X(i\Delta t)\,e^{-j\omega_n i\Delta t} + \hat{G}_\tau(\omega_n)$$

(2.3-7)

where $\hat{G}_\tau(\omega_n)$ is a complex (both in form and in value) modification term. In the application of the time delay to a control, it is reasonable to assume that the (perturbed) control state is zero (corresponding to the trim position) prior to the application of a test input

signal, and is zero at the end of a time record corresponding to the free response, in both cases for a time span of length at least τ seconds: hence the signal is periodic and $\hat{G}_\tau(\omega_n)$ is zero since all the higher derivatives are zero. For time delays in the controls (and for the test input signals used in practice) and for delays in other quantities periodic in the measurement window, we can use the result given by (2.3-7), with the modification term $\hat{G}_\tau(\omega_n)$ set equal to zero.

Changes to the Model Equations

By formulating the estimation problem in the frequency domain, the inclusion of time delays (in the controls $\underset{\sim}{U}$ and measurements $\underset{\sim}{Z}$) results in a relatively simple modification to the frequency-domain state equations given by (2.2-37) and (2.2-38). Additional diagonal matrices of the form:

$$D_{\iota K}(\omega_n) \triangleq e^{-\tau_\iota \omega_n j} = \cos(\tau_\iota \omega_n) - j \sin(\tau_\iota \omega_n) \; ; \; \iota = K$$

$$D_{\iota K}(\omega_n) = 0 \; ; \; \iota \neq K \qquad (2.3\text{-}8)$$

are required to premultiply the corresponding vectors. Using $B_2(\omega)$ and $H_2(\omega)$ as the diagonal matrices of delays for the controls and measured responses respectively, the frequency-domain model representation becomes:

$$\hat{\dot{\underset{\sim}{X}}}(\omega) = A \hat{\underset{\sim}{X}}(\omega) + B \cdot B_2(\omega) \hat{\underset{\sim}{U}}(\omega) \qquad (2.3\text{-}9)$$

$$H_2(\omega)\,\hat{\underset{\sim}{Z}}(\omega) = H\,\hat{\underset{\sim}{X}}(\omega) + \hat{\underset{\sim}{V}}(\omega) \qquad (2.3\text{-}10)$$

with $\hat{\dot{X}}(\omega)$, and the discrete values of ω used, defined by (2.2-39). The implementation of the estimation algorithm, with time delays in the model, is explained in detail in Section 4.2.2.

Incorporating Delays into the Modification Term

For the inclusion of time delays in the measurement system, the term $\Delta\underset{\sim}{Z}$ (occurring in equation (2.2-40) and used to obtain $\Delta\underset{\sim}{X}$ for the modification term for a non-periodic measurement window) must incorporate the current values of the time delays in $\underset{\sim}{Z}$. Linear interpolation is used in estimating $\Delta\underset{\sim}{X}$, and there is a requirement for the storage of a small portion of time-history data immediately before and after the transformed portion, in order to accommodate time delays in the modification term. For control terms which are time derivatives and have time delays, linear interpolation is also used in obtaining the appropriate modification term.

Some Further Remarks Regarding the Incorporation of Delays in the Model

Some justification for the use of a time delay in a control in order to more correctly model higher-order

rotor transient effects on the rigid-body model was presented in Section 1.2.5. This potentially useful innovation for helicopter system identification is demonstrated using simulated data in Section 2.3.2, and using real flight data in Section 2.3.3 (as well as in the results presented in various sections of Chapter 4). The incorporation of time delays into the estimation problem is facilitated by the frequency-domain formulation used.

An interpretation of the time delays on the control input vector $\underset{\sim}{U}(t)$ has been given. Time delays, or relative phase shifts, may also be identified for the measured observations $-\underset{\sim}{Z}(t)$; these may be introduced by pre- filtering procedures carried out on the raw flight-data, prior to the estimation. In addition, time shifts can be introduced into the measured observations as a result of the data sampling interval: for a sample interval of Δt seconds, the sampled value of one quantity can be separated by up to Δt seconds from the sample of another quantity in the same time frame.

As was pointed out in Section 1.3.1, there may be some dynamic lags associated with some of the measurement instrumentation; it was pointed out that under certain conditions these could be adequately modelled using time delays.

It is important to bear in mind the point made at the end of Section 1.2.5, that a component of the identified delay associated with a control term may be

due to the transmission of the signal from the pilot's control to the control surface (i.e. the main-rotor disc or the tail-rotor disc): for the purpose of identification the two components cannot be distinguished separately.

The sensitivity of the maximum-likelihood estimator to small time, or phase, shifts has been noted by some authors (e.g. IL1F001); in this reference the author presents a case from an aircraft parameter-estimation problem carried out in the time-domain, where a positive time shift of 0.1 seconds in an aileron control-surface time history resulted in almost a 50% error in the estimated value of the roll-rate to side-slip stability derivative. There was, however, no facility, for the identification of delays in the example presented in the reference.

2.3.2 Effect of Sampling Interval on Estimates of the Delay

A linearised model representing the coupled fuselage and rotor states was given by equations (1.2-5) and (1.2-6) in Section 1.2.4. The quasi-static model, which assumes that rotor-dynamics can be neglected, was also discussed in Section 1.2.4; in this type of model, it is considered adequate to include only fuselage states and controls in the identification with the contribution of the steady- state rotor effects being lumped into the

identified fuselage derivatives. In reality, however, the effective neglect of rotor-dynamical effects can lead to identification difficulties for some parameters. As was discussed in Section 1.2.4, this is a well known and reported problem in the application of system identification techniques to helicopters. In Section 1.2.5, the basis for a new approach to accounting for rotor-dynamical effects in the identification, was developed by the current author, involving the use of a time delay in the control used by the pilot in applying the test-input signal.

In this section, an investigation into the incorporation of a time delay in the applied control, for the use of a six-degrees-of-freedom model in describing a nine- degrees-of-freedom system will be carried out. Simulated data from the HELISTAB program, briefly described in Section 1.2.6, will be used to represent the nine degrees-of-freedom system, and in addition, the six degrees-of-freedom quasi-static linear model will also be provided. The rotor states included in the model represent the flapping states β_0, β_{1c} and β_{1s} defined by (1.2-4) in Section 1.2.4 (i.e. a first-order rotor representation).

The flight condition used was for straight and level flight at 80 knots. The eigenvalues of the 11 x 11 system (8 fuselage states and 3 rotor states) are given in Table 2-1. The first three entries in the table correspond to those modes of the eleventh order system for which the

rotor states feature significantly. Mode 1 is a subsidence mode for which the coning angle - β_0 is the mode dominant rotor state. Mode 2 and 3 is an oscillatory mode for which the longitudinal and lateral cyclic flapping angles - β_{1c} and β_{1s} are the most dominant rotor states.

Using the frequency-domain output-error program - OUTMOD, developed by the current author, and explained in detail in Chapter 4 (and BLAC006), the helicopter stability and control derivatives included in the 'estimated' model were fixed at the six-degrees-of-freedom quasi-static linear model values. The only free parameter in the estimation was the time delay. For the nine-degrees-of- freedom data generated, the upper frequency value used in the estimation was 0.5 Hz., covering the range of the rigid-body modes. With this experiment, some indication of the requirement for a time delay in obtaining an improved model fit for the reduced-order model, can be established.

Descriptions of Inputs and Results Obtained

The set of control inputs used initially were longitudinal-cyclic doublets. The estimated time delay as a function of sampling interval, is shown in Figure 2-3. For one particular sampling interval of 0.015 seconds (approximately equal to the sampling interval for the flight data - 1/64th second - used in the work covered in

this document), the estimated delay for each of the controls when a '3211' test input signal is applied to that control alone, is shown.

As the results show, a positive time delay was strongly identified for the longitudinal-cyclic and lateral- cyclic inputs. For the longitudinal-cyclic doublet inputs, it is shown that as the sampling interval was increased, the estimated time delay decreased. This is because increasing the sampling interval effectively filters out the high-order rotor flapping effects. The points in Figure 2-3 representing the doublet inputs are extrapolated to zero time delay, and it can be seen that the corresponding sampling interval is very near to the time constant of 0.11 seconds, given in Table 2.1 for mode 2 and 3).

The original estimation of the time delay was carried out in the frequency-domain, and the time-domain predictions of the data generated from the nine-degrees-of-freedom model, for the six-degrees-of-freedom model, without and with the time delay, are shown in Figures 2-4 a) and b). It can be seen clearly that a much closer match with the nine-degrees-of-freedom data is obtained, using the six-degrees-of-freedom model, when the time delay is included. An improvement in a model fit is to be expected for the inclusion of an additional parameter; however, some justification that the extra parameter (i.e. the time delay) represents an actual physical effect has been

provided, and its inclusion leads to a marked improvement.

In the case of the collective input, the small value estimated for the delay, is probably associated with mode 1 in Table 2-1 (of which the coning angle is the most dominant rotor state), which in comparison to mode 2 and 3, has a very small time constant. For the tail rotor control there are no dynamics modelled in the HELISTAB program: the small delay estimated (less than the sampling interval) is the result of numerical noise. Results using real flight-data, however, have demonstrated the importance of having a delay associated with this control; these results are presented in Section 4.3.2. For the longitudinal-cyclic '3211' input, the estimated delay is almost identical to that obtained for the doublet input.

It was also found that when activity was present on both longitudinal and lateral-cyclic controls, significant delays were identified for both controls. The presence of noise on the controls was found to increase the values of the identified delays.

These results have indicated that the inclusion of time delays, in some of the controls, may be a useful feature in the estimation of lower-order models, where the sampling interval is significantly less than the time constants of modes not included in the model. Increasing the sampling interval to a value of the order of the time constant of mode 2 and 3 (longitudinal and lateral cyclic

flapping angles are the dominant rotor states), for example, would seem to be an alternative approach to circumvent the difficulties caused by the rotor transients. However, this can have some unpredictable results, and as will be shown in Section 2.3.3 using real flight-data, more satisfactory parameter estimates, and model fits, are obtained using the delay in preference to a larger sampling interval, for the frequency-domain identification.

2.3.3 A Demonstration of the Use of a Time Delay Using Real Flight Data

Description of Flight Data and Model Structure Used

A flight-data set corresponding to a longitudinal-cyclic doublet input applied to a Puma helicopter in straight and level flight at a speed of 100 knots, was used in the investigation. The length of the data record was 13.3 seconds. The estimation of longitudinal, and longitudinal/lateral-coupling parameters was carried out (using the frequency-domain output-error program - OUTMOD) over a frequency range of 0.075 to 0.602 Hz: the magnitudes of the Fourier transforms were very small beyond this range. The structure of the model used was as shown below, with the lateral states incorporated into an extended control vector. As was pointed out in Section 1.2.1, this enables the identification problem to be cast

in a manageable form for the application of a single control input (See Appendix 1).

$$\begin{bmatrix} \dot{U}(t) \\ \dot{W}(t) \\ \dot{q}(t) \\ \dot{\theta}(t) \end{bmatrix} = \begin{bmatrix} X_u & X_w & X_q - W_e & X_\theta - g\cos\theta_e \\ Z_u & Z_w & Z_q + U_e & Z_\theta - g\sin\theta_e \\ M_u & M_w & M_q - W_e & 0 \\ 0 & 0 & 1 & 0 \end{bmatrix} \begin{bmatrix} U(t) \\ W(t) \\ q(t) \\ \theta(t) \end{bmatrix} + \begin{bmatrix} 0 & 0 & X_{\eta_{1s}} \\ 0 & Z_p & Z_{\eta_{1s}} \\ M_\beta & M_p & M_{\eta_{1s}} \\ 0 & 0 & 0 \end{bmatrix} \begin{bmatrix} \beta(t) \\ p(t) \\ \eta_{1s}(t-\tau) \end{bmatrix} \qquad (2.3\text{-}11)$$

The measure variables are related to the state variables by the additional equation (i.e. the longitudinal portion of Equation 2.2-33):

$$\begin{bmatrix} V_m(t) \\ \alpha_m(t) \\ q_m(t) \\ \theta_m(t) \end{bmatrix} = \begin{bmatrix} 1 & 0 & l_z^v & 0 \\ 0 & 1/U_e & -l_x^\alpha / U_e & 0 \\ 0 & 0 & 1 & 0 \\ 0 & 0 & 0 & 1 \end{bmatrix} \begin{bmatrix} U(t) \\ W(t) \\ q(t) \\ \theta(t) \end{bmatrix} + \begin{bmatrix} V_{OFF} \\ \alpha_{OFF} \\ q_{OFF} \\ \theta_{OFF} \end{bmatrix}$$

(2.3-12)

The terms in the above equation were explained in Section 2.2.4.

A number of the parameters in these equations are known to be insignificant (measures of parameter significance as explained in Section 3.2.4 were used) and were excluded from the estimation process. Initial parameter estimates for the output-error method were

obtained from equation-error fits for each of the rows.

Description of Results Obtained

Three different cases for the estimation were considered:

(1) estimation without a time delay in the longitudinal-cyclic control (i.e. the delay in the above model is effectively fixed at a zero value), using the flight-data sampling time of 0.015625 seconds;
(2) estimation with a time delay in the longitudinal-cyclic control using the flight-data sampling time of 0.015625 seconds; and
(3) estimation without a time delay, but using an increased sampling time of (6 x 0.015625 =) 0.09375 seconds. The final estimates obtained on convergence of the estimation algorithm, are given in Table 2-2, along with theoretical values from the HELISTAB program.

Examination of the results for cases (1) and (2) reveals that the inclusion of the time delay resulted in a smaller cost-function value (the frequency-domain output- error cost function is derived in Section 4.2.1) at convergence, for the sampling interval of 0.015625 seconds: that is to say a better fit with the observed flight data was obtained for case (2). The estimate of the important pitch-rate-damping parameter M_q without the

delay is very much underestimated in comparison to theory, but with time delay estimated in the model, the agreement is excellent. The underestimation of this parameter in helicopter parameter identification studies is reported by some authors (e.g. PADF002), where the assumption of quasi-static rotor dynamics in the simplified six-degrees-of-freedom models is cited as the most probable cause. The inclusion, and estimation, of the time delay in the longitudinal-cyclic control appears to have made a considerable improvement to the situation. For the case with the time delay, excellent estimates are obtained for the cross-coupling parameters: M_β and M_p. The control sensitivity $M_{\eta_{1s}}$ agrees very well with theory for the inclusion of the delay. The time delay itself is estimated with confidence; its estimated value is of the same order of magnitude as the time constant for longitudinal and lateral cyclic flapping. For the derivative M_w, it is seen that the theoretical HELISTAB prediction represents a more stable aircraft that is suggested by the results; the change in sign obtained for this parameter, when the time delay is included in the model, indicates that there may be some strong correlation between M_q and M_w. The normal-force derivative: Z_w, is estimated with a small error-bound, and is unaffected by the time delay.

Looking now at case (3), it can be seen that by increasing the sampling interval to 0.09375 seconds, the most significant features of the results obtained in case

(2) are repeated: namely, the significant improvements in the estimates of M_q and $M_{\Delta_{1s}}$ over those obtained for case (1); and the reversal in sign for the estimate of M_w. Improvements in the quasi-static estimates of some parameters, such as pitch-rate damping and control sensitivity, obtained by increasing the sampling interval, were demonstrated in the reference PADF002 using simulated data and time-domain equation-error estimation. These observations have now been confirmed using real flight-data, and a more advanced frequency-domain output-error technique. This improvement is because, as was indicated in Section 2.3.3, the higher-order rotor transient effects are effectively filtered out for large sampling-intervals. It was also pointed out, however, that this is not the approach advocated here: the use of a time delay with a small sampling-interval is preferred - the superiority of this approach will be made apparent in the rest of this section.

The cost-function value at convergence for case (3) is smaller than case (2); however, because the sampling interval in case (3) is six times that in case (2), the two values are not directly commensurable. Examination of Table 2-2 reveals that the cross-coupling derivatives: M_β and M_p, have a less satisfactory agreement with theory than case (2). In fact, plots of the frequency-domain fits for the three cases, shown in Figures 2-5a), b) and c), reveal that case (2) (with the time delay in the

control and the small sampling interval) gives the best frequency-domain fit; this is especially true for the pitch rate.

Using the parameters identified in the frequency-domain, a time-domain output-error procedure can then be used to estimate initial state conditions, and measurement zero offsets - quantities not identifiable in the frequency- domain because of the exclusion of the zero frequency to obtain the time-domain fits of the estimated model. This was done using the program: OFBIT, developed by the current author; the theoretical basis of the method, and the computer implementation, is explained in detail in Chapter 5 and in the reference BLAC006. The time-domain fits obtained for three cases above, are shown in Figures 2-6 a), b) and c). Case (2) is again the most satisfactory, having the best time-domain reconstruction. The inclusion of the time delay results in a much tighter fit between the observed and predicted time-domain responses, especially for the pitch rate: q. A comparison of the pitch-rate fits in Figures 2-6 a) and b), shows clearly the improvement resulting from the inclusion, and estimation of, the time delay in the longitudinal-cyclic control. The lateral variables used as 'pseudo controls' in the extended control vector, along with the longitudinal- cyclic control are shown in Figure 2-6 d).

Summary of Chapter 2

The use of the the discrete Fourier transform as a means of representing a linearised state-space model of a helicopter in the frequency-domain, was presented. The model was extended to include time delays in the measurements and controls; and the ease with which the time delays can be incorporated into the frequency-domain model was emphasized.

In addition to the state-space equation, consideration was given to the frequency-domain representation of the measurement system: it was explained that a linearised representation was necessary because of the practical difficulties encountered in applying a linear transformation, such as the discrete Fourier transformation, to non-linear equations in general. It was pointed out that a drawback of the frequency-domain approach was its limitation to small-perturbation models (non-linear only in the sense that time delays are permissible). Another drawback of the frequency-domain approach was explained: namely that errors are introduced into the identification as a result of representing the response as a Fourier series whose coefficients are calculated using a finite-length record.

However, the potential advantages for helicopter system identification, gained by formulating the problem in the frequency domain are manifold. Some examples of the advantages were given in both this and the previous

chapter, and are brought out in detail, or demonstrated, in the remaining chapters of this document. These include:

1) Noisy flight data can be used directly in the system identification. There is no pressing requirement for pre-estimation techniques, such as Extended-Kalman-Filter state estimation, in order to remove high-frequency noise, or to construct unmeasured quantities, such as the time derivatives of states; thus cutting down considerably on the time required to perform an identification.

2) The ability to easily introduce selectivity in the frequencies used in the identification is useful for models valid for a specified frequency range; however, the resultant reduction in the number of data is also computationally beneficial. For the helicopter flight data used by the current author, there was found to be typically a 1:50 reduction in the amount of data actually used in the frequency-domain identification algorithm, in comparison to the original time-domain data. This kind of reduction in the amount of data augurs well for identification techniques based on cost functions involving summations. It should also be pointed out that obtaining the Fourier transforms of the measured time-domain data can be done very quickly using standard FFT routines, such as the NAG routine C06FAF, mentioned in Section 2.2.2. The availability of frequency-domain

records provides a useful indication of the degree of excitation of the system at frequencies of interest, and there is no requirement for the creation of new data sets each time the frequency range used in the identification changes.

3) By excluding the zero frequency value from the range used in the identification, there is a reduction in the number of parameters that have to be estimated using the frequency domain. Zero-offset terms are decoupled from the rest of the model. These can be estimated at a later stage, along with initial state conditions, using the time domain.

4) Expressing the identification problem in the frequency-domain has some important practical benefits for the estimation algorithms, and their computer implementation. The problem of obtaining the estimated model output, and other quantities, becomes algebraic; in the time-domain, numerical integration is required for the corresponding operations.

Finally in this chapter, the usefulness of a new approach (i.e. the incorporation and identification of a time delay in the control used) in overcoming some of the problems associated with quasi-static derivatives was demonstrated using both simulated data and real flight-data. For real flight-data, the parameter estimates obtained compared favourably, in most cases, with the theoretical values provided by the HELISTAB

program, when a time delay was identified in the longitudinal cyclic input. The improvement was also apparent in the time-domain reconstructions of the models identified in the frequency-domain.

Results from simulated data indicated that in some cases, there would be no requirement for the inclusion of a time delay in the collective input channel because of its association with high-frequency coning effects, and because of the sampling interval used in the flight data; results obtained by the current author using real flight-data, have confirmed this. The HELISTAB program does not include the modelling of tail-rotor dynamics, however, results for pedal inputs using real flight-data, and presented in Section 4.3.2, show the inclusion of a time delay in the pedal control, to be an important modelling requirement.

CHAPTER 3

3.0 Initial Stages In The Identification Methodology, And A Consideration Of Some Relevant Identification Techniques.

3.1 Introduction And Overview Of The Methodology.

The three basic elements of the identification methodology are developed and discussed separately in each of the remaining chapters of this document, culminating in a summary of the salient points for each stage in the final Sections of Chapter 5. These three elements are: a frequency-domain equation-error method; a frequency-domain output-error method; and a time-domain output-error method (see Figure 5-1). The ordering of the chapters represents the natural sequence of application for each of these stages, where the results from one stage are used to initiate the next stage.

Initial parameter estimates are obtained at the equation-error stage; these estimates, which are biased in the presence of noise on the independent variables used in the equations, may then be used as initial guesses for the iterative frequency-domain output-error method, which is capable of producing unbiased estimates in the absence of process (or model) noise. Both the equation-error and output-error identifications are carried out over a restricted frequency range appropriate

to the assumed form of model, namely one which describes the rigid-body motions of a helicopter. Convergence of the frequency-domain output-error method is assisted by having good initial estimates of the unknown parameters; the singular-value-decomposition implementation of the equation-error method, presented in this Chapter, is seen as a means of improving the estimates obtained at the equation-error stage. For the frequency-domain output-error method implemented here, options exist for investigating the effects of different model structures on the estimates. Results from the equation-error stage can also assist in isolating weak, or insignificant, parameters to be fixed, or excluded, from the state-space model used in the output-error identification.

The final stage of the identification methodology involves the estimation of initial conditions and zero-offsets which are uncoupled from the frequency-domain identification, but which are necessary for a final time-domain verification of the model. Stability and control derivatives, and time delays, estimated at the frequency-domain output-error stage (together with those elements of the model fixed for that identification) are fixed for the time-domain output-error identification.

There are some issues which relate to both the frequency-domain equation-error and output-error methods, such as the selection of an appropriate frequency range, and the selection of an appropriate length of time-domain record for transformation. These are discussed in this

Chapter since it is at the equation-error stage that they are first encountered. In addition, the comments made about attempts to apparently increase the frequency resolution through the use of zero pads in this Chapter, also apply to their use at the output-error stage.

The equation-error method is a widely used approach to system identification. This is so, mainly because of its simplicity and easy application to linear or non-linear models. In the reference KLEI001, the author pays tribute to the equation-error method: "Despite all these degradations in the accuracy of the estimates resulting from real flight-data [because of violations of the assumed noise properties], the equation-error method is often used, sometimes with very consistent results in comparison with more sophisticated techniques". Some previously reported applications of the equation-error technique are discussed in appropriate Sections of this Chapter.

3.2 The Frequency-Domain Equation-Error Stage In The Identification Methodology.

3.2.1 The Basic Method And Some Comments On The Frequency-Domain Formulation.

The equation-error technique is based on the least-squares principle, and is well-known for its application to curve fitting or regression analysis. With this

approach, the solution aims to minimise the sum of squares of deviations between measured data points and corresponding points obtained from the solution, where the measured data is to be represented by a functional relationship, or smooth curve.

For the estimation of parameters of a dynamical system with state-space form (as given by Equation 2.2-15), it is necessary to consider one row of the matrix-equation at a time for the equation-error method. Consider an element of the state time-derivative vector $\dot{X}_i$ as the dependent variable, with unknown parameters a_{ij} corresponding to the ith row of state matrix A, and b_{ik} corresponding to the ith row of the control dispersion matrix B. It is assumed that the state $\underset{\sim}{X}$ and control vector $\underset{\sim}{U}$ are measured without error, whereas the measured values $\underset{\sim}{Y}$ of the dependent variable X_i are corrupted with zero-mean uncorrelated Gaussian measurement noise such that

$$\underset{\sim}{Y}(r) = \dot{X}_i(r) + \varepsilon(r) \tag{3.2-1}$$

$$\underset{\sim}{Y}(r) = a_{i1} X_1(r) + a_{i2} X_2(r) + \dots a_{in} X_n(r) + b_{i1} U_1(r) + \dots b_{im} U_m(r) + \varepsilon(r) \tag{3.2-2}$$

for an nxn state matrix A and nxm control dispersion matrix B. The error term $\varepsilon(r)$ in (3.2-1) can represent process (i.e. modelling) noise on the model, in addition to measurement noise on the dependent variable $\dot{X}_i$ -

assuming, of course, that a zero-mean uncorrelated Gaussian representation is appropriate. The least-squares criterion in defined as the minimisation of the cost function:

$$J(\Theta) = 1/2 \sum_{r=1}^{N} (Y(r) - \alpha_{L1} X_1(r) - \alpha_{L2} X_2(r) \ldots \beta_{Lm} U_m(r))^2 \tag{3.2-3}$$

where Θ is the set of parameter estimates: $\alpha_{L1}, \alpha_{L2}, \alpha_{L3} \ldots \beta_{Lm}$.

In order to succinctly express the solution to the least-squares problem, Equation (3.2-2) will be written in the following form:

$$\underset{\sim}{Y} = \mathbf{X} \underset{\sim}{\Theta} + \underset{\sim}{\varepsilon} \tag{3.2-4}$$

where the vector $\underset{\sim}{Y}$ is constructed from the N measured values of the dependent variable; the NxP matrix $\mathbf{X}$ (where P is the number of parameters to be estimated) is constructed from the independent-variable values: $X_i(r)$, $U_i(r)$ arranged in columns; and the vector: $\underset{\sim}{\Theta}$ represents the P parameters to be estimated. For the estimates of the unknown parameters, represented as $\hat{\underset{\sim}{\Theta}}$, using (3.2-4), we can write the cost function in (3.2-3) as:

$$J(\Theta) = 1/2 (\underset{\sim}{Y} - \mathbf{X} \hat{\underset{\sim}{\Theta}})^T (\underset{\sim}{Y} - \mathbf{X} \hat{\underset{\sim}{\Theta}}) \tag{3.2-5}$$

A necessary condition for the minimum of $J(\Theta)$ is given

by:

$$\frac{\partial J(\boldsymbol{\Theta})}{\partial \hat{\underset{\sim}{\Theta}}} = \underset{\sim}{0} \tag{3.2-6}$$

From which it can easily be shown that the least-squares solution for $\hat{\underset{\sim}{\Theta}}$ is given by (e.g. GELB001):

$$\hat{\underset{\sim}{\Theta}} = [\mathbf{X}^T\mathbf{X}]^{-1}\mathbf{X}^T\underset{\sim}{y} \tag{3.2-7}$$

<u>Biased Estimates.</u>

The parameter estimates will only be unbiased if the independent variables - corresponding to columns of $\mathbf{X}$ are measured error-free, and if the equation-error vector $\underset{\sim}{\xi}$ represents a zero-mean uncorrelated Gaussian random variable; this is shown in the reference KLEI001 by substituting (3.2-4) into (3.2-7) to give:

$$\hat{\underset{\sim}{\Theta}} = [\mathbf{X}^T\mathbf{X}]^{-1}\mathbf{X}^T(\mathbf{X}\underset{\sim}{\Theta} + \underset{\sim}{\xi}) \tag{3.2-8}$$

and by taking the expected value of both sides of the Equation to give:

$$E[\hat{\underset{\sim}{\Theta}}] = \underset{\sim}{\Theta} + E[[\mathbf{X}^T\mathbf{X}]^{-1}\mathbf{X}^T\underset{\sim}{\xi}] \tag{3.2-9}$$

If $\underset{\sim}{\xi}$ has the properties given above, then we can write:

$$E[[\mathbf{X}^T\mathbf{X}]^{-1}\mathbf{X}^T\underset{\sim}{\xi}] = E[[\mathbf{X}^T\mathbf{X}]^{-1}\mathbf{X}^T] \cdot E[\underset{\sim}{\xi}] = \underset{\sim}{0} \tag{3.2-10}$$

otherwise the expected parameter estimates will be biased by an amount given by the second term on the right-hand side of Equation (3.2-9).

Covariance Matrix.

Some indication of the accuracy of the parameter estimates which are given by (3.2-7), is given by the covariance matrix defined as:

$$\mathrm{Cov}(\hat{\underset{\sim}{\theta}} - \underset{\sim}{\theta}) \triangleq E[(\hat{\underset{\sim}{\theta}} - \underset{\sim}{\theta})(\hat{\underset{\sim}{\theta}} - \underset{\sim}{\theta})^T] \qquad (3.2\text{-}11)$$

Using (3.2-9), and for the conditions on the noise given above, it can be shown easily that (e.g. KLEI001):

$$\mathrm{Cov}(\hat{\underset{\sim}{\theta}} - \underset{\sim}{\theta}) = \sigma^2 (X^T X)^{-1} \qquad (3.2\text{-}12)$$

where σ^2 is the variance of the noise, assumed to be a stationary random process. In the time domain a stationary random process is one whose statistical properties are invariant in time (e.g. GELB001); the concept can be extended to the frequency domain, when a random variable is distributed identically for all discrete frequency values. The variance σ^2 is defined by:

$$E[\underset{\sim}{\xi}\underset{\sim}{\xi}^T] = \sigma^2 I \qquad (3.2\text{-}13)$$

where I is the identity matrix, the order of which corresponds to the number of points used in the identification. Because of the equidistribution of power between the real and imaginary parts of the transform of an uncorrelated stationary random variable (as shown in Section 2.2.5), and because the real and imaginary parts of both sides of a frequency-domain equation-error problem can be considered independently, allowing the estimation to have the appearance of a real-valued problem (explained shortly), than Equation (3.2-13) also holds for the frequency-domain application of the method considered here. However, the variance σ^2 is not usually known, and its estimate S^2, obtained from the calculated fit, can be used as an approximation instead:

$$S^2 = 1/(N-P) \sum_{r=1}^{N} e^2(r) \qquad (3.2\text{-}14)$$

The residuals $e(r)$ are obtained from the measured data and the calculated fit as follows:

$$e(r) = Y(r) - X_{rJ} \hat{\Theta}_J \qquad (3.2\text{-}15)$$

<u>Frequency-Domain Formulation.</u>

If we consider one row of the frequency-domain state space model (as given by Equation 2.2-16), then the general equation-error representation given by Equation (3.2-2), will consist of complex-valued quantities, and r

will represent discrete values of frequency. However, by equating the real and imaginary parts of both sides of (3.2-2) - where we are replacing $Y(r)$, $X_1(r)$ etc. by the complex-valued quantities: $\hat{Y}(r)$, $\hat{X}_1(r)$ etc. - it can be seen that two Equations occur for a given value of frequency, both having exactly the same coefficients:

$$Re[\hat{Y}(r)] = a_{11} Re[\hat{X}_1(r)] + a_{12} Re[\hat{X}_2(r)] + \ldots + b_{1m} Re[\hat{U}_m(r)] + Re[\hat{\underset{\sim}{\xi}}(r)] \qquad (3.2\text{-}16)$$

$$Im[\hat{Y}(r)] = a_{11} Im[\hat{X}_1(r)] + a_{12} Im[\hat{X}_2(r)] + \ldots + b_{1m} Im[\hat{U}_m(r)] + Im[\hat{\underset{\sim}{\xi}}(r)] \qquad (3.2\text{-}17)$$

It is conceivable that either the real or imaginary Equations could be used separately to perform the identification. Algebraically, it would not be incorrect to add together the real and imaginary parts of corresponding terms in Equations (3.2-16) and (3.2-17): this would be equivalent to the application of the discrete Hartley transform (BRAC001) to the original time-domain data. There is a reduction - by a factor of 2 - in the number of points needed to represent a given frequency range; however, it should be pointed out that by examining the corresponding cost function, defined in terms of the transformed equation-error term: $\hat{e}(r)$

$$J_H(\boldsymbol{\theta}) \triangleq 1/2 \sum_{r=1}^{q} \left(Re[\hat{e}(r)] + Im[\hat{e}(r)] \right)^2 \qquad (3.2\text{-}18)$$

we can see that for a given contribution to the cost function $J_H(\boldsymbol{\theta})$, corresponding to a frequency value r,

equal weighting is given to both the solutions

$$R_e[\hat{e}(r)] = -I_m[\hat{e}(r)] \tag{3.2-19}$$

$$R_e[\hat{e}(r)] = I_m[\hat{e}(r)] = 0 \tag{3.2-20}$$

for the contribution to be a minimum, namely zero in value. For the matching of the frequency characteristics of the model and the observed measurements we require solutions corresponding to Equation (3.2-20) and not (3.2-19) which represents the worst-case scenario for the addition of the real and imaginary parts of the transform for use in the identification.

The Hartley transform is discussed in detail in the reference BRAC001 as a transform which resembles the discrete Fourier transform, but one which permits faster computing because it is real valued and since one complex multiplication equals four real multiplications; however, such advantages are not relevant in the current context. Interestingly, identification results using the addition of the real and imaginary parts of the transformed quantities, were found by the current author, to be similar in many cases, to results obtained using the approach finally adopted, and described in the following paragraph.

By forming a vector in which the real and imaginary components alternate, we have for example in the case of the dependent variable $\underset{\sim}{Y}$, given in (3.2-4):

$$\underset{\sim}{Y} \triangleq (R_e[\hat{Y}(1)], I_m[\hat{Y}(1)], R_e[\hat{Y}(2)], I_m[\hat{Y}(2)], \ldots R_e[\hat{Y}(q)], I_m[\hat{Y}(q)])^T \qquad (3.2\text{-}21)$$

for a frequency range, given by r=1, 2..q, used in the identification. By similarly constructing vectors for the independent variables: $\hat{X}_1(r)$, $\hat{X}_2(r)$ ... $\hat{U}_m(r)$ in (3.2-16) and (3.2-17), we can perform the identification using both the real and imaginary parts, and are thus minimising the cost function:

$$J(\boldsymbol{\theta}) \triangleq 1/2 \sum_{r=1}^{q} (R_e^2[\hat{e}(r)] + I_m^2[\hat{e}(r)]) \qquad (3.2\text{-}22)$$

The cost function defined in (3.2-22) can only have zero contribution at a given frequency r, when (3.2-20) holds.

<u>Instrumental Variable Technique.</u>

The requirement for a zero-mean uncorrelated Gaussian error-term in the equation-error method (in addition to error-free measurements of the independent variables) is pointed out in references to the equation-error method (e.g. KLEI001); this was expressed by Equations (3.2-9) and (3.2-10) as a necessary condition for obtaining unbiased estimates (i.e. estimates without systematic errors). In the context of time-domain estimation, a technique which attempts to overcome the difficulties of correlated noise is through the use of an

instrumental-variable matrix Z_{IV} (BOOM001, KLEI001); the instrumental-variable matrix Z_{IV} premultiplies all the original quantities in the equation-error estimation problem given by Equation (3.2-4) to give, by analogy with (3.2-9):

$$E[\hat{\underset{\sim}{\Theta}}_{IV}] = \Theta + E[((Z_{IV}X)^T(Z_{IV}X))^{-1}(Z_{IV}X)^T(Z_{IV}\underset{\sim}{\varepsilon})] \tag{3.2-23}$$

where the properties of the instrumental-variable matrix Z_{IV}, are such that:

$$|(Z_{IV}X)^T(Z_{IV}X)| > 0 \tag{3.2-24}$$

$$E[Z_{IV}\underset{\sim}{\varepsilon}] = 0 \tag{3.2-25}$$

For a positive-definite Hermitian matrix (e.g. STOE001) as defined by (3.2-24), and for an uncorrelated effective noise source, as given by (3.2-25), we have that the second term on the right-hand side of Equation (3.2-23) has an expected value of zero, resulting in unbiased estimates of $\underset{\sim}{\Theta}$.

An important property of equation-error estimates (in the case of uncorrelated noise) and of instrumental-variable estimates is that of consistency. Basically, a consistent estimator in the time-domain is one whose covariance matrix (i.e. the parameter error bounds) tends to the null matrix (i.e. zero error bounds) as the number of points used in the identification increases. This

will be demonstrated for parameter estimates obtained using real flight data in Section 3.3.3. The property of consistency is defined by:

$$\lim_{N \to \infty} \mathrm{Cov}(\hat{\underset{\sim}{\Theta}} - \underset{\sim}{\Theta}) = 0 \qquad (3.2\text{-}26)$$

In the reference KLEI001, the consistency of equation-error estimates (in the case of uncorrelated and stationary noise) is proven; the consistency of instrumental-variable estimates is also stated, but not proven, though it can be easily shown that the proof of consistency follows in a similar fashion.

With regard to the requirements given by (3.2-24) and (3.2-25), it is suggested in the reference KLEI001, that the instrumental variables (i.e. the rows of Z_{IV}), could be obtained as the output from a Kalman filter with known input variables, and approximate values for the stability and control derivatives.

<u>Use Of A Restricted Frequency Range.</u>

It was observed by the current author that the solution to the frequency-domain equation-error estimation problem, carried out over a restricted frequency range, could be written in a form analogous to the instrumental-variable formulation for time-domain estimation, given by Equation (3.2-23). Unbiased estimates are obtained for requirements similar to those

given by (3.2-24) and (3.2-25). In addition, the estimates are consistent for an increase in the number of frequency-domain points within the frequency range valid for the model; this corresponds to (3.2-26).

To show that the above is true, consider first that the discrete Fourier transformation of a time-domain quantity which is represented as a column vector, is achieved through pre-multiplying it by a complex-valued matrix - Z'_{FR}, whose elements - $Z'_{FR_{LK}}$ are:

$$Z'_{FR_{LK}} \triangleq 1/\sqrt{N}\ \exp(-j\,2\pi(L-1)(K-1)/N) \qquad L,K = 1,2,3 \ldots N \tag{3.2-27}$$

Now the method devised by the current author for using what are essentially complex-valued quantities in the estimation, was to alternate the real and imaginary parts of a column vector, as shown in (3.2-21). If we use a real-valued matrix Z_{FR}, where alternative rows correspond respectively to the real and imaginary parts of a discrete Fourier transform, defined by:

$$Z_{FR_{2L-1,K}} \triangleq 1/\sqrt{N}\ \cos 2\pi(L-1)(K-1)/N$$

$$Z_{FR_{2L,K}} \triangleq -1/\sqrt{N}\ \sin 2\pi(L-1)(K-1)/N \qquad L,K = 1,2,3 \ldots N \tag{3.2-28}$$

then the frequency-domain equation-error problem can be written in terms of the matrix Z_{FR} and the original time-domain quantities. Pre-multiplying Equation (3.2-4) by Z_{FR}, we have:

$$Z_{FR}\underset{\sim}{Y} = Z_{FR}\mathbf{X}\underset{\sim}{\Theta} + Z_{FR}\underset{\sim}{\xi} \tag{3.2-29}$$

By excluding the rows in (3.2-28) corresponding to $i=1$, we will exclude the zero frequency from the identification; in addition, if we define Z_{FR} such that it only has rows corresponding to $2 \leq i \leq q+1 < N/2$, then we are performing the identification on a restricted range of lower frequencies.

By analogy with Equation (3.2-23), we have that:

$$E[\hat{\underset{\sim}{\Theta}}_{FR}] = \underset{\sim}{\Theta} + E[((Z_{FR}\mathbf{X})^T(Z_{FR}\mathbf{X}))^{-1}(Z_{FR}\mathbf{X})(Z_{FR}\underset{\sim}{\xi})] \tag{3.2-30}$$

assuming the frequency range implied by the rows of Z_{FR} is the appropriate one for the identification of the model.

Using the definition of Z_{FR} given by (3.2-28), constructed for a reduced frequency range, we can see that provided the sums of the squared magnitudes of the transforms (i.e. the power within the stipulated frequency range - see Parseval's theorem discussed in Section 2.2.2) are 'sufficiently' large for each of the independent variables in Equation (3.2-29), then no terms having a small magnitude will occur in the leading diagonal of the real-valued matrix product, whose diagonal terms are defined below:

$$(Z_{FR}\mathbf{X})^T(Z_{FR}\mathbf{X})_{ii} = \sum_j (\hat{X}_{2j-1,i})^2 + (\hat{X}_{2j,i})^2 \tag{3.2-31}$$

where $\hat{X}_{jk}$ are elements of the matrix defined by:

$$(Z_{FR} X) \triangleq \hat{X} \tag{3.2-32}$$

In addition, provided the frequency-domain responses of the independent variables are 'sufficiently' uncorrelated, we will then have a condition analogous to (3.2-24):

$$|(Z_{FR} X)^T (Z_{FR} X)| > 0 \tag{3.2-33}$$

The above discussion relating to the expression given in (3.2-33) is in fact centred upon the condition number of the frequency-domain information matrix (i.e. the matrix whose determinant is considered in 3.2-33), which is affected by both the sensitivities of, and correlations between, the independent variables; these concepts are considered in more detail in Section 3.2.5.

In order to finally complete the analogy between the time-domain instrumental variable technique and the frequency-domain equation-error method (using a restricted frequency range), consider the matrix $Z_{FR}.\underset{\sim}{\xi}$. For helicopter flight test data, the original time-domain noise source $\underset{\sim}{\xi}$, for a six-degrees-of-freedom model that includes fuselage states only, will not, in general, be adequately modelled as a zero-mean uncorrelated Gaussian disturbance. Consequently, biased parameter estimates

and poor fits will be obtained when the original time-domain data, or equivalently the entire frequency range available, is used in the identification; this is shown graphically in Section 3.3.2 using real flight data. However, if the restricted frequency range used in the identification of a six-degrees-of-freedom model is such that the frequency-domain noise source $Z_{FR}\underset{\sim}{\xi}$ is adequately modelled as a zero-mean uncorrelated noise source, then we will have a property for the real-valued matrix Z_{FR}, identical to that for the time-domain instrumental-variable matrix Z_{IV}, given by (3.2-25), that is:

$$E[Z_{FR}\underset{\sim}{\xi}] = \underset{\sim}{0} \tag{3.2-34}$$

Hence we have, for an appropriate frequency range implied by the rows of Z_{FR}, and using (3.2-33) and (3.2-34), that:

$$E[((Z_{FR}X)^T(Z_{FR}X))^{-1}(Z_{FR}X)(Z_{FR}\underset{\sim}{\xi})] =$$

$$E[((Z_{FR}X)^T(Z_{FR}X))^{-1}(Z_{FR}X)]\cdot E[Z_{FR}\underset{\sim}{\xi}] = \underset{\sim}{0} \tag{3.2-35}$$

From Equation (3.2-30) we can see that this results in unbiased parameter estimates (i.e. $E[\hat{\underset{\sim}{\Theta}}_{FR}] = \hat{\underset{\sim}{\theta}}$).

Despite the violation of the assumption of no noise for the identification of real flight data, it will be demonstrated in later Sections of this Chapter using real flight data, that useful results can still be obtained using the frequency-domain equation-error approach over a restricted frequency range.

Direct Transformation Of Flight Data.

When the states to be used in the identification and the flight-test measurements are related linearly, we have:

$$R_e[\hat{\underset{\sim}{Z}}(\omega)] = H\, R_e[\hat{\underset{\sim}{X}}(\omega)]$$

$$I_m[\hat{\underset{\sim}{Z}}(\omega)] = H\, I_m[\hat{\underset{\sim}{X}}(\omega)] \qquad (3.2\text{-}36)$$

The real and imaginary parts of the transformed quantities can be arranged in the same way as the vector defined in (3.2-21), and a single matrix-linear Equation solved for the relatively few frequency-domain points used in helicopter system identification, in order to obtain $\hat{\underset{\sim}{X}}(\omega)$. The same approach is used to obtain the transforms of time derivatives.

3.2.2 Subset Regression.

The equation-error approach to helicopter and fixed-wing system identification problems is mostly discussed in the available literature in the context of a subset (or stepwise) regression procedure, using time-domain data (e.g. PADF005 [current author is a co-author], KLEI002, KLEI003, DUVA001).

The subset regression procedure allows for some

investigation in determining the 'best' model structure from a pool of possible model structures; that is, the 'best' subset of independent variables from a set of variables specified by the analyst. The procedure applies least-squares fits in a sequence of steps, where at each step a variable is added to, or removed from the model, on the basis of objective statistical tests. The process terminates when, according to some criteria specified by the analyst, the 'best' structure is obtained, and no further improvement can be made either by the addition, or the removal, of a variable from the Equation. The subset-regression procedure is described in the reference KLEI002, and is outlined below.

From a pool of possible independent variables to be included in the Equation, the variable chosen at each stage of the procedure, for entry into the Equation, will have the highest partial correlation coefficient r_{jy}, defined by:

$$r_{jy} = \frac{\sum_{i}^{N} [X_j^*(i) - \bar{X}_j^*][Y^*(i) - \bar{Y}^*]}{\left(\sum_{i}^{N} [X_j^*(i) - X_j^*]^2 \sum_{i}^{N} [Y^*(i) - \bar{Y}^*]^2\right)^{1/2}} \qquad (3.2\text{-}37)$$

where Y^* is the residual left when the current model fit is subtracted from the dependent variable. At the start of the algorithm this will correspond to the dependent variable to which the model is being fitted - i.e. p=o in (3.2-28). For stage p+1 we have:

$$Y^*(r) = Y(r) - \alpha_1 X_1(r) - \alpha_2 X_2(r) \ldots - \alpha_p X_p(r) \qquad (3.2\text{-}38)$$

X_j^* is associated with the variable X_j, which is a candidate for inclusion in the model; it is obtained by regressing X_j against all the variables currently in the model: X_1, X_2 ... X_p to obtain the coefficients β_1, β_2 ... β_p, finally using the residual defined as:

$$X_j^*(r) = X_j(r) - \beta_1 X_1(r) - \beta_2 X_2(r) \ldots - \beta_p X_p(r) \qquad (3.2\text{-}39)$$

At every stage of the procedure, variables which are already incorporated into the model, and the variable selected for possible inclusion in the model (on the basis of its partial correlation) are subjected to the partial-F test. The partial-F statistic is defined in (3.2-40):

$$F_p = \alpha_i^2 / S^2(\alpha_i) \qquad (3.2\text{-}40)$$

where α_i is a parameter estimate and $S^2(\alpha_i)$ is the estimated variance of the estimate α_i. This statistic is evaluated for each of the variables under consideration, and is compared with a pre-defined value set by the analyst. If it is less than the pre-defined value, then the variable is removed from, or prevented from entering into, the model. This amounts to performing a hypothesis test using the appropriate F-distribution (e.g. MOOD001), where the null hypothesis postulates that the true value of the parameter is zero (i.e. the variable is not

present in the model). The procedure continues until no more variables can be admitted to, or removed from, the model Equation.

The partial-F statistic is an indicator of the relative accuracy of a parameter estimate, since it is defined as the square of the ratio of estimated parameter value to estimated standard error.

The squared multiple-correlation coefficient - R^2 provides a measure of the accuracy of the fit (the fractional portion of the dependent variable which can be attributed to linear effects), and is defined by:

$$R^2 \triangleq \frac{\sum_{i=1}^{N} (\hat{Y}(i) - \bar{Y}(i))^2}{\sum_{i=1}^{N} (Y(i) - \bar{Y}(i))^2} \qquad (3.2\text{-}41)$$

where $\hat{Y}(i)$ are the model predictions and $Y(i)$ the measured responses.

The total F-ratio provides a measure of the confidence that can be attributed to the fit, and is defined by:

$$F_{TOTAL} \triangleq \frac{R^2/(P-1)}{(1-R^2)/(N-P)} \qquad (3.2\text{-}42)$$

where N is the number of data points used in the identification and p is the number of parameters in the linear model.

Whilst the tests for deciding the 'best' model are objective, a subjective component of the process of model-structure determination exists; this is because the

selection of the 'best' model is made from a finite set of possibilities specified by the analyst. In addition, most applications of the method allow the analyst to force terms into the model, regardless of the fact that they would not be selected by the automatic process. This feature is present in the optimal-subset-regression program OSR, developed at NASA Ames specifically for helicopter system identification (HALL002). In the reference KLEI002, a procedure termed "modified stepwise regression" is described; here the aerodynamic force and moment coefficients are described using multivariable polynomials in response and control variables (i.e. a Taylor-series expansion about the initial steady-state flight condition, including terms higher than first order), and in applying the stepwise regression procedure, the significant linear terms are forced into and kept in the Equation, with the testing for entry or removal carried out only on the higher-order terms. It should be pointed out that some analysts prefer not to use the statistical approach for the selection of significant non-linear terms; in the reference ROSS001 the author points out that some flight dynamicists have reservations in 'leaving out the physics' from the identification.

Results obtained in the application of the subset regression procedure to real flight-data, using the time domain, are presented in the reference PADF005 [current author is a co-author]. In that paper, attention is

focussed on the rolling and yawing moment Equations; it was observed that the 'best' parameter estimates - in terms of their physical realism, and accuracy indicated by individual partial-F statistics - were obtained for the primary stiffness (N_v, L_v), primary damping (N_r, L_p), and control derivatives (N_{Δ_p}, L_{Δ_p}) when each of the Equations contained only the three indicated terms. When further terms were brought into the Equation by the subset regression procedure, a deterioration in the physical realism, and a collapse in the value of the partial-F statistics was observed. As would be expected for an increasing number of parameters, the squared correlation coefficient continued to increase for the higher-order, but less satisfactory models.

The reduced-order models corresponding to the first three steps of the subset regression procedure were judged to be the 'best' representative models. The concept of obtaining the best representative model based on the choice of one particular model structure from a set of possible structures, will be discussed in Section 3.2.5, using an approach known as singular-value decomposition.

3.2.3 The Method Of Successive Residuals.

In addition to the subset-regression method, another approach to the use of the equation-error technique in helicopter system identification, called "the method of

successive residuals", has been suggested in the references - DUVA001 and WANG001. This method involves partitioning the fuselage six-degrees-of-freedom model into longitudinal, lateral, and cross-coupling subsets, shown here:

$$\begin{pmatrix} \dot{\underset{\sim}{X}}_{LONG} \\ \dot{\underset{\sim}{X}}_{LAT} \end{pmatrix} = \begin{pmatrix} A_{11} & A_{12} \\ A_{21} & A_{22} \end{pmatrix} \begin{pmatrix} \underset{\sim}{X}_{LONG} \\ \underset{\sim}{X}_{LAT} \end{pmatrix} + \begin{pmatrix} B_{11} & B_{12} \\ B_{21} & B_{22} \end{pmatrix} \begin{pmatrix} \underset{\sim}{U}_{LONG} \\ \underset{\sim}{U}_{LAT} \end{pmatrix} \qquad (3.2\text{-}43)$$

It is proposed that the partition matrices: A_{11} and B_{11}, are best identified by applying the equation-error technique to data generated by a longitudinal input, and neglecting the effects of the lateral states and controls. Once these matrices have been identified, a constraint Equation is constructed as:

$$\underset{\sim}{Y} = \dot{\underset{\sim}{X}}_{LONG} - A_{11} \underset{\sim}{X}_{LONG} - B_{11} \underset{\sim}{U}_{LONG} \qquad (3.2\text{-}44)$$

The new dependent variable $\underset{\sim}{Y}$ is generated from a lateral-input manoeuvre, and is the residual due to the unidentified cross-coupling terms (A_{11} and B_{11} were identified at the previous longitudinal-input stage). The cross-coupling terms are then estimated by applying the equation-error technique to the data-set generated from the lateral input, using the Equation:

$$\underset{\sim}{Y} = A_{12} \underset{\sim}{X}_{LAT} + B_{12} \underset{\sim}{U}_{LAT} \qquad (3.2\text{-}45)$$

The cross-coupling matrices A_{12} and B_{12} are thus

estimated in such a way that they are consistent with the A_{11} and B_{11} matrices obtained from the longitudinal manoeuvre. A similar approach is used in identifying the lateral force and moment matrices.

It is pointed out in the reference DUVA001, that in theory, the method could be used to identify rotor derivatives corresponding to fast modes and fuselage derivatives corresponding to slow modes independently, whilst combining them in a consistent fashion. The frequency content of each manoeuvre would be separated into a high and low frequency portion, and a process similar to that outlined above for the fuselage derivatives alone, could be carried out.

In the reference DUVA001, some results are presented where "the method of successive residuals" is applied to time-domain data generated for a linear simulation. A comparison was made of the estimates of the cross-coupling derivates obtained from this approach, with those obtained by identifying uncoupled and cross-coupled terms simultaneously on a data set containing longitudinal and lateral manoeuvres. This data set involved one set of time-history records placed directly after another, and the stacking of data in this way is permissible because the regression looks only for correlations, and is unaffected by discontinuities. The estimates of the cross-coupling terms were found to be superior when "the method of successive residuals" was used.

The use of combined data sets from several manoeuvres has been a commonly used, and advocated, approach for helicopter system identification (e.g. KALE001, MOLU001); however, as is pointed out in DUVA001: the problem with this approach is that some states are poorly excited in one manoeuvre, and well excited in another, so that combining the data tends to degrade the identification, in comparison to that obtained using only the well-excited data.

"The method of successive residuals" was investigated by the current author using simulated linear data obtained from the HELISTAB program. Noise was added to the dependent variables (i.e. the state time derivatives) to make the simulation more realistic. A variation on the originally proposed method was also tried, where for example with a longitudinal input, the lateral states were not assumed to be negligible, and all parameters known to non-zero were included in the initial stage of the identification procedure. The cross-coupling estimates obtained at the initial stage were then effectively disgarded; the intention being to estimate these at the second stage, using a lateral test input.

Results obtained from this investigation are presented in the reference BLAC003. It was also concluded by the current author, that "the method of successive residuals" was better in estimating the cross-coupling derivatives than the use of stacked data.

However, in some cases the variation on the original method (as described before) gave the best estimates, whilst in others the originally proposed method gave the best estimates. When there was a substantial difference in accuracy (i.e. when compared to the true values) this was seen to be reflected in the relative values of the partial-F statistics.

The main results obtained from this study, which were carried forward into the identification methodology developed in this document - remembering that the equation-error technique is seen more in terms of providing good initial estimates for use in the output-error method, than in being an end in itself - were as follows:

Firstly, single-run identification, where only one control at a time is used in applying the test input signal, is not an unreasonable approach to the problem of helicopter system identification. Data sets at exactly the same flight condition may not be available to apply the multirun approach, and also as was pointed out earlier, the use of such data often leads to the deterioration of some estimates in comparison to the single-run case.

Secondly, provision for the effects of lateral states for models identified using longitudinal inputs (and vice versa) should be made. This is accomplished in the implementation of the equation-error technique described in Section 3.2.5, and demonstrated using real

flight-data in the sub-Sections corresponding to 3.3. In the application of the frequency-domain output-error method, where for example a longitudinal test input is used, the lateral states are included in an extended control vector; this was shown for the example given in Section 2.3.3, and the corresponding case for the application of a lateral test input is shown in Section 4.3.2, where the cross-coupling derivatives are estimated as if they were elements of the control dispersion matrix.

And finally, the fact that some derivatives were best estimated with one model structure, and some with another (e.g. the inclusion or exclusion of cross-coupling terms) emphasized the importance of investigating the effect of model structure, and of determining a suitable one. The method for the determination of a suitable model structure, proposed in this document for the equation-error technique, has similarities with some of the features associated with the two applications of the equation-error method described in this Section (method of successive residuals), and in the previous Section (subset regression).

3.2.4 Parameter Significance Values.

There is a requirement to determine which parameters are contributing significantly towards the helicopter

motion, and which parameters are not, and can therefore be excluded from the identification, where the identification technique in mind is the output-error method. We would expect that parameters which only have a minor influence on the vehicle motion would not be estimated with great confidence. An indication of whether a parameter is weak or strong can be provided by the equation-error stage.

In the reference KALE001, the author defines measures of significance for individual parameters, based on the absolute integral of the time response over the time span used in the identification multiplied by the estimated parameter value, and normalised by the absolute integral of the dependent variable. Any other 'vector norm' which gives some indication of the size of the response, such as the root-mean square, could equally well be used instead. Taking the example of the pitching-moment Equation in the time domain, this leads to measures such as:

$$|M_u| \int |u(t)|\,dt \Big/ \int |\dot{q}(t)|\,dt$$

(3.2-46)

$$|M_w| \int |w(t)|\,dt \Big/ \int |\dot{q}(t)|\,dt$$

The same concept was extended into the frequency domain by the current author. Here, the integration is carried out over the range of frequencies used in the identification, and the magnitudes of the Fourier transform are used instead of the magnitudes of the time responses. These frequency-domain measures of parameter

significance take the form:

$$|M_u| \int |\hat{U}(\omega)|\, d\omega \Big/ \int |\hat{q}(\omega)|\, d\omega$$

$$|M_w| \int |\hat{W}(\omega)|\, d\omega \Big/ \int |\hat{q}(\omega)|\, d\omega \qquad (3.2\text{-}47)$$

Parameter significance values are demonstrated in Section 3.3.5 using real flight-data.

3.2.5 An Implementation Of The Equation-Error Method Using Singular-Value Decomposition.

Ill Conditioning Of The Information Matrix.

We can see from Equation (3.2-7) that the parameter estimates $\hat{\underset{\sim}{\Theta}}$, for the equation-error method, are obtained formally by solving a linear matrix Equation; that is by inverting the square matrix $(X^T X)$ (i.e. the equation-error information matrix - though strictly speaking $\frac{1}{\sigma^2} X^T X$ is the maximum-likelihood information matrix, whose inverse gives the parameter covariance matrix). From the expression for the parameter covariance matrix given in (3.2-12), we can see that in order to have uncorrelated parameter estimates, we would require the responses of the independent variables, written as columns of the matrix X, to be orthogonal; this would result in a diagonal parameter covariance matrix. The precision of the parameter estimates (i.e. the error bounds) are given by the diagonal elements of the matrix $(X^T X)^{-1}$.

Correlations between some of the response variables will result in some columns of X^TX being almost linearly dependent; in addition, the presence of insensitive variables in the model will result in some of the columns of X^TX being all zero: in both cases the result is the same - the matrix X^TX will be 'nearly singular'.

If we write the matrix linear Equation which represents the solution to the equation-error problem in the form

$$A\hat{\underset{\sim}{\Theta}} = \underset{\sim}{b} \tag{3.2-48}$$

we have from Equation (3.2-7)

$$A \triangleq X^TX \tag{3.2-49}$$

$$\underset{\sim}{b} \triangleq X^T\underset{\sim}{y} \tag{3.2-50}$$

A measure of the sensitivity of the relative error in $\hat{\underset{\sim}{\Theta}}$ to changes in the right-hand-side vector $\underset{\sim}{b}$, and to changes in the matrix A, is given by the condition number of A (STOE001). There are several ways of defining the condition number. It can be shown that the ratio of the largest and smallest eigenvalues of the matrix A can be used. An inequality relating the relative change in the solution, to the condition number of the matrix A, and to a relative change in the right-hand-side vector $\underset{\sim}{b}$ is derived in the reference STOE001; in the context of the

equation-error solution considered here, it can be written as:

$$\|\Delta\hat{\underset{\sim}{\theta}}\| / \|\hat{\underset{\sim}{\theta}}\| \leqslant \|A\| \, \|A^{-1}\| \, \|\Delta \underset{\sim}{b}\| / \|\underset{\sim}{b}\| = \mathrm{Cond}(A) \, \|\Delta \underset{\sim}{b}\| / \|\underset{\sim}{b}\| \qquad (3.2\text{-}51)$$

where $\| \; \|$ represents a norm, and the condition number: $\mathrm{Cond}(A) \triangleq \|A\| \, \|A^{-1}\|$. It is also shown in STOE001 that the condition number can be used to measure the sensitivity of the solution to changes in the matrix A.

If the information matrix (i.e. $X^T X$) - represented in the foregoing discussion as A - is 'nearly singular', it will have at least one relatively small eigenvalue, and consequently has a large condition number.

From (3.2-51) it can be seen that it is desirable from the point of view of the accuracy of the parameter estimates, to have a small condition number for the information matrix. This is true of the equation-error technique discussed here, and the output-error technique discussed in Chapter 4 (the conditioning of the output-error information matrix is discussed in Section 4.2.3). It is observed by the current author that the lowest upper-bound of the parameter-estimate errors - defined in terms of the norm $\| \; \|$ - is proportional both to the condition number of the information matrix and the relative-error in the vector $\underset{\sim}{b}$ (again defined in terms of the norm $\| \; \|$). Furthermore, we can use the definition of $\underset{\sim}{b}$, given in (3.2-50), to associate errors in $\underset{\sim}{b}$ with the

noise on the dependent variable $\underset{\sim}{Y}$. These observations are consistent with the expression for the parameter-estimates error given in Equation (3.2-12), which has two independent components: a scalar component σ^2 - estimated as S^2 given in Equation (3.2-14) - and which can be associated with $\|\Delta b\|/\|b\|$ in (3.2-51); and a matrix component $(X^TX)^{-1}$ which can be associated with $\mathrm{Cond}(A)$ in (3.2-51).

The implementation of the equation-error method used by the current author, and which is described in detail below, allows information matrices, which are of reduced rank, but which have a lower condition number, to be used in the identification. The ill-conditioning of the higher-rank problem is seen as an indication of the requirement to restructure the model; and it is observed by the current author that this is equivalent to the introduction of relational constraints between the parameter values. The derivation of the solution of the least-squares problem using singular-value decomposition, is in essence, the same as is presented in the reference NASH001; some additional references to singular-value decomposition are JACO001 and KERR001.

<u>Singular-Value Decomposition.</u>

Consider the NxP matrix X given in Equation (3.2-4) containing the values for each of the independent variables arranged in columns. We can find a PxP

orthogonal matrix V which transforms X into another NxP matrix B, whose columns are orthogonal. We will have:

$$B = XV = (b_1, b_2, \ldots b_p) \qquad (3.2\text{-}52)$$

where $b_i^T b_j = 0 \quad i \neq j$
$\qquad\qquad\quad = s_i^2 \quad i = j$

s_i^2 represents the squared magnitude of each of the NX1 column vectors b_i; the positive squared roots of these are referred to as the singular values of the matrix X. For non-zero singular values we may obtain unit-orthogonal vectors from:

$$U_i = b_i / s_i \qquad (3.2\text{-}53)$$
$$s_i \neq 0$$

We may separate the matrix of unit-orthogonal vectors, and the corresponding magnitudes of the original orthogonal vectors, into two matrices.

$$B = US \qquad (3.2\text{-}54)$$

S is a diagonal matrix with the singular values arranged in descending order down the leading diagonal. Equating (3.2-52) and (3.2-54), and using the orthogonal property of V, we have the singular-value decomposition of the matrix X.

$$X = USV^T \tag{3.2-55}$$

If we write the least-squares problem given in (3.2.4) as

$$\underset{\sim}{Y} \doteq X\hat{\underset{\sim}{\Theta}} \tag{3.2-56}$$

and use (3.2-54) and (3.2-55) in the above, we have

$$\underset{\sim}{Y} \doteq USV^T\hat{\underset{\sim}{\Theta}} = US\hat{\underset{\sim}{\phi}} = B\hat{\underset{\sim}{\phi}} \tag{3.2-57}$$

$$V^T\hat{\underset{\sim}{\Theta}} = \hat{\underset{\sim}{\phi}} \tag{3.2-58}$$

The matrix B contains in its columns the principal components of the matrix X; these correspond to new sets of orthogonal independent-variable responses that relate to the new set of parameters $\underset{\sim}{\phi}$. Estimates of the original model parameters $\underset{\sim}{\Theta}$ can be obtained from estimates of $\underset{\sim}{\phi}$, remembering that the matrix V is orthogonal.

From (3.2-57), it can be seen that the normal Equations corresponding to the least-squares solution of $\underset{\sim}{Y} \doteq B\hat{\underset{\sim}{\phi}}$ are:

$$B^T\underset{\sim}{Y} = B^TB\hat{\underset{\sim}{\phi}} = S^2\hat{\underset{\sim}{\phi}} \tag{3.2-59}$$

Since S^2 is a square diagonal matrix, least-squares solutions for $\underset{\sim}{\phi}$ are easily obtained as:

$$\hat{\underset{\sim}{\phi}} = S^{-2} B^T \underset{\sim}{Y} \tag{3.2-60}$$

And using (3.2-54) we have:

$$\hat{\underset{\sim}{\phi}} = S^{-1} U^T \underset{\sim}{Y} \tag{3.2-61}$$

where it is assumed that all the singular values are non zero. In the case of real data this will almost certainly be the case. However, the problem of zero singular values can still be overcome in the quest for a solution, by effectively setting the corresponding element of $\hat{\underset{\sim}{\phi}}$ in (3.2-59) to zero. In fact, for relatively small non-zero singular values, it may be desirable to assume that the corresponding element of $\hat{\underset{\sim}{\phi}}$ is zero. The solution can still be written in a form equivalent to Equation (3.2-61), where S_{ii}^{-1} is replaced by S_{ii}^{+}, which is defined as:

$$\begin{aligned} S_{ii}^{+} &= 1/s_i \qquad i \leq r \\ &= 0 \qquad i > r \end{aligned} \tag{3.2-62}$$

where r is the number of non-zero singular values retained in the diagonal matrix S and arranged in descending order of magnitude down the leading diagonal. Solutions corresponding to the inclusion of the r most significant singular values in the solution are known as principal component solutions. This may be summarised by the following.

$$\tilde{\underset{\sim}{\phi}} = S^{+}U^{T}\underset{\sim}{Y} \tag{3.2-63}$$

$$\hat{\tilde{\phi}}_i = 0 \qquad i > r \tag{3.2-64}$$

$$\hat{\underset{\sim}{\tilde{\phi}}}(r) \triangleq (\hat{\tilde{\phi}}_1, \hat{\tilde{\phi}}_2, \ldots \hat{\tilde{\phi}}_r, 0, 0, 0)^{T} \tag{3.2-65}$$

Using (3.2-58), we can relate the parameter estimates $\hat{\underset{\sim}{\Theta}}$ for the original least-squares problem given in (3.2-56), in terms of the estimates of the transformed variables $\hat{\underset{\sim}{\tilde{\phi}}}(r)$ given by (3.2-63 - 3.2-65):

$$\hat{\underset{\sim}{\Theta}} = V^{T}\hat{\underset{\sim}{\tilde{\phi}}}(r) \tag{3.2-66}$$

It is noted by the current author that by using $\hat{\underset{\sim}{\tilde{\phi}}}(r)$, as defined in (3.2-65), in order to estimate $\hat{\Theta}$, P-r relational constraints are introduced into the estimation; this means that the estimation is carried out in a subspace of the original parameter space.

<u>Covariance Matrix.</u>

Expressions for the covariance matrix of the parameter estimates corresponding to principal component solutions are not given in the reference NASH001, but are easily derived as follows. Using (3.2-54) and (3.2-57), we have from (3.2-12) that

$$\mathrm{Cov}(\tilde{\underset{\sim}{\phi}} - \underset{\sim}{\phi}) = \sigma^{2} S^{-2} \tag{3.2-67}$$

And using (3.2-58) we have that

$$\mathrm{Cov}(\hat{\underset{\sim}{\Theta}} - \underset{\sim}{\Theta}) = V\,\mathrm{Cov}(\hat{\underset{\sim}{\phi}} - \underset{\sim}{\phi})V^{T} \qquad (3.2\text{-}68)$$

In the case of principal component solutions indicated by (3.2-66) S^{-1} is replaced by S^{+} defined in (3.2-62).

<u>Reduction In The Expected Value Of The Residual Sum Of Squares.</u>

For estimates $\hat{\underset{\sim}{\Theta}}$, and measurements of the dependent variable $\underset{\sim}{Y}$, we can write the residual sum of squares as:

$$\sum_i e^2(i) = (\underset{\sim}{Y} - X\hat{\underset{\sim}{\Theta}})^{T}(\underset{\sim}{Y} - X\hat{\underset{\sim}{\Theta}}) = (\underset{\sim}{Y} - B\hat{\underset{\sim}{\phi}})^{T}(\underset{\sim}{Y} - B\hat{\underset{\sim}{\phi}}) \qquad (3.2\text{-}69)$$

This can be easily rearranged to give:

$$\sum_i e^2(i) = \underset{\sim}{Y}^{T}\underset{\sim}{Y} - \underset{\sim}{Y}^{T}B\hat{\underset{\sim}{\phi}} - \hat{\underset{\sim}{\phi}}^{T}B^{T}(\underset{\sim}{Y} - B\hat{\underset{\sim}{\phi}}) \qquad (3.2\text{-}70)$$

In NASH001, the expression:

$$\sum_i e^2(i) = \underset{\sim}{Y}^{T}\underset{\sim}{Y} - \underset{\sim}{Y}^{T}B\hat{\underset{\sim}{\phi}} \qquad (3.2\text{-}71)$$

is written, without comment, as a strict equality; however, this assumes that the term $\hat{\underset{\sim}{\phi}}^{T}B^{T}(\underset{\sim}{Y} - B\hat{\underset{\sim}{\phi}})$ is exactly zero, which is not true. Certainly, if the residuals: $(\underset{\sim}{Y} - B\hat{\underset{\sim}{\phi}})$ are zero-mean and uncorrelated, the expected value of the residual sum of squares is given by the right-hand

side of (3.2-71), that is:

$$E[\sum_i e^2(i)] = \underset{\sim}{Y}^T \underset{\sim}{Y} - \underset{\sim}{Y}^T B \hat{\underset{\sim}{\phi}} \tag{3.2-72}$$

Using (3.2-54) and (3.2-63) we can rewrite (3.2-72) as:

$$E[\sum_i e^2(i)] = \underset{\sim}{Y}^T \underset{\sim}{Y} - \sum_{i=1}^{r} (U^T \underset{\sim}{Y})_i^2 \tag{3.2-73}$$

where r is the number of orthogonal components used. Hence as r increases, it is the expected value of the residual sum of squares which must decrease rather than the calculated residual sum of squares, for an increase in the number of orthogonal components used. As can be seen from (3.2-70), the predicted values of the dependent variable (i.e. $B\hat{\underset{\sim}{\phi}}$) would have to differ substantially from the measured values $\underset{\sim}{Y}$ over a sizeable portion of the data for the calculated residual sum of squares to increase, for the inclusion of an extra orthogonal component in the solution. This is possible for helicopter flight-data represented in the frequency domain even when good fits, with large values of the squared correlation coefficient R^2, are obtained. If there is a region of the frequency range used in the identification, where the discrete Fourier transforms have a relatively small magnitude in comparison to the important modal effects which are modelled by the fit, a small decrease in the calculated residual sum of squares could occur for the inclusion of an additional orthogonal

component that does not contribute to any real improvement in the fit; this would indicate that further orthogonal components should not be included in the model.

Some Comments On The Condition Number And On Ill-Conditioning Due To Bad Scaling.

Equation-error solutions for the use of the r most significant orthogonal components correspond to the use of an information matrix which is better conditioned than that for the usual equation-error solution where all the orthogonal components are present. This is because the condition number of the information matrix can be defined as the ratio of its largest and smallest eigenvalues. It is shown below that the use of only a subset of the most significant orthogonal components corresponds to the removal of the smallest eigenvalues from the information matrix; whether this is a valid modelling step or not is a separate issue.

For the equation-error information matrix $X^T X$, we have, using the singular-value decomposition of the matrix X given in Equation (3.2-55) that:

$$X^T X = (USV^T)^T (USV^T) = V \Omega V^T \qquad (3.2\text{-}74)$$

where $\Omega_{ii} = S_{ii}^2$. This is the familiar eigenvalue-eigenvector factorisation result often given in texts on

linear algebra (e.g. MURD001). The P eigenvalues of the information matrix X^TX are equal to the squared singular values of the matrix X.

If the dependent variable $\underset{\sim}{Y}$ is best approximated by an orthogonal variable corresponding to a column of B associated with a small singular value, then the problem is ill-conditioned due to bad scaling of the data. For applications of regression, it is often recommended that if the independent variables differ substantially in order of magnitude that a correlation transformation be applied, where the variables are described as perturbations about their estimated mean values, normalised by the respective estimated standard deviations.

3.2.6 Practical Application Of The Singular-Value-Decomposition Approach To Frequency-Domain System Identification.

The singular-value-decomposition approach was implemented in a FORTRAN-77 program - SINGVAL; details of the program are given in BLAC006. The program was written especially to perform frequency-domain identification, and incorporates all the features outlined in this document that are special to the frequency-domain implementation of the equation-error method.

The program enables the user to investigate with ease, the effect on the identification of varying the

number of orthogonal components. That is, it provides information concerning the effect of changing the model structure on the estimated parameter values, on the indicated accuracy of individual parameters (using partial-F statistics), on the indicated significance of individual parameters (using parameter significance values), and on indicators of the accuracy and goodness of the overall fit (using the total F statistic and the squared correlation coefficient).

For the practical application of the method to helicopter flight-data using the frequency domain, the most convenient approach was found to involve building up the model from a small number of orthogonal components - possibly 1 - up to the case where all the orthogonal components are used, corresponding in form to the usual least-squares solution obtained using the matrix pseudo inverse. It is the value of the squared-correlation coefficient R^2 which is the most immediate and most useful indicator of how additional orthogonal components are affecting the solution. A progressive increase in the value of R^2 as the number of orthogonal components increases up to a certain number, followed by negligible increases for additional components, may indicate that the orthogonal components corresponding to the smaller singular values should be excluded from the solution, since these components will consist essentially of noise. In addition, factors including the physical realism of the estimates themselves, and their indicated accuracies,

can be used by the analyst in choosing the 'optimum' number of orthogonal components for the solution. In the reference NASH001, the use of tolerances relating to the magnitudes of the singular values, is presented as a means of deciding if a particular orthogonal component should be excluded from the least-squares solution. For the relatively few points used in helicopter frequency-domain identification it is possible to consider the effect of all possible combinations of orthogonal components on the solution, very quickly, thus rendering the specification of tolerances on the singular values unnecessary.

The ideas given above on the selection of an appropriate number of orthogonal components are demonstrated using real flight-data in Section 3.3.4.

<u>(NAG) Library Routines Used To Carry Out The Singular-Value Decomposition And Computational Details.</u>

The program SINGVAL uses the NAG routine F02WAF (NAG004) to carry out the singular-value decomposition of the frequency-domain independent-variable matrix X.

As a result of the reduction in the amount of data used in the identification, when the frequency domain is used, the dimensions of the vector and matrix quantities involved in performing the singular-value decomposition will be relatively small when compared to those involving the use of time-domain data. For example, the number of

data points in the flight-data sets used for the work carried out in this document, is typically 1500; when transformed into the frequency domain, the number of data points (i.e. real and imaginary parts) used in the identification is about 20. For N data values and P parameters, the timing of the singular-value decomposition of the NxP matrix for the NAG routine F02WAF is quoted as being approximately proportional to $P^2(N+6P)$ (NAG004); this means that for the Figures quoted before, the time to perform a singular-value decomposition using frequency-domain data is only 1.3% of the time required to carry out the corresponding calculation in the time domain. For equation-error identification, this is a strong point in favour of the use of frequency-domain data.

3.2.7 Some Comments On The Use Of Zero Pads In Frequency-Domain Identification.

For the discrete Fourier transform, the frequency resolution is determined solely by the length of the time-domain record used. This is unfortunate in the context of helicopter system identification in view of the difficulty of obtaining long records. In the reference PADF002, the use of zero-pads is suggested as a possible means of reducing the spacing between the frequency-domain points; the motivation being a more accurate estimation of the low-frequency modes which are

difficult to identify from a data record of limited duration. Zero-padding has been used in spectral analysis to smoothen the appearance of calculated power spectra (e.g. BUCK002). However, the use of zero-padding is, in the opinion of the current author, not an appropriate technique for system identification. A proof is offered below which shows that when zero-padding is used, the modelled noise term is in fact correlated with itself over a range of frequencies. It follows from the discussion given in Section 3.2.1, and in particular from Equation (3.2-30), that this will lead to biased estimates.

The argument proposed by the current author first shows that zero-padding the time-domain data is equivalent to using a complex-valued, unit magnitude, set of weights on the original time-domain data in order to obtain an expression for the discrete Fourier transform at a frequency value lying between two integer multiples of the fundamental. Consider a data record of N sampled values padded with an additional (L-1) x N zeros, where L is a positive integer. We have for the discrete Fourier transform of a quantity $V(i\Delta t)$:

$$\hat{V}(\omega_K) = 1/\sqrt{N} \sum_{i=0}^{LN-1} V(i\Delta t)\, e^{-j\omega_K i\Delta t} \qquad (3.2\text{-}75)$$

where $\omega_K = 2\pi K/LN\Delta t$, $K = 0,1,2 \ldots LN-1$; $V(i\Delta t) = 0$ for $i > N-1$; and $\omega_F \triangleq 2\pi/N\Delta t$. We can write:

$$\omega_K = [K/L]\,\omega_F + q/L\,\omega_F \tag{3.2-76}$$

Hence (3.2-75) can be rewritten as:

$$\hat{V}(\omega_K) = 1/\sqrt{N} \sum_{i=0}^{N-1} V(i\Delta t)\, e^{-j([K/L]\omega_F + q\omega_F/L)i\Delta t} \tag{3.2-77}$$

If we write the integer [K/L] as r, and the fraction of the fundamental frequency $q\omega_F/L$ as $q\Delta\omega_F$, we have that:

$$\hat{V}(\omega_r + q\Delta\omega_F) = 1/\sqrt{N} \sum_{i=0}^{N-1} \left(V(i\Delta t)\, e^{-jq\Delta\omega_F i\Delta t}\right) e^{-j\omega_r i\Delta t} \tag{3.2-78}$$

For integer multiples of the fundamental frequency, i.e. q=0, Equation (3.2-78) corresponds to the usual discrete Fourier transform; however, $\hat{V}$ is also defined for equi-spaced frequency values lying between integer multiples of the fundamental, with the spacing $\Delta\omega_F = \omega_F/L$, dependent on the L-1 sets of zero pads used.

For a zero-mean, uncorrelated, stationary random variable : $V(i\Delta t)$ defined for $i=0,1,\ldots N-1$, it will now be proved that $\hat{V}(\omega_r)$ is correlated with all $\hat{V}(\omega_r + q\Delta\omega_F)$ defined for all the interspersed frequencies $q\Delta\omega_F = q\omega_F/L \neq K\omega_F$, where K is an integer. We have using Equation (3.2-78) for the scalar quantity $V(i\Delta t)$ that:

$$E[\hat{V}(\omega_r)\hat{V}^*(\omega_r + q\Delta\omega_F)] =$$

$$E\left[1/N \sum_{i,m=0}^{N-1} V(i\Delta t)V(m\Delta t)\, e^{-j\omega_r i\Delta t} \cdot e^{j\omega_r m\Delta t} \cdot e^{-jq\Delta\omega_F i\Delta t}\right] \tag{3.2-79}$$

For a random variable with the characteristics given

above, and whose variance is given by σ_N^2, we have, taking the expectation operator into the summation, and noting that:

$$E[V(i\Delta t)V(m\Delta t)] = \sigma_N^2 \qquad i = m$$
$$= 0 \qquad i \neq m \tag{3.2-80}$$

the following result:

$$E[\hat{V}(\omega_r)\hat{V}^*(\omega_r + q\Delta\omega_F)] = \sigma_N^2/N \sum_{i=0}^{N-1} e^{-jq\Delta\omega_F i\Delta t} \tag{3.2-81}$$

The case corresponding to q=0 has already been effectively considered in Section 2.2.5, (where the equi-distribution between the real and imaginary parts of the transform of an appropriately conditioned random variable was shown); this gives:

$$E[\hat{V}(\omega_r)\hat{V}^*(\omega_r)] = \sigma_N^2/N \sum_{i=0}^{N-1} 1 = \sigma_N^2 \tag{3.2-82}$$

For $q\Delta\omega_F = K\omega_F$, that is for a separation equal to an integer multiple K of the fundamental frequency; we have:

$$E[\hat{V}(\omega_r)\hat{V}^*(\omega_{r+K})] = \sigma_N^2/N \sum_{i=0}^{N-1} e^{-jK\omega_F i\Delta t} =$$

$$\sigma_N^2/N \sum_{i=0}^{N-1} e^{\frac{-j2\pi iK}{N}} = \frac{(1 - e^{-j2\pi K})}{(1 - e^{\frac{-j2\pi K}{N}})} = 0 \tag{3.2-83}$$

where $1 \leqslant K < N$. This shows that $\hat{V}(\omega_r)$ and $\hat{V}(\omega_{r+K})$, which correspond to frequencies considered for the usual application of the discrete Fourier transform, are

uncorrelated. For all the other interspersed frequencies, we have from (3.2-81), that:

$$\sigma_N^2/N \sum_{i=0}^{N-1} e^{-jq\Delta\omega_F i\Delta t} = \sigma_N^2/N \sum_{i=0}^{N-1} e^{-\frac{jqi2\pi}{LN}} =$$

$$\sigma_N^2/N \frac{(1 - e^{\frac{-j2\pi q}{L}})}{(1 - e^{\frac{-j2\pi q}{LN}})} \neq 0 \qquad (3.2\text{-}84)$$

for $q/L \neq K$, where K is an integer. Hence the modelled noise term is correlated when zero padding is used, thus rendering the use of zero pads to be inappropriate for identification purposes, if biased parameter estimates are to be avoided. The occurrence of biased estimates when zero-padding is used was demonstrated practically by the current author by obtaining some equation-error fits with zero-padded data sets. In fact, it was the results from the practical application of the technique which first suggested that biased estimates were being obtained; the proof given above was then formulated.

3.2.8 A Summary Of Section 3.2.

The equation-error method has been presented as the first stage in the identification methodology, providing initial estimates of model parameters. A frequency-domain formulation of the method, using the real and imaginary parts of the Fourier transform, was derived. Also, a means of determining a suitable model structure, through the use of singular-value decomposition, was

advocated. It was pointed out that the equation-error stage can also be used to indicate the significance of a given parameter in the aircraft motion, thus assisting in the determination of a suitable model structure for the output-error method.

Some observations relating to the frequency-domain aspect of the identification method were made. These included the implications for algorithmic efficiency as a result of using a relatively small number of data, similarities between the use of an instrumental-variable matrix in the time domain and the use of a restricted frequency range in the identification, following a discrete Fourier transformation of the data, and the fact that zero-padding used in an attempt to increase frequency resolution, will result in biased parameter estimates.

3.3 Applications Of The Singular-Value-Decomposition Frequency-Domain Equation-Error Method To Flight Data.

3.3.1 Flight Data Sets And Basic Model Equations Used.

The singular-value-decomposition frequency-domain equation-error method will be demonstrated using real flight data. Several data sets will be used, and results presented, with a view to highlighting some important aspects of the identification. Two data sets which are

considered in detail, correspond to the application of longitudinal cyclic and pedal doublet inputs. The longitudinal-cyclic data set is that which was considered in Section 2.3.3, where the output-error method was applied, although in practice, the equation-error method was used before the output-error method. This flight-data set is labelled as run R0201A. The pedal data set is labelled as run R1201L, and is also used in the application of the output-error method in Section 4.3.2. Both flight-data sets are taken from a Puma helicopter, in straight and level flight, with a nominal trim speed of 100 knots. The data is sampled at a frequency of 64 Hz.

Longitudinal Equations.

The data from the single longitudinal-cyclic manoeuvre was directly transformed into the frequency domain. The portion of data used was about 13.3 seconds in length, giving a spacing between points in the frequency domain of about 0.0752 Hz. The frequency-domain values of quantities used in the actual identification were obtained from the frequency-domain values of measured quantities using the Equations given in (3.3-36). The two longitudinal Equations considered (pitching moment and normal force) have the following frequency-domain representation:

$$\hat{q}(\omega) = M_u \hat{U}(\omega) + M_w \hat{W}(\omega) + M_q \hat{q}(\omega) + M_v \hat{V}(\omega) + M_p \hat{p}(\omega) + M_{\eta_{1s}} \hat{\eta}_{1s}(\omega) \tag{3.3-1}$$

$$\hat{\dot{W}}(\omega) - U_e \hat{q}(\omega) = Z_u \hat{U}(\omega) + Z_w \hat{W}(\omega) + Z_\theta \hat{\Theta}(\omega) + Z_v \hat{V}(\omega) + Z_p \hat{p}(\omega) + Z_\phi \hat{\phi}(\omega) + Z_{\eta_{1s}} \hat{\eta}_{1s}(\omega) \tag{3.3-2}$$

where U_e represents the forward trim velocity. The transforms of time derivatives $\hat{\dot{q}}(\omega)$ and $\hat{\dot{W}}(\omega)$ are obtained from the transforms $\hat{q}(\omega)$ and $\hat{W}(\omega)$ as described in Section 2.2.3.

<u>Lateral Equations.</u>

For the pedal-doublet data set, the two lateral Equations considered (rolling moment and yawing moment) have following frequency-domain representation:

$$\hat{\dot{p}}(\omega) = L_u \hat{U}(\omega) + L_w \hat{W}(\omega) + L_q \hat{q}(\omega) + L_v \hat{V}(\omega) + L_p \hat{p}(\omega) + L_r \hat{r}(\omega) + L_{\eta_p} \hat{\eta}_p(\omega) \tag{3.3-3}$$

$$\hat{\dot{r}}(\omega) = N_u \hat{U}(\omega) + N_w \hat{W}(\omega) + N_q \hat{q}(\omega) + N_v \hat{V}(\omega) + N_p \hat{p}(\omega) + N_r \hat{r}(\omega) + N_{\eta_p} \hat{\eta}_p(\omega) \tag{3.3-4}$$

The portion of data used was about 26.6 seconds in length, giving a spacing between points in the frequency domain of about 0.0376 Hz.

Incorporation Of Time Delays Into The Equations.

The incorporation and estimation of a time delay in the control channel used by the pilot is an important feature of the identification methodology developed in this document. It is primarily seen as a feature most appropriately and most easily accomplished at the frequency-domain output-error stage of the identification methodology. However, using a first-order approximation to the complex exponential $e^{-j\omega\tau}$ (valid for small delays τ and small frequency values ω, as explained in Section 1.2.5) the following means for the estimation of delays using the equation-error method was developed by the current author. For a time-delayed quantity $C(t-\tau)$, where τ is the delay, and whose coefficient in an Equation (such as those given in 3.3-1 - 3.3-4) is K_c, we have for the frequency-domain representation that:

$$K_c(1-j\omega\tau)\hat{C}(\omega) \doteq K_c e^{-j\omega\tau}\hat{C}(\omega) \qquad (3.3\text{-}5)$$

Taking the first-order form and splitting it into its real and imaginary components, we have:

$$K_c(1-j\omega\tau)\hat{C}(\omega) = K_c(R_e[\hat{C}(\omega)] + \omega\tau I_m[\hat{C}(\omega)]) +$$

$$jK_c(I_m[\hat{C}(\omega)] - \omega\tau R_e[\hat{C}(\omega)]) \qquad (3.3\text{-}6)$$

The right-hand-side of Equation (3.3-6) can be rewritten with terms having the same coefficient:

$$K_c(1-j\omega\tau)\hat{C}(\omega) = K_c R_e[\hat{C}(\omega)] + jK_c I_m[\hat{C}(\omega)] + K_s R_e[\hat{S}(\omega)] + jK_s I_m[\hat{S}(\omega)] \tag{3.3-7}$$

where

$$R_e[\hat{S}(\omega)] \triangleq \omega I_m[\hat{C}(\omega)]$$

$$I_m[\hat{S}(\omega)] \triangleq -\omega R_e[\hat{C}(\omega)] \tag{3.3-8}$$

$$K_s \triangleq K_c\tau$$

We may thus construct another independent variable in the frequency domain $\hat{S}(\omega)$, with coefficient K_s. Using the implementation of the frequency-domain equation-error method described in detail in Section 3.2.1, we have from the definitions given in (3.3-8) that the estimate of the delay can be obtained by taking the ratio of the estimates of the two coefficients K_s and K_c:

$$K_s / K_c = \tau \tag{3.3-9}$$

For the incorporation of a time delay in the control input, an additional independent variable, constructed as explained above, is included in Equations (3.3-1) to (3.3-4).

3.3.2 Selection Of Frequency Range.

The magnitudes of the Fourier-transform quantities

can be used as an indication of a suitable frequency range for use in the identification of rigid-body parameters. For example, the magnitudes of transforms used in the pitching-moment Equation, are shown in Figure 3-1 (for a magnitude log-frequency scale). It can be seen that above about 0.54Hz. (i.e. $\log_{10} f_c \sim -0.25$) the magnitudes of the Fourier transforms are small in comparison.

The number of data points used in frequency-domain helicopter system identification is relatively small, and it is an easy matter to investigate the effect of frequency range on the estimates. For the pitching-moment Equation, the effect of using a progressively higher upper-limit of frequency in the identification (the lower limit of frequency is fixed at the smallest non-zero value of 0.0752 Hz) is shown in Figures 3-2 and 3-3, where some parameter estimates and their partial-F statistics are shown in terms of both the frequency range and the number of orthogonal components used. The squared-correlation coefficient for the pitching-moment Equation is shown similarly in Figure 3-4. Focussing on the results corresponding to 5 orthogonal components, it can be seen in Figure 3-3 that peaks in the partial-F statistics (indicating highest confidence in the corresponding parameter estimates) are observed for an uppermost frequency of about 0.75 Hz.. The parameter estimates shown in Figure 3-2 have stabilised over this region for 5 orthogonal components.

Hence all the indicators - the magnitudes of the transforms, and the partial-F statistics - point to the use of an upper frequency value in the range 0.5 to 0.75 Hz., with the parameter estimates themselves showing no significant changes over this range. In Figure 3-5, the squared-correlation coefficient R^2 is presented as in Figure 3-4 except that the entire frequency range available (with an upper limit corresponding to the Nyquist folding frequency of 32 Hz.) is used. The value of R^2 can be seen to fall away from the high levels associated with a low frequency range as higher-order effects, not accounted for in the model, are brought into play. It is interesting to note that the final low value of the squared-correlation coefficient corresponds to carrying out the identification on the original raw flight-data in the time domain.

Equivalent Time-Domain Reconstruction For A Selected Frequency Range.

In Section 2.2.2, an interpretation of the use of a restricted frequency range in terms of an equivalent time-domain response was given. For one quantity (forward velocity) the effect of progressively increasing the number of frequency-domain points used (i.e. terms used in the Fourier series approximation) is shown in Figure 3-6, up to the point where all available points are used (corresponding to the original measured

response).

3.3.3 Length Of Time-Domain Record Used.

Figure 3-7 shows, for the pitching-moment Equation, the effect of the record length used on the parameter estimates obtained; the frequency range used in the identification is approximately up to 0.5 Hz., with 5 orthogonal components used for the solutions (this choice is discussed in the next Section). The estimates are seen to reach almost constant values as the record length approaches the time span used for the results presented here; however, it is clear in some cases, such as for $M_{\dot{p}}$, that a longer record than that which was available would have been desirable for the identification. The error bounds on the estimates are clearly decreasing with increasing record length: this is the consistency property of the estimator given by (3.2-26) in Section 3.2.1.

It is of interest to note that the parameters estimated with the greatest confidence, namely M_u and $M_{\eta_{is}}$, approach their final estimated values for much shorter record lengths than some of the other parameters.

If any credence is to be given to the identified model, it is important to ensure that the data records are of a duration which has allowed the parameter estimates to converge.

3.3.4 Selection Of An Appropriate Number Of Orthogonal Components.

Pitching Moment Equation.

Consider first the pitching-moment Equation, where the frequency-domain form of the Equation is as given by (3.3-1). The model incorporating an approximation to a time-delay in the control input will be considered secondly, and the form of Equation (3.3-1) corresponds to the results shown in Figures 3-2 - 3-4; tabulated parameter estimates for different numbers of orthogonal components are presented in Table 3-1 a).

For this example, the squared-correlation coefficient (R^2) is seen to increase. This is as would be expected in the statistical sense and is consistent with the discussion in Section 3.2.5 on the expected reduction of the residual sum of squares as more orthogonal components (associated with singular values of a progressively smaller magnitude) are used in the solution. The size of the increase in R^2 in going from one structure to another, can be seen from Table 3-2 a), to be associated with the 'significance' of the newly introduced orthogonal component. A convenient measure of 'parameter significance' (see Section 3.2.4) was seen by the current author to be given by the absolute product of the estimated coefficient of the orthogonal component - which remains unchanged for the addition of further

orthogonal components - and the associated singular value (which, as was explained in Section 3.2.5, represents the squared magnitude of the orthogonal component). In Table 3-2 b) partial-F statistics of the orthogonal variables are presented for the principal component solutions. It is interesting to note that for the solution corresponding to six orthogonal components (i.e. the conventional least squares solution), the least significant orthogonal component ϕ_6 is seen to have a partial-F statistic of less than unity, implying that the estimate is an approximation to zero: the sixth component may well be associated mostly with noise. The sixth orthogonal component can also be seen, from Table 3-2 a), to have a relatively small measure of 'parameter significance', defined by the absolute product of the orthogonal-variable estimate and the corresponding singular value (given in the Table as ABS. PRODUCT a) x b)).

The relatively small difference between the high values of R^2 given by 5 and 6 orthogonal components is one indicator that the solution corresponding to 5 orthogonal components may be selected. In deciding on the number of orthogonal components to use, the physical realism of the model estimates can also be taken into account, along with indicators of parameter accuracy (partial-F statistics and parameter significance). For example, the solution corresponding to 5 orthogonal components is seen to give the highest values of

partial-F statistics for the important parameters, M_u, M_q, $M_{\eta_{1s}}$ (see Figure 3-3); five orthogonal components also give the most physically realistic estimates - over all the other solutions shown - of pitch-damping M_q, M_p and control sensitivity $M_{\eta_{1s}}$.

The parameters M_q and M_p do not play a significant part in the solutions - and consequently, are estimated poorly - for the inclusion of up to 4 orthogonal components. For 5 orthogonal components, relatively large entries in the 3rd and 5th columns of the 5th row of the matrix V^T (relate to Equation 3.2-58 in Section 3.2.5), which is shown in Table 3 c), corresponds to the effective use of pitch rate and roll rate in the estimation. In Figure 3-8 'parameter significance' values are given for the model variables, for all the principal component solutions. They show the importance of M_u, M_w and $M_{\eta_{1s}}$ in the first few principal component solutions. However, the solution corresponding to 5 orthogonal components shows for the stability derivatives, 'parameter significance' values which are all of similar magnitude; these are included in Table 3-1 b).

The incorporation of a time delay in the control has been advocated throughout this document as a more appropriate means of producing parameter estimates that can be compared with theoretical values obtained from a quasi-static model. An approximate method for the incorporation, and estimation, of time delays using the frequency-domain equation-error method was offered in

Section 3.3.1. Parameter estimates are given in Table 3-3 a) and these are discussed in detail in the next Section. Using the same approach as for the case without the delay, it can be seen that this time, all the evidence points to the selection of the model with 7 orthogonal components. There are no principal-component solutions, with high values of R^2, which appear to have (associated with the smaller singular values) orthogonal components that are relatively insignificant (see Table 3-4 a), or that have very small partial-F statistics (see Table 3-4 b). 'Parameter significance' values and partial-F statistics of the model parameters, for the selected number of orthogonal variables are given by Table 3-3 b).

Tables 3-5 a) and 3-5 b) contain parameter estimates for the pitching-moment Equation without and with a time delay in the control respectively, for a wider frequency range of 0.075 to 0.753 Hz.; it can be seen that there is no significant difference from the estimates obtained for 0.075 to 0.527 Hz., for the selected number of orthogonal components.

Normal Force Equation.

The parameters in the normal force Equation, where the frequency-domain form is given by Equation (3.3-2), were estimated using the same frequency range as the pitching-moment Equation. The parameter estimates are

presented in Table 3-6 a); it can be seen that the squared-correlation coefficient levels out in value once 5 orthogonal components are used. The use of 7 orthogonal components would correspond to the conventional least-squares solution. However, from Table 3-6 c), it can be seen that there are 2 relatively insignificant orthogonal components associated with the 2 smallest singular values. It should be stressed that it is not possible to make the final choice of the number of orthogonal components to be used in the solution completely objective, but on the basis of the information given in Table 3-6 a) and 3-6 c), 5 orthogonal components is a justifiable choice. For the selected number of orthogonal components, the 'parameter significance' values and partial-F statistics are presented in Table 3-6 b). It can be seen here that Z_W is the most significant parameter by far in the Equation; the control sensitivity $Z_{n_{1s}}$ is the next most significant parameter, and has a fairly large partial-F statistic. The 'parameter significance' values are shown in Figure 3-9.

It is useful to remember that the equation-error approach is seen in the identification methodology developed in this document both as a means of obtaining initial guesses for the output-error method and in isolating insignificant parameters through the use of 'parameter significance' values. If the normal-force Equation, with parameters identified using the equation-error approach, was itself intended for use, then further

model simplifications would be required in order to give the model satisfactory predictive qualities. Insignificant parameters, estimated with great error, would be removed to give the simplest model adequate for the intended application.

For the normal-force Equation with a time delay estimated in the control, the parameter estimates are presented in Table 3-7 a). The evidence points to the selection of 6 orthogonal components: the levelling-off of the squared-correlation coefficient; the presence of 2 relatively insignificant orthogonal components associated with the 2 smallest singular values (see Table 3-7 c)); and the emergence of an estimate of the time delay in the control which is very close to the value also given from the corresponding pitching-moment results (c.f Table 3-3 a)).

For the selected number of orthogonal components, the 'parameter significance' values and partial-F statistics are presented in Table 3-7 b): the most important and most confidently estimated stability and control derivatives are once again Z_w and $Z_{\Delta_{1s}}$.

<u>Yawing-Moment And Rolling-Moment Equations.</u>

Tables 3-8 a), b), c) relate to the yawing-moment Equation (frequency-domain form given by Equation (3.3-4)). The corresponding results for the model with the delay in the control are given in Tables 3-9 a) and b).

The selected number of orthogonal components are 6 and 7 respectively: for the selected models - particularly for the model with the delay - the important yaw-damping parameter estimate N_r is very close to theory. Results for the rolling-moment Equation, when a time delay is estimated in the control, are given in Tables 3-10 a) and b). The selected model corresponding to the use of 7 orthogonal components gives the estimate of the important (as evidenced by Table 3-10 b)) derivative, L_v, that is closest to theory. It should be pointed out that the rolling-moment Equation has exactly the same independent variables as the yawing-moment Equation: consequently the associated singular values are identical in both cases (compare Tables 3-10 c) and 3-9 c)); for the two Equations, the smallest singular value was judged to be an approximation to zero.

3.3.5 Comparison Of Estimates With Theoretical Values.

Since actual experimental flight data have been analysed in the application of the equation-error method demonstrated here, there is no set of 'true' parameter values with which the estimates can be compared. The helicopter flight mechanics package HELISTAB provides theoretical parameter values which may be considered alongside the estimates obtained from flight data.

For the pitching-moment results presented in Table 3-1 a), it can be seen that the selected model,

corresponding to the use of 5 orthogonal components, results in estimates of the parameters M_q, M_p and $M_{\eta_{1s}}$ which are closer to theory than the conventional least-squares solution (given by 6 orthogonal components). M_u compares very well with theory, whilst M_w and M_v are estimated with relatively small error bounds and are of the same order of magnitude as the theoretical values.

At this stage in the discussion of pitching-moment results it is of interest to consider the results given in Table 3-11 a) obtained from flight data for a Puma helicopter at a trim speed of 80 knots with a longitudinal cyclic '3211' input applied. For the selection of 5 orthogonal components, the results for the 80 knots case display some similar characteristics to those obtained for the 100 knots case. The emergence of the most physically realistic estimate of M_q is significant and an estimate of M_p which compares very well with theory, and which has a small error bound is another important feature of the results which contrasts with the estimate for 6 orthogonal components. In addition, the estimate of M_u compares very well with theory, whilst M_v is estimated with a relatively small error bound and the magnitude-trend for M_v (i.e. the change in going from 100 to 80 knots) is consistent with theory.

The most significant discrepancy between the flight-data estimates and theoretical quasi-static values in the case of the results presented in Tables 3-1 a) and 3-11

a) was the underestimation of the parameter M_q. From Table 3-3 a) it can be seen that when an approximation to a time delay is incorporated and estimated in the longitudinal cyclic control, the pitch-rate damping parameter M_q is significantly bigger in magnitude, and compares very well with theory. The control sensitivity $M_{\eta_{1s}}$ also compares much better with theory than the case without the delay. It is reassuring to note that the approximate time delay estimate is almost identical to the value obtained for the application of the output-error method to the same data set, described in Section 2.3.3; in fact, a great many similarities can be found when the two sets of results are compared. It is worthwhile pointing out that in the case of a time delay in the control, the iterative procedure for the output-error results of Section 2.3.3 was initiated using equation-error results corresponding to an estimation without a time delay in the control; an initial guess of zero was used for the time delay.

For the normal-force-Equation results presented in Tables 3-6 a) and 3-7 a) - without and with a time delay in the control respectively - it is only worth discussing estimates of the dominant parameters: Z_w and $Z_{\eta_{1s}}$. For the selected models, the time delay is shown not to affect the estimates of Z_w; this observation was also made for the output-error identification. The selected Z_w estimates have relatively small error bounds, and are seen to be of a slightly greater magnitude than the

theoretical value. The selected $Z_{\eta_{1s}}$ estimates compare favourably, in both cases, with the theoretical value, and have relatively small error bounds. The time delay is estimated with a value that is almost identical to that obtained for the pitching-moment Equation, and ipso facto it is in close agreement with the value obtained for the application of the output-error method in Section 2.3.3. There is a large difference between the estimated delay for the selected model (6 orthogonal components) and that which is offered for the conventional least-squares solution (8 orthogonal components); this observation constitutes a strong argument in favour of the selected model in preference to the conventional least-squares solution.

For the yawing-moment results presented in Table 3-8a), it can be seen that the selected model, corresponding to the use of 6 orthogonal components, results in an estimate of the yaw-rate damping parameter N_r that is both substantially different from the value offered for the conventional least-squares solution (7 orthogonal components), and is closer to the theoretical value of the parameter. The estimate of N_v is slightly greater than theory, and this parameter is estimated with a relatively small error bound; conversely, the estimate of the control sensitivity N_{η_p} is slightly smaller in magnitude than theory, and is also estimated with a relatively small error bound. The estimate of N_p has a relatively large accompanying error bound, and differs

somewhat from theory. On the basis of the 'parameter significance' values presented in Table 3-8 b) the lateral/longitudinal coupling parameters: N_u, N_w and N_q play a relatively insignificant role in the Equations; this contrasts with the pitching-moment Equation where longitudinal/lateral coupling intensity was shown to be significant for the flight condition considered.

With a time delay in the control there is a noticeable reduction in the indicated error bounds of the important yawing-moment derivatives: N_v, N_p, N_r and N_{η_p} for the selected model over the case without a delay, as shown in Table 3-9 a). In addition, the estimate of the yaw-rate damping N_r is in very close agreement with theory as a result of the time delay being used in the control.

Estimates of the rolling-moment Equation are presented in Table 3-10 a), and it can be seen from Table 3-10 b), that like the yawing-moment results, lateral/longitudinal coupling effects are relatively insignificant. For the selected model (7 orthogonal components) it can be seen that the estimate of L_v matches very well with theory, and has a relatively small error bound. The estimate of L_p is smaller in magnitude than its theoretical counterpart, whilst conversely the estimate of L_r is larger than theory suggests. The tendency for the derivatives L_p and L_r to have this reciprocal relationship is considered again later in Section 4.3.2, where the estimation of yawing-moment and

rolling-moment derivatives is examined in detail using the frequency-domain output-error method with rank-deficient solutions; it is shown that more satisfactory estimates of lateral parameters, particularly L_p and L_r, can be obtained, than by considering the yawing-moment and rolling-moment Equations in isolation, as is the case with the equation-error method.

Measured And Predicted Frequency-Domain Values.

In addition to consideration of the individual parameter estimates themselves, further evidence of the overall validity of an identified model can be obtained by comparing measured frequency-domain values with corresponding values predicted by the model. A convenient way of displaying the fits is to use the magnitudes of the complex-valued quantities, remembering that the identification is performed by fitting both the real and imaginary parts of both sides of an Equation. In Figures 3-10 a), b) the frequency-domain fits for the pitching-moment Equation, without and with a time delay estimated in the control, respectively, are presented for solutions obtained for different numbers of orthogonal components, including the selected model. similarly, Figures 3-11 a), b); 3-12 a), b); and 3-13 a),b) are provided for the normal-force, yawing-moment, and rolling-moment fits respectively.

3.3.6 An Equation-Error Multirun Example.

An investigation into the use of four combined manoeuvres for frequency-domain equation-error identification was carried out. The manoeuvres involve the use of all four controls, and consisted of: a collective doublet; a longitudinal cyclic '3211'; a pedal doublet; and a lateral cyclic step input. The responses were stacked to produce a record length of just over 60 seconds as shown in Figure 3-14. Frequency-domain fits for the pitching-moment, normal-force, yawing-moment and rolling-moment Equations are presented in Figure 3-15. The frequency range used extended up to about 0.5 Hz. with 35 different frequencies used in the identification. It was observed that the estimates of some longitudinal parameters were closer to theoretical values than for the single-input longitudinal-cyclic case described earlier, for the selected model, namely M_w and M_p - estimated as -0.0040 [0.0009] and -0.1965 [0.07] respectively (where the square brackets indicate the estimated error bounds). The corresponding theoretical values are given in Table 3-1 a). On the other hand, some important longitudinal parameters, namely M_u and M_q - estimated as 0.0015 [0.0003] and -0.0593 [0.15] respectively, had estimates which were worse than the single-input longitudinal-cyclic case in terms of physical realism. These findings appear to support the comments made in the reference DUVA001 - mentioned in Section 3.2.3 - about

the shortcomings of using several stacked data sets in the identification. It should be noted however that the data used for the investigation do not constitute an ideal set. The fact that a step input, rather than a (small amplitude) multistep input which involve a return to the trim setting, was used, is one notable deficiency. This choice of lateral input was dictated by the available test records for the flight condition. The results for the multirun identification are presented in more detail in the reference BLAC005.

The presence of discontinuities presents no problems for the use of time-domain data in equation-error identification, however, for the frequency-domain approach exemplified in this Section, the Gibb's oscillation effect - described in Section 2.2.2 - will be a source of error in the identification.

3.3.7 Consideration Of The Predictive Qualities Of A Model.

If there are sufficient flight-data sets available to the analyst, the identified model should be tested on a completely independent data set. Figures 3-16 a), b) provide examples of this type of assessment, where frequency-domain values are shown for the response to a longitudinal cyclic '3211', together with predictions based on the identified model using the longitudinal - cyclic doublet (discussed in Section 3.3.5 and

corresponding to Table 3-1 a)). In addition, the response to the longitudinal-cyclic doublet input, and predictions based on the multirun model, considered in the last Section, are also shown. The overall agreement between the measured and predicted responses is reasonable in both cases.

CHAPTER 4

4.0 THE FREQUENCY-DOMAIN OUTPUT-ERROR STAGE IN THE IDENTIFICATION METHODOLOGY.

4.1 Introduction.

4.1.1 Background To The Use Of The Output-Error Technique.

The frequency-domain output-error method is presented here as a special case of the more general maximum-likelihood method, where there is the assumption of no process (i.e. modelling) noise. The original features of the method presented here are given in Sections 4.2.2 to 4.2.4, and are associated with model representation and computer implementation; the cost function used as the basis for the method is the same as that derived in KLEI004.

A significant distinction between the output-error and equation-error techniques is that the former requires start-up values, or initial guesses, to perform the estimation. For the implementation used in this work the minimisation of the cost-function is performed iteratively using the Gauss-Newton method (with an additional line-search modification). Good initial guesses are required for rapid convergence because of the representation of the cost-function in the vicinity of

the minimum by a quadratic. Whereas the equation-error method can only be used to identify one equation at a time, the output-error method identifies state-space type models. The frequency-domain output-error method is presented here, as the second, and most important stage in the helicopter system identification methodology that is developed.

4.1.2 Previous Applications Of The Technique.

Maximum-likelihood/output-error methods have featured often in previous helicopter and aircraft system identification work. Most reported applications have used the time domain (e.g. FOST001, FOST002, ROSS001, KLEI007, STEP001, FEIK002). Applications to the problem of helicopter system identification include: HALL001, MOLU001, MOLU002, MOLU003. Real progress with these techniques for helicopter system identification, however, have been disappointing, with few reported successes in the literature. The large computation times required, coupled with the dificulties of obtaining an adequate model structure in the time-domain, (without introducing a formidable amount of complexity into the problem through, for example the inclusion of rotor states), have severely limited the use of this method for helicopter system identification.

The use of the frequency domain, for the output-error method, is advantageous for several reasons,

including the ease with which innovative modelling features can be incorporated (e.g. the use of delays in the controls, and the use of a specific frequency range for the estimation). In addition, use of the frequency domain can lead to a reduction in the amount of data (and hence computation time) required. In the reference FUKH 001, the authors report some success in the application to helicopter flight data of a frequency-domain identification technique based on the same cost-function as that developed in section 4.2.1. In MARC002, the authors present some results, again using the frequency-domain technique, to data generated from an in-flight-simulator. Defined time delays existed between the commanded control inputs (pitch stick, roll stick) and the corresponding control surfaces (elevator, rudder), and these were successfully identified leading to improved fits. In Chapter 2, the idea of using time delays to account for higher-order rotor effects, in addition to any purely transport effects, was advanced as a new and original tactic in helicopter system identification. Some results using real flight data were used to demonstrate the resulting improvement. Further examples of the use of a time delay with this interpretation, are presented later in this chapter (and in the references BLAC005, BLAC007).

A Further Comment.

Although not used to estimate the stability and control derivatives, time-domain estimation does have a place in the estimation methodology presented in this document. It is used to estimate zero-offset and initial state conditions (see chapter 5), following a frequency domain identification of the main model parameters.

4.2 Development Of The Frequency-Domain Output-Error Algorithm.

4.2.1 Formulation Of The Frequency-Domain Cost Function.

Set Of Transformed Measurements.

Consider the following equations representing the state-space model and the measurement system (delays in the controls and measurements have been omitted from the notation here for clarity), and using the same notation as in section 2.2.4:

$$\dot{\underset{\sim}{X}}(t) = A\underset{\sim}{X}(t) + B\underset{\sim}{U}(t) + \underset{\sim}{W}(t) \qquad (4.2\text{-}1)$$

$$\underset{\sim}{Z}(t) = H\underset{\sim}{X}(t) + \underset{\sim}{K} + \underset{\sim}{b} + \underset{\sim}{V}(t) \qquad (4.2\text{-}2)$$

$\underset{\sim}{W}(t)$ is a process (or modelling) noise term.

Transforming the above into the frequency domain, we have:

$$\hat{\dot{\underset{\sim}{X}}}(\omega_K) = A\hat{\underset{\sim}{X}}(\omega_K) + B\hat{\underset{\sim}{U}}(\omega_K) + \hat{W}(\omega_K) \qquad (4.2\text{-}3)$$

$$\hat{\underset{\sim}{Z}}(\omega_K) = H\hat{\underset{\sim}{X}}(\omega_K) + \hat{V}(\omega_K) \qquad (4.2\text{-}4)$$

where $\omega_K \neq 0$, and $\omega_K = K2\pi/N\Delta t$ for N time-domain samples of interval Δt. Let Z_q be the set of q frequency-domain measurement values. If $\underset{\sim}{W}(t)$ and $\underset{\sim}{V}(t)$ are independent Gaussian random variables, then so are the transformed quantities $\hat{\underset{\sim}{W}}(\omega_K)$ and $\hat{\underset{\sim}{V}}(\omega_K)$ (SCHO001). We can define the following set:

$$Z_q \triangleq \{\hat{\underset{\sim}{Z}}(\omega_1), \hat{\underset{\sim}{Z}}(\omega_2), \ldots \hat{\underset{\sim}{Z}}(\omega_q)\} \qquad (4.2\text{-}5)$$

where $0 < q \leq N/2 - 1$

<u>Maximum-Likelihood Principle.</u>

The maximum-likelihood principle can be defined as follows: Given an experiment whose outcome depends on a set of unknown parameters γ, the maximum-likelihood estimates of the unknown parameters are those values of γ, for which the observed values in the experiment, are most likely to occur. This involves maximization of the conditional probability-density function of the observations given γ; and is called the likelihood

function. For the set of measured values Z_q, this can be stated as:

$$\Upsilon_{est} = \max P[Z_q/\Upsilon] \tag{4.2-6}$$

$P[Z_q/\Upsilon]$ is the probability density of Z_q conditioned on Υ, and Υ_{est} are the maximum-likelihood estimates of Υ. The probability of obtaining the set Z_q can be obtained by concatenating conditional probabilities (using Baye's theorem):

$$P[Z_q/\Upsilon] = P[\hat{\underset{\sim}{Z}}(\omega_q)/Z_{q-1},\Upsilon] \cdot P[Z_{q-1}/\Upsilon] \tag{4.2-7}$$

Repeated application results in:

$$P[Z_q/\Upsilon] = \prod_{i=1}^{q} P[\hat{\underset{\sim}{Z}}(\omega_i)/Z_{i-1},\Upsilon] \tag{4.2-8}$$

To find the probability distribution of $\hat{\underset{\sim}{Z}}(\omega_i)$ given Z_{i-1} and Υ, the mean value and variance are determined first. Let us define:

$$E[\hat{\underset{\sim}{Z}}(\omega_i)/Z_{i-1},\Upsilon] \triangleq \hat{\hat{\underset{\sim}{Z}}}(\omega_i/i-1) \tag{4.2-9}$$

$$E[(\hat{\underset{\sim}{Z}}(\omega_i) - \hat{\hat{\underset{\sim}{Z}}}(\omega_i/i-1))\overline{(\hat{\underset{\sim}{Z}}(\omega_i) - \hat{\hat{\underset{\sim}{Z}}}(\omega_i/i-1))^T}] \tag{4.2-10}$$

$$\triangleq S(\omega_i)$$

In order to obtain $\hat{\hat{\underset{\sim}{Z}}}(\omega_i/i-1)$, consider first the discrete steady-state Kalman Filter representation of the system given by (4.2-1) and (4.2-2) (e.g. KLEI004; $\underset{\sim}{K}$ and $\underset{\sim}{b}$ added by current author)

$$\bar{\underset{\sim}{X}}(n+1\,\Delta t) = \phi\,\bar{\underset{\sim}{X}}(n\Delta t) + D\underset{\sim}{U}(n\Delta t) + K\underset{\sim}{v}(n\Delta t) \qquad (4.2\text{-}11)$$

$$\underset{\sim}{Z}(n\Delta t) = H\bar{\underset{\sim}{X}}(n\Delta t) + \underset{\sim}{K} + \underset{\sim}{b} + \underset{\sim}{v}(n\Delta t) \qquad (4.2\text{-}12)$$

The Kalman Filter (KALM001, or e.g. GELB001) is a linear procedure for obtaining minimum-variance estimates of the states $\bar{\underset{\sim}{X}}(t)$ (the bar denotes a mean or expected estimate). The minimum-variance estimate is the conditional mean of the state vector (regardless of its probability density function). The Kalman-gain matrix $-K$ (see Appendix 4) is a function of the noise statistics of the process noise term $\underset{\sim}{W}(t)$ and measurement noise term $\underset{\sim}{V}(t)$ given in (4.2-1) and (4.2-2); for the steady-state case, K is constant.

If we transform the discrete equations representing the model into the frequency domain, we have, for the measurement system given in (4.2-12):

$$\hat{\underset{\sim}{Z}}(\omega_K) = H\hat{\hat{\underset{\sim}{X}}}(\omega_K) + \hat{\underset{\sim}{v}}(\omega_K) \quad ; \omega_K \neq 0 \qquad (4.2\text{-}13)$$

The vector $\underset{\sim}{v}(t)$ (of innovations) is obtained from a

linear combination of terms having Gaussian distributions, and is thus itself distributed in a Gaussian manner. It follows that the transformed innovations $\underset{\sim}{\gamma}(\omega_k)$ are also Gaussian random variables, with

$$E[\hat{\underset{\sim}{\gamma}}(\omega_k)] = 0 \quad , \quad E[\hat{\underset{\sim}{\gamma}}(\omega_k)\hat{\underset{\sim}{\gamma}}^*(\omega_k)] = S \qquad (4.2\text{-}14)$$

where the covariance matrix S is independent of frequency for white time-domain Gaussian noise sources $\underset{\sim}{V}(t)$ and $\underset{\sim}{W}(t)$.

<u>Output Errors Instead Of Kalman-Filter Innovations.</u>

If we assume that there is no process noise term $\underset{\sim}{W}(t)$ (i.e. no modelling errors) in (4.2-1), then the steady-state Kalman-gain matrix K is zero (APPENDIX 4). The innovations $\hat{\underset{\sim}{\gamma}}(\omega_k)$ become output-errors $\hat{\underset{\sim}{V}}(\omega_k)$. Hence we have for (4.2-13):

$$\hat{\underset{\sim}{Z}}(\omega_k) = H\hat{\underset{\sim}{X}}(\omega_k) + \hat{\underset{\sim}{V}}(\omega_k) \quad ; \quad \omega_k \neq 0 \qquad (4.2\text{-}15)$$

For $\hat{\underset{\sim}{Z}}(\omega_i/i-1)$ defined in (4.2-9), we can see from (4.2-15) that it is dependent solely on the model output at that particular frequency, and is consequently only conditioned on the model parameters γ.

Log Likelihood Function.

Returning to (4.2-8), we may now write the conditional probabilities:

$$P[Z_q/\mathcal{Y}] = \prod_{i=1}^{q} P[\hat{\underset{\sim}{Z}}(\omega_i)/\mathcal{Y}] \qquad (4.2\text{-}16)$$

Using the Gaussian probability density function, the following argument for the derivation of the likelihood function is similar to that presented in the references KLEI004 and KLEI005, except that output- errors have been used instead of innovations, following the assumption of no process noise given earlier. The probability density function for the Gaussian variable $\hat{\underset{\sim}{Z}}(\omega_i)$ conditioned on $\mathcal{Y}$ is given by:

$$[(2\pi)\,|S|]^{-\frac{1}{2}} \cdot \exp[-\tfrac{1}{2}(\hat{\underset{\sim}{V}}(\omega_i)^* S^{-1} \hat{\underset{\sim}{V}}(\omega_i))] \qquad (4.2\text{-}17)$$

Including terms of the form given in (4.2-17) into the product given in (4.2- 16), and taking the natural logarithm of both sides, we have:

$$\log_e P[Z_q/\mathcal{Y}] = \sum_{i=1}^{q} \log_e P[\hat{\underset{\sim}{Z}}(\omega_i)/\mathcal{Y}] \qquad (4.2\text{-}18)$$

And using (4.2-17) where:

$$\log_e P[\hat{\underset{\sim}{Z}}(\omega_i)/\Upsilon] = -1/2 \log_e |S| - 1/2\, \hat{\underset{\sim}{V}}(\omega_i)^* S^{-1} \hat{\underset{\sim}{V}}(\omega_i) - 1/2 \log_e (2\pi) \qquad (4.2\text{-}19)$$

we have:

$$-\log_e P[Z_q/\Upsilon] = 1/2 \sum_{i=1}^{q} (\hat{\underset{\sim}{V}}^*(\omega_i) S^{-1} \hat{\underset{\sim}{V}}(\omega_i) + \log_e |S|) + \text{Constant} \qquad (4.2\text{-}20)$$

Ignoring the constant term, which is of no consequence for the optimization, and noting that the log function is monotonic increasing, a suitable cost function is given by:

$$J(\Upsilon, S) = 1/2 \sum_{\omega} (\hat{\underset{\sim}{V}}^*(\omega) S^{-1} \hat{\underset{\sim}{V}}(\omega) + \log_e |S|) \qquad (4.2\text{-}21)$$

This is the cost function for the frequency-domain output-error method used in this document. The change of sign in Equation (4.2-21), as compared with Equation (4.2-20), should be noted. It can be seen that the cost function is a function of the model parameters Υ (i.e. elements of the matrices A, B and H given in (4.2-1) and (4.2-2), in addition to any time delays included in the model), and elements of the frequency-domain error-

covariance matrix S (defined in (4.2-10), but independent of frequency for white measurement noise). The cost-function summation is carried out over the desired frequency range for the estimation.

Some Further Comments.

It is appreciated by the current author that the above justification for the cost function, based on a probabilistic argument, may be considered unsatisfactory for a number of reasons. Firstly, the assumption that there are no modelling errors might seem to be patently unjustified. In the context of helicopters, obvious modelling errors which spring to mind, are ones arising from non-linearities (i.e. large excursions from the trim), and the coupling of rigid-body dynamics with rotor dynamics. In the case of non-linearities, the use of more appropriate control inputs (discussed in section 1.4.2) can reduce this problem. This is a situation where prevention is better than a 'cure', because non-linearities are deterministic effects which are obviously not appropriately modelled as a Gaussian random effect. For the effect of rotor dynamics on rigid-body states, the use of time delays to re-model the effective control input has already been discussed, and it has been emphasized that this is only an approximate method. There is also the problem of having noise on the controls, and this is commented on in section 4.2.5.

The cost-function given in (4.2-21) is of the familiar least-squares form when the error-covariance matrix S is known, and this is the sort of ad-hoc cost function which one might define as the basis for a model fitting technique. However, when S is unknown, and has to be estimated in addition to the model parameters γ, then the logarithmic component must be included. Finally, it should be mentioned that the cost-function given in (4.2-21) can be modified, when a statistical model is available for the parameters as well as the measurements, by the inclusion of an additional term. This corresponds to a Bayesian estimation approach (e.g. GELB001), and for the estimates (4.2-6) is replaced by:

$$\gamma_{est} = \max P[Z_q/\gamma] \cdot P[\gamma] \qquad (4.2\text{-}22)$$

As is pointed out in MAIN002, the probability distribution of parameters in a model, such as $P[\gamma]$, does not represent any randomness in the value of γ, but reflects knowledge or information about the value of γ. For the work covered in this report, however, there is no assumption of an a priori distribution of the parameter values.

4.2.2 Implementation Of Gauss-Newton Minimisation Algorithm.

The cost-function given in (4.2-21) is to be

minimised with respect to the unknown parameters in the model. The values of the parameters at the minimum of the cost-function are taken as the estimates. The minimization scheme used is a modified Newton-Raphson technique; this is also known as a Gauss-Newton method (e.g. MAIN002, WALS001). An additional scalar line-search algorithm (FOST002 and Appendix 3) is also used.

A Convenient Symbolic Representation Of The Model.

A convenient symbolic representation of the frequency-domain model, which facilitates the formulation of required terms for the minimisation, is that developed in Section 2.2.4. This involves the stacking of the real components of a complex-valued vector on top of the imaginary components; and the development of the corresponding matrix terms through equating separately the real and imaginary parts of both sides of an expression. Let us define the following shorthand notation:

$$\check{\underset{\sim}{X}}(\omega) \triangleq \begin{bmatrix} Re[\hat{\underset{\sim}{X}}(\omega)] \\ Im[\hat{\underset{\sim}{X}}(\omega)] \end{bmatrix} \qquad \mathcal{A}(\omega) \triangleq \begin{bmatrix} -A & -\omega I \\ \omega I & -A \end{bmatrix}$$

$$\check{\underset{\sim}{U}}(\omega) \triangleq \begin{bmatrix} Re[\hat{\underset{\sim}{U}}(\omega)] \\ Im[\hat{\underset{\sim}{U}}(\omega)] \end{bmatrix} \qquad \mathcal{B} \triangleq \begin{bmatrix} B & 0 \\ 0 & B \end{bmatrix}$$

(4.2-23)

$$\check{\underset{\sim}{G}}(\omega) \triangleq -\sqrt{N}/T \begin{bmatrix} \Delta \underset{\sim}{X} \cos \frac{\omega \Delta t}{2} \\ \Delta \underset{\sim}{X} \sin \frac{\omega \Delta t}{2} \end{bmatrix} \qquad \mathcal{H} \triangleq \begin{bmatrix} H & 0 \\ 0 & H \end{bmatrix}$$

For the frequency-domain model (i.e. system and measurement equations) we can thus write:

$$\mathbb{A}(\omega)\,\check{\underset{\sim}{X}}(\omega) = \mathbb{B}\,\check{\underset{\sim}{U}}(\omega) + \check{\underset{\sim}{G}}(\omega) \tag{4.2-24}$$

$$\check{\underset{\sim}{Z}}(\omega) = \mathbb{H}\,\check{\underset{\sim}{X}}(\omega) + \check{\underset{\sim}{V}}(\omega) \tag{4.2-25}$$

If we include time delays in the model, then the $\check{\underset{\sim}{U}}(\omega)$ and $\check{\underset{\sim}{Z}}(\omega)$ vectors are pre-multiplied by matrices whose elements are frequency-dependent sinusoidal and cosinusoidal functions of the time delays (See Equation 2.3-8 in Section 2.3-1). Representing these matrices by $\mathbb{B}_2(\omega)$ and $\mathbb{H}_2(\omega)$, then in place of the above equations we have:

$$\mathbb{A}(\omega)\,\check{\underset{\sim}{X}}(\omega) = \mathbb{B}\,\mathbb{B}_2(\omega)\,\check{\underset{\sim}{U}}(\omega) + \check{\underset{\sim}{G}}(\omega) \tag{4.2-26}$$

$$\mathbb{H}_2(\omega)\,\check{\underset{\sim}{Z}}(\omega) = \mathbb{H}\,\check{\underset{\sim}{X}}(\omega) + \check{\underset{\sim}{V}}(\omega) \tag{4.2-27}$$

For the case of r controls, the definition of $\mathbb{B}_2(\omega)$ must be:

$$\mathbb{B}_2(\omega) \triangleq \left[\begin{array}{ccc|ccc} \cos\omega\tau_1 & & & \sin\omega\tau_1 & & \\ & \cos\omega\tau_2 & 0 & & \sin\omega\tau_2 & 0 \\ 0 & & \ddots & 0 & & \ddots \\ & & \cos\omega\tau_r & & & \sin\omega\tau_r \\ \hline -\sin\omega\tau_1 & & & \cos\omega\tau_1 & & \\ & -\sin\omega\tau_2 & 0 & & \cos\omega\tau_2 & 0 \\ 0 & & \ddots & 0 & & \ddots \\ & & -\sin\omega\tau_r & & & \cos\omega\tau_r \end{array}\right] \tag{4.2-28}$$

The matrix $\mathcal{H}_2(\omega)$ is defined in an identical fashion to $\mathcal{B}_2(\omega)$.

A Convenient Symbolic Representation Of The Cost Function.

Using (4.2-15) and (4.2-21), and the definitions:

$$\mathcal{S} \triangleq \begin{bmatrix} S & 0 \\ 0 & S \end{bmatrix} \tag{4.2-29}$$

$$\check{\underset{\sim}{\mathcal{X}}}(\omega) \triangleq \begin{bmatrix} \mathrm{Re}[E[\hat{\underset{\sim}{Z}}(\omega)]] \\ \mathrm{Im}[E[\hat{\underset{\sim}{Z}}(\omega)]] \end{bmatrix} \tag{4.2-30}$$

where, for white measurement noise - $E[\check{\underset{\sim}{V}}(\omega)] = \underset{\sim}{0}$, we can re-express the frequency-domain cost function as:

$$J(\Psi, S) = 1/2 \sum_{\omega} \left((\check{\underset{\sim}{Z}}(\omega) - \check{\underset{\sim}{\mathcal{X}}}(\omega))^T \mathcal{S}^{-1} (\check{\underset{\sim}{Z}}(\omega) - \check{\underset{\sim}{\mathcal{X}}}(\omega)) \right.$$

$$\left. + \log_e |\mathcal{S}| \right) \tag{4.2-31}$$

For white Gaussian measurement noise, the error-covariance matrix $\mathcal{S}$ is independent of frequency, and so for N_ω frequency values used in the estimation, we have:

$$J(\Psi, S) = 1/2 \sum_{\omega} \left((\check{\underset{\sim}{Z}}(\omega) - \check{\underset{\sim}{\mathcal{X}}}(\omega))^T \mathcal{S}^{-1} (\check{\underset{\sim}{Z}}(\omega) - \check{\underset{\sim}{\mathcal{X}}}(\omega)) \right)$$

$$+ 1/2 N_\omega \log_e |\mathcal{S}| \tag{4.2-32}$$

Minimisation Of The Cost Function.

Since the objective is to minimise the cost function with respect to the unknown parameters, which are γ (the set of model parameters) and s (the set of elements of the error covariance matrix S), then we must have:

$$\left(\partial/\partial\gamma_1, \partial/\partial\gamma_2, \ldots \partial/\partial\gamma_m\right)^T J(\gamma, s) = \underset{\sim}{0} \qquad (4.2\text{-}33)$$

$$\left(\partial/\partial s_1, \partial/\partial s_2, \ldots \partial/\partial s_n\right)^T J(\gamma, s) = \underset{\sim}{0} \qquad (4.2\text{-}34)$$

Assuming that the matrix S (and hence $\mathcal{S}$) is completely unknown, except for the restriction that it be positive semi-definite, then for (4.2-33) and (4.2-34) respectively (using matrix differentiation results for (e.g. MAIN007, GELB001), we have

$$\partial J/\partial\gamma_i = \underset{\sim}{0} = \sum_{\omega}\left(\left(\check{\underset{\sim}{z}}(\omega) - \check{\underset{\sim}{\chi}}(\omega)\right)^T \mathcal{S}^{-1} \partial/\partial\gamma_i \left[\check{\underset{\sim}{z}}(\omega) - \check{\underset{\sim}{\chi}}(\omega)\right]\right) \qquad (4.2\text{-}35)$$

$$\partial J/\partial s_i = \underset{\sim}{0} = -1/2\, \mathcal{S}^{-1} \sum_{\omega}\left(\left(\check{\underset{\sim}{z}}(\omega) - \check{\chi}(\omega)\right)\left(\check{\underset{\sim}{z}}(\omega) - \check{\chi}(\omega)\right)^T \mathcal{S}^{-1}\right.$$

$$+ 1/2\, N_\omega\, \mathcal{S}^{-1} \qquad (4.2\text{-}36)$$

Using (4.2-36), gives

$$S_{est} = 1/N_\omega \sum_\omega (\check{\underset{\sim}{Z}}(\omega) - \check{\underset{\sim}{X}}(\omega))(\check{\underset{\sim}{Z}}(\omega) - \check{\underset{\sim}{X}}(\omega))^T \quad (4.2\text{-}37)$$

The result given in (4.2-37) is consistent with the definition of S (with the dependence on frequency omitted) given in (4.2-10) because of the equi-distribution of power between the real and imaginary parts of the transform of a Gaussian random variable, discussed in section 2.2.5.

<u>Separate Algorithms For The Estimation Of γ And S.</u>

A distinction has already been made between the model parameters: γ, and elements of the error-covariance matrix: S . In terms of the minimisation of the cost-function, the conditions for the minimum, in terms of each of these sets of parameters, were given in (4.2-35) and (4.2-36). It would be possible to apply the same optimization technique to both sets of parameters simultaneously, and for a gradient minimisation scheme the right-hand sides of (4.2-35) and (4.2-36) would be used to supply the required first-order partial derivatives. An alternative approach, and one which is used here because of its ease of application, uses separate algorithms for the estimation of γ and S. This

approach is called axial iteration, and is one which has been widely, and successfully, used in optimization problems analogous to the present one (e.g. FEIK002, FOST002, MAIN002). Convergence in both algorithms is required for the estimation procedure to terminate. The Gauss-Newton method is used in the estimation of γ, and is written as:

$$\underset{\sim}{\gamma}_{est}^{K+1} = \underset{\sim}{\gamma}_{est}^{K} - M^{K^{-1}} \underset{\sim}{g}^{K} \qquad (4.2\text{-}38)$$

where the super-script refers to the iteration number. M^K is a linearised approximation to the Hessian matrix (this will be explained in more detail shortly), at the Kth iteration, such that:

$$M^K \doteq \begin{bmatrix} \partial^2 J / \partial\gamma_1 \partial\gamma_1 & \cdots & \partial^2 J / \partial\gamma_1 \partial\gamma_m \\ & \ddots & \\ & & \partial^2 J / \partial\gamma_m \partial\gamma_m \end{bmatrix} \qquad (4.2\text{-}39)$$

where the second-order partial derivatives are evaluated for the parameter estimates at the Kth iteration. $\underset{\sim}{g}^K$ is the gradient vector of the cost function at the Kth iteration (similarly evaluated for the current parameter estimates), such that:

$$\underset{\sim}{g}^{k} = [\partial J/\partial \gamma_1, \partial J/\partial \gamma_2, \ldots \partial J/\partial \gamma_m] \qquad (4.2\text{-}40)$$

Elements of S are estimated at each iteration step using (4.2-37), where the model output terms $\check{\underset{\sim}{\chi}}(\omega)$ are calculated using the current estimates of γ. By using two separate algorithms, the dimension of the unknown parameter vector that would have to be used in (4.2-38), is reduced.

<u>Summary Of The Axial Iteration Algorithm.</u>

The procedure may be summarised as follows:

1) Estimate S using (4.2-37) and the current estimate of γ
2) Perform one iteration of the Gauss-Newton algorithm (using 4.2-38) to revise the estimate of γ
3) Repeat steps 1 and 2 until some convergence criterion is satisfied

Only one iteration of the Gauss-Newton algorithm is carried out at stage 2, because it is pointless improving on the estimates of γ for a given S any further, if S itself is to be changed at the next pass through the overall procedure.

The situation could be further simplified if S was

known and fixed throughout the estimation. This would correspond to a weighted least-squares type estimation (FOST001), with the logarithmic component of the cost function becoming a constant, irrelevant to the optimization. The elements of S are fixed by the analyst in this type of estimation (in fact S^{-1} is the weighting matrix used), and can be chosen to reflect the importance attached to the fitting of each measured quantity. For the applications of the method presented in this document, this will not be the mode of operation used: S and γ will both be estimated using the axial iteration procedure. However, the ability to fix elements of the matrix S at user-defined values for the first few iterations of the procedure, is a very useful feature. This is standard procedure for the application of minimisation schemes similar to the one described here. Experience has shown that if the initial parameter guesses (necessary to start the iterative procedure) are far from their true values, then the corresponding estimate of S (and hence $\hat{S}$) given by (4.2-37) will be very poor because of the significant modelling errors. This, consequently, could result in a divergence of the algorithm.

<u>Convergence Of The Non-Logarithmic Component Of The Cost Function.</u>

It can be seen by substituting for the converged

estimate of $\hat{S}$ into the non-logarithmic component of the cost function in (4.2-32), that for convergence of the estimation algorithm, the non-logarithmic component of the cost function should tend towards the integer value - $N_x \times N_\omega$, where N_x is the number of states in the state-space equation, and N_ω is the number of frequency points used in the estimation.

$$\tfrac{1}{2} \sum_{\omega} 2 \cdot N_x = N_x \cdot N_\omega \qquad (4.2\text{-}41)$$

This was found by the current author to be a useful check that the algorithm was converging correctly.

<u>Expressions For The Sensitivities (Or Partial Derivatives).</u>

Expressions for the elements of the matrix M^k and the vector $\underset{\sim}{g}^k$ given in (4.2-39) and (4.2-40) respectively are obtained as follows. Using (4.2-35) for a point away from the minimum (thus dropping the equality with zero), we have for an element of $\underset{\sim}{g}^k$, corresponding to the unknown parameter γ_L :

$$\partial J / \partial \gamma_L = \sum_{\omega} \left(\left(\underset{\sim}{\check{z}}(\omega) - \underset{\sim}{\check{x}}(\omega) \right)^T S^{-1} \partial / \partial \gamma_L \left[\underset{\sim}{\check{z}}(\omega) - \underset{\sim}{\check{x}}(\omega) \right] \right.$$

(4.2-42)

By partially differentiating (4.2-42) with respect to a second parameter - γ_m, we have:

$$\partial^2 J / \partial \gamma_L \partial \gamma_m = \sum_{\omega} \left(\left(\check{\underset{\sim}{z}}(\omega) - \check{\underset{\sim}{\chi}}(\omega) \right)^T S^{-1} \partial^2 / \partial \gamma_L \partial \gamma_m \left[\check{\underset{\sim}{z}}(\omega) - \check{\underset{\sim}{\chi}}(\omega) \right] \right.$$

$$\left. + \partial / \partial \gamma_m \left[\check{\underset{\sim}{z}}(\omega) - \check{\underset{\sim}{\chi}}(\omega) \right]^T S^{-1} \partial / \partial \gamma_L \left[\check{\underset{\sim}{z}}(\omega) - \check{\underset{\sim}{\chi}}(\omega) \right] \right)$$

(4.2-43)

If we use only the first-order derivative terms on the right-hand side of (4.2-43), the resultant expression for $\partial^2 J / \partial \gamma_L \partial \gamma_m$ is known as a quasi-linear approximation (MAIN002). Computing the second-order partial derivative terms would add greatly to the complexity of the computer implementation of the method with negligible improvement in algorithmic performance. Hence, after linearisation, we have:

$$\partial^2 J / \partial \gamma_L \partial \gamma_m \simeq \sum_{\omega} \left(\partial / \partial \gamma_m \left[\check{\underset{\sim}{z}}(\omega) - \check{\underset{\sim}{\chi}}(\omega) \right] S^{-1} \partial / \partial \gamma_L \left[\check{\underset{\sim}{z}}(\omega) - \check{\underset{\sim}{\chi}}(\omega) \right] \right)$$

(4.2-44)

It is the use of this linearised approximation to the matrix of second-order partial derivatives (the Hessian matrix), which constitutes the Gauss-Newton method.

Line-Search Modification.

The line-search modification to the Gauss-Newton (FOST002) attempts to use an optimal scalar multiple of the update increment $\Delta \underset{\sim}{\gamma}$ (this incremental change in parameter estimates is implied in (4.2-38)). For the cost function at the (K+1)th iteration, with scalar

multiple α of $\Delta\underset{\sim}{\gamma}$, we have:

$$J(\alpha) \triangleq J(\underset{\sim}{\gamma}^{k}_{est} + \alpha \Delta\underset{\sim}{\gamma}) \qquad (4.2\text{-}45)$$

With the one-dimensional line search, we seek a value of α which minimises $J(\alpha)$. The method is explained in detail in Appendix 3.

Of the method, it has been said (MAIN002) that the Gauss-Newton method works well enough in most cases, and that one-dimensional line searches cannot measurably improve convergence, and may in fact result in a large total computation time. In contrast to this view, the current author has found that for the application covered here, the line search can measurably improve performance. A typical figure for the reduction in C.P.U. time, over a case where the line search was not used, but converged to the same minimum, is 16%. This may be connected with the fact that the line-search algorithm requires the frequent computation of the cost value. Since the frequency-domain estimation is usually carried out using a relatively small number of data points comparison to the time domain, there are less terms in the summation which defines the cost function, and consequently this can be carried out fairly quickly.

<u>Calculating The Expressions For The Sensitivities (Partial Derivatives).</u>

As a result of working in the frequency domain, all the necessary operations in the implementation of the Gauss-Newton minimisation algorithm are, as will be shown here, algebraic. This contrasts with the use of the time domain, where numerical integration of the model equations for the full time span used, is required to obtain the model output and sensitivities (e.g. FOST002) for each iteration.

For the terms in expressions (4.2-42) and (4.2-44), the first step is to obtain $\check{\underset{\sim}{Z}}(\omega)$ and $\check{\underset{\sim}{\mathcal{X}}}(\omega)$. $\check{\underset{\sim}{Z}}(\omega)$ is obtained by transforming the flight-data measurements into the frequency domain. $\check{\underset{\sim}{\mathcal{X}}}(\omega)$ is obtained, for each frequency value ω, as follows:

1) For a known input vector - $\check{\underset{\sim}{U}}(\omega)$ (obtained by transforming the flight-data measurements into the frequency-domain), and known correction term for non-periodic measurement windows $\check{\underset{\sim}{G}}(\omega)$, and for the current parameter estimates γ, solve the linear equation given in (4.2-26) for $\check{\underset{\sim}{X}}(\omega)$.
2) Using the definition of $\check{\underset{\sim}{\mathcal{X}}}(\omega)$ given in (4.2-30), we have from (4.2-27) that:

$$\mathcal{H}_2(\omega)\,\check{\underset{\sim}{\mathcal{X}}}(\omega) = \mathcal{H}\,\check{\underset{\sim}{X}}(\omega) \qquad (4.2\text{-}46)$$

The above linear equation is solved for $\check{\underset{\sim}{\mathcal{X}}}(\omega)$, again using the current estimates of γ. For zero-valued delays in

the measurements, $\mathcal{H}_2(\omega)$ becomes the identity matrix.

The next step in the calculation of the sensitivities is to consider terms of the form: $\frac{\partial}{\partial \gamma_L}[\check{\underset{\sim}{Z}}(\omega)]$ (noting that $\frac{\partial}{\partial \gamma_L}[\check{\underset{\sim}{Z}}(\omega)] = \underset{\sim}{0}$, i.e. the measurements are not influenced by the parameters in the model). If we partially differentiate the model equations given in (4.2-26) and (4.2-27), we have, after rearrangement:

$$\mathcal{A}(\omega)\frac{\partial \check{\underset{\sim}{X}}(\omega)}{\partial \gamma_L} = \frac{\partial}{\partial \gamma_L}[-\mathcal{A}(\omega)]\check{\underset{\sim}{X}}(\omega) + \frac{\partial}{\partial \gamma_L}[\mathcal{B}]\cdot\mathcal{B}_2(\omega)\check{\underset{\sim}{U}}(\omega)$$

$$+ \mathcal{B}\cdot\frac{\partial}{\partial \gamma_L}[\mathcal{B}_2(\omega)]\check{\underset{\sim}{U}}(\omega) \qquad (4.2\text{-}47)$$

$$\mathcal{H}_2(\omega)\frac{\partial \check{\underset{\sim}{Z}}(\omega)}{\partial \gamma_L} = \frac{\partial}{\partial \gamma_L}[-\mathcal{H}_2(\omega)]\check{\underset{\sim}{Z}}(\omega) + \frac{\partial}{\partial \gamma_L}[\mathcal{H}]\cdot\check{\underset{\sim}{X}}(\omega)$$

$$+ \mathcal{H}\cdot\frac{\partial \check{\underset{\sim}{X}}(\omega)}{\partial \gamma_L} \qquad (4.2\text{-}48)$$

The steps required to solve for $\frac{\partial}{\partial \gamma_L}[\check{\underset{\sim}{Z}}(\omega)]$, for each frequency value ω, are as follows:

3) Using known quantities, and those calculated at stage 1 (i.e. $\check{\underset{\sim}{X}}(\omega)$), solve the linear equation given in (4.2-47) for $\frac{\partial \check{\underset{\sim}{X}}(\omega)}{\partial \gamma_L}$.

4) Similarly using known quantities, and $\frac{\partial \check{\underset{\sim}{X}}(\omega)}{\partial \gamma_L}$ calculated at stage 3, solve the linear equation given in (4.2-48) for $\frac{\partial \check{\underset{\sim}{Z}}(\omega)}{\partial \gamma_L}$.

Hence, for each frequency point, we can calculate the terms within the summations, given in (4.2-42) and (4.2-

44). By carrying out the summations over the stipulated frequency range, we can build up the full numerical values of the terms in (4.2-42) and (4.2-44), for use in the minimisation scheme given by (4.2-38).

Expressions like: $\frac{\partial}{\partial \gamma_L}[\underline{\mathbb{B}}]$, $\frac{\partial}{\partial \gamma_L}[-\underline{A}(\omega)]$ and $\frac{\partial}{\partial \gamma_L}[\underline{\mathbb{B}}_2(\omega)]$ etc., follow straight from the definitions of the corresponding matrices given in (4.2-23) and (4.2-28). And so we have that:

$$\frac{\partial[\underline{\mathbb{B}}]}{\partial \gamma_L} = \left[\begin{array}{c|c} \frac{\partial B}{\partial \gamma_L} & 0 \\ \hline 0 & \frac{\partial B}{\partial \gamma_L} \end{array}\right]$$

$$\frac{\partial[-\underline{A}(\omega)]}{\partial \gamma_L} = \left[\begin{array}{c|c} \frac{\partial A}{\partial \gamma_L} & 0 \\ \hline 0 & \frac{\partial A}{\partial \gamma_L} \end{array}\right]$$

$$\frac{\partial[\underline{\mathbb{B}}_2(\omega)]}{\partial \gamma_L} = \left[\begin{array}{c|c} \begin{matrix} -\frac{\partial \tau_1}{\partial \gamma_L}\omega\sin\omega\tau_1 & & 0 \\ & \ddots & \\ 0 & & -\frac{\partial \tau_r}{\partial \gamma_L}\omega\sin\omega\tau_r \end{matrix} & \begin{matrix} \frac{\partial \tau_1}{\partial \gamma_L}\omega\cos\omega\tau_1 & & 0 \\ & \ddots & \\ 0 & & \frac{\partial \tau_r}{\partial \gamma_L}\omega\cos\omega\tau_r \end{matrix} \\ \hline \begin{matrix} -\frac{\partial \tau_1}{\partial \gamma_L}\omega\cos\omega\tau_1 & & 0 \\ & \ddots & \\ 0 & & -\frac{\partial \tau_r}{\partial \gamma_L}\omega\cos\omega\tau_r \end{matrix} & \begin{matrix} -\frac{\partial \tau_1}{\partial \gamma_L}\omega\sin\omega\tau_1 & & 0 \\ & \ddots & \\ 0 & & -\frac{\partial \tau_r}{\partial \gamma_L}\omega\cos\omega\tau_r \end{matrix} \end{array}\right]$$

(4.2-49)

Some Further Remarks On The Algorithm.

Good initial guesses are required for the parameters that are to be estimated, in order to ensure a quick convergence to the true cost-function minimum. This requirement arises because in the vicinity of the minimum, the Gauss-Newton algorithm uses a quadratic approximation to the cost function. On the use of second-order methods, such as Gauss-Newton, the following words are said in the reference MAIN002: "Second-order methods tend to converge quite rapidly in regions where they work well. There is usually such a region around the minimum point; the size of the region is problem dependent. The price paid for this region of excellent convergence is that the second-order methods often converge poorly or diverge in regions far from the minimum".

In order to perform a successful identification, the analyst must be confident that values of the parameters fixed throughout the estimation (including those fixed or set to zero) are correct. It can be appreciated that the fixing of some parameters at constant values, is a form of axial iteration (by analogy with the fixing of the error-covariance matrix elements for each iteration of the Gauss-Newton method), since these parameters could be estimated at a later stage, with the previously estimated model parameters fixed at the converged values! The fixing of some parameters at constant values can be

considered to be a constraint on the estimation. Other types of constraints are considered in section 4.2.3.

The Information Matrix.

The Cramer-Rao inequality for maximum-likelihood estimators can be shown (e.g. (MAIN001) to be given by:

$$E[(\underset{\sim}{\gamma}_{est} - \underset{\sim}{\gamma})(\underset{\sim}{\gamma}_{est} - \underset{\sim}{\gamma})^T] \geqslant M^{-1}_{true} \qquad (4.2\text{-}50)$$

where M_{true} is the Hessian matrix (defined by the right-hand side of (4.2-39)) evaluated at the true parameter values. The maximum achievable accuracy in the estimation is hence given by M^{-1}_{true}. It is stated in the reference MAIN001, that the calculated value of M^{-1}, (or rather the calculated value obtained using the first-order approximation whose elements are given by (4.2-44)) based on the estimated parameters from a maximum-likelihood procedure, rather than the true (and hence unknown) parameter values, is a good approximation. This is true even when the parameter estimates are far from their true values, because M tends to be relatively insensitive to changes in γ. In the current context, the matrix M is called the information matrix, and its inverse the parameter covariance matrix.

For the computer implementation of the frequency-domain output-error method, the squared roots of the diagonal elements of the inverse of the information

matrix (corresponding to the 1σ bounds) are used to indicate the accuracy of estimates.

4.2.3 Constrained Optimization.

Defined Relationships Between Sets Of Parameters.

If relationships are known to exist between different parts of the model structure, then they can be incorporated into the estimation. Expressions such as those given in (4.2-49) would be calculated taking the relationships into consideration. Only one of a set of related parameters would be estimated in the algorithm, and the related parts of the model would be updated on the basis of the known relationship to the single estimated parameter, using its current estimate. Specifying relationships between parameters is a form of constrained optimization, which reduces the dimensions of the quantities used in the minimisation scheme given in (4.2-38).

In the computer implementation of the frequency-domain output-error method developed in this chapter, the user has the facility to specify relationships between different parts of the model structure. For linear relationships, the matrix partial differentiation required for the calculation of the sensitivities, is done automatically within the software. Non-linear relationships can also be specified, but the user must be

able to write the analytic form of the partial derivative in a special subroutine. An example of the application of this facility is given in section 4.3.2.

Defining Allowable Regions For The Solution.

In the computer implementation of the frequency-domain output-error method developed in this document, which uses the Gauss-Newton minimisation technique, it is possible to constrain the parameters being estimated to lie within a specified region (defined by upper and lower bounds on allowable parameter values). If during the estimation, a particular parameter is given an update increment that would move it outside its allowable range, then the current estimate remains unchanged. If no constraints are required, then the user can specify a very wide range for the allowable parameter values, well outside a realistic range of parameter values. This facility is useful if we know from physical considerations that a parameter must lie within a specific range; for example, we may know that a certain parameter cannot be negative. In FOST002, the lack of such a facility in the software implementation of the time-domain maximum likelihood method developed in the reference, is cited as a notable deficiency by the author. It is also pointed out in the reference MAIN002, that constraints on the allowable range of estimates can have a stabilizing effect on the convergence of

second-order methods.

Rank-Deficient Solutions.

The use of singular-value decomposition in the equation-error approach was discussed and demonstrated in chapter 3. It was shown that the use of only a subset of the available orthogonal components in the solution, was equivalent to the removal of insignificant eigenvalues from the equation-error information matrix. The interpretation of this, given by the current author, was that each insignificant eigenvalue removed from the equation-error information matrix, corresponded to the introduction of a relational constraint into the estimation. The evidence for the requirement of a relational constraint originates from the measurement data used in the estimation. It manifests itself in the form of small singular values - S_i of the matrix $\mathbf{X}$ of independent-variable responses, and equivalently, small eigenvalues of the equation-error information matrix - λ_i, through the relationship implied in section 3.2.5, namely $S_{ii} = \sqrt{\lambda_i}$.

The information matrix used in the iterative Gauss-Newton estimation technique given in (4.2-38) can also be calculated with the most insignificant eigenvalues removed; this results in what is known as a rank-deficient solution. The technique of using a rank-deficient information matrix has been applied, with some

reported success, to time-domain aircraft identification problems by some researchers (e.g. STEP001).

In order to implement a facility for rank-deficient solutions in the output-error method developed here, the current author decided that applying a singular-value decomposition directly to the information matrix, would be a good approach numerically, for the decomposition into its eigenvalues and eigenvectors.

Consider a singular-value decomposition of the information matrix M, where for the special case of a p x p square symmetrical matrix, (where p is the number of parameters requiring update increments) this corresponds to the eigenvalue-factorisation result often given in texts on linear algebra (e.g. MURD001). This expression is given in (4.2-51); the diagonal matrix S (=Diag(λ_i)) will have the eigenvalues (i.e. the singular values) of M in descending order of magnitude down the leading diagonal, and the orthogonal matrix V will be composed of the eigenvectors V_i arranged in columns.

$$M = VSV^T \tag{4.2-51}$$

The iterative Gauss-Newton method, given by (4.2-38) can be written in terms of the update increments $\Delta\underset{\sim}{Y}$, as:

$$M\Delta\underset{\sim}{Y} = -\underset{\sim}{g} \tag{4.2-52}$$

Applying (4.2-51) to (4.2-52) we have

$$VSV^T\Delta\underset{\sim}{\varsigma} = -\underset{\sim}{g} \tag{4.2-53}$$

which implies that:

$$S\Delta\underset{\sim}{\phi} = -V^T\underset{\sim}{g} \tag{4.2-54}$$

where we have that:

$$V^T\Delta\underset{\sim}{\varsigma} = \Delta\underset{\sim}{\phi} \tag{4.2-55}$$

The diagonal nature of S allows (4.2-54) to be solved easily for the linearly-transformed set of parameter update increments.

$$\Delta\phi_i = (-V^T\underset{\sim}{g})_i / \lambda_i \tag{4.2-56}$$

We may obtain rank-deficient increments by setting the most insignificant elements of the linearly-transformed update increment vector $\Delta\underset{\sim}{\phi}$ (corresponding to small eigenvalues of M) to zero, and using the inverse of the linear transform to obtain the increments in terms of the original set of variables:

$$\Delta\underset{\sim}{\varsigma} = V\underset{\sim}{\phi}(r) \tag{4.2-57}$$

where:

$$\Delta \underset{\sim}{\phi}(r) = (\phi_1, \phi_2, \phi_3, \ldots \phi_r, 0, 0, 0)^T \qquad (4.2\text{-}58)$$

For the symmetrical matrix M we can formally write the following expression for the inverse of a rank-deficient M:

$$M^{-1} = \sum_{i=1}^{p-r} \lambda_i^{-1} (V_i V_i^T) \qquad (4.2\text{-}59)$$

where r is the number of eigenvalues removed from the information matrix M. Whilst the above expression is not used in calculating a rank-deficient M, it highlights the fact that the smallest eigenvalues are associated with directions in the parameter space that have the most uncertainty associated with them.

An example of the application of rank-deficiency is given in section 4.3.2. Using (4.2-58) in (4.2-55) it can be seen that the removal of insignificant eigenvalues corresponds to the introduction of relational constraints on the update increments $\Delta \underset{\sim}{\zeta}$. As with the case where there are known relationships between sets of parameters, there is a reduction in the dimension of the parameter space effectively used in the estimation. The advantage of the use of rank-deficiency is that it may not be possible for the analyst to easily define the relationships (or correlations) that exist between a large set of

parameters. However, with the rank-deficient approach, the relationships (associated with near-zero eigenvalues) are effectively constructed automatically from the measured data used in the identification; more will be said of this in the context of the practical examples given in section 4.3.2.

4.2.4 Controlling Convergence Of The Algorithm.

The Gauss-Newton iterative technique used in the minimisation of the cost function J requires the specification of criteria to indicate when the estimates are acceptable. There are several possible ways of doing this. These include the following, suggested in the reference FOST002: (1) inspect the size of $\frac{\partial J}{\partial \underset{\sim}{\gamma}}$, and end the search when the elements of this vector become small; (2) end the search when the change in J is small; and (3) end the search for small changes in each of the elements of $\underset{\sim}{\gamma}$. As pointed out in FOST002, the problem with the first approach is that it is difficult to define what constitutes a small gradient vector in a way that is readily appreciable. It is also pointed out that the problem with the second approach is that, for parameters weakly defined by the observation data, the algorithm can terminate at values which are highly dependent on initial guesses. The third approach is given as the most desirable, where what constitutes a small change is specified individually for each parameter. This is

better than using percentage changes for all the parameters, because it avoids difficulties that could be experienced for parameters whose true value is near zero; in addition, it indicates acceptable levels of accuracy for each of the parameters, which as the author points out in FOST002, is no bad thing.

A problem that may be experienced is that the algorithm may converge not to the desired global minimum, but to a local minimum. It should be apparent when this occurs from the un-realistic (or non-physical) parameter estimates obtained on completion; in addition, the cost value will be higher than might be expected, based on experience from similar runs. As was stressed in section 4.2.2, the performance of the identification algorithm is very dependent on the initial guesses - hence the requirement for good initial guesses to ensure rapid convergence.

4.2.5 Some Further Comments On Neglecting Process-Noise Terms.

<u>The Problem Of Noisily Observed Inputs.</u>

In the development of the cost function for the frequency-domain output-error method presented in section 4.2.1, it was assumed that there was no process noise. This assumption was made to avoid the considerable complexity that would be incurred as a result of

formulating the model output in terms of a Kalman filter. This decision was then rationalized by saying that the effect of some unmodelled inputs could be lessened: for example, avoiding the use of large amplitude and/or large clock-period test inputs to lessen problems due to non-linearities. In addition, in the case of unmodelled rotor effects, the incorporation and estimation of a time delay in some controls, could improve the modelling of the effective control input. However, the problem of having noise on the control inputs is not one which is easily dismissed. This is particularly so for the approach presented in this document: that of using an extended control vector to include in addition to the applied pilot control (possibly with a time delay), additional (noisy) terms to drive the state-space model. This approach was convenient because it enabled the helicopter identification problem to be cast in a manageable size.

The problem of having noisily observed inputs is equivalent to having a process noise term in the model. As in the case of measurement noise on the independent variables in the equation-error approach, the presence of process noise in the output-error approach will lead, in general, to biased estimates. One possible approach, which if not a solution, is at least a palliative, is to use a state estimator, such as the Extended Kalman Filtering program DEFKIS, mentioned in section 1.3.3. This technique may be able to remove some of the noise (or uncertainty) associated with those quantities to be

included in the extended control vector, used to drive the reduced-order model. It will, however, add considerably to the time and cost required to carry out an identification.

Estimation Of Kalman Gains.

For the state-space model given by equations (4.2-1) and (4.2-2) the corresponding continuous-time Kalman-Filter equations (which enable the expected-value quantities which are defined in (4.2-9) and (4.2-10), and are required for the maximum-likelihood formulation of the problem, to be obtained) are given by (e.g. GELB001, and APPENDIX 4):

$$\dot{\bar{\underset{\sim}{X}}}(t) = A\bar{\underset{\sim}{X}}(t) + B\underset{\sim}{U}(t) + K\underset{\sim}{V}(t) \qquad (4.2\text{-}60)$$

$$\underset{\sim}{Z}(t) = H\bar{\underset{\sim}{X}}(t) + \underset{\sim}{V}(t) \qquad (4.2\text{-}61)$$

The zero-offset terms are dropped from the above formulation, since they disappear anyway for transformation into the frequency domain, with the condition that $\omega \neq 0$. In addition, the steady-state Kalman gains K are used (transients associated with uncertainties about the initial state conditions have decayed, and the noise statistics are assumed stationary).

The steady-state Kalman-Filter representation of the

system given by (4.2-60) and (4.2-61) can be rearranged to give:

$$\dot{\bar{\underset{\sim}{X}}}(t) = A_2 \bar{\underset{\sim}{X}}(t) + B_2 \underset{\sim}{U}_2(t) \qquad (4.2\text{-}62)$$

where: $A_2 = A - KH$; $B_2 = (B, K)$; $\underset{\sim}{U}_2(t) = (\underset{\sim}{U}(t), \underset{\sim}{Z}(t))^T$

By transforming equations (4.2-61) and (4.2-62) into the frequency domain, the frequency-domain innovations vector $\hat{\underset{\sim}{\gamma}}(\omega)$ can be obtained for use in the probability density function given in (4.2-17), instead of $\hat{\underset{\sim}{V}}(\omega)$. In addition, the covariance matrix of the innovations S, can also be obtained from the Kalman-filter algorithm. Strictly speaking, the Kalman-gain matrix K, implicit in (4.2-62), is not an independent entity which could be estimated as if it was part of a control dispersion matrix B_2, but is subject to the constraints of both its definition and the matrix Riccati equation (governing the propagation of the error-covariance matrix of the state estimates through time) (e.g. GELB001).

The above discussion of the inclusion of Kalman gains (and by implication, the inclusion of process noise terms) in the estimation, is not presented in detail, because no results were obtained applying the method. It was included to show the possibility of future work in this direction, though it would also be important to assess whether the considerable increase in complexity incurred as a result, would justify its use for helicopter system identification.

In the references KLEI004 and KLEI005, an algorithm for the frequency-domain identification of a linear system using maximum likelihood estimation, was developed. The algorithm is based on the transformation of discrete-time system equations into the frequency domain. However, the elements of the Kalman-gain matrix are estimated as if they were free parameters and are not subject to the constraints of the discrete-time Kalman filter algorithm such as the definition of the steady-state Kalman gain matrix, the error-covariance extrapolation and error-covariance update equations (see Appendix 4). (As an aside, it is also assumed in the derivation that the measurement window is periodic: the output-error method developed in this document incorporates a non-periodic measurement window correction term at the outset). Before the implications of neglecting the constraints and treating the Kalman-gain matrix elements as if they were ordinary parameters are discussed, it is worth pointing out that such an estimation could be carried out using the frequency-domain output-error method developed in this document. By formulating the estimation problem in terms of equation (4.2-62), and using the control vector extended to include the measured responses, and making use of the ability to include any relationships between different parts of the model, an identification could be carried out. There will be a substantial increase in the number of parameters to be estimated because of the need to

estimate the gain matrix K as part of the control dispersion matrix. Because this approach requires no modification to existing software, it is a possible area for future research.

It is pointed out in the reference FOST002, that by using the simple method, whereby the Kalman gains are treated as if they were independent parameters, the parameter search will take place in a space with many more dimensions than necessary. For a time-domain maximum likelihood method, the author in FOST002 reports some success with the simple method, but recommends a more rigourous implementation of the Kalman-filter algorithm, and develops some analytical expressions for the implementation of the algorithm.

4.2.6 Summary Of Section 4.2.

A frequency-domain output-error method has been developed and implemented in a FORTRAN-77 program: OUTMOD. The Gauss-Newton minimisation method, with an additional line-search facility, was used. A separate estimation algorithm was used for the elements of the error-covariance matrix.

The output-error method was implemented with many unique and potentially useful features. The frequency-domain representation of the model equations, developed by the current author, facilitated the development and implementation of both the required expressions for the

estimation algorithm, and the useful features of the program OUTMOD. These include: the ability to define relations between different parts of the model structure (i.e. a relational constraint); the ability to restrict the allowable range of individual parameter values; and the facility for obtaining rank-deficient solutions (linear relational constraints) using a singular-value decomposition of the information matrix.

In addition, time delays in the observed control inputs and measured responses can be estimated, as well as elements of the model matrices: A, B, H. The correction term for a non-periodic measurement window, discussed in section 2.2.4, is also incorporated in the algorithm. The program OUTMOD, is to the best of the current author's knowledge, the best and most versatile frequency-domain state-space identification software available to date.

4.3 Applications Of The Frequency-Domain Output-Error Method To Flight Data.

4.3.1 Applications Involving Longitudinal Test Inputs.

The frequency-domain output-error method has been applied to a large number of data sets, although, only a representative set of results is included in this document. These examples serve to illustrate important features of the method and the computer implementation.

In Section 2.3.3, results were presented using real flight data for a longitudinal-cyclic input. It was shown that the output-error method produced estimates, which in the case with a time delay incorporated, compared favourably with theoretical estimates; the plots showing the frequency-domain fits and the time-domain verification also indicated a successful identification. Figure 4-1 shows the estimates of the parameters, and the total cost-function value and its non-logarithmic component, as a function of iteration number. The estimated diagonal elements of the inverse of the error-covariance matrix as a function of iteration number are shown in Figure 4-2; these elements were fixed at specified values (obtained by estimating the relative noise levels using the original flight-data records) for the first iteration, to prevent possible initial divergence of the algorithm due to the use of an estimated error-covariance matrix which could be greatly in error due to the initial parameter estimates being far from their true values.

Twelve model parameters and four diagonal elements of the error-covariance matrix (estimated using the axial iteration algorithm explained in Section 4.2.2) were estimated. It can be seen from Figure 4-1 that convergence is reached after about 16 iterations although the exact number will vary according to the tolerances specified on the update increments for each of the parameters individually. This is of the order of one

iteration per unknown parameter. The total C.P.U. time for the run was about 4 minutes on a VAX 11/750 computer with V.M.S. operating system. The cost-function value shown in Figure 4-2 is progressively reduced after each iteration until it levels out to a value of about -131.4; and the non-logarithmic component (as explained in section 4.2.2) converges to the value of 64, corresponding to the product of the number of states in the model and the number of frequency points used in the identification. It should be noted that an additional factor of 2 is present because the cost-function minimised in the implementation here is not premuliplied by 1/2; this is, however, taken into consideration when the error-bounds are calculated. The non-logarithmic component should always reach the value indicated above, and is a useful additional check that the identification algorithm has converged correctly. The results shown in Figure 4-2, for the error-covariance matrix, also confirm that its elements have converged.

A Transfer Function Example.

An alternative to the formulation of the identification in terms of the linearised equations of motion in state-space form, is provided by a single-input single-output transfer function representation. The use of single-input single-output transfer functions valid over a defined frequency range for chosen flight

conditions, is an approach which has been used by some researchers (e.g. TISC001) using the chirp Z transform. The transfer-function response for the measured data is obtained from cross and input auto spectra (as outlined in section 2.2.1). The approach adopted by the current author was to use the frequency-domain output-error method developed in this document: this is possible because the transfer-function models can be written in an equivalent state-space form.

The classical pitch rate and normal acceleration responses to a longitudinal-cyclic input for the short period mode are given by:

$$\frac{q(s)}{\eta_{1s}(s)} = \frac{M_{\eta_{1s}}(s + 1/T_\theta)\, e^{-s\tau_\theta}}{s^2 + 2\zeta\omega_{sp}s + \omega_{sp}^2} \qquad (4.3\text{-}1)$$

$$\frac{a_z(s)}{\eta_{1s}(s)} \quad \frac{Z_{\eta_{1s}}\, e^{-s\tau_{az}}}{s^2 + 2\zeta\omega_{sp}s + \omega_{sp}^2} \qquad (4.3\text{-}2)$$

where $q(s)/\eta_{1s}(s)$ is the Laplace-transformed pitch-rate response to a longitudinal-cyclic input, and s is the Laplace operator. The parameter $M_{\eta_{1s}}$ is the longitudinal-cyclic pitch sensitivity, and τ_θ is the effective time delay on the input for pitch rate. The parameter T_θ is given by (PADF006):

$$T_\theta = \frac{M_{\eta_{1s}}}{M_w Z_{\eta_{1s}} - Z_w M_{\eta_{1s}}} \qquad (4.3\text{-}3)$$

where ζ and ω_{sp} are the equivalent short-period mode damping and natural frequency respectively. In equation (4.3-2), the term $a_z(s)/\eta_{1s}(s)$ is the Laplace-transformed normal acceleration response to a longitudinal-cyclic input, whilst $Z_{\eta_{1s}}$ is the longitudinal-cyclic normal-force sensitivity. The effective time delay on the input, τ_{az}, was assumed to be negligible for this investigation. The denominator parameters are identical to those in the pitch-rate transfer function.

Equations (4.3-1) and (4.3-2) may be written in time-domain state-space form as:

$$\begin{bmatrix} \dot{q}(t) \\ \ddot{q}(t) \\ \dot{a}_z(t) \\ \ddot{a}_z(t) \end{bmatrix} = \begin{bmatrix} 0 & 1 & 0 & 0 \\ -\omega_{sp}^2 & -2\zeta\omega_{sp} & 0 & 0 \\ 0 & 0 & 0 & 1 \\ 0 & 0 & -\omega_{sp}^2 & -2\zeta\omega_{sp} \end{bmatrix} \begin{bmatrix} q(t) \\ \dot{q}(t) \\ a_z(t) \\ \dot{a}_z(t) \end{bmatrix}$$

$$+ \begin{bmatrix} 0 & 0 & 0 \\ M_{\eta_{1s}}/\tau_\theta & M_{\eta_{1s}} & 0 \\ 0 & 0 & 0 \\ 0 & 0 & Z_{\eta_{1s}} \end{bmatrix} \begin{bmatrix} \eta_{1s}(t-\tau_\theta) \\ \dot{\eta}_{1s}(t-\tau_\theta) \\ \eta_{1s}(t-\tau_{az}) \end{bmatrix} . \qquad (4.3\text{-}4)$$

The identification problem is thus formulated now in a way that allows the frequency-domain output-error method to be used. Use can be made of the facility in the software to relate parameters within the model structure, because ω_{sp}^2, $2\zeta\omega_{sp}$ and τ_θ all occur twice. By specifying the equalities which exist between the elements in the second and fourth rows of the state

matrix in equation (4.3-4), we are effectively imposing equality in the denominator coefficients for the transfer functions shown in equations (4.3-1) and (4.3-2).

Using flight-data for a longitudinal-cyclic doublet input (input and response time histories shown in Figure 2-6), estimates were obtained, using the transfer-function formulation, for ω_{sp}^2, $2\zeta\omega_{sp}$, etc .. Results are shown in Table 4-1 for three cases, representing : (1) an identification using only the pitch-rate terms - that is the subsystem of equation (4.3-4) corresponding to a state-space formulation of the transfer function given by (4.3-1); (2) an identification using (4.3-4, with the equalities existing between elements in the model structure specified; and finally (3), an identification also using (4.3-4), but with the acceleration measurements modelled such that the actual acceleration is lagged relative to the measured acceleration, with the acceleration time-constant estimated as an unknown parameter. Before the results are considered, some additional remarks concerning the third case would be of use. The acceleration time-constant τ_m is modelled as a delay in the corresponding measurement channels; this is a satisfactory approximation when $|\omega\tau_m| \ll 1$ (see equations (1.2-17) - (1.2-22) in section 1.2.5).

Comparing the results for cases (1) and (2) in Table 4-1, it can be seen that by using both pitch-rate and acceleration measurements to estimate the transfer-

function parameters (using equation 4.3-4), a substantial improvement is obtained in the parameter estimates, both in terms of their comparison with theoretical values and their estimated error bounds, when compared to those obtained for the single pitch-rate transfer-function. Finally, it can be seen that the case (3) estimates are in essence very similar to those obtained for case (2). Both sets of estimates agree within the indicated 1σ error bounds, however, it is remarkable that $2\zeta\omega_{s_{\tilde{q}}}$ and $M_{\eta_{1s}}$ compare more favourably with theory for case (3), and have smaller error bounds. The acceleration time-constant is estimated with great uncertainty in this example, - in fact, a zero value for τ_m, corresponding effectively to case (2), lies within the indicated 1σ error bound. However, the example shown here serves to illustrate a potentially useful idea which could be used in future applications for lagged (or phase-shifted measurements.

A noticeable feature of all three cases shown in Table 4-1, is that the time delay τ_θ in the longitudinal-cyclic control is estimated consistently to be around 0.2 seconds, and has a relatively small error bound for cases (2) and (3).

It can be seen from equation (4.3-4) that implicit in the formulation is the assumption that measurements of $\dot{q}(t)$ and $\dot{a}_z(t)$ are available. In fact, for the example presented, they were not, and the problem of having to construct time-derivative signals was tackled by

differentiating a signal constructed using only the first few Fourier coefficients (corresponding to a frequency range similar to that used in the identification). The facility for differentiating a filtered signal over a specified frequency range is available in the frequency-domain output-error program OUTMOD. One drawback with this approach, is that, as pointed out in section 2.2.2, the 'filtered' signal might suffer from Gibb's-oscillation effects, resulting in some errors in the differentiated signal if the beginning and end of the response are very different. There is no requirement to differentiate a control-signal time history in the same way, because when the model equations are transformed into the frequency domain, the relationship between the Fourier transform of a given quantity and the Fourier transform of its time derivative can be used, as explained in section 2.2.3.

The normal acceleration signal used in the identification, was effectively obtained from measurements of the incidence angle, using:

$$W + W_e = U_e \alpha + l_x^{\alpha} q - l_y^{\alpha} p \qquad (4.3\text{-}5)$$

(from equation (2.2-33) in section 2.2.4)

We have, using the result for the normal-force equation in APPENDIX 1 (for a first-order approximation), the following relationship between the measured quantities and those in the state-space model:

$$\begin{bmatrix} q_m \\ \dot{q}_m \\ \dot{W} \\ \ddot{W} \end{bmatrix} \simeq \begin{bmatrix} 1 & 0 & 0 & 0 \\ 0 & 1 & 0 & 0 \\ U_e & 0 & 1 & 0 \\ 0 & U_e & 0 & 1 \end{bmatrix} \begin{bmatrix} q \\ \dot{q} \\ a_z \\ \dot{a}_z \end{bmatrix} \qquad (4.3\text{-}6)$$

Figure 4-3 shows the 'measured' signals $q_m, \dot{q}_m, \dot{W}_m, \ddot{W}_m$. The frequency-domain fits (corresponding to case (3) in Table 4-1) are shown in Figure 4-4; and apart from the lowest frequency value, (possibly associated with non-linearities) the correspondence between measured and predicted value is good for $q, \dot{q}$ and $\dot{W}$.

<u>A Run With A Defined Non-Linear Relationship (Using A Combination Of Data For Two Test-Input Signals Applied To The Longitudinal-Cyclic Control).</u>

An identification was carried out using a combination of two longitudinal-cyclic inputs - a '3211' and a doublet. Both sets of data represent the same nominal flight condition: a speed of 100 knots in straight and level flight. The form of model used in the identification is the same as that given in section 2.3.3. The data corresponding to each input is combined using the linear principle of superposition. This is possible in the present context, even when a non-linear feature, namely a time delay, is incorporated and estimated in the longitudinal-cyclic control, because we

can assume that the time delay is the same for both test-input signals. Some evidence for the validity of this assumption can be provided by the investigation carried out in section 2.3.2 using simulated data from the HELISTAB program, where, as shown in Figure 2-3, the estimated delays for both a doublet and a 3211, are identical within the limits of the indicated accuracy.

The combined time-domain (averaged) responses are shown as part of Figure 4-5. For a linear system, whether the data is transformed into the frequency domain and then combined, or the perturbation data is combined in the time domain and then transformed into the frequency domain, should be immaterial; both approaches are attempted and are referred to as cases (1) and (2) respectively.

A feature of the identification carried out here for the combined data set, was the specification of a non-linear relationship between an element of the system matrix A and an element of the measurement transition matrix H. The system matrix and measurement transition matrix are defined in section 2.3.3 by equations (2.3-11) and (2.3-12) respectively. The non-linear relationship defined was:

$$A_{23} = 1/H_{22} \tag{4.3-7}$$

where A_{ij} and H_{ij} are the ijth elements of the matrices. It was assumed that A_{23} was equal to the trim value of

the forward velocity component U_e , and that the derivative Z_q was negligible in comparison - from which, the relationship specified by equation (4.3-7) follows.

The identification was carried out over a frequency range up to 0.60 Hz, with the transformed record length being about 13.3 seconds in length (see Figure 4-5). Thirteen independent model parameters, in addition to the parameter A_{23} defined by equation (4.3.7), were estimated. A third case was attempted where $1/U_e$ (and U_e) were fixed at the values indicated for the flight condition.

The parameter estimates for all three cases are given in Table 4-2. It can be seen that the results, on the basis of individual parameter estimates, are not as good as those obtained for the use of the doublet-input data alone (results shown in Table 2-2, case (2), in section 2.3.3). This is apparent for several parameters which previously had estimates which compared favourably with theory, and which had relatively small error bounds, namely: M_q, M_p, M_β, $M_{\eta_{1s}}$ and $Z_{\eta_{1s}}$. The parameter $1/U_e$ estimated for the relationship defined by equation 4.3.7 is, however, for case (1), estimated with a relatively high degree of confidence, and is in close agreement with what would be expected for a nominal trim speed of 168.9 ft/s (100 knots). For case (2), the estimate of $1/U_e$ is smaller in value; the reason for the difference is not clear, but may be associated with the strong non-linearities (i.e. large excursions from the trim)

apparent for the speed time history shown as part of Figure 4-7. In fact a comparison of the responses shown in Figures 4-7 and 2-6, shows that the combined run has much larger excursions in the measurements, which is not good for the identification of a model based on the assumption of small perturbations.

The estimates of Z_w, shown in Table 4-2, are consistent for all three cases and compare very favourably with theory. The values of the time delay obtained are in agreement with that obtained for the single-input doublet run, within the limits of indicated accuracy.

The frequency-domain fits obtained at convergence are shown in Figure 4-6, and, unfortunately, provide little useful information. It is apparent that the combined run has resulted in responses which are poorly excited above 0.15Hz.. The poor excitation above 0.15 Hz., together with the large excursions in the measurements, are major factors in causing the estimates to be inferior to the single doublet-input case.

When the one-second clock-period '3211' input (i.e. a total of 7 seconds in length) alone was used, the identification algorithm diverged. It was pointed out in section 1.4.1 that the use of this input is far from ideal for the identification of small perturbation models. The effective input for the combined run, shown in Figure 4-5, represents an improvement, but is demonstrably inferior to the two-second clock-period

doublet input. The estimated auto-spectra for the two cases are shown in Figures 4-8 a), b).

The time-domain predictions of the model, following a time-domain output-error estimation of initial conditions and zero offsets are shown as part of Figure 4-7.

An Output-Error Multirun Example.

In the reference MARC002, the combination of data sets in the frequency domain, corresponding to the application of test-inputs on different controls, is an approach which is advocated for multirun identification. This requires all the data sets - representing the same flight condition - to be of equal length. Time histories of the data used in a multirun identification presented in the reference MARC002 reveal that the test-input signals, applied on all four controls, are all of the same general shape. Although no parameter values are presented and final fits between measured and estimated time histories only are given, it is the opinion of the current author that this is likely to lead to identification difficulties, particularly for elements of the true control dispersion matrix. The reason for this can be appreciated by examination of the state-equation, where it can be seen that if two controls have similarly shaped test-input signals and are dispersed onto a given state, then the two corresponding row entries in the

control dispersion matrix are indistinguishable for identification purposes.

A multirun identification was carried using two data sets; one corresponding to the application of a longitudinal-cyclic doublet (as used in section 2.3.3), and the other corresponding to a collective doublet. The test-input signals are shown in Figure 4-9, along with the time-histories of the effective lateral-state responses incorporated as pseudo-controls in an extended control vector. The form of the model used is as given by equations (2.3-11) and (2.3-12) in section 2.3.3, except that an additional collective control term is present.

If we consider Figure 4-11, and for the time being concentrate only on the measured responses of the longitudinal variables, it can be seen that the excursions from the initial trim values are small in comparison to those given by Figure 4-7. This indicates that the small-perturbation modelling assumption is likely to be more satisfactory in this case. It may, however, have been more satisfactory to use different test-input signals rather than two two-second clock-period doublets, because of the reasons discussed earlier. The choice of data sets used was dictated by availability.

Results for the identification, which was carried out over a frequency range up to 0.60 Hz., are given in Table 4-3. Also shown are results corresponding to the use of an information matrix of rank 13 (14 model

parameters in total were estimated). The full-rank and rank-deficient solutions are referred to in the table as Cases 1 and 2 respectively.

Examination of the results given for Case 1 in Table 4-3 for the multirun data, and a comparison of the results given in Table 2-2 (Case 2) for the single-run data, shows that for this example, the use of multirun data in the identification has tended to degrade the estimates in comparison to the single-run case. Estimates of parameters which had previously compared well with theory, and were estimated with a relatively high degree of confidence, no longer correspond with theory, in the majority of cases.

The use of a rank-deficient information matrix resulted in an improvement in the estimates obtained in a few cases, especially for M_q. The value of the time delay estimated in the longitudinal-cyclic control is in agreement with the value obtained for the single-run case, and is estimated with a relatively high degree of confidence. It is also interesting to note that a smaller value, which is less significant on the basis of the indicated error bounds, is obtained for the delay on the collective control channel. The investigation carried out in section 2.3.2 using simulated data, indicated that a time delay in the collective was likely to be of less importance than a time delay in the longitudinal-cyclic control, for the identification of a quasi-static model using flight-data contaminated with

rotor transient effects. A further reduction in the rank of the information matrix did not give, in general, appreciably better results: more physically realistic estimates of M_p and M_β emerged, but this was found to coincide with less satisfactory estimates of other parameters, particularly for the time delay in the longitudinal-cyclic control.

The frequency-domain fits obtained for the rank-13 solution are given in Figure 4-10. The least satisfactory frequency-domain fit is obtained for the speed channel. A time-domain verification of the model, following a time-domain output-error estimation of initial conditions and zero-offsets, is shown as part of Figure 4-11.

It can be concluded that if multirun data sets are to be used as a means for identifying more robust models than single-run data sets, then more consideration of the test-input signals used on each of the control channels is required. The use of multirun data sets for the attempted identification of a full 8-state model, involving the application of uncorrelated test-input signals on the longitudinal and lateral control channels is a task to which the identification software could be applied.

Other Applications To The Identification Of Longitudinal Models.

Some other attempted applications of the frequency-domain output-error method to the identification of longitudinal models involved mostly the use of one-second clock-period 3211 test inputs. The unsatisfactory nature of this test-input signal for the identification of models relating to the Puma helicopter has already been emphasized. Nevertheless, despite obtaining in most cases poorer parameter estimates, some of the features of the more successful applications discussed here for longitudinal models, and in the next section for lateral models, could be seen in the results obtained. In particular, an improvement was found in the fits, and in some of the parameter estimates, for the incorporation and estimation of a time delay in the longitudinal-cyclic control. Results are presented in Table 4-4 for two flight-data sets corresponding to a Puma helicopter, trimmed at a speed of 80 knots in straight and level flight.

4.3.2 Applications Involving Lateral Test Inputs, With A Consideration Of Trends In The Estimates For Different Flight Conditions.

Previously Reported Problems.

The tendency for primary-rate damping derivatives, such as M_q and L_p to be underestimated, is a recurring theme in previously published studies on helicopter parameter estimation studies (e.g. PADF002). The incorporation and estimation of a time delay in the applied control for the output-error method is an approach advocated in this document for the identification of quasi-static derivatives when using a six-degrees-of-freedom model; this approach was demonstrated in section 2.3.3 for a longitudinal model. In addition to the problem of the underestimation of roll-damping L_p, the results obtained in PADF002 using the equation-error approach, show that the accompanying estimate of the derivative L_r was very high compared to theory; this anomaly has also been observed by the current author, for a range of flight conditions between 60 and 100 knots in level flight, using the equation-error approach.

If we consider the response (shown for the lateral variables as part of Figures 4-17, 4-18, and 4-19) to a pedal doublet input (Figure 4-12), for a Puma helicopter flying at a nominal trim sped of 100 knots, in straight

and level flight, altitude 6000 ft., it can be seen that there is a strong correlation between the roll and yaw rate responses. The damped sinusoidal roll and yaw rate responses are almost π radians out of phase with each other, and are associated with a 'Dutch-Roll' type mode. It can therefore be expected that difficulties in estimating some of the parameters associated with these variables will occur due to the ill-conditioning of the information matrix. Ill-conditioning of the information matrix was considered in section 3.2.5 in the context of the equation-error method; and in section 4.2.3 the facility for producing a rank-deficient - and therefore better conditioned - information matrix for the output-error method was explained. The presence of one, or more, relatively small eigenvalues in the information matrix is an indication that the parameter set used does not constitute a truly independent set of parameters, and that a better identification may be carried out using a rank-deficient information matrix; indeed, convergence problems can be experienced in the use of an ill-conditioned - nearly singular - information matrix.

Before results obtained in applying the rank-deficient frequency-domain output-error technique for the identification of lateral derivatives are presented, it is worth noting that, in addition to the problems resulting from linear dependence, the information matrix will also be nearly singular, if one or more of the parameters to be estimated are weakly defined. In terms

of the cost- function surface defined in the parameter space, this means that in the vicinity of the minimum, the surface is relatively flat in at least one direction: a relatively insignificant change in the cost-function value would occur for a relatively large change in the parameter value. For the iterative output-error estimation scheme where a rank-deficient information matrix was used, the final estimate of a weakly-defined parameter will depend very much on the initial guess. Consequently, weak or insignificant parameters should be excluded from the identification at the outset; 'parameter significance' values obtained at the equation-error stage can be used as a basis for judgement.

Pedal Input - 100 Knots.

Consider the pedal-doublet run described earlier. The full-rank, and rank-deficient results, obtained using the frequency-domain output-error estimation technique are shown in Tables 4-5 a) and b). The results are also represented graphically for the important lateral derivatives, the delay, and the cost-function value in figure 4-13. Full-rank solutions with, and without, a delay in the control are also presented for comparison.

In total, 12 stability and control parameters were estimated for each of the rank-deficient solutions. The number of time-domain points input to the estimation

program, and transformed into the frequency domain was 1700, sampled at 64 Hz., making a record of length 26.6 seconds. The frequency range used in the estimation was 0.03765 - 0.4894 Hz., corresponding to 13 complex-valued frequency-domain points, and was chosen on the basis of magnitude plots of the Fourier transforms, obtained at the equation-error stage. Initial guesses for the parameters were also obtained at the equation-error stage, except for the delay which had an initial guess of zero.

The incorporation and estimation of a delay in the control, results in a substantially lower cost value at convergence. Figures 4-14 and 4-15 show the frequency-domain fits obtained for these two cases. The improvement obtained as a result of the delay is particularly visible for frequencies on either side of the peak at about 0.22 Hz.. In general, the agreement between measured and predicted frequency-domain responses is very good, especially the rolling and yawing moment fits. The delay itself is estimated to be about 0.2 seconds, and has a relatively small error bound.

In the case of the rolling-moment parameters, the inclusion of a delay results in estimates that are in much better agreement with theory, than in the case without the delay. As the rank of the solution is decreased to 9, there is a noticeable change in the estimates of L_v and L_r; L_v agrees very well with theory, whilst the L_r estimate is much closer to theory than the

higher-rank cases. The roll damping L_p is lower than the theoretical prediction, but it is larger than corresponding estimates obtained from the equation-error approach (values of -0.9 and 0.86 for L_p and L_r respectively). The incorporation of a delay in the control has thus increased the estimate of L_p. The combination of the use of the output-error technique, the incorporation and estimation of a delay in the control, and the use of rank-deficiency in the information matrix - in particular, for an information matrix of rank 9 - has led to rolling moment parameter estimates that are in generally good agreement with theory.

Consider now the yawing-moment derivatives: the rank-9 estimate of N_r is in excellent agreement with theory. N_p differs somewhat from theory, but is estimated with a relatively small error bound. N_v is estimated to be larger than the theoretical prediction, but is still of comparable magnitude. The pedal control sensitivity to yaw N_{η_p} is smaller than theory suggests; however, the estimate obtained from the rank-9 solution is the closest to theory. The frequency-domain fits obtained at convergence for the rank-9 solution are shown in Figure 4-16. It can be seen that they are very similar to those for the full-rank case with delay presented in Figure 4-15.

Following a frequency-domain estimation of the stability and control derivatives, the next stage in the identification scheme is to perform a time-domain output-

error estimation to obtain estimates of the zero-offsets, and initial state conditions, with a view to obtaining a time-domain verification of the model identified in the frequency domain. This stage in the identification methodology is explained in Chapter 5. This was done for the estimated model obtained in the following three cases: 1) full rank with no delay in the control 2) full rank with delay in the control and 3) rank-9 solution with delay in the control. The time-domain verification results following from the time-domain estimation are shown in Figures 4-17 to 4-19. First comparing Figures 4-17 and 4-18 for the full-rank solutions: it can be seen that for the roll rate channel in particular, the inclusion of the delay leads to a much tighter fit over the first few seconds of data, when the control input is applied; the rank-9 solution also shows this, and in comparison to the full rank case in Figure 4-18, the time-domain fit is only slightly degraded towards the end of the time record.

The preference for the rank-9 solution was based on comparisons of the predicted theoretical values with corresponding estimates. It is accepted that all the parameter estimates obtained from flight data need not equal the theoretical values, since the purpose of system identification in the current context is both to confirm some aspects of the theoretical model, and to update others. However, important primary effects should be able to be predicted by relatively simple theory, and so the

estimates of parameters strongly influencing these effects may be used as an indicator of how good the model is, along with the time-domain reconstructions and predictions of the model.

In going from rank 9 to rank 8 there is a substantial degradation in the estimates of most of the important parameters, such as: L_p, L_r and N_r. Figure 4-20 shows for one iteration of the frequency-domain output-error method a typical reduction in cost-function value (normalised to the full-rank case) that would obtained as the rank of the information matrix is increased from 1 up to the full-rank case; this is obtained using the total differential:

$$\Delta J \simeq \frac{\partial J}{\partial \gamma_1}\Delta\gamma_1 + \frac{\partial J}{\partial \gamma_2}\Delta\gamma_2 + \frac{\partial J}{\partial \gamma_3}\Delta\gamma_3 + \dots \frac{\partial J}{\partial \gamma_p}\Delta\gamma_p \tag{4.3-8}$$

There is clearly a distinction between the rank-9, and rank-8 and lower-rank cost-reductions, whereas the rank-9 reduction is of comparable magnitude to the higher-rank cost-reductions. This observation seems to reflect the degradation observed in the parameter estimates for ranks lower than 9.

Longitudinal measurements were included in an extended deterministic control vector for the four-state lateral model used in the estimation, with the significant cross coupling terms identified as elements of the control dispersion matrix B. Table 4-5 b) shows

the values of the estimated lateral-longitudinal cross-coupling terms. In regard to the agreement with theory for these parameters, it can be seen that whilst there is not even any approximate matching, there is some evidence that rank-deficiency produces estimates which are at least of the correct order of magnitude. It can be appreciated that the degree of coupling-intensity between lateral and longitudinal states, in the 6 degrees-of-freedom (6DOF) model, will determine the ease with which satisfactory estimates of these parameters can be obtained. As pointed out earlier, the use of rank-deficiency in situations where the information matrix is 'near singular' because of the presence of one or more weakly-defined parameters, can result in situations where the estimates of the weak parameters are dependent on initial guesses. Indeed, for the current data set, there was found to be some evidence that for the cross-coupling terms, the rank-deficient solutions were dependent on the initial guesses, although estimates of the expected order of magnitude were still found. A contributory factor to the disagreement between estimates and theory for the cross-coupling terms could also be due to the fact that in directly incorporating longitudinal measurements into the extended control vector, any offsets relative to the centre of gravity of the corresponding measurement devices were not taken into consideration. In the case of the measurements that relate to the states in the linear model, offsets are accounted for through the measurement transition matrix

H. For the extended control vector, this would require extra measurements to be included in the control vector, and extra parameters to be estimated in the B matrix.

It should also be noted that the use of noisy measurements - such as $\alpha(t)$ and $q(t)$ - as deterministic pseudo-controls is a possible source of error in the estimates, where in the estimation algorithm there is the inherent assumption that these are noise free. It is assumed that there is no process noise on the model. Larger models incorporating all longitudinal and lateral states would avoid the problem of noise on the controls, but would mean the estimation of a larger number of parameters, and would require the use data sets generated from control inputs that excite both the longitudinal and lateral modes.

Lateral Cyclic Input - 60 Knots.

Consider now the results obtained for a lateral-cyclic doublet input, for a Puma helicopter flying at a nominal trim level of 60 knots, in straight and level flight, altitude 1000 ft.. The input is shown in Figure 4-21, and the lateral response variables are shown as part of Figure 4-24. The length of record available for estimation is much shorter than in the previous case, with 800 points transformed into the frequency domain, sampled at 64 Hz., making a record of length 12.5 seconds. The frequency range used in the estimation was

0.08 to 0.56 Hz., corresponding to 7 complex-valued frequency-domain points.

The important lateral stability derivatives obtained from the frequency-domain output-error estimation are shown in Figure 4-22(a), together with the estimates obtained from the previous 100-knots case, in order to clearly visualise any trends that may be apparent in the estimated values. Theoretical HELISTAB values are also shown for comparison. Error bounds are shown only for the rank-9 case in order to avoid the figure becoming too cluttered; the error bounds for the other cases are of a similar magnitude.

Concentrating first on the rolling-moment parameters, it can be observed that in the case of L_r the substantial improvement in the estimate that was obtained in the 100-knots case, as a result of using rank-deficiency, is not repeated for the 60-knots case; the lower-rank solutions are, however, smaller than the full-rank case. Once again, the estimate of L_v is improved by rank-deficiency, with the rank-10 and rank-9 estimates in excellent agreement with theory. The rank-10 and rank-9 estimates of L_p, whilst as with the 100-knots case are lower than theory, are consistent with the magnitude order predicted by theory.

For the yawing-moment derivatives, there is close agreement with theory for estimates of N_r, with the rank-10 and rank-9 solutions. A value higher than the theoretical prediction is obtained once again for N_p,

though the value obtained for all the ranks is on the whole larger than the 100-knots case, and this trend is predicted by theory. The N_v estimate is in excellent agreement with theory for the rank-10 case.

In Figure 4-22(b) are shown estimates of the lateral- cyclic control sensitivity with respect to roll rate; the estimated delay in the control; and the final cost- function value at convergence. The rank-10 and rank-9 estimates of the control sensitivity are identical within the range of error. The estimated delay is not as large for the lateral-cyclic input as it was for the pedal input, and is not estimated with the same degree of confidence, although it is of a magnitude comparable to the time constant of the main-rotor longitudinal and lateral cyclic flapping modes.

It appears that for the lateral-cyclic case at 60 knots, the rank-10 solution gives the most satisfactory agreement with theory. The frequency-domain fits obtained at convergence for the rank-10 solution are shown in Figure 4-23. In Figure 4-24, the time-domain reconstruction is shown for the rank-10 estimates, following a time-domain output-error estimation of the zero offsets, and initial state conditions.

Tail-Rotor - 60 Knots.

Data obtained for a pedal-doublet input, for a Puma helicopter flying at a nominal trim level of 60 knots, in

straight and level flight, altitude 1000 ft., was also analysed. The input is shown in Figure 4-25. As with the 60-knots lateral-cyclic case, the length of record available for use was 12.5 seconds; this is considerably shorter than the 26.5 seconds of data available for the 100-knots tail-rotor case. The magnitude of the doublet input, however, in this case is larger than the 100-knots case: the result being that the corresponding excursions from the nominal trim levels are large. This is not good for the estimation of a small-perturbation model, and highlights the important point concerning control-input design made in Section 1.4.1: attention should be addressed not only to the shape or frequency content of any applied input signal, but also to its amplitude and the magnitudes of the excursions likely to be produced.

The frequency range used in the estimation was the same as the lateral-cyclic case - 0.08 to 0.56 Hz., corresponding to 7 complex-valued frequency-domain points. Estimates of the important lateral stability derivatives obtained from the frequency-domain output-error estimation are shown in Figure 4-26. The full-rank case failed to converge, but by turning to rank-deficient solutions, convergence was obtained for the output-error method.

The results shown in Figure 4-26 also include the estimates obtained for a full-rank solution when the L_r parameter is considered to be linearly related to L_p; the L_p parameter is estimated freely and the L_r estimate is

constrained using the theoretical HELISTAB ratio of the two parameters:

$$L_r = R_{ar} \cdot L_p \tag{4.3-9}$$

The result is that there are 11 free stability and control parameters to be estimated, and one additional related parameter which is updated at each iteration; the sensitivities are calculated within the output-error algorithm taking the defined relation into consideration. The ability to define relations between sets of parameters, is one of the features of the estimation program OUTMOD.

It can be seen that the cost-value obtained for the case with the relation between L_p and L_r is almost identical to the rank-11 cost-value obtained at convergence. In addition, the parameter estimates shown are identical, within the bounds of accuracy. For the rolling-moment parameters, there is good agreement with theory for L_v, L_p and L_r, in both cases. In reality, the correlation is not usually between pairs of parameters, but may involve a large number of unknown parameters, and so the technique of fixing relationships between parameters is not a practical solution to the problem of correlations between parameters. The example shown, however, does perhaps reinforce earlier statements about likely problems in the estimation caused by strong correlations between the roll and yaw responses. The fact

that for the results presented in the two previous cases, solutions of rank-9 and rank-10 respectively, gave the best estimates, where the full-rank case was of rank 12, does indicate that the existing correlations were indeed between more than simply L_p and L_r.

If we consider the yawing-moment parameters, it is seen that they are not estimated very well for the rank-11, and full-rank case with the defined relationship (i.e. rank 11), but require lower-rank solutions in order to approach the indicated theoretical values. On the whole, the estimated delay value is very similar to that obtained for the 100-knots tail-rotor case.

Comparing the cost-function values given in Figures 4-26 and 4-22 b), it can be seen that for the 60-knots cases, they are, for all the rank-deficient solutions presented, much greater for the pedal input than for the lateral-cyclic input. This is reflected in the better parameter estimates obtained in the latter case. It should be noted that the larger the cost value obtained at convergence, the poorer is the fit, and that comparisons of this type are valid here because the same number of frequency-domain points were used in the estimation process in both cases. It is felt that the large amplitude of the pedal input, and as a result, the less satisfactory adherence to the small-perturbation modelling assumption of the responses is to blame for this.

CHAPTER 5

5.0 FINAL STAGE OF THE IDENTIFICATION METHODOLOGY AND A SUMMARY OF THE COMPLETE IDENTIFICATION APPROACH.

5.1 Estimation of Zero Offsets and Initial Conditions.

5.1.1 Introduction.

By excluding the zero frequency value from those values used in the identification, the estimation of the stability and control derivatives, and time delays, is carried out independently of the zero offsets and initial state conditions. However, for a time-domain verification of the model identified in the frequency- domain, it is necessary to estimate these quantities. This is seen as the final stage of the identification methodology, and is carried out using a time-domain output-error method. Those parameters estimated using the frequency domain are considered fixed for the purpose of the time-domain identification.

5.1.2 Minimisation of Time-Domain Cost Function.

The Time-Domain Cost Function and Model.

The time-domain maximum-likelihood cost function is well known (eg. FEIK002). For the implementation of the

method by the current author, Kalman-filter innovations are replaced by output-errors; this is analogous to the simplifications made in the frequency-domain application of the method, discussed in Section 4.2.1.

$$J_T = 1/2 \sum_t \left(\underset{\sim}{V}^T(t) R^{-1} \underset{\sim}{V}(t) + \log_e |R| \right) \qquad (5.1\text{-}1)$$

$\underset{\sim}{V}(t)$ are the output-errors and R is the time-domain error-covariance matrix. The state equation and the output-errors are given by:

$$\dot{\underset{\sim}{X}}(t) = A \underset{\sim}{X}(t) + B(\underset{\sim}{U}(t, \tau_c) - \underset{\sim}{K}_c) \qquad (5.1\text{-}2)$$

$$\underset{\sim}{V}(t) = H \underset{\sim}{X}(t) + \underset{\sim}{K}_m - \underset{\sim}{Z}(t, \tau_m) \qquad (5.1\text{-}3)$$

where τ_c and τ_m are the set of time delays in the controls and measurements respectively; $\underset{\sim}{K}_c$, $\underset{\sim}{K}_m$ are the zero-offset vectors in the controls and measurements, and together with the initial state conditions: $\underset{\sim}{X}(0)$, they represent the unknowns in the estimation.

It is assumed that elements of the state matrix $-A$, the control dispersion matrix $-B$, the measurement transition matrix $-H$, and the sets of time delays $-\tau_c$, τ_m are known, or have been estimated using the frequency domain; these are fixed throughout the estimation.

The discrete representation of (5.1-2) and (5.1-3) may be written as:

$$\underset{\sim}{X}(n+1\Delta t) = \Phi \underset{\sim}{X}(n\Delta t) + D(\underset{\sim}{U}(n\Delta t, \tau_c) - \underset{\sim}{K}_c) \tag{5.1-4}$$

$$\underset{\sim}{V}(n\Delta t) = H \underset{\sim}{X}(n\Delta t) + \underset{\sim}{K}_m - \underset{\sim}{Z}(n\Delta t, \tau_m) \tag{5.1-5}$$

where the following are defined (e.g. GELB001):

$$\Phi(t_2, t_1) \triangleq e^{A(t_2 - t_1)} \tag{5.1-6}$$

$$\Phi \triangleq e^{A\Delta t} \tag{5.1-7}$$

$$D \underset{\sim}{U}(n\Delta t, \tau_c) \triangleq \int_{n\Delta t}^{n+1\Delta t} \Phi(n+1\Delta t, \theta) B \underset{\sim}{U}(\theta, \tau_c) d\theta \tag{5.1-8}$$

For small Δt we may use the following approximation:

$$D \doteq B\Delta t \tag{5.1-9}$$

And for $\Phi = e^{A\Delta t}$, a truncated form of the expansion:

$$\Phi = I + A\Delta t + A^2\Delta t^2/2! + \ldots \tag{5.1-10}$$

<u>Expressions for the Sensitivities.</u>

As with the frequency-domain output-error method, the Gauss-Newton method is used in the minimisation of the cost function given by (5.1-1). For the elements of the vector of partial derivatives, and approximate Hessian matrix given by:

$$\partial J_T / \partial \gamma_L = \sum_t \underset{\sim}{V}^T(t) R^{-1} \partial \underset{\sim}{V}(t) / \partial \gamma_L \qquad (5.1\text{-}11)$$

$$\partial^2 J_T / \partial \gamma_L \partial \gamma_m = \sum_t \partial \underset{\sim}{V}(t) / \partial \gamma_L R^{-1} \partial \underset{\sim}{V}(t) / \partial \gamma_m \qquad (5.1\text{-}12)$$

we require expressions for terms of the form: $\frac{\partial \underset{\sim}{V}(t)}{\partial \gamma_L}$; these can be obtained easily using (5.1-4) - (5.1-10), giving:

$$\partial \underset{\sim}{V}(n\Delta t) / \partial \gamma_L = \partial \underset{\sim}{K}_m / \partial \gamma_L \qquad \gamma_L \in K_m \qquad (5.1\text{-}13)$$

$$\partial \underset{\sim}{V}(n\Delta t) / \partial \gamma_L = -(H \sum_{i=0}^{n-1} \Phi^i) D \, \partial \underset{\sim}{K}_c / \partial \gamma_L \qquad \gamma_L \in K_c \qquad (5.1\text{-}14)$$

$$\partial \underset{\sim}{V}(n\Delta t) / \partial \gamma_L = H \Phi^n \, \partial \underset{\sim}{X}(0) / \partial \gamma_L \qquad \gamma_L \in X_0 \qquad (5.1\text{-}15)$$

where n = 0, 1, 2 ..., and γ_L is a given unknown parameter belonging to one of the sets: K_m , K_c , X_0 , whose members are elements of the vectors implied.

Computer Implementation.

A Fortran 77 program called OFBIT was written by the current author to implement the time-domain output-error method. The program is similar in structure to the frequency-domain program - OUTMOD, and has many of the same features.

5.1.3 Correlations Between the Sets of Parameters

On re-arranging equation (5.1-5), we have that measured quantities are related to the state vector by:

$$\underset{\sim}{Z}(n\Delta t, \tau_m) = H\underset{\sim}{X}(n\Delta t) + \underset{\sim}{K}_m + \underset{\sim}{V}(n\Delta t) \quad (5.1\text{-}16)$$

where $\underset{\sim}{V}(n\Delta t)$ is modelled as a white noise source. In the reference FEIK002, the maximum-likelihood estimation of bias terms in the measurements is considered, and it is pointed out that in the absence of measurement noise there will be relationships between the biases and initial state conditions. In the present context an identical situation can be seen to occur: measurement zero-offsets $-\underset{\sim}{K}_m$ and initial state conditions $-\underset{\sim}{X}(o)$ are related if $\underset{\sim}{V}(n\Delta t) \doteq \underset{\sim}{0}$, since:

$$\underset{\sim}{Z}(0, \tau_m) \doteq H\underset{\sim}{X}(0) + \underset{\sim}{K}_m \quad (5.1\text{-}17)$$

$$\underset{\sim}{V}(n\Delta t) \doteq \underset{\sim}{0} \quad (5.1\text{-}18)$$

As an example, consider the measurement system for longitudinal quantities, described in Section 2.3.3, evaluated at time t=o, and assuming $\underset{\sim}{V}(n\Delta t) = \underset{\sim}{0}$:

$$\begin{bmatrix} V_m(0) \\ \alpha_m(0) \\ q_m(0) \\ \theta_m(0) \end{bmatrix} = \begin{bmatrix} 1 & 0 & L_z^{\nu} & 0 \\ 0 & 1/U_e & -L_x^{\alpha}/U_e & 0 \\ 0 & 0 & 1 & 0 \\ 0 & 0 & 0 & 1 \end{bmatrix} \begin{bmatrix} U(0) \\ W(0) \\ q(0) \\ \theta(0) \end{bmatrix} + \begin{bmatrix} V_{OFF} \\ \alpha_{OFF} \\ q_{OFF} \\ \theta_{OFF} \end{bmatrix} \quad (5.1\text{-}19)$$

We have that:

$$\underset{\sim}{K}_m = (V_{OFF}, \alpha_{OFF}, q_{OFF}, \Theta_{OFF})^T$$
$$\underset{\sim}{X}(0) = (U(0), W(0), q(0), \Theta(0))^T \qquad (5.1\text{-}20)$$

Since the measurement transition matrix H is known and fixed for the application of the time-domain output-error technique required here, it can be seen from (5.1-19) that there are only four independent parameters amongst those given by (5.1-20).

The relationships between $\underset{\sim}{K}_m$ and $\underset{\sim}{X}(0)$ could be incorporated into the estimation if the conditions given by (5.1-17) and (5.1-18) were close approximations to reality. Also, the use of rank-deficiency (described in Section 4.2.3) is a relevant possibility in these circumstances (the program OFBIT has the facility for rank-deficient solutions). The author of the reference FEIK002 investigates the incorporation of the constraint given by (5.1-17) into the identification, even when measurement noise is present. The best results with measurement noise, were obtained when all parameters including initial conditions were independently extracted. However, the current author is of the opinion that rank-deficiency offers a better approach to the problem, than deciding to fix cast-iron relational constraints into the estimation at the outset. As was

pointed out in Section 4.2.3, potential relationships between sets of parameters are effectively constructed automatically from the measured data used in the identification, and are associated with, and evidenced by, near-zero eigenvalues of the information matrix.

It can be seen from (5.1-14) and (5.1-15) that a perfect correlation will exist between the initial conditions of a given state, and those elements of the control zero- offset vector: $\underset{\sim}{K}_c$, dispersed onto the state through the discrete control dispersion matrix D. Consequently these two sets of parameters cannot be identified independently. The control zero-offset term $\underset{\sim}{K}_c$ was incorporated into the previous analysis to draw attention to the fact that the observed control time histories are not obtained from the flight-data files as perturbed quantities, but as total stick and pedal position. For frequency-domain identification using flight-data records, there is no need to consider the estimation of $\underset{\sim}{K}_c$ when the zero frequency value is excluded from the frequency range used.

5.2 Summary of the Complete Identification Methodology

The basic elements of the estimation methodology are shown in Figure 5.1. Details of each stage, and specific features of the software implementations, are summarised below.

5.2.1 Stage 1: Frequency-Domain Singular-Value-Decomposition Equation-Error Identification

Measured flight-data is transformed directly into the frequency domain. The time derivatives of quantities (i.e. dependent variables) need not be measured: the transforms of these quantities can be obtained from a known algebraic relationship. The transforms of variables used in the model can be obtained from the transforms of the measurements by solving the relevant linear equations, for the relatively few points used in the frequency- domain identification.

The frequency range used in the identification is based on the required range for the model; the magnitudes of the Fourier transforms are a useful indicator of the frequency range over which the rigid-body states have been excited. Also by investigating the effect of increasing the frequency range on the parameter estimates and their associated confidences (indicated by Partial-F statistics), a suitable frequency range for the identification can be found; this frequency range can also be used for the output-error identification at Stage 2). The zero frequency value is excluded from the identification, obviating the need to estimate zero-offset terms.

No a-priori values are required for the identification to take place, and it is carried out for one equation (a row of the state-space model) at a time. The

equation-error method is formulated in terms of the singular-value decomposition of the Matrix X which has the independent variable (frequency-domain) values in its columns. The analyst can decide upon an 'optimum' number of orthogonal components to be used in obtaining the estimates, on the basis of model-fit parameters such as the squared-correlation coefficient, partial-F statistics, etc., and on the reasonableness of the estimates when compared with the predicted theoretical values. The singular-value-decomposition approach, whilst allowing for an estimation in a subset of the available parameter space, finally provides a full set of parameter values for use as initial guesses in Stage 2).

Finally, for the selected model, the parameter significance values which indicate the relative contributions to the dependent variable, can be used to determine insignificant parameters for exclusion from the model used in the next stage of the identification.

Stage 1) is implemented in the Fortran-77 program - SINGVAL, developed by the current author.

5.2.2 Stage 2: Frequency-Domain Output-Error Identification (With Options for the Inclusion of Constraints)

As with the equation-error stage, measured flight-data is transformed directly into the frequency domain. Initial guesses are required for the parameters in the

model to be estimated; other parameters are fixed at known or theoretical values. The model used is in a state-space form that can include time delays in the controls and in the measurements. Time delays in the controls have been shown to be an important feature for the successful identification of quasi-static model derivatives; these are estimated with ease using the frequency domain. In addition to the stability and control derivatives, and time delays, elements of the measurement transition matrix which relates measurements to model states, can be estimated.

The control vector has the facility for up to 9 control terms, enabling for example in the identification of a longitudinal model using a single pilot control input, the inclusion, and estimation, of longitudinal/lateral cross-coupling terms, as elements of a control dispersion matrix; thus enabling the formulation of the identification problem in a manageable size. The terms in the extended control vector can also be quantities which are differentiated with respect to time.

Relationships between different elements of the model structure can be explicitly defined by the analyst at the outset: one parameter is estimated, and the related elements are updated in accordance with the relationship. Rank-deficient solutions can also be obtained, meaning also in effect, that relationships exist between different parts of the model structure;

this is indicated by the data set used, and the presence of near-zero eigenvalues in the information matrix. Whatever rank of information matrix is used in the identification, a full set of parameter values are finally provided.

The iterative optimization technique used is Gauss-Newton, with an additional scalar line-search incorporated; a range of facilities are available for terminating the algorithm. Parameters can also be constrained to lie within an allowable range of values.

Stage 2) is implemented in the Fortran-77 program-OUTMOD, developed by the current author.

5.2.3 Stage 3: Time-Domain Output-Error Identification (With Options for the Inclusion of Constraints)

The estimation of zero-offsets and initial state conditions, is seen as the final stage in the identification methodology. The stability and control derivatives, elements of the measurement transition matrix, and the delays, are fixed during this estimation. The original measured time-domain flight data is used in the estimation.

Initial guesses for the zero offsets are provided by the zero frequency values for the Fourier transforms, obtained at Stage 2) (and given as part of the output from the program - OUTMOD); initial guesses for the initial state conditions are obtained using the measured

responses and the measurement transition matrix.

As with the frequency-domain output-error computer implementation, rank-deficient solutions can also be obtained; these may be required because of the possibility of strong correlations between some of the zero-offset terms and some of the initial state conditions. Once again, the optimization technique used is Gauss-Newton.

Time-domain verification of the model identified in the frequency-domain, is also provided at this stage.

Stage 3) is implemented in the FORTRAN -77 program - OFBIT, developed by the current author.

CHAPTER 6

6.0 CONCLUSIONS AND RECOMMENDATIONS FOR FUTURE WORK

The purpose of this document has been primarily to present, and justify, a methodology for the identification of helicopter mathematical models from flight data. Central to the philosophy of the identification methodology here is the use of the frequency-domain. The ability to use a restricted frequency range has been shown to be essential for the successful identification of low-order helicopter rigid-body models from measured flight data. The formulation of the identification problem in the frequency domain also facilitates the estimation of time delays in the model. The incorporation, and estimation, of time delays in some of the controls used by the pilot when applying a test input signal, is an important feature of the methodology developed here for the improved estimation of quasi-static derivatives known to be susceptible to rotor-transient effects which are not included in the assumed model structure. This feature was demonstrated using real flight-data, and was shown to result in an improved identification of quasi-static models and to be a more satisfactory way of dealing with the unmodelled high-frequency rotor effects than their attempted exclusion through the use of larger sampling intervals.

The formulation of the identification problem in the

frequency domain was also shown to be of practical benefit from the point of view of algorithmic implementation in comparison to the use of the time domain: sequences of numerical integrations are replaced by simple algebraic manipulation. In addition, there is a reduction in the number of data points used in the identification, hence allowing for a faster computation. Cost-function summations are not required for a large number of indices and, as a consequence of the relatively small amount of data used, the dimensions of the arrays used in singular-value-decomposition calculations for the equation-error method are small.

The singular-value-decomposition technique provides a means of investigating different model structures for the equation-error stage in the identification methodology. Various indicators of model quality, relating to the individual parameters in the model, the orthogonal variables from which a model is built up, and overall measures of the model fit, all have to be taken into account when selecting a model. It can be concluded that the technique is much more satisfactory than the conventional pseudo-inverse least-squares technique, both from a numerical point of view, and because of its flexibility. What is more, it retains some similarities with the widely used subset-regression procedure, whilst still retaining a fixed number of parameters in the final selected model. Having a full set of parameter values is useful because the equation-error method is seen here,

primarily, as a means of providing initial guesses for all the parameters included in the model for the frequency-domain output-error method. The frequency-domain singular-value-decomposition equation-error method has been implemented in a FORTRAN-77 program - SINGVAL.

The frequency-domain output-error method was presented as the most important stage in the identification methodology. The implementation presented here was based on the minimisation of an already well-established cost-function, but includes many features that are original, or untried in this context, relating to the form of model used and the minimisation algorithm. The symbolic representation of the frequency-domain model for the output-error method, developed in this document, was shown to facilitate both the calculation of symbolic expressions relating to the method, and their subsequent computer implementation. In addition, features of the model- such as the ability to incorporate delays, and features of the minimisation algorithm- such as the ability to define relationships between different parts of the model structure, are consequently implemented with ease. The use of a rank-deficient information matrix was presented as one of the several means of constrained optimization available in the software implementation. Some previously reported problems in the identification of lateral stability derivatives, associated with strong correlations between some of the response variables in the 'Dutch-roll' type

mode, have been tackled using rank-deficient information matrices. This was shown to lead to marked improvements in the estimates of important lateral derivatives.

The frequency-domain output-error method was used in obtaining results for longitudinal and lateral parameters over a range of nominal flight conditions; and close agreement with theory was found for many important parameters. The theoretical values were obtained using the helicopter flight-mechanics package HELISTAB, which also proved invaluable in testing the frequency-domain output-error program OUTMOD during development.

Whilst the equation-error method will only produce unbiased estimates in the absence of measurement noise on each of the independent variables, the output-error method requires the absence of process (or model) noise, including noise on the controls. The possibility of including Kalman gains in the identification in an attempt to account for process noise was suggested, cautiously, as one possible area for future research; it was pointed out that a simple option, whereby the Kalman gains are treated as independent and free parameters, can be carried out using the current version of the OUTMOD program.

A time-domain output-error estimation program OFBIT was developed especially for the estimation of zero-offsets and initial conditions, following a frequency-domain identification of the state-space model parameters. It was shown that a requirement for

rank-deficient solutions existed at this stage of the identification methodology also, because the initial conditions and zero-offset terms may not always constitute an independent set of parameters; this was implemented in the program OFBIT. Time-domain verification of the identified models presented in this document was accomplished using OFBIT. In future work, when the identification methodology is applied to more high-quality data sets, especially for situations where several data sets are available for the same flight condition using different test-input signals, this program could be of value for testing the robustness of identified models.

It was pointed out that a drawback of using a frequency-domain state-space model in the identification, was its limitation to small-perturbation data. In relation to this problem, attention was drawn to the effect of test-input amplitude and shape on inducing a large excursion (i.e. 'non-linear' response) from the trim, and it was suggested that some currently available test inputs (e.g. '3211's' with a 1.0 second clock period) are not adequate for identification work using the Puma helicopter, and that there is a strong need for test inputs which produce small excursions from the trim, thus also ensuring the availability of longer data records.

The problem of obtaining data records which are of sufficient length to ensure a satisfactory identification

is a major problem in helicopter system identification; this was highlighted by some results presented in Chapter 3 for a longitudinal input. Longer data records can be obtained through the use of stability augmentation systems, however, correlations between input and response variables (and hence between the stability and control derivatives) would be expected to degrade the identification. Nevertheless, by using rank-deficiency, it might be possible to obtain better estimates of the stability derivatives for the longer data records; this is seen as one possible area for future research.

One, possibly, surprising aspect of the results presented here was that good fits (initially in the frequency-domain) and realistic parameter estimates (in comparison with theoretical values) could be obtained using a relatively small (in comparison to the number of time-domain data) number of frequency-domain data points. An advantage of this, is that the identification can be carried out quickly. However, the fact that a small number of data points are used will be reflected in the precision, or error bounds, of the estimates. For a given frequency range of interest, the number of frequency-domain points available, when the discrete Fourier transform is used, is determined solely by the record length. The use of zero-padding to apparently decrease the spacing between the frequency-domain points was shown by the current author to result in biased estimates. One facility of the frequency-domain

formulation of the identification problem, which has yet to be looked into, is that of weighting individual frequencies differently - that is, using a frequency-dependent error-covariance matrix; this could be used if the assumption that the measurement noise can be modelled as a band-limited white-noise source, was thought to be greatly in error.

The methodology developed in this document for helicopter system identification represents a synthesis of new and innovative, and already-established, techniques and ideas, in addition to some which have not been applied in this context. The theoretical basis of the identification methodology was presented, implemented in terms of software and applied successfully to real flight-data. Some recommendations for future areas of research and application were given.

Table 2-1 9 DOF Eigenvalues
HELISTAB Puma model, 80 Kn.

Mode	Time Constant (s)	Real Part	Imag. Part	Modulus
1	0.033	-30.282	0.000	30.282
2	0.109	-9.190	5.224	10.571
3	0.109	-9.190	-5.224	10.571
4	0.478	-2.094	0.000	2.094
5		-0.961	0.724	1.203
6		-0.961	-0.724	1.203
7		-0.138	0.979	0.989
8		-0.138	-0.979	0.989
9		-0.00644	0.245	0.2454
10		-0.00644	-0.245	0.2454
11		-0.102	0.000	0.102

Table 2-2 Results Showing the Effect of Inclusion of Delay and the Effect of Sampling Interval in the Estimation.

Parameter	Case (1) Estimates	Case (2) Estimates	Case (3) Estimates	Theoretical Helistab Values
M_u	0.00337	0.00432	0.00295	0.0024
	(0.00014)†	(0.00028)	(0.00016)	
M_w	-0.00237	0.00135	0.00125	-0.0051
	(0.00057)	(0.0011)	(0.00074)	
M_q	-0.372	-0.861	-0.803	-0.835
	(0.070)	(0.14)	(0.10)	
M_β	-1.378	-1.362	-1.113	-1.368‡
	(0.074)	(0.083)	(0.094)	
M_p	-0.421	-0.233	-0.100	-0.210
	(0.052)	(0.071)	(0.055)	
$M_{\eta_{1s}}$	-0.0302	-0.0398	-0.0377	-0.0376
	(0.0014)	(0.0027)	(0.0021)	
Z_u	0.0336	0.0332	0.0463	-0.0316
	(0.014)	(0.011)	(0.013)	
Z_w	-0.789	-0.782	-0.815	-0.696
	(0.013)	(0.0096)	(0.016)	
$Z_{\eta_{1s}}$	0.628	0.520	0.752	0.618
	(0.096)	(0.077)	(0.126)	
X_u	-0.0622	-0.112	-0.150	-0.0265
	(0.036)	(0.044)	(0.037)	
$X_{\eta_{1s}}$	0.485	1.956	-0.162	0.180
	(0.27)	(0.38)	(0.43)	
τ		0.158		
		(0.032)		
Cost	- 123.0	-131.4	-163.76	

† Estimated 1σ error bound

‡ Using HELISTAB value of M_w to calculated M_β

Table 3-1a) Equation-Error Results Pitching-Moment Equation Puma, 100 KN, Run R0201A, Long Cyclic Input.

Parameter Estimates
Frequency Range: (0.075-0.527 Hz)

Number of Orthogonal Components:	1	2	3	4	5	6	Theoretical Quasi-Static Values.
Parameters							
M_u	.	.	.	0.00224	0.00289	0.00267	0.00244
				(0.00095)	(0.00064)	(0.00069)	
M_w	.	.	.	-0.00262	-0.00225	-0.00376	-0.0052
				(0.00090)	(0.0006)	(0.0016)	
M_q	.	.	.	0.00036	-0.330	-0.186	-0.835
				(0.00005)	(0.0880)	(0.170)	
M_v	.	.	.	-0.00359	-0.00486	-0.00595	-0.0013
				(0.0031)	(0.0020)	(0.0023)	
M_p	.	.	.	-0.0000043	-0.298	-0.458	-0.210
				(0.000019)	(0.079)	(0.180)	
$M_{\eta_{1s}}$	.	.	.	-0.0285	-0.0325	-0.0303	-0.0376
				(0.0037)	(0.0027)	(0.0034)	
R^2	0.0386	0.4152	0.4190	0.9100	0.9664	0.9725	
F total	0.0643	1.136	1.153	16.126	45.987	56.591	

Table 3-1 b) Parameter Significance Values and Partial-F Statistics for the Selection of 5 Orthogonal Components.

Parameter	Signif. Value	Partial-F
M_u	0.24	20.00
M_w	0.21	14.07
M_q	0.25	14.07
M_v	0.15	56.21
M_p	0.19	14.10
$M_{\eta_{1s}}$	0.85	147.80

Table 3-2a) Equation-Error Results Pitching-Moment Equation Puma, 100KN, Run R0201A, Long-Cyclic Input. Estimates of Orthogonal Variables with Singular Values, and Associated Partial-F Statistics for Different Numbers of Orthogonal Components. Frequency Range: (0.075 - 0.527 Hz.)

a)						
Orthogonal Variables:	ϕ_1	ϕ_2	ϕ_3	ϕ_4	ϕ_5	ϕ_6
Estimates:	-0.0016	-0.0064	-0.0028	-0.0280	0.445	0.216
b)						
Singular Values	134.4	92.10	30.76	24.64	0.5184	0.2832
Significance Value = (Abs. Prod. a) x b))	0.215	0.589	0.086	0.690	0.231	0.0612

Table 3-2b)

Numbers of Orthogonal Variables:	1	2	3	4	5	6
Partial-F Statistics of Orthogonal Variables						
1	0.678	1.007	0.936	5.509	12.73	12.72
2		7.311	6.791	39.99	92.38	92.33
3			0.146	0.8613	1.990	1.989
4				54.77	126.5	126.5
5					14.10	14.09
6						0.995

Table 3-2c) Matrix V^T

0.6016	0.7959	0.0047	-0.0567	-0.0032	0.0385
-0.7956	0.5963	0.0003	0.0022	-0.0028	0.1073
-0.0207	-0.0644	-0.0046	-0.9719	0.0061	0.2253
0.0691	-0.0827	-0.0127	0.2284	0.0004	0.9675
0.0015	0.0008	-0.7432	-0.0029	-0.6690	-0.0089
-0.0010	-0.0070	0.6689	-0.0051	-0.7432	0.0098

Table 3-3a) Equation-Error Results. Pitching-Moment Equation (with Delay in Control). Puma, 100 KN, Run R0201A, Long Cyclic Input.
Parameter Estimates
Frequency Range: (0.075-0.527 Hz.)

Number of Orthogonal Components:	1	2	3	4	5	6	7[□]	Theoretical Quasi-Static Values.
Parameters								
Mu	.	.	.	.	0.00216	0.00277	0.00414	0.00240
					(0.00097)[†]	(0.00062)	(0.00086)	
Mw	.	.	.	.	-0.00242	-0.00411	0.0000422	-0.0052
					(0.00095)	(0.00073)	(0.0022)	
Mq	.	.	.	.	0.000325	-0.2002	-0.868	-0.835
					(0.000048)	(0.051)	(0.34)	
Mv	.	.	.	.	-0.00321	-0.00656	-0.00534	-0.0013
					(0.0032)	(0.0021)	(0.0019)	
Mp	.	.	.	.	-0.0000196	-0.519	-0.261	-0.210
					(0.000023)	(0.13)	(0.17)	
$M\eta_{1s}$	.	.	.	.	-0.0288	-0.0303	-0.0387	-0.0376
					(0.0038)	(0.0024)	(0.0046)	
Approx τ[‡]	.	.	.	.	0.0583	0.0400	0.157	.
R^2	0.0404	0.4121	0.4170	0.4174	0.9149	0.9751	0.9819	
F total	0.00492	0.8180	0.8345	0.8357	12.546	45.728	63.366	

† Estimated 1σ error bound.
‡ See Section 3.3.1 for explanation of how approx. τ value is obtained
□ Selected number of orthogonal components (=7)

Table 3-3 b) Parameter Significance Values and Partial-F Statistics for the Selection of 7 Orthogonal Components.

Parameter	Signif. Value	Partial-F
M_u	0.34	22.86
M_w	0.0039	0.00038
M_q	0.65	6.66
M_v	0.17	7.71
M_p	0.17	2.33
$M_{\eta_{1s}}$	1.01	68.92

Table 3-4a) Equation-Error Results. Pitching-Moment Equation (with Delay in Control), Puma, 100 KN, Run R0201A, Long-Cyclic Input.

Estimates of Orthogonal Variables, with Singular Values, and Associated Partial-F Statistics for Different Numbers of Orthogonal Components. Frequency Range: (0.075 - 0.527 Hz.)

a)							
Orthogonal Variables:	ϕ_1	ϕ_2	ϕ_3	ϕ_4	ϕ_5	ϕ_6	ϕ_7
Estimates:	-0.0017	-0.0063	-0.0009	-0.0022	0.0283	0.5567	0.7163
b)							
Singular Values	134.6	92.64	47.34	30.02	24.58	0.4144	0.1404
Significance Value =							
(Abs. Prod. a) x b))	0.229	0.584	0.043	0.066	0.696	0.231	0.101

Table 3-4b)

Numbers of Orthogonal Variables:	1	2	3	4	5	6	7
Partial-F Statistics of Orthogonal Variables							
1	0.706	1.046	0.962	0.882	5.537	14.36	19.77
2		7.264	6.681	6.121	38.44	99.71	137.2
3			0.037	0.034	0.215	0.557	0.767
4				0.079	0.493	1.279	1.761
5					53.80	139.5	192.1
6						15.34	21.12
7							4.011

Table 3-5a) Equation-Error Results. Pitching-Moment Equation, Puma, 100 KN, Run R0201A, Long-Cyclic Input

Parameter Values for a Frequency Range 0.075 - 0.753 Hz, for the Selection of 5 Orthogonal Components.

Parameter	M_u	M_w	M_q	M_v	M_p	$M_{\eta_{1S}}$	R^2	F tot
Estimate:	0.00285	-0.00226	-0.327	-0.00485	-0.300	-0.0324	0.9622	71.345
Error Bound	(0.00052)	(0.00048)	(0.070)	(0.0017)	(0.064)	(0.0021)	.	.

Table 3-5b) Parameter Values for a Frequency Range 0.075 - 0.753 Hz, (With Delay in Control) for the Selection of 7 Orthogonal Components.

Parameter	M_u	M_w	M_q	M_v	M_p	$M_{\eta_{1s}}$	Approx τ ‡	R^2	F total
Estimate:	0.00392	-0.000559	-0.774	-0.00549	-0.301	-0.0374	0.145	0.9777	94.949
Error Bound	(0.00068)	(0.0017)	(0.26)	(0.0016)	(0.13)	(0.0036)	.	.	.

‡ See Section 3.3.1 for explanation of how approx. τ value is obtained.

Table 3-6a) Equation-Error Results. Normal Force Equation, Puma, 100 KN, Run R0201A, Long Cyclic Input.
Parameter Estimates.
Frequency Range: (0.075-0.527 Hz)

Number of Orthogonal Components:	1	2	3	4	5 ▫	6	7	Theoretical Quasi-Static Values.
Parameters								
Z_u	.	-0.0764	-0.0815	-0.514	-0.00311	-0.0133	-0.0217	-0.0317
	.	(0.049)†	(0.046)	(0.036)	(0.026)	(0.036)	(0.11)	
Z_w	.	-0.720	-0.736	-0.772	-0.897	-0.877	-0.868	-0.696
	.	(0.044)	(0.042)	(0.034)	(0.039)	(0.062)	(0.13)	
Z_θ	.	-0.00949	-0.00683	-0.0117	2.507	0.228	-0.910	0.222
	.	(0.00082)	(0.0018)	(00021)	(0.65)	(5.31)	(14.9)	
Z_v	.	0.0345	-0.208	-0.109	0.0628	0.113	0.100	0.0258
	.	(0.0021)	(0.15)	(0.12)	(0.087)	(0.15)	(0.22)	
Z_p	.	0.00304	0.00456	0.00473	-1.827	2.314	1.551	2.15
	.	(0.00019)	(0.00094)	(0.00072)	(0.47)	(9.58)	(13.8)	
Z_ϕ	.	0.00944	0.00439	0.0140	-5.865	-0.813	-8.381	-0.806
	.	(0.00064)	(0.0031)	(0.0039)	(1.51)	(5.47)	(6.59)	
$Z_{\eta_{1s}}$	.	-0.0694	-0.00850	0.414	0.523	0.538	0.535	0.618
	.	(0.0060)	(0.035)	(0.14)	(0.095)	(0.11)	(0.12)	
R^2	0.8167	0.9674	0.9770	0.9943	0.9949	0.9949	0.9949	
F total	5.197	34.537	49.533	201.474	228.582	226.407	227.007	

† Estimated 1σ error bound.
▫ Selected number of orthogonal components (=5).

Table 3-6 b) Parameter Significance Values and Partial-F Statistics for the Selection of 5 Orthogonal Components.

Parameter	Signif. Value	Partial-F
Zu	0.0035	0.0140
Zw	1.14	532.4
$Z\theta$	0.047	14.93
Zv	0.026	0.522
Zp	0.016	14.99
$Z\phi$	0.15	15.00
$Z\eta_{1s}$	0.19	30.19

Table 3-6c) Estimates of Orthogonal Variables with Associated Singular Values.

a)							
Orthogonal Variables:	ϕ_1	ϕ_2	ϕ_3	ϕ_4	ϕ_5	ϕ_6	ϕ_7
Estimates:	-0.6238	-0.3754	-0.2490	-0.4368	-6.658	5.242	1.393
b)							
Singular Values	134.4	92.11	30.77	24.64	1.328	0.1972	0.1511
Significance Value =							
(Abs. Prod. a) x b))	83.84	34.58	7.662	10.76	8.842	1.034	0.210

Table 3-7a) Equation-Error Results. Normal Force Equation (with Delay in Control), Puma, 100 KN, Run R0201A, Long Cyclic Input. Parameter Estimates
Frequency Range: (0.075-0.527 Hz)

Number of Orthogonal Components:	1	2	3	4	5	6□	7	8	Theoretical Quasi-Static Values.
Parameters									
Zu	.	.	.	-0.0877 (0.044)†	-0.0576 (0.032)	-0.0138 (0.026)	-0.0216 (0.029)	-0.179 (0.12)	-0.031
Zw	.	.	.	-0.719 (0.041)	-0.757 (0.031)	-0.871 (0.040)	-0.849 (0.054)	-0.664 (0.14)	-0.696
Zθ	.	.	.	-0.00687 (0.0016)	-0.0119 (0.0019)	2.033 (0.61)	-0.2018 (3.59)	-21.40 (15.8)	0.222
Zv	.	.	.	-0.163 (0.14)	-0.0795 (0.10)	0.0559 (0.082)	0.135 (0.15)	-0.0557 (0.20)	0.0258
Zp	.	.	.	0.00413 (0.0011)	0.00456 (0.00077)	-1.616 (0.48)	4.685 (9.98)	-5.229 (11.87)	2.15
Zφ				0.00481 (0.0028)	0.0145 (0.0035)	-5.157 (1.54)	-8.013 (4.80)	-13.30 (5.94)	-0.806
$Z\eta_{1s}$	.	.	.	-0.0200 (0.0028)	0.395 (0.13)	0.498 (0.092)	0.519 (0.100)	0.466 (0.10)	0.618
Approx τ‡	.	.	.	-7.393	0.327	0.143	0.146	0.273	.
R^2	0.8244	0.9722	0.9738	0.9794	0.9957	0.9962	0.9962	0.9973	
F total	4.024	29.931	31.918	40.651	200.268	222.598	222.595	310.888	

† Estimated 1σ error bound.
‡ See Section 3.3.1 for explanation of how approx. τ value is obtained.
□ Selected number of orthogonal components (=6).

Table 3-7 b) Parameter Significance Values and Partial-F Statistics for the Selection of 6 Orthogonal Components.

Parameter	Signif. Value	Partial-F
Zu	0.016	0.292
Zw	1.11	468.9
$Z\theta$	0.038	11.11
Zv	0.024	0.462
Zp	0.014	11.2
$Z\phi$	0.13	11.2
$Z\eta_{1s}$	0.18	29.59

Table 3-7c) Equation-Error Results. Normal Force Equation (With Delay in Control), Puma, 100KN, Run R0201A, Long-Cyclic Input.
Estimates of Orthogonal Variables with Associated Singular Values.

a) Orthogonal Variables:	ϕ_1	ϕ_2	ϕ_3	ϕ_4	ϕ_5	ϕ_6	ϕ_7	ϕ_8
Estimates:	-0.6256	-0.3709	-0.1039	-0.1839	-0.4264	5.796	7.271	-23.99
b) Singular Values	134.6	92.66	47.34	30.03	24.58	1.245	0.1945	0.1204
Significance Value = (Abs. Prod. a) x b))	84.21	34.37	4.919	5.523	10.48	7.216	1.414	2.888

Table 3-8a) Equation-Error Results. Yawing Moment Equation, Puma 100 KN, Run R1201L, Pedal Input.
Parameter Estimates
Frequency Range: (0.0376-0.489 Hz).

Number of Orthogonal Components:	1	2	3	4	5	6 ◻	7	Theoretical Quasi-Static Values.
Parameters								
N_u	.	.	.	.	-0.00078 (0.00098)†	0.00037 (0.0010)	-0.00075 (0.00096)	
N_w	. .	. .	. .	. .	0.000044 (0.00085)	-0.00137 (0.00097)	-0.00552 (0.0017)	
N_q	.	.	.	.	0.0264 (0.0048)	0.0846 (0.025)	0.853 (0.28)	-0.328
N_v	.	.	.	.	0.0110 (0.00051)	0.00907 (0.00095)	0.0109 (0.0011)	0.00605
N_p	.	.	.	.	0.134 (0.025)	-0.184 (0.14)	-0.184 (0.12)	-0.0009
N_r	.	.	.	.	-0.136 (0.025)	-0.438 (0.13)	-0.290 (0.13)	-0.528
N_{η_p}	.	.	.	.	-0.0253 (0.0024)	-0.0264 (0.0022)	-0.0249 (0.0020)	-0.043
R^2	0.9108	0.9110	0.9162	0.9728	0.9891	0.9913	0.9938	
F total	32.331	32.398	34.635	113.078	286.23	358.90	504.09	

† Estimated 1σ error bound.
◻ Selected number of orthogonal components (=6).

Table 3-8 b) Parameter Significance Values and Partial-F Statistics for the Selection of 6 Orthogonal Components.

Parameter	Signif. Value	Partial-F
Nu	0.016	0.13
Nw	0.054	1.99
Nq	0.029	11.66
Nv	0.77	91.68
Np	0.14	1.85
Nr	0.29	11.60
$N\eta_p$	0.37	147.4

Table 3-8c) Estimates of Orthogonal Variables with Associated Singular Values.

a)							
Orthogonal Variables:	ϕ_1	ϕ_2	ϕ_3	ϕ_4	ϕ_5	ϕ_6	ϕ_7
Estimates:	-0.00967	-0.00037	-0.00304	-0.0242	-0.1931	-0.4423	0.7822
b)							
Singular Values	374.3	137.3	86.80	37.27	2.480	0.4274	0.2428
Significance Value =							
(Abs. Prod. a) x b))	3.619	0.051	0.264	0.902	0.479	0.189	0.190

Table 3-9a) Equation-Error Results. Yawing-Moment Equation (with Delay in Control). Puma, 100 KN, Run R1201L, Pedal Input.
Parameter Estimates
Frequency Range: (0.0376-0.489 Hz)

Number of Orthogonal Components:	1	2	3	4	5	6	7[□]	8	Theoretical Quasi-Static Values.
Parameters									
N_u	.	.	.	.	0.00007 (0.0015)[†]	-0.00098 (0.00087)	0.00048 (0.00071)	-0.00028 (0.00073)	
N_v	.	.	.	.	0.00311 (0.0010)	-0.00037 (0.00077)	-0.00253 (0.00074)	-0.00493 (0.0013)	
N_q	.	.	.	.	0.00002 (0.00001)	0.0324 (0.0048)	0.143 (0.025)	0.613 (0.22)	-0.328
N_w	.	.	.	.	0.00932 (0.00063)	0.0114 (0.00047)	0.00894 (0.00066)	0.0101 (0.00081)	0.00605
N_p	.	.	.	.	-0.00010 (0.000017)	1.157 (0.023)	-0.259 (0.097)	-0.244 (0.089)	-0.0009
N_r	.	.	.	.	0.00012 (0.000025)	-0.154 (0.023)	-0.554 (0.093)	-0.441 (0.10)	-0.528
N_{η_p}	.	.	.	.	-0.0244 (0.0036)	-0.0254 (0.0021)	-0.0268 (0.0015)	-0.0258 (0.0015)	-0.043
Approx τ	.	.	.	.	0.0154	0.109	0.131	0.117	
R^2	0.9106	0.9108	0.9162	0.9164	0.9728	0.9923	0.9958	0.9967	
F total	26.192	26.250	28.114	28.196	92.035	330.946	614.802	780.110	

† Estimated 1σ error bound.
□ Selected number of orthogonal components (=7).

Table 3-9 b) Parameter Significance Values and Partial-F Statistics for the Selection of 7 Orthogonal Components.

Parameter	Signif. Value	Partial-F
Nu	0.019	0.400
Nw	0.10	11.53
Nq	0.049	31.37
Nv	0.76	185.6
Np	0.23	7.187
Nr	0.37	35.55
$N\eta_p$	0.38	302.9

Table 3-9c) Estimates of Orthogonal Variables with Associated Singular Values.

a)								
Orthogonal Variables:	ϕ_1	ϕ_2	ϕ_3	ϕ_4	ϕ_5	ϕ_6	ϕ_7	ϕ_8
Estimates:	-0.00967	-0.00038	-0.00308	0.00066	-0.0242	0.2228	-0.5877	0.4836
b)								
Singular Values	374.5	137.3	86.84	78.26	37.26	2.331	0.4172	0.2315
Significance Value =								
(Abs. Prod. a) x b))	3.621	0.0522	0.2675	0.0516	0.9016	0.5193	0.2452	0.1120

Table 3-10a) Equation-Error Results. Rolling-Moment Equation (with Delay in Control). Puma, 100 KN, Run R1201L, Pedal Input.
Parameter Estimates
Frequency Range: (0.0376-0.489 Hz)

Number of Orthogonal Components:	1	2	3	4	5	6	7[a]	8	Theoretical Quasi-Static Values.
Parameters									
Lu	.	.	.	.	.	0.00076	0.00113	-0.00045	
					.	(0.0014)[†]	(0.0016)	(0.0017)	
Lw	.	.	.	.	.	-0.00017	-0.00073	-0.0060	
					.	(0.0013)	(0.0017)	(0.0030)	
Lq	.	.	.	.	.	-0.217	-0.188	0.834	0.839
					.	(0.0080)	(0.059)	(0.51)	
Lv	.	.	.	.	.	-0.0198	-0.0204	-0.0178	-0.022
					.	(0.00078)	(0.0015)	(0.0019)	
Lp	.	.	.	.	.	-1.052	-1.161	-1 128	-2.05
					.	(0.039)	(0.22)	(0.21)	
Lr	.	.	.	.	.	1.035	0.9310	1.178	0.294
					.	(0.038)	(0.22)	(0.24)	
$L\eta_p$	.	.	.	.	.	0.0184	0.0181	0.0203	
					.	(0.0034)	(0.0036)	(0.0035)	
Approx τ	.	.	.	.	.	0.408	0.405	0.414	
R^2	0.3397	0.6185	0.6218	0.6350	0.6433	0.9903	0.9905	0.9922	
F total	1.323	4.169	4.228	4.473	4.638	262.793	266.971	326.584	

† Estimated 1σ error bound.
[a] Selected number of orthogonal components (=7).

Table 3-10 b) Parameter Significance Values and Partial-F Statistics for the Selection of 7 Orthogonal Components.

Parameter	Signif. Value	Partial-F
Lu	0.037	0.472
Lw	0.022	0.178
Lq	0.049	10.07
Lv	1.31	178.6
Lp	0.76	26.67
Lr	0.46	18.56
$L\eta_p$	0.19	25.51

Table 3-10c) Estimates of Orthogonal Variables with Associated Singular Values.

a)								
Orthogonal Variables:	ϕ_1	ϕ_2	ϕ_3	ϕ_4	ϕ_5	ϕ_6	ϕ_7	ϕ_8
Estimates:	0.00903	-0.02172	0.00689	0.00806	0.01288	-1.492	-0.1532	1.052
b)								
Singular Values	374.5	137.3	86.84	78.26	37.26	2.331	0.4172	0.2315
Significance Value =								
(Abs. Prod. a) x b))	3.382	2.982	0.5983	0.6308	0.4800	3.478	0.0639	0.2435

Table 3-11a) Equation-Error Results. Pitching-Moment Equation. Puma, 80 KN, Run R0106F, Long Cyclic Input. Parameter Estimates
Frequency Range: (0.0376-0.489 Hz)

Number of Orthogonal Components:	1	2	3	4	5[□]	6	Theoretical Quasi-Static Values.
Parameters							
M_u	.	.	.	0.00202	0.00296	0.00292	0.0025
				(0.00084)[†]	(0.00062)	(0.00061)	
M_w	.	.	.	0.00718	0.00655	0.00754	-0.00455
				(0.0010)	(0.00075)	(0.00098)	
M_q	.	.	.	0.00023	-0.322	-0.199	-0.774
				(0.00004)	(0.064)	(0.103)	
M_v	.	.	.	-0.00407	-0.00723	-0.00870	-0.00154
				(0.0011)	(0.0010)	(0.0014)	
M_p	.	.	.	0.00008	-0.2400	-0.405	-0.212
				(0.000011)	(0.048)	(0.119)	
$M_{\eta_{1s}}$	.	.	.	-0.0167	-0.0217	-0.0200	
				(0.0027)	(0.0021)	(0.0023)	
R^2	0.0080	0.5938	0.6756	0.8581	0.9317	0.9388	
F total	0.0035	6.433	9.164	26.603	60.031	67.517	

† Estimated 1σ error bound.

□ Selected number of orthogonal components (=5).

Table 3-11b) Parameter Significance Values and Partial-F Statistics for the Selection of 5 Orthogonal Components.

Parameter	Signif. Value	Partial-F
M_u	0.27	22.65
M_w	0.54	77.26
M_q	0.27	25.24
M_v	0.48	52.45
M_p	0.19	25.26
$M_{\eta_{1s}}$	0.67	104.0

Table 4-1 Frequency-domain Output-error Estimates. Longitudinal Cyclic Doublet Input, Puma 100 Kn, Transfer Function Identification. Run R0201A.

Parameter	Case 1 Estimates	Case 2 Estimates	Case 3 Estimates	Helistab Value
ω_{sp}^2	1.592 (0.68)	0.942 (0.47)	1.110 (0.54)	0.93
$2\zeta\omega_{sp}$	1.890 (1.26)	1.952 (0.29)	1.812 (0.28)	1.76
$M\eta_{1s}/T_\theta$	-0.0236 (0.034)	-0.0340 (0.014)	-0.0302 (0.014)	
$M\eta_{1s}$	-0.0511 (0.013)	-0.0448 (0.0064)	-0.0386 (0.0061)	-0.0376
$Z\eta_{1s}$		4.104 (1.27)	2.868 (1.38)	0.618
τ_θ	0.195 (0.091)	0.203 (0.058)	0.213 (0.071)	
Measurement System Parameter				
τ_m			0.0439 (0.053)	

Table 4-2 Frequency-domain Output-error Estimates. Combined Run: Longitudinal Cyclic Doublet (Run R0201A) and 3211 (Run R0501A). Puma, 100Kn.

Parameter	Case 1 Combination In Frequency Domain (1/Ue est.)	Case 2 Combination In Time Domain (1/Ue est.)	Case 3 Combination In Time Domain (1/Ue fixed)	Helistab Value
M_u	0.00344 (0.00049)†	0.00334 (0.00041)	0.00393 (0.00043)	0.0024
M_w	0.00245 (0.0025)	0.00173 (0.0011)	0.00379 (0.0015)	-0.0051
M_q	-1.261 (0.32)	-1.190 (0.27)	-1.537 (0.28)	-0.835
M_β	0.112 (0.19)	0.0945 (0.19)	0.161 (0.19)	-1.368
M_p	0.389 (0.17)	0.363 (0.16)	0.545 (0.16)	-0.210
$M_{\eta_{1s}}$	-0.0465 (0.0053)	-0.0452 (0.0045)	-0.0489 (0.0045)	-0.0376
Z_u	-0.0259 (0.022)	0.000859 (0.020)	0.0165 (0.013)	-0.0316
Z_w	-0.703 (0.020)	-0.720 (0.016)	-0.737 (0.0011)	-0.696
$Z_{\eta_{1s}}$	-0.492 (0.23)	-0.0539 (0.28)	-0.231 (0.17)	0.618
X_u	0.144 (0.019)	0.143 (0.019)	0.147 (0.018)	-0.0265
$X_{\eta_{1s}}$	3.784 (0.45)	3.781 (0.43)	3.865 (0.43)	0.180
$\tau(\eta_{1s})$	0.195 (0.045)	0.173 (0.043)	0.212 (0.037)	
1/Ue*	0.00625 (0.00036)	0.00496 (0.00015)		
Cost Val.	X	-130.278	-138.129	

* the parameter estimated for the relationship defined by Equation 4.3-7
† estimated 1σ error bound
X exact value not recorded $\approx$ - 130

Table 4-3 Frequency-domain Output-error Estimates. Multirun: Longitudinal Cyclic Doublet (Run R0201A) and Collective Doublet (Run R1501V). Puma, 100 Kn.

Parameter	Case 1 Full Rank Solution	Case 2 Rank 13 Solution	Helistab Value
M_u	0.00575 (0.00096)†	0.00540 (0.00088)	0.0024
M_w	0.000904 (0.0014)	0.00258 (0.00069)	-0.0051
M_q	-0.691 (0.15)	-0.828 (0.15)	-0.835
M_β	-0.979 (0.13)	-1.069 (0.091)	-1.368
M_p	-0.0323 (0.064)	-0.0503 (0.061)	-0.210
$M_{\eta_{1s}}$	-0.0460 (0.0033)	-0.0473 (0.0032)	-0.0376
M_{η_0}	0.0133 (0.0015)	0.0141 (0.0015)	
Z_w	-0.672 (0.036)	-0.625 (0.034)	-0.696
$Z_{\eta_{1s}}$	0.227 (0.17)	0.132 (0.18)	0.618
Z_{η_0}	-0.504 (0.052)	-0.448 (0.051)	
X_u	0.203 (0.075)	0.104 (0.034)	-0.0265
$X_{\eta_{1s}}$	1.192 (0.70)	2.226 (0.015)	0.180
$\tau(\eta_{1s})$	0.106 (0.038)	0.154 (0.035)	
$\tau(\eta_0)$	0.113 (0.052)	0.115 (0.057)	
Cost Value	-136.334	-135.736	

† estimated 1σ error bound.

Table 4-4 Freqency-domain Output Error Estimates. Longitudinal Cyclic 3211 Input, Puma, 80 Kn, Runs: RO311A (=case 1); RO312A (= Case 2).

Parameter	Case 1a) (no delay)	Case 1b) (delay)	Case 2a)* (no delay)	Case 2b) (delay)	Helistab Values
M_u	0.0000734 (0.00042)†	0.00216 (0.00033)	-0.00104 (0.001)	0.00132 (0.00045)	0.0025
M_w	0.000504 (0.00041)	0.00128 (0.00027)	0.00101 (0.00107)	0.00213 (0.00042)	-0.00455
M_q	-0.593 (0.12)	-1.24 (0.11)	-0.335 (0.28)	-1.030 (0.14)	-0.774
M_p	0.754 (0.12)	0.440 (0.092)	0.860 (0.20)	0.764 (0.10)	-0.212
$M_{\eta_{1s}}$	-0.0251 (0.0014)	-0.0390 (0.0017)	-0.0250 (0.0020)	-0.038 (0.0020)	
M_β	1.300 (0.19)	0.396 (0.15)	1.380 (0.36)	0.647 (0.18)	
$X_{\eta_{1s}}$	-0.527 (0.27)	-0.144 (0.26)	-0.408 (0.44)	-0.354 (0.27)	
$Z_{\eta_{1s}}$	5.66 (0.97)	6.79 (0.80)	6.58 (0.87)	5.95 (0.83)	
$\tau(M_{\eta_{1s}})$	.	0.246 (0.016)	.	0.249 (0.020)	
Cost Value	-23.505	-55.480	-33.497	-52.938	

* rank 7 solution, rank 8 failed to converge.

† estimated 1σ error bound.

Table 4-5a) Frequency-domain Output-error Estimates. Pedal Doublet Input, Puma, 100 Kn, run R1201L. Lateral Derivatives (Uncoupled).

Parameter	Full rank No delay	Full rank Delay	Rank 11	Rank 10	Rank 9	Rank 8	Theory
Lv	-0.0112 (0.0012)†	-0.0138 (0.0014)	-0.0188 (0.0016)	-0.0226 (0.0018)	-0.0228 (0.00076)	-0.0212 (0.00071)	-0.022
Lp	-1.317 (0.14)	-1.539 (0.14)	-1.408 (0.17)	-1.524 (0.19)	-1.491 (0.042)	-1.212 (0.041)	-2.05
Lr	1.237 (0.13)	1.097 (0.13)	0.748 (0.16)	0.563 (0.099)	0.444 (0.044)	0.965 (0.039)	0.294
$L\eta_p$	0.0455 (0.0041)	0.0325 (0.0044)	0.0229 (0.0046)	0.0195 (0.0052)	0.0174 (0.0052)	0.0248 (0.0050)	
Nv	0.00765 (0.00056)	0.00865 (0.00060)	0.00867 (0.00063)	0.00822 (0.00067)	0.00841 (0.00061)	0.00728 (0.00046)	0.00605
Np	-0.353 (0.061)	-0.227 (0.066)	-0.254 (0.068)	-0.281 (0.074)	-0.283 (0.056)	-0.353 (0.041)	-0.0009
Nr	-0.494 (0.062)	-0.500 (0.062)	-0.518 (0.067)	-0.565 (0.057)	-0.525 (0.058)	-0.671 (0.017)	-0.528
$N\eta_p$	-0.0264 (0.0015)	-0.0312 (0.0014)	-0.0319 (0.0014)	-0.0326 (0.0016)	-0.0326 (0.0016)	-0.0311 (0.0014)	-0.043
$\tau(N\eta_p)$	*	0.204 (0.031)	0.204 (0.031)	0.226 (0.031)	0.210 (0.029)	0.223 (0.033)	*
Cost Value	-160.6	-178.9	-164.9	-153.7	-152.1	-148.4	*

† Estimated 1σ error bound.

Table 4-5b) Lateral/longitudinal Cross-coupling Derivatives

L_α	-3.954	-3.700	-1.951	-0.839	-0.941	-0.200	-0.046
	(0.31)	(0.28)	(0.17)	(0.10)	(0.022)	(0.010)	
L_q	2.737	2.822	1.117	0.400	0.105	0.354	0.839
	(0.32)	(0.30)	(0.16)	(0.13)	(0.023)	(0.019)	
N_q	-0.0468	-0.304	-0.210	-0.308	-0.183	-0.400	-0.328
	(0.12)	(0.12)	(0.13)	(0.10)	(0.059)	(0.027)	

KEY TO PLOTS

FREQUENCY-DOMAIN FITS

(Magnitudes of FFT's are used to display fits)

Measured : —

Predicted : X

TIME-DOMAIN FITS

Measured :

Predicted :

UNITS

Angular measurements are in radians.
Speed is measured in Knots.

State-space angular quantities are in radians.
State-space translational velocities are in ft/s.

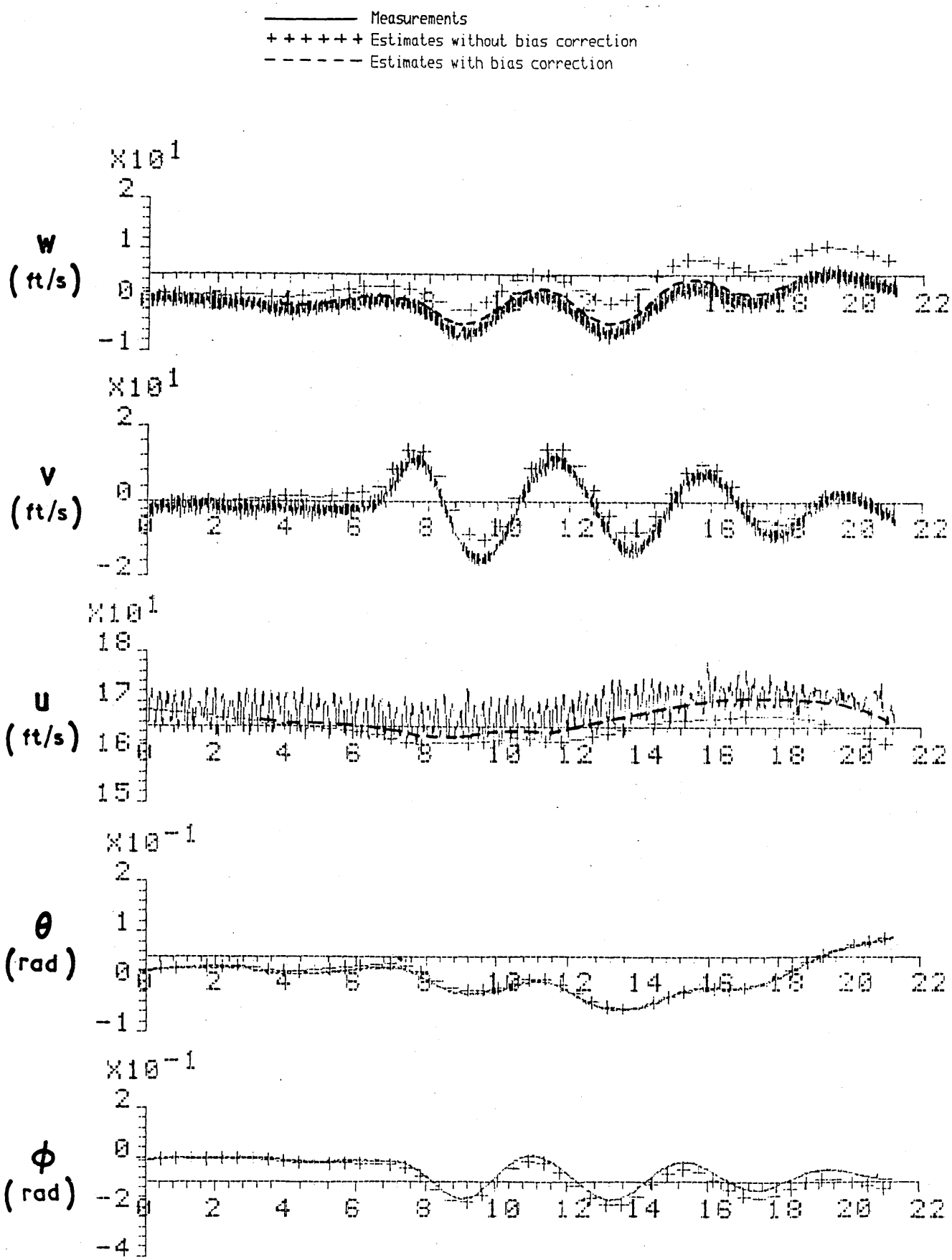

FIGURE 1-1 DETECTION AND REMOVAL OF BIASES IN ACCELEROMETERS USING THE PROGRAM KINECON

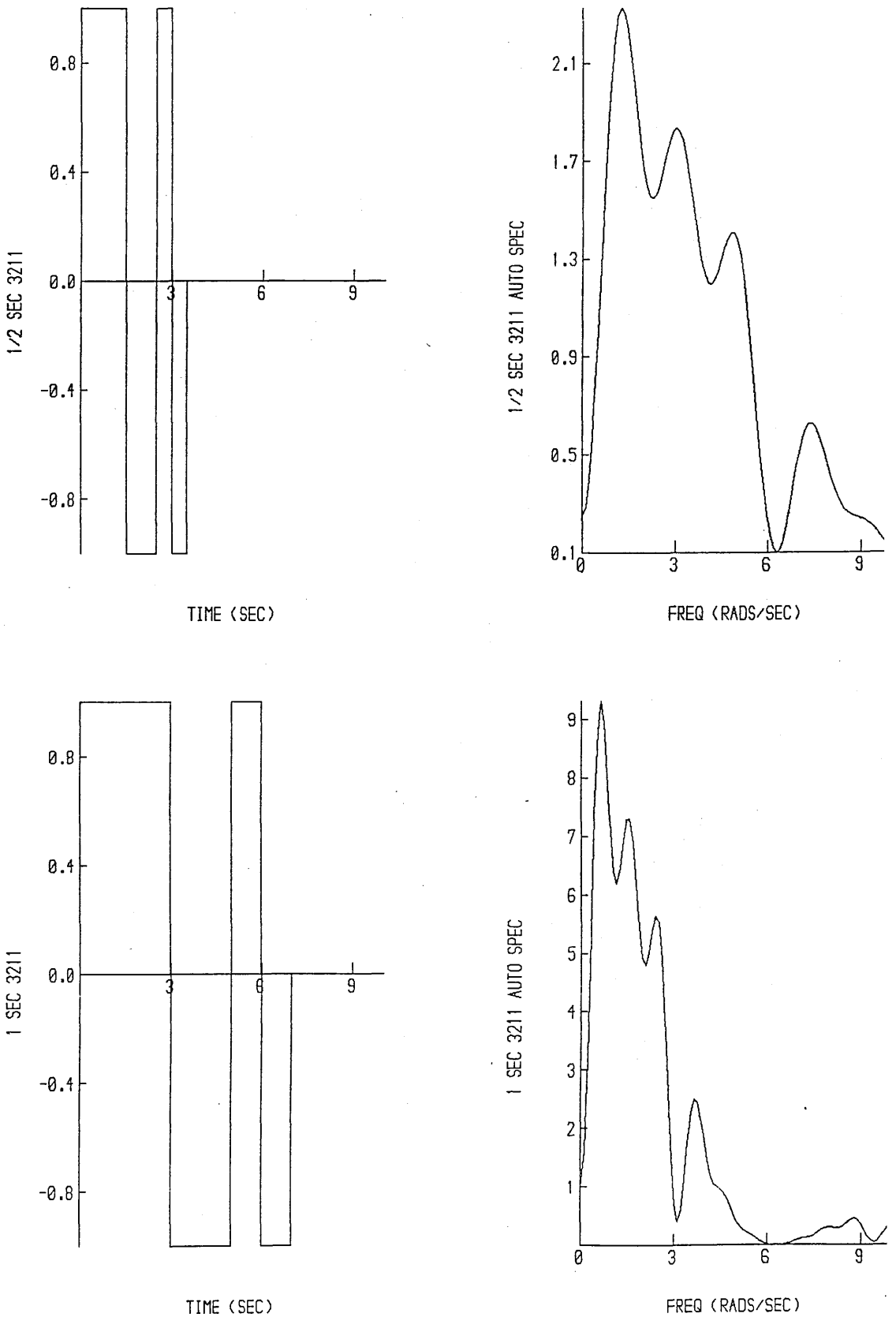

FIGURE 1-2 TIME HISTORIES AND AUTO-SPECTRA OF 1/2 SECOND AND 1 SECOND 3211 INPUTS

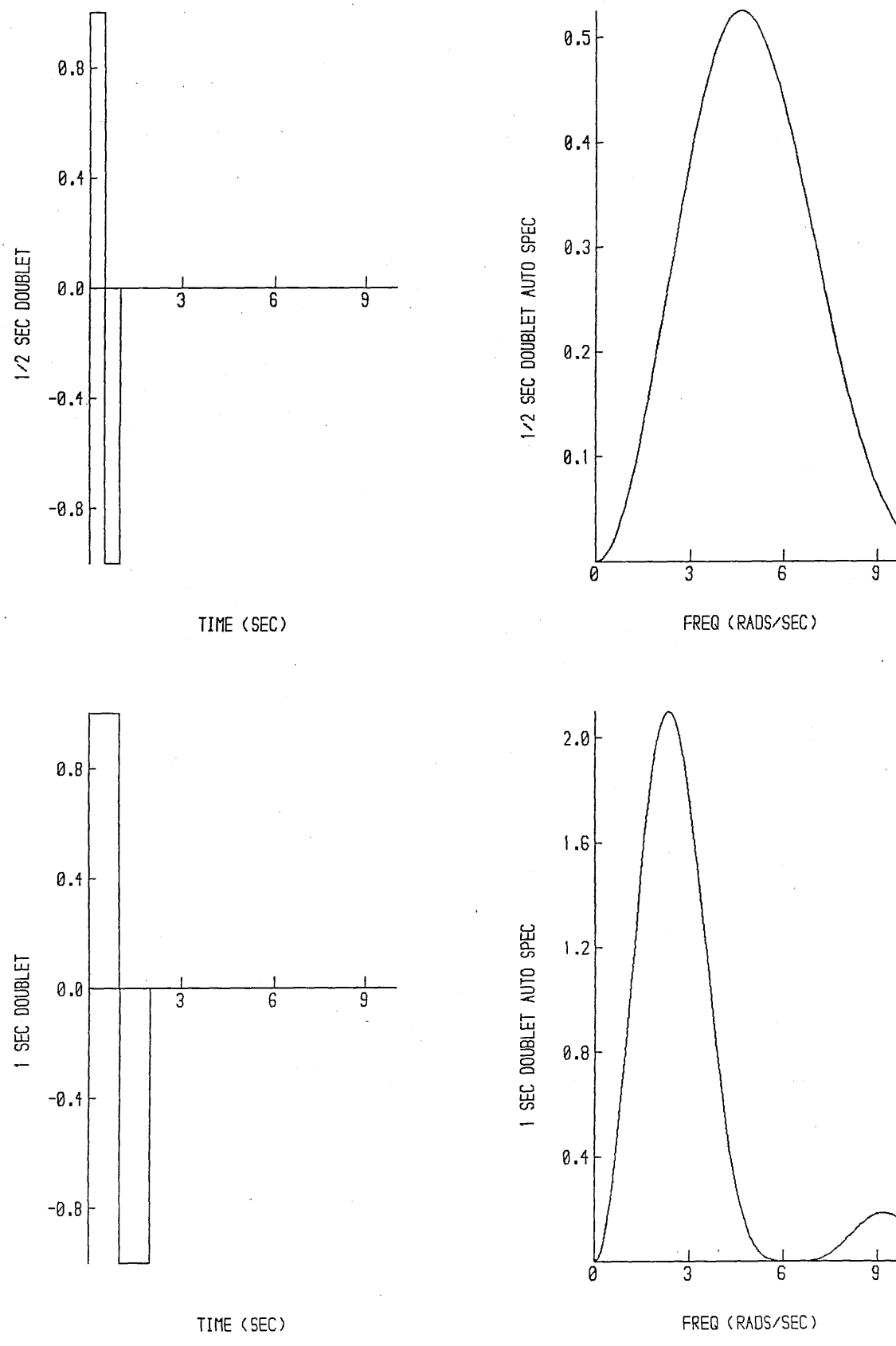

FIGURE 1-3 TIME HISTORIES AND AUTO-SPECTRA OF 1/2 SECOND AND 1 SECOND DOUBLET INPUTS

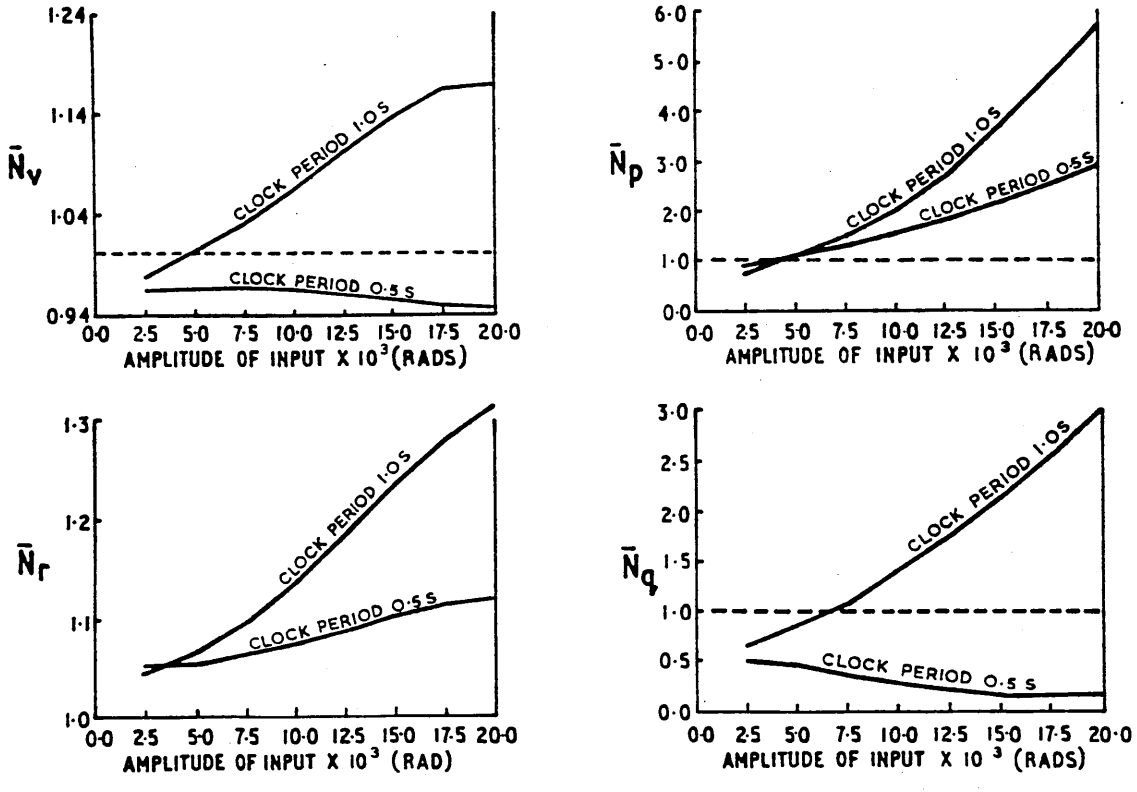

FIGURE 1-4 THE EFFECT OF INPUT SIZE AND CLOCK PERIOD ON ESTIMATED YAWING-MOMENT DERIVATIVES. (ESTIMATES NORMALISED WITH RESPECT TO LINEAR MODEL VALUES: HELISTAB SIMULATED DATA; PUMA 80 KNOTS, LATERAL CYCLIC 3211 INPUT

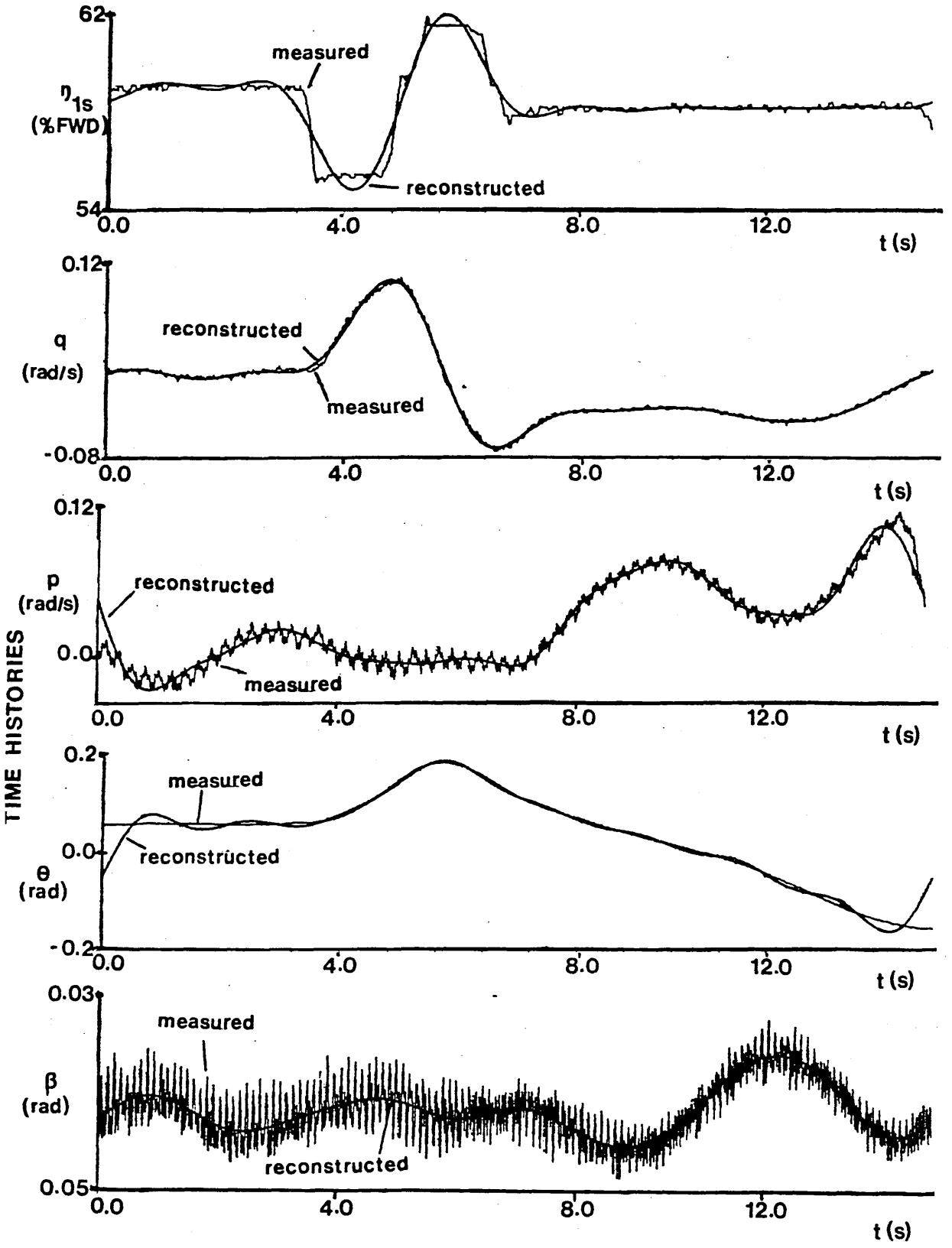

FIGURE 2-1 MEASURED TIME HISTORIES TOGETHER WITH LOW-FREQUENCY RECONSTRUCTIONS

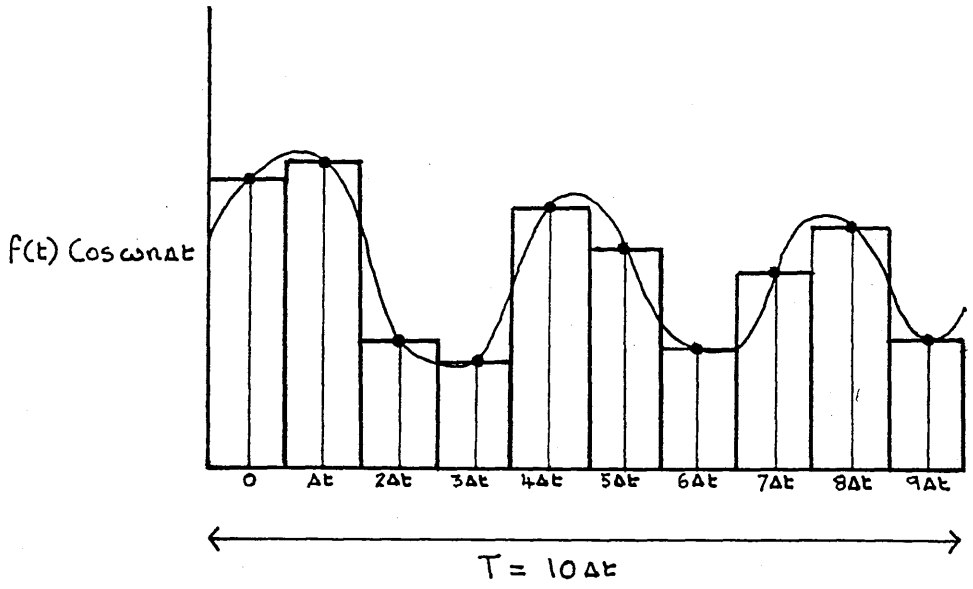

FIGURE 2-2 THE FOURIER TRANSFORM AS AN APPROXIMATION TO THE FOURIER INTEGRAL USING MIDPOINT INTEGRATION

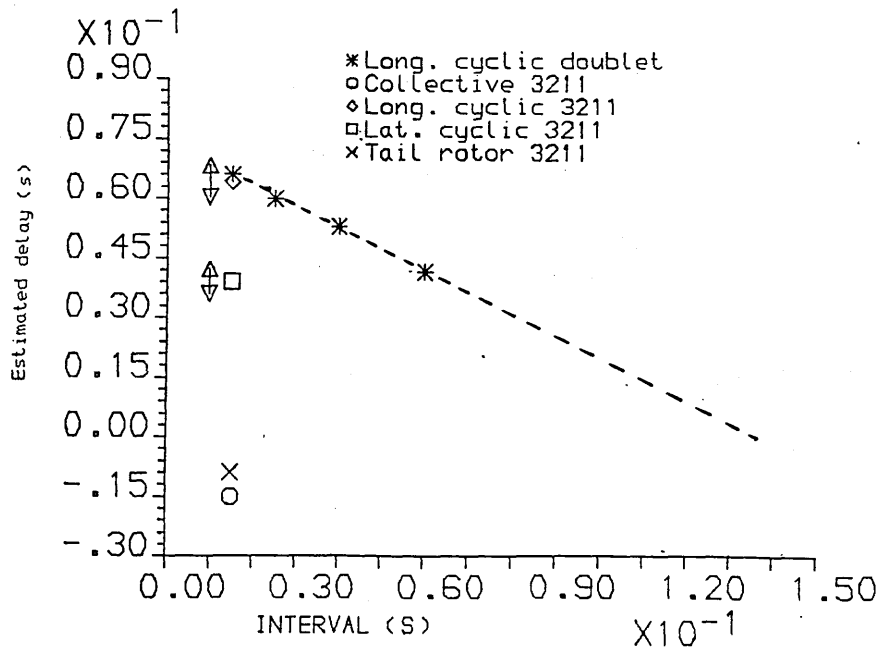

FIGURE 2-3 ESTIMATED TIME DELAY VERSUS SAMPLING INTERVAL USING 9 DOF SIMULATED DATA AND A 6 DOF ESTIMATION MODEL (HELISTAB)

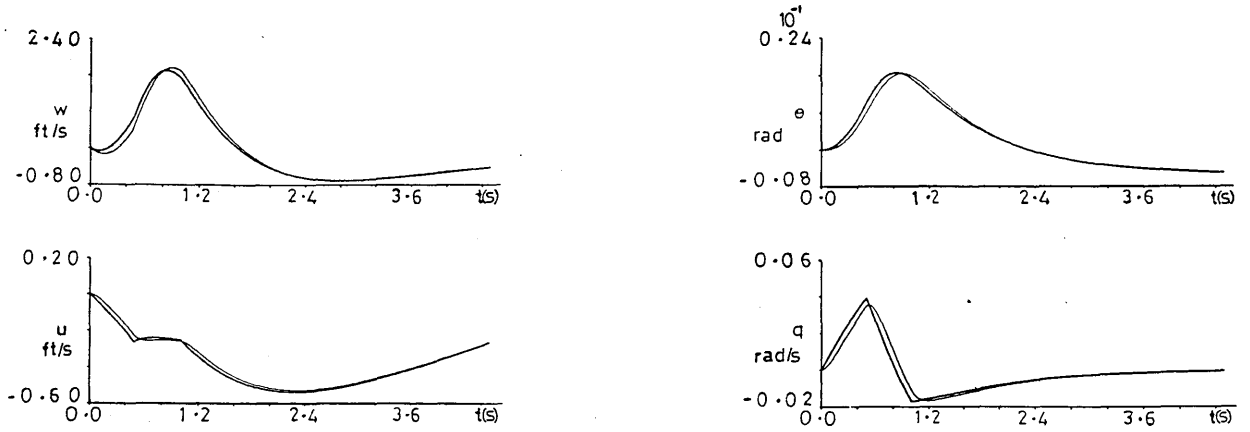

FIGURE 2-4 a) TIME-DOMAIN FITS. 9 DOF DATA AND 6 DOF MODEL WITHOUT TIME DELAY. HELISTAB, 80 KNOTS, LONGITUDINAL-CYCLIC DOUBLET

9 DOF RESPONSE: ~
6 DOF PREDICTION WITHOUT DELAY: ~

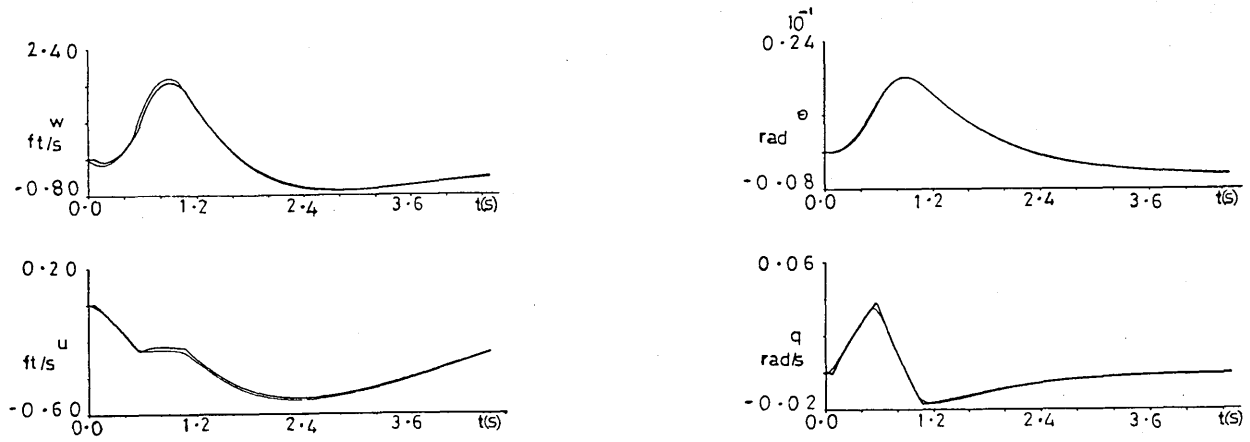

FIGURE 2-4 b) TIME-DOMAIN FITS. 9 DOF DATA AND 6 DOF MODEL WITH TIME DELAY. HELISTAB, 80 KNOTS, LONGITUDINAL-CYCLIC DOUBLET

9 DOF RESPONSE: ~
6 DOF PREDICTION WITH DELAY: ~

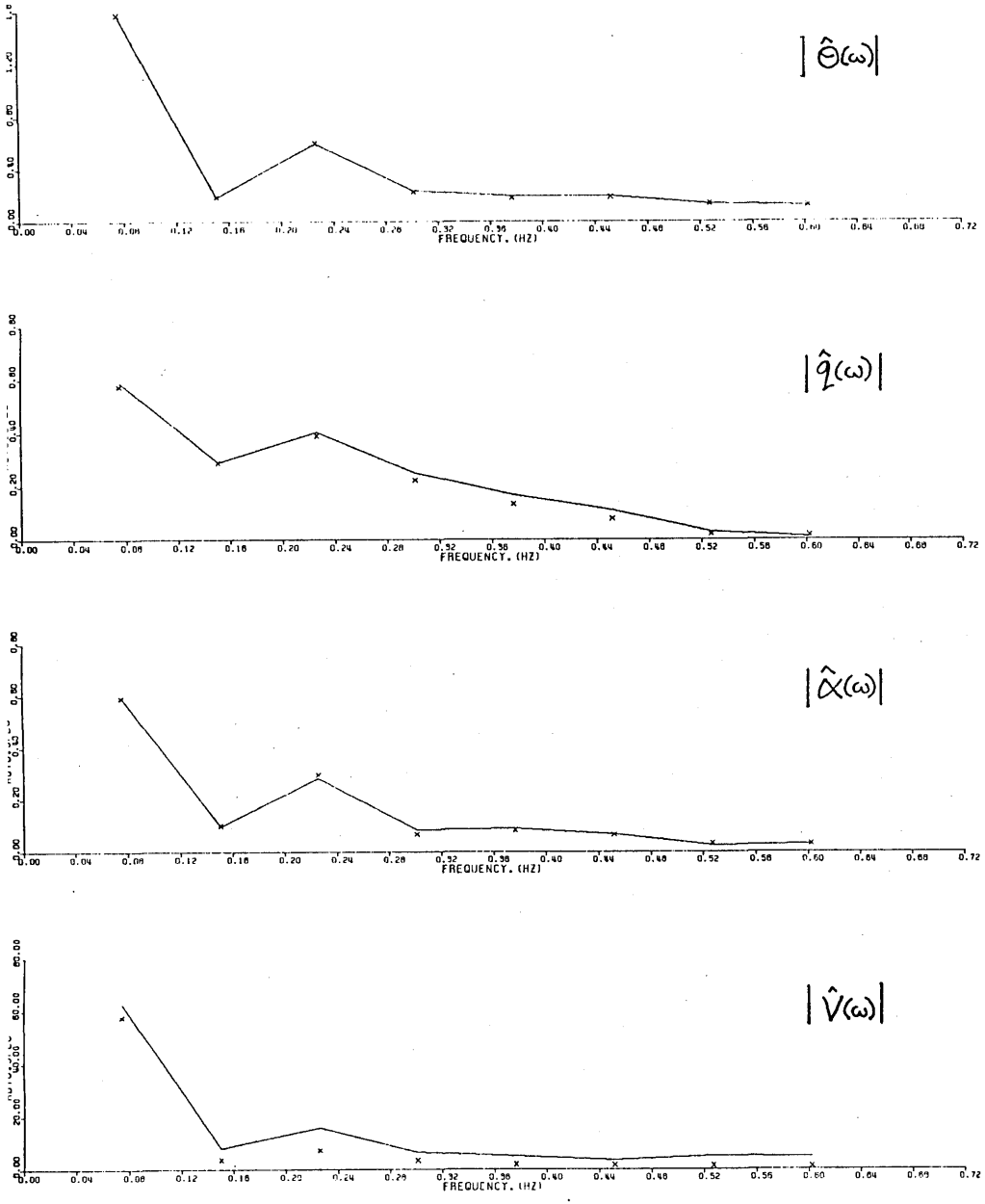

FIGURE 2-5 a) FREQUENCY-DOMAIN FITS (OUTPUT-ERROR METHOD)
CASE 1: SAMPLING INTERVAL 0.015625 SECONDS;
NO TIME DELAY IN MODEL.
PUMA, 100 KNOTS, RUN R0201A

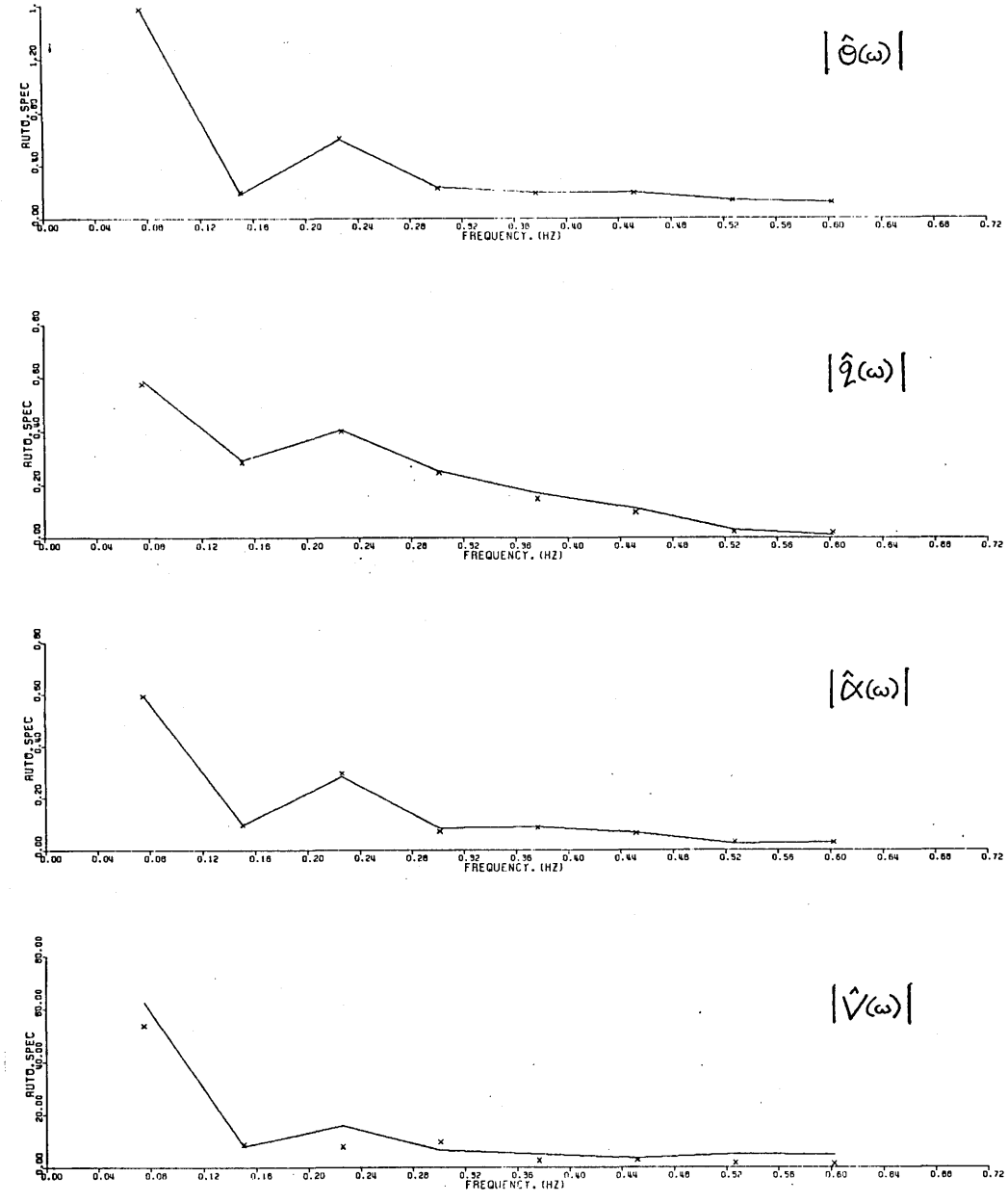

FIGURE 2-5 b) FREQUENCY-DOMAIN FITS (OUTPUT-ERROR METHOD)
CASE 2: SAMPLING INTERVAL 0.015625 SECONDS;
TIME DELAY IN MODEL.
PUMA, 100 KNOTS, RUN R0201A

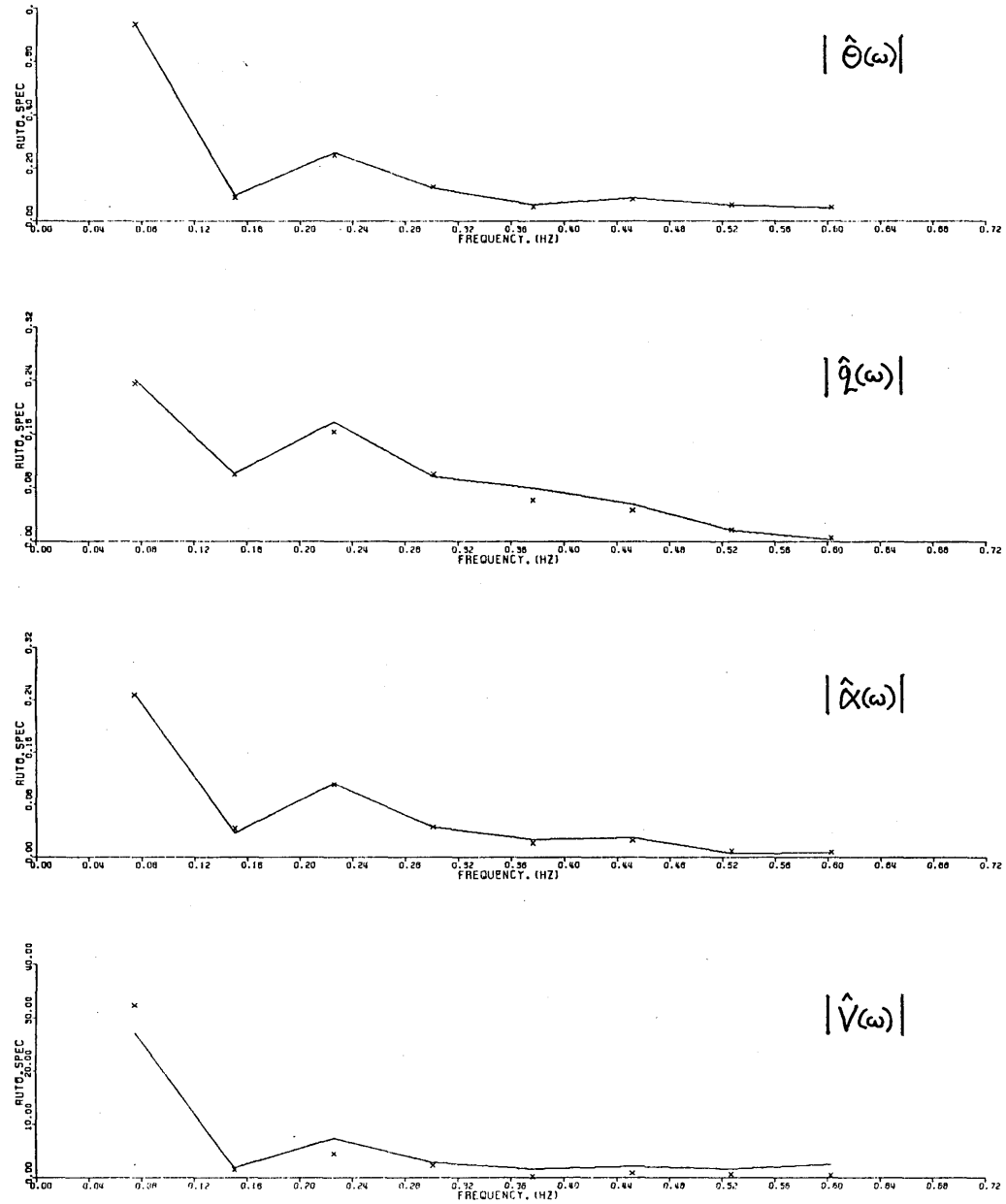

FIGURE 2-5 c) FREQUENCY-DOMAIN FITS (OUTPUT-ERROR METHOD)
CASE 3: SAMPLING INTERVAL 0.09375 SECONDS;
NO TIME DELAY IN MODEL.
PUMA, 100 KNOTS, RUN R0201A

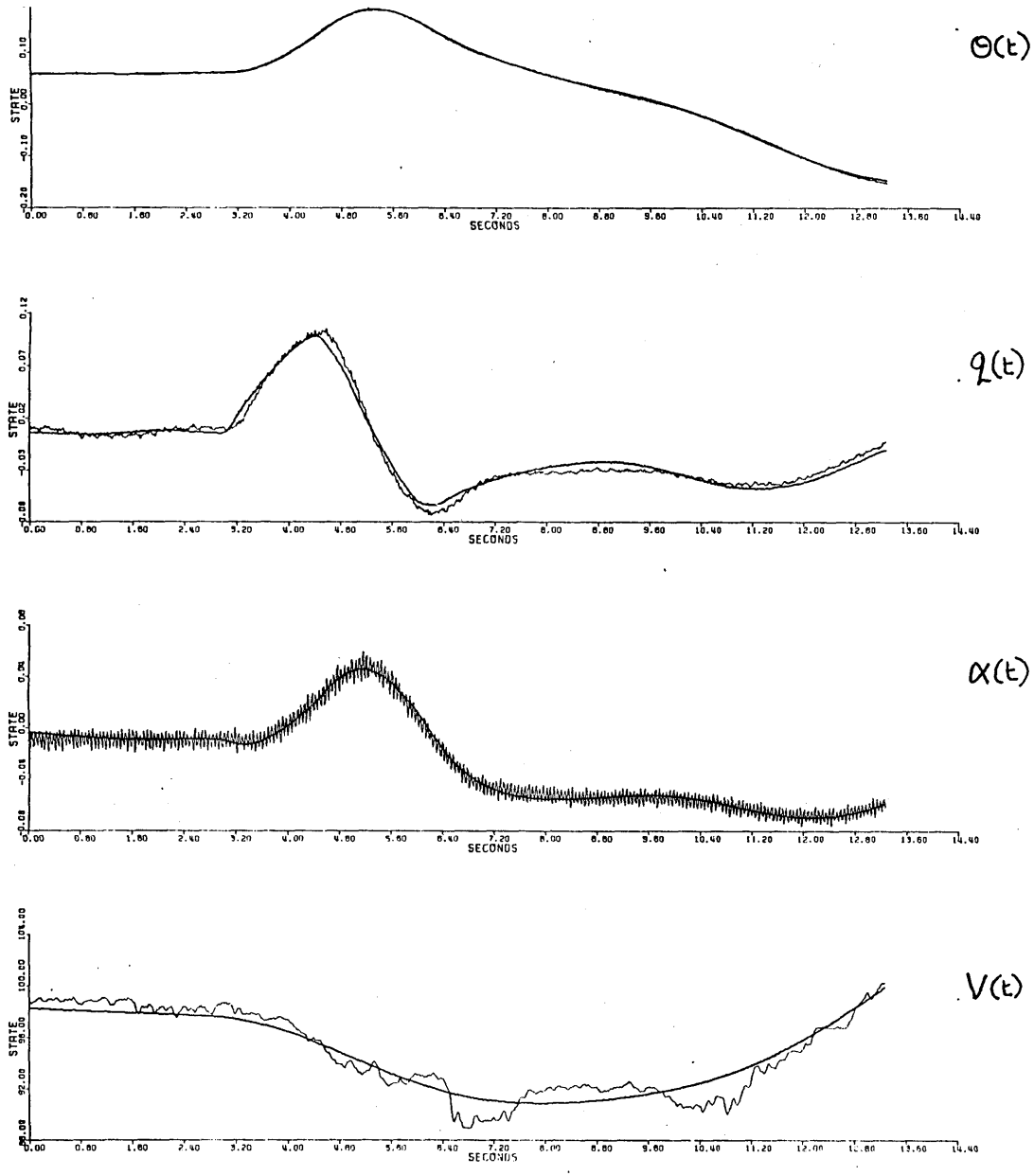

FIGURE 2-6 a) TIME-DOMAIN VERIFICATION (OUTPUT-ERROR METHOD)
CASE 1: SAMPLING INTERVAL 0.015625 SECONDS;
NO TIME DELAY IN MODEL.
PUMA, 100 KNOTS, RUN R0201A

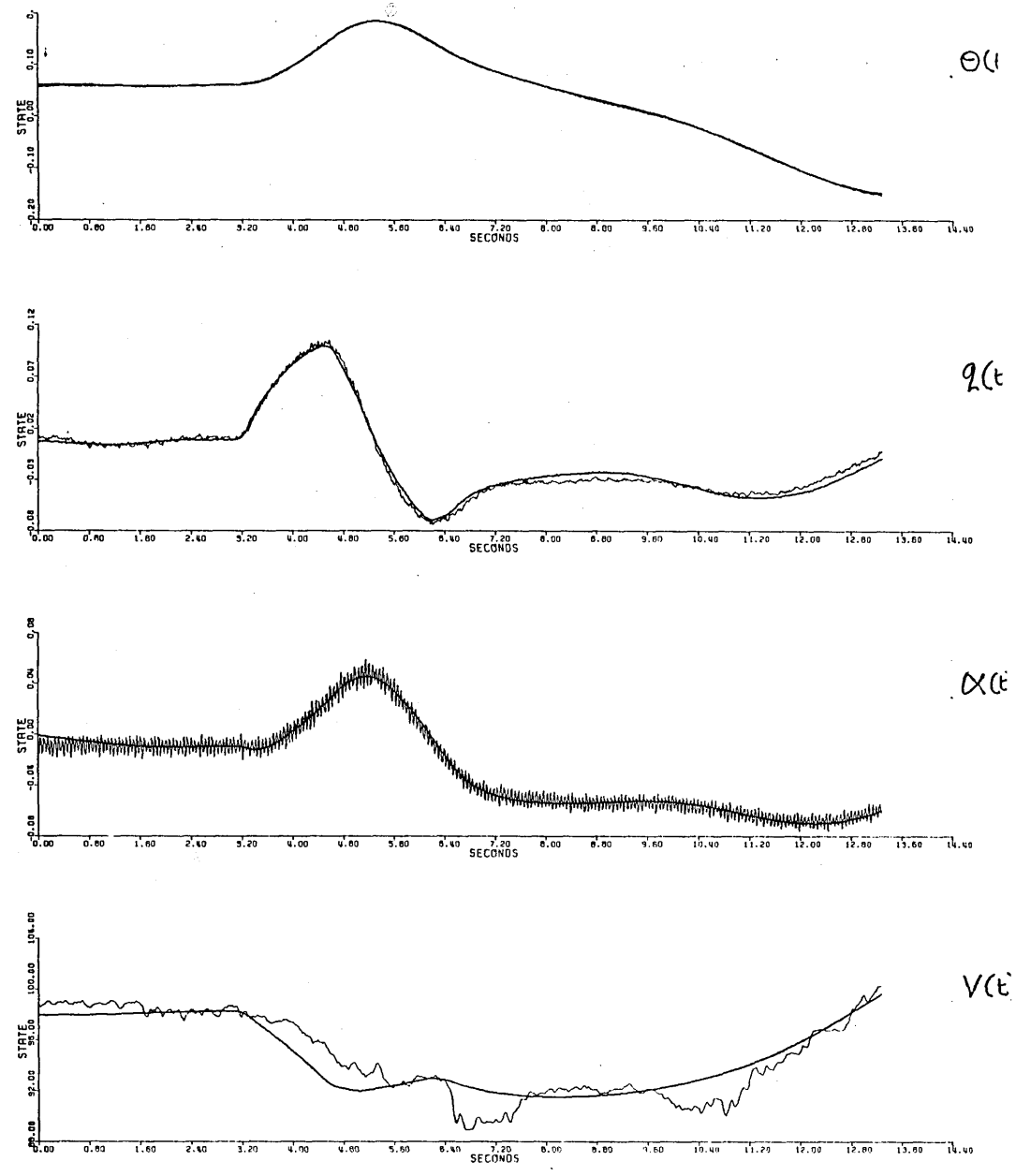

FIGURE 2-6 b) TIME-DOMAIN VERIFICATION (OUTPUT-ERROR METHOD)
CASE 2: SAMPLING INTERVAL 0.015625 SECONDS;
TIME DELAY IN MODEL.
PUMA, 100 KNOTS, RUN R0201A

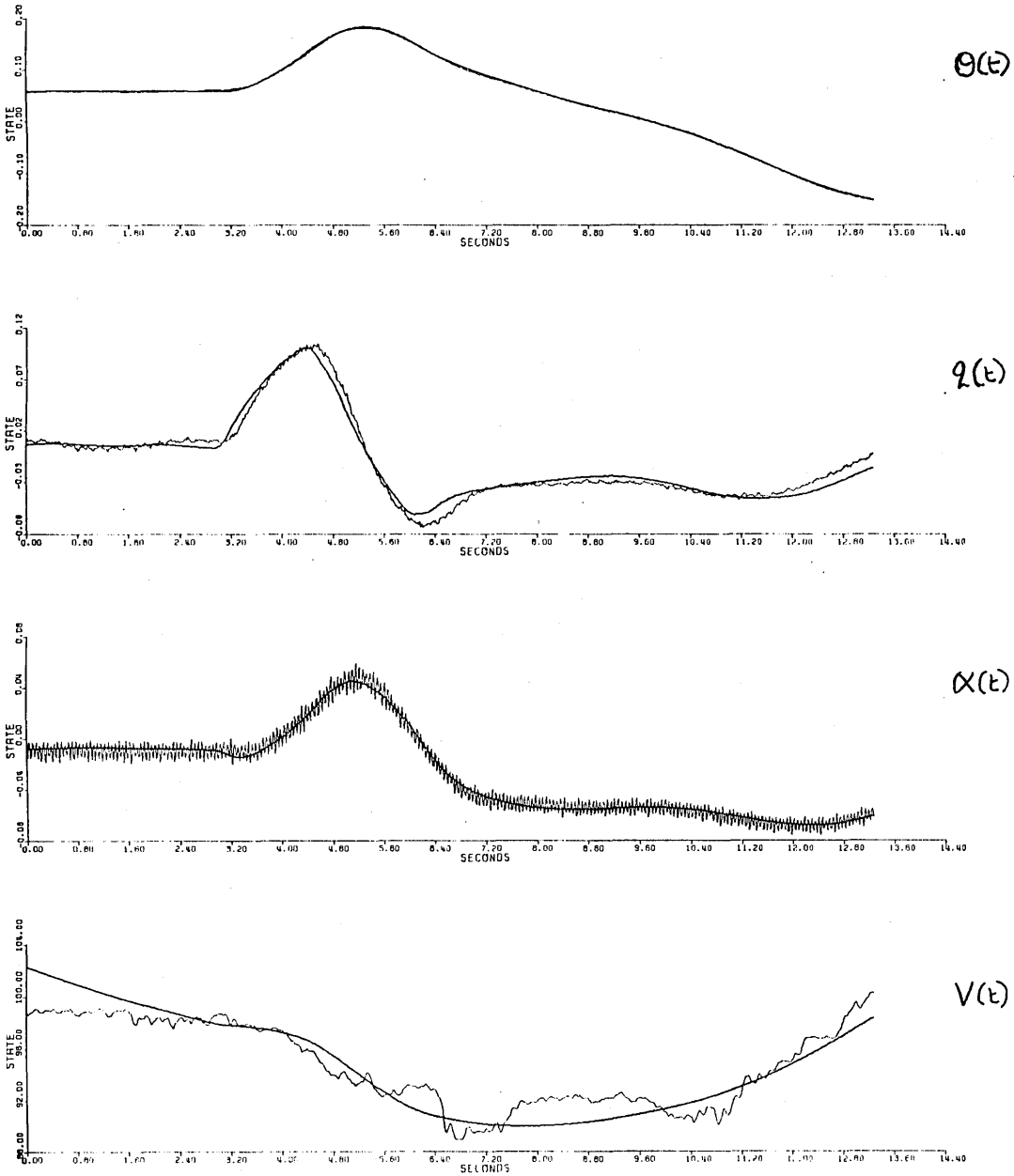

FIGURE 2-6 c) TIME-DOMAIN VERIFICATION (OUTPUT-ERROR METHOD)
CASE 3: SAMPLING INTERVAL 0.09375 SECONDS;
NO TIME DELAY IN MODEL.
PUMA, 100 KNOTS, RUN R0201A

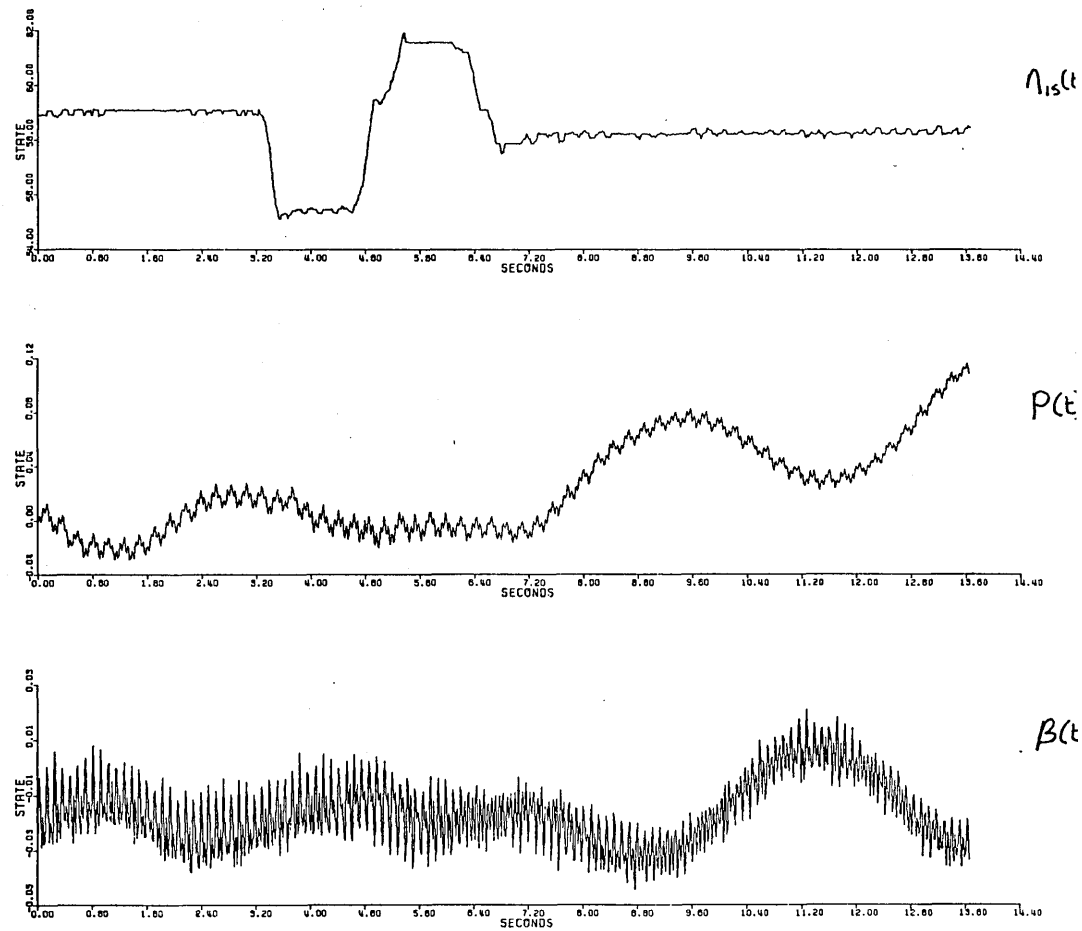

FIGURE 2-6 d) TIME HISTORIES OF THE LONGITUDINAL-CYLIC CONTROL
AND LATERAL PSEUDO CONTROL TERMS

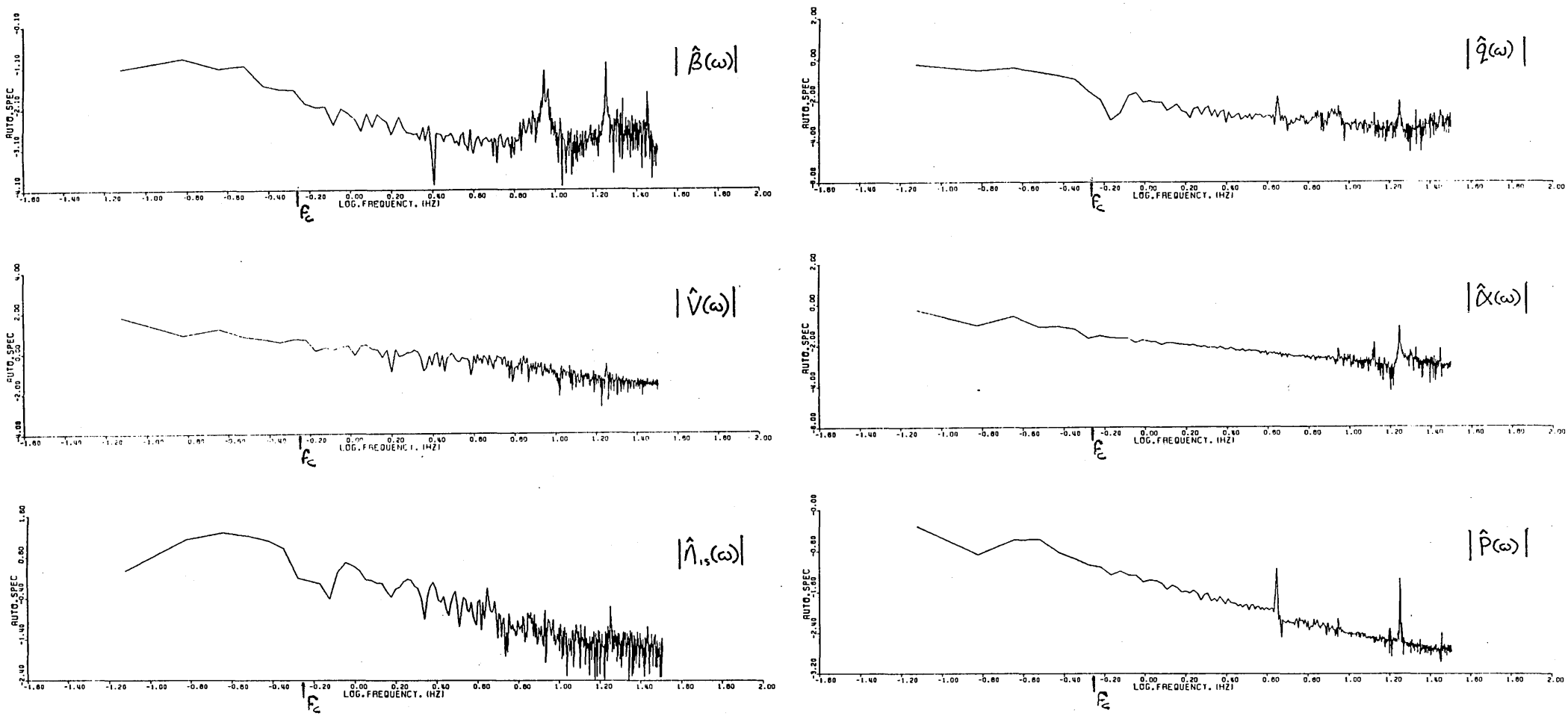

FIGURE 3-1 LOG-MAGNITUDE LOG-FREQUENCY PLOTS OF VARIABLES
USED IN THE PITCHING-MOMENT EQUATION

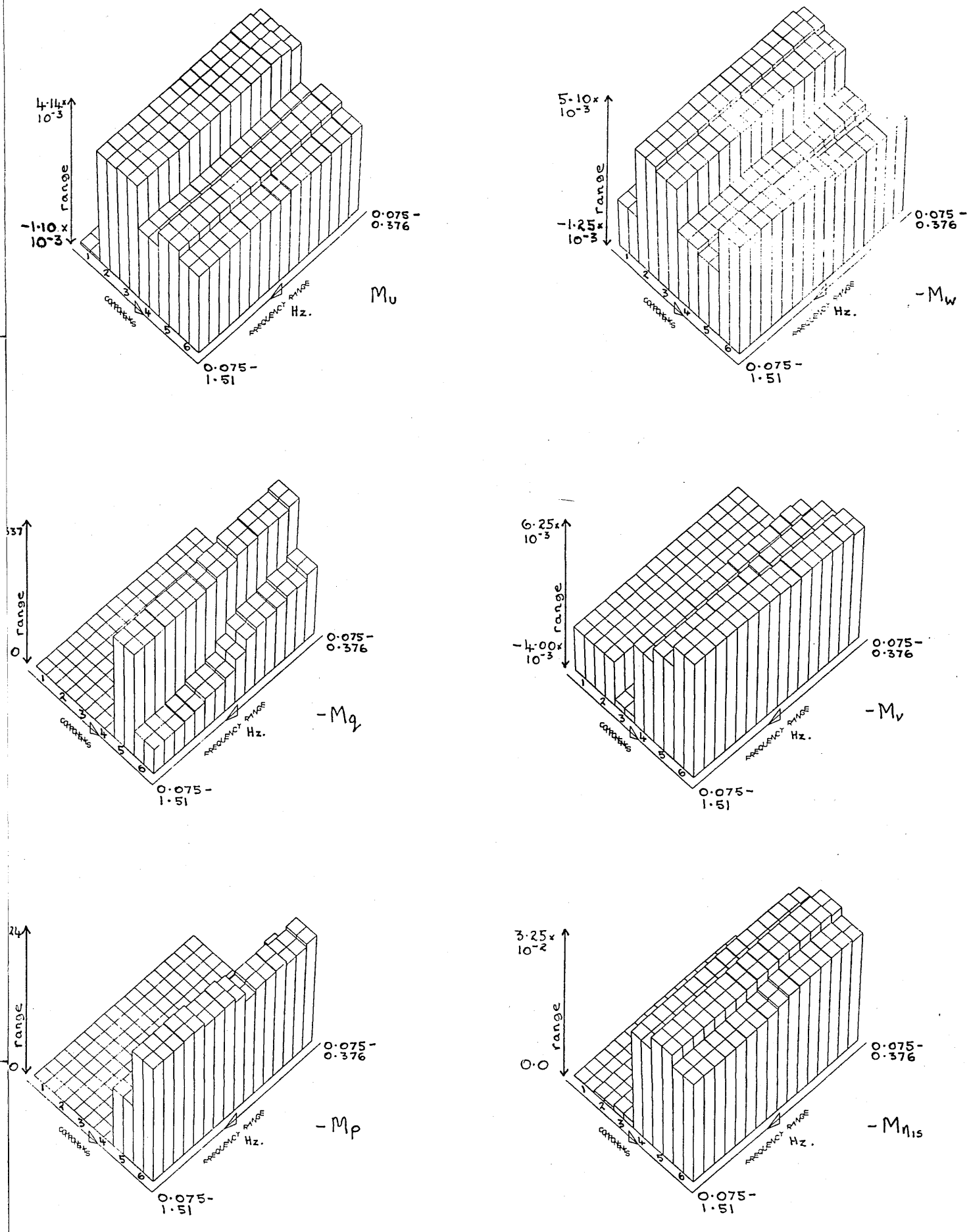

FIGURE 3-2 THE DEPENDENCE OF PARAMETER ESTIMATES ON THE FREQUENCY RANGE AND THE NUMBER OF ORTHOGONAL COMPONENTS USED. RUN R0201A

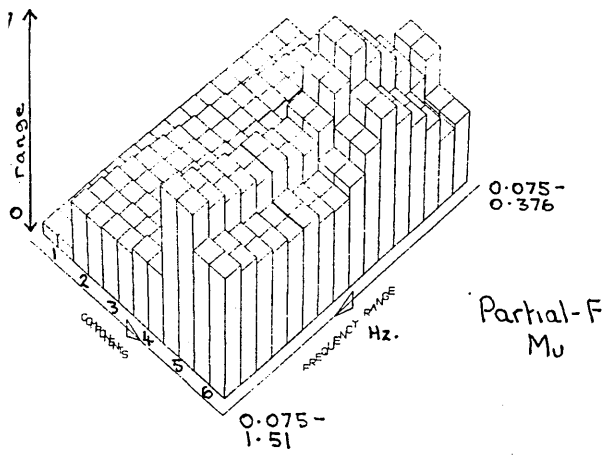

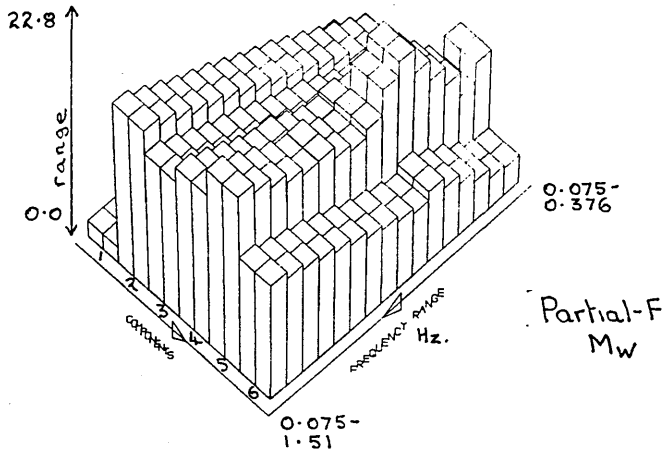

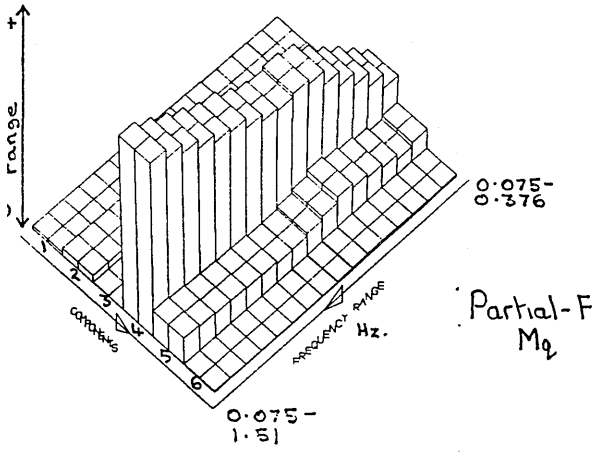

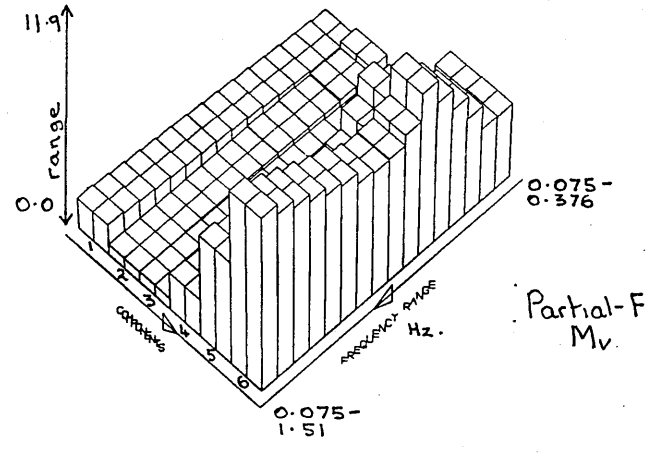

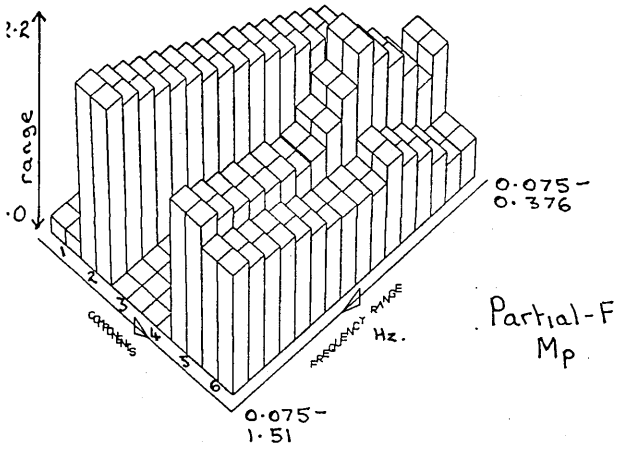

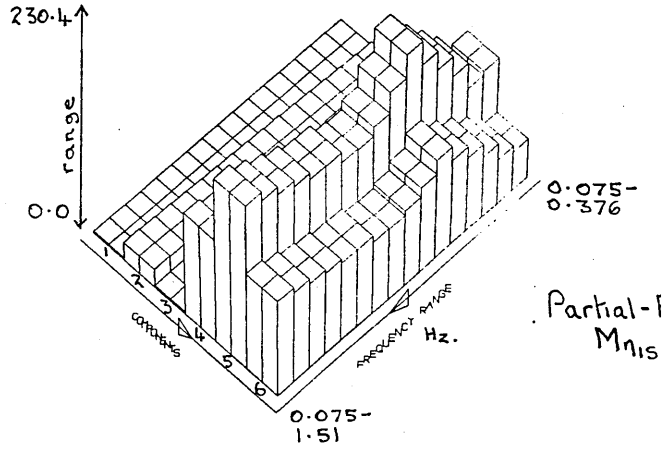

FIGURE 3-3 THE DEPENDENCE OF PARTIAL-F RATIOS ON THE FREQUENCY RANGE AND THE NUMBER OF ORTHOGONAL COMPONENTS USED. RUN R0201A

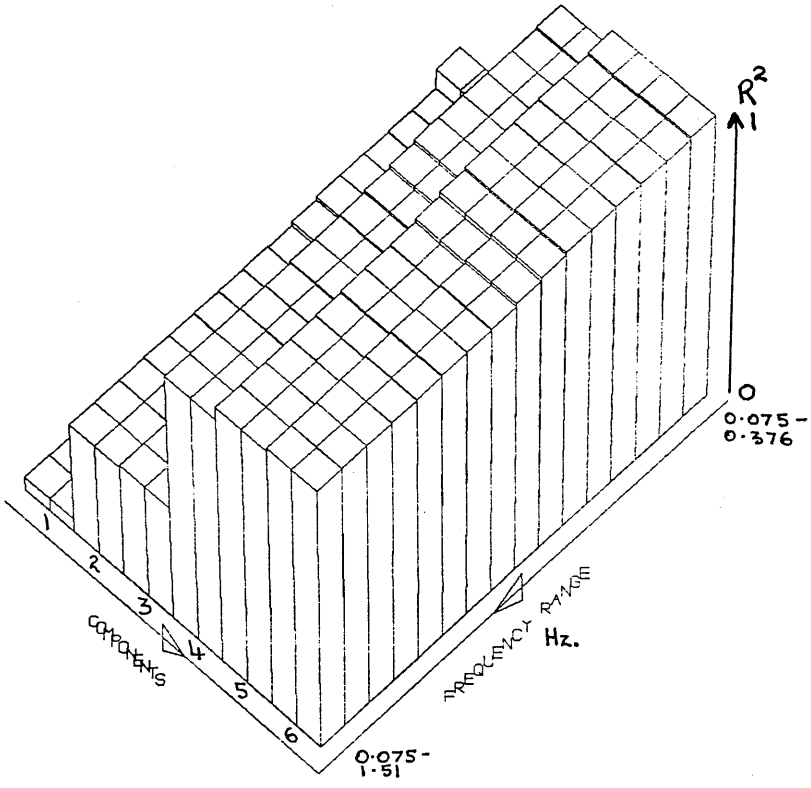

FIGURE 3-4 THE DEPENDENCE OF THE SQUARED-CORRELATION COEFFICIENT ON THE FREQUENCY RANGE AND THE NUMBER OF ORTHOGONAL COMPONENTS USED FOR THE PITCHING-MOMENT EQUATION. RUN R0201A

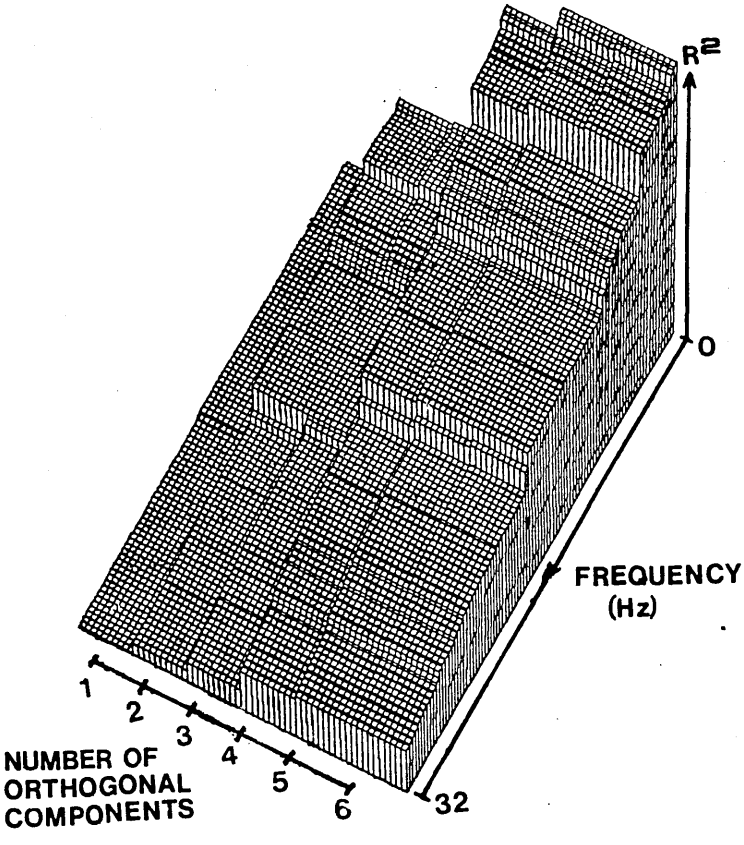

FIGURE 3-5 THE DEPENDENCE OF THE SQUARED-CORRELATION COEFFICIENT ON THE FREQUENCY RANGE AND THE NUMBER OF ORTHOGONAL COMPONENTS USED FOR THE PITCHING-MOMENT EQUATION (FOR FULL RANGE OF FREQUENCIES. RUN R0201A)

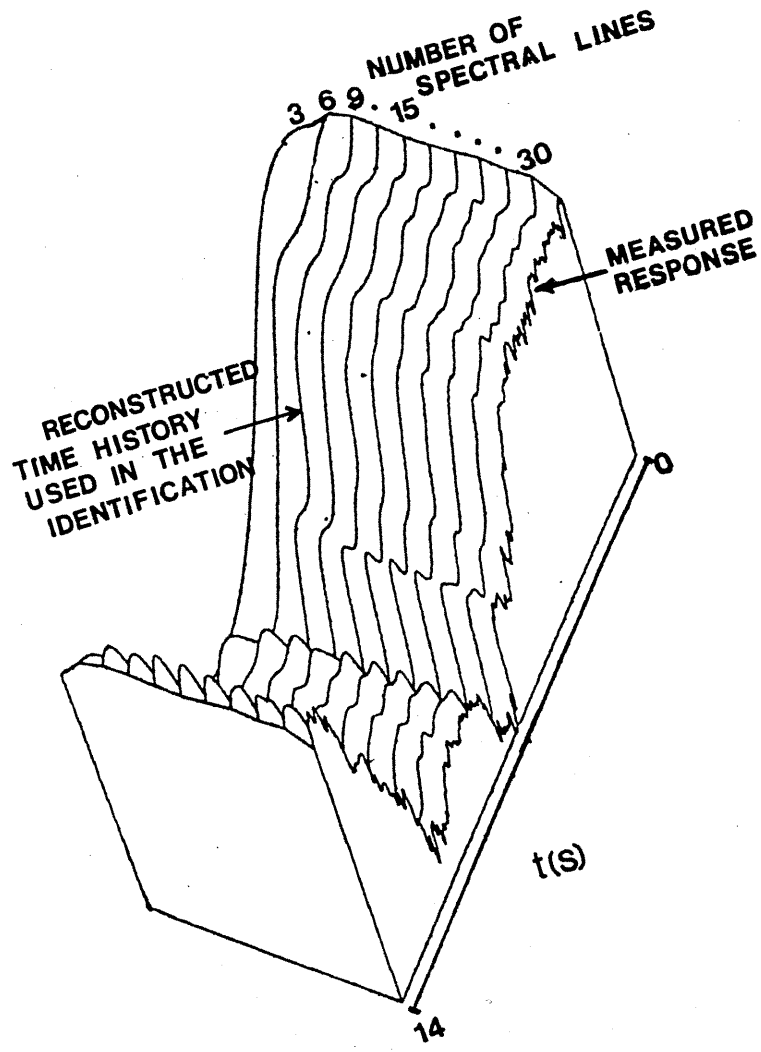

FIGURE 3-6 FORWARD VELOCITY RECONSTRUCTIONS IN THE TIME DOMAIN, SHOWING THE EFFECT OF INCREASING THE NUMBER OF FREQUENCY-DOMAIN POINTS USED. RUN R0201A

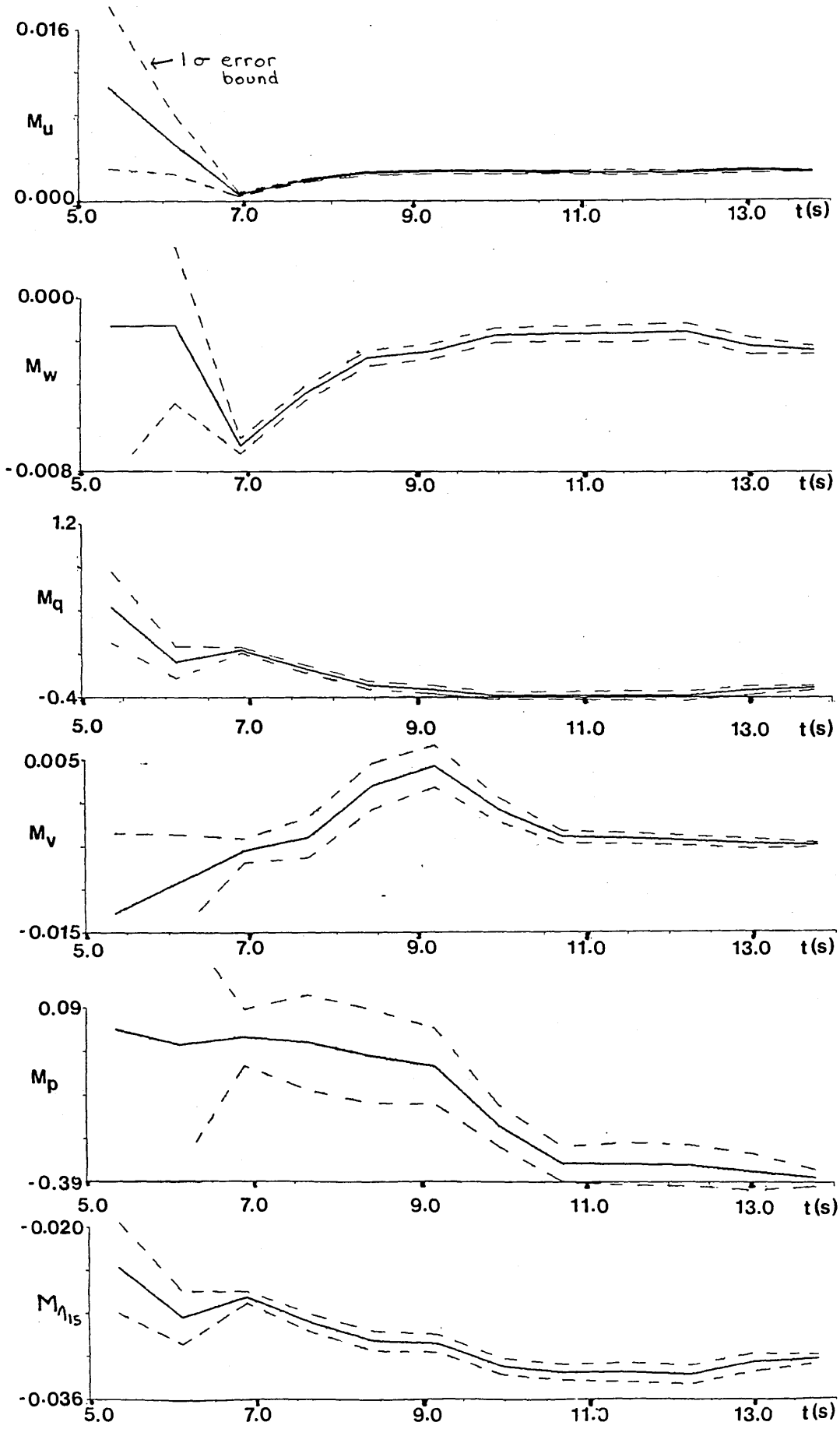

FIGURE 3-7 VARIATION OF ESTIMATES AND ERROR BOUNDS (BROKEN LINES) WITH LENGTH OF RECORD USED. RUN R0201A

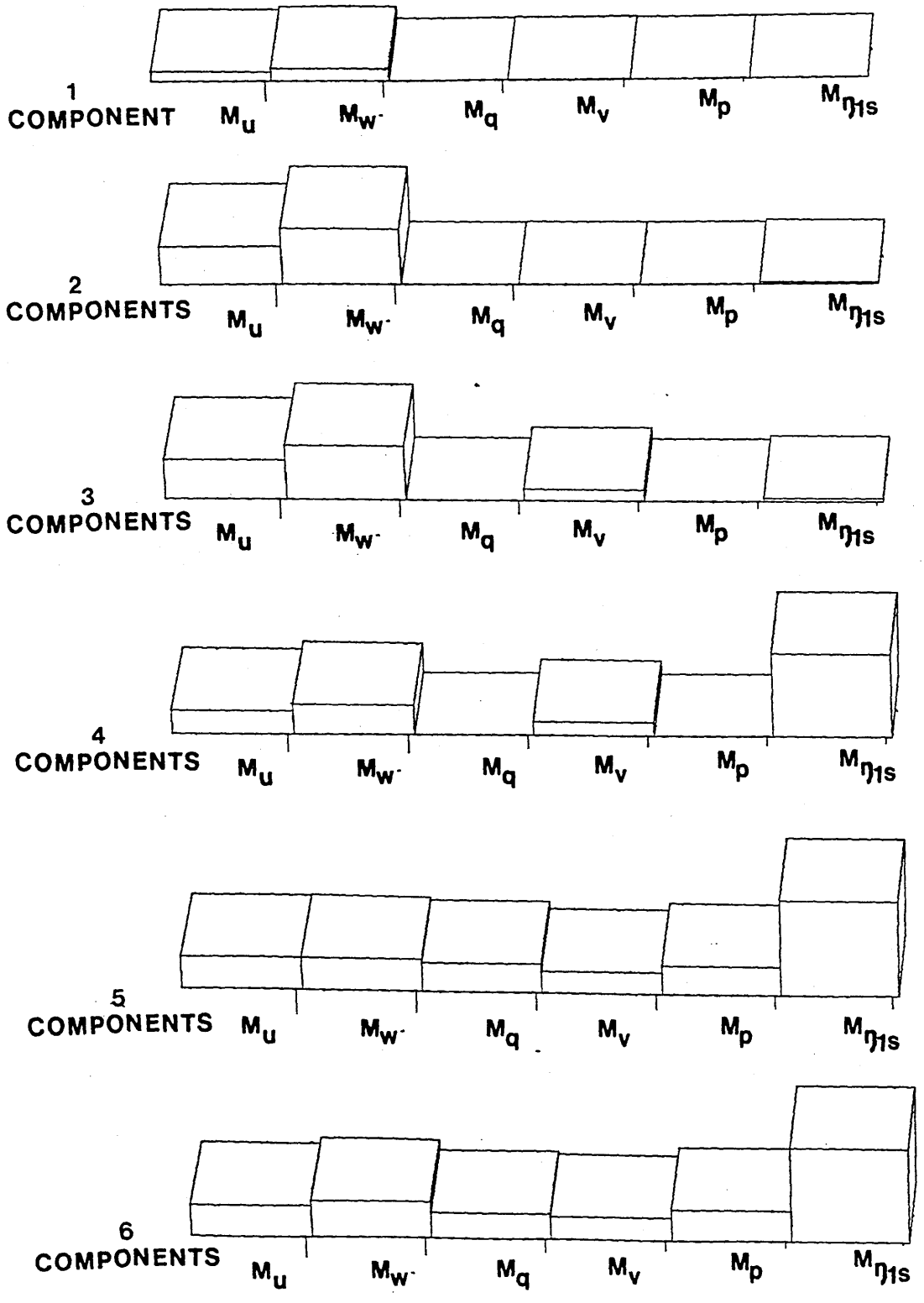

FIGURE 3-8 PARAMATER SIGNIFICANCE VALUES.
PITCHING-MOMENT EQUATION. RUN R0201A

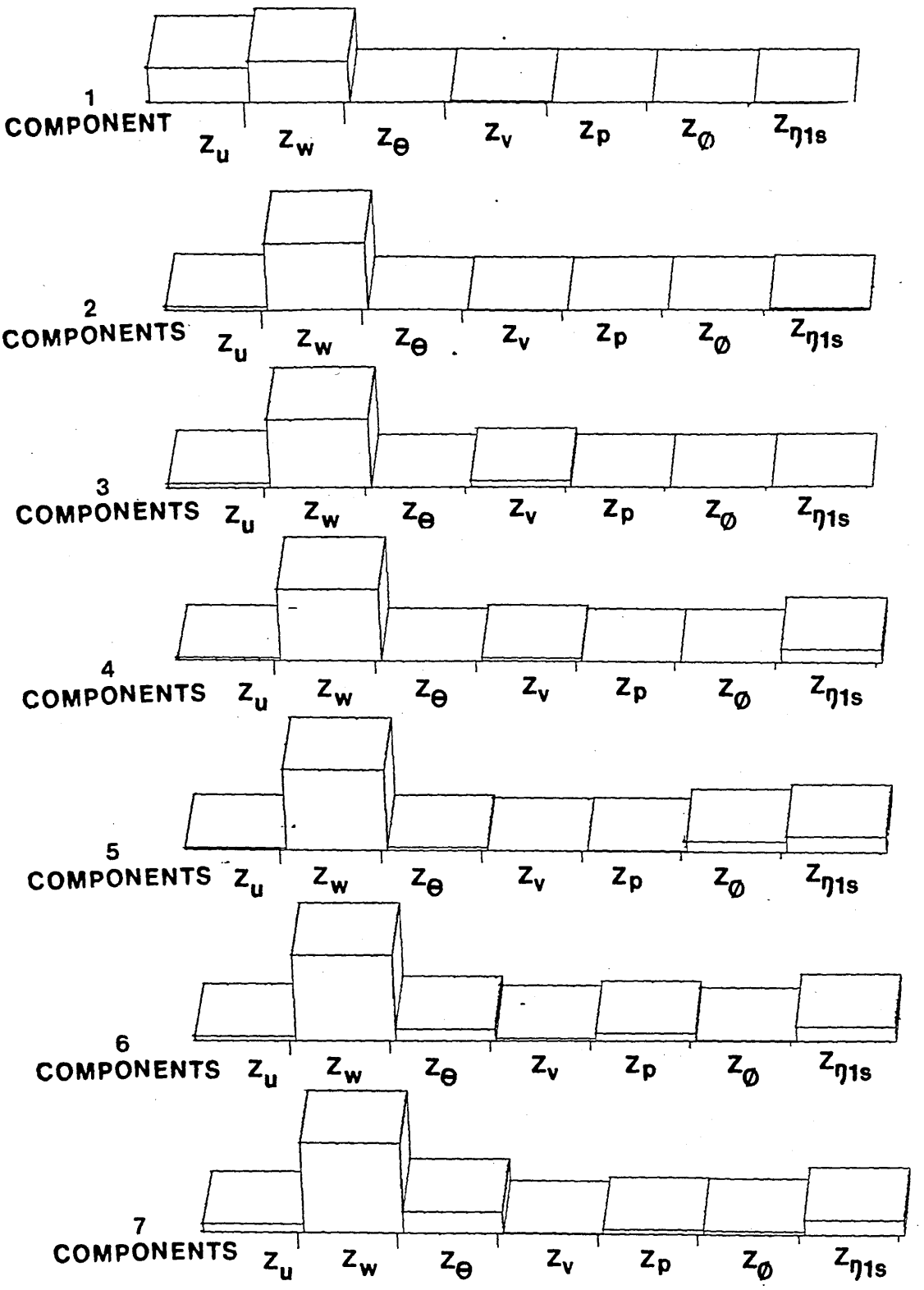

FIGURE 3-9 PARAMETER SIGNIFICANCE VALUES.
NORMAL-FORCE EQUATION. RUN R0201A

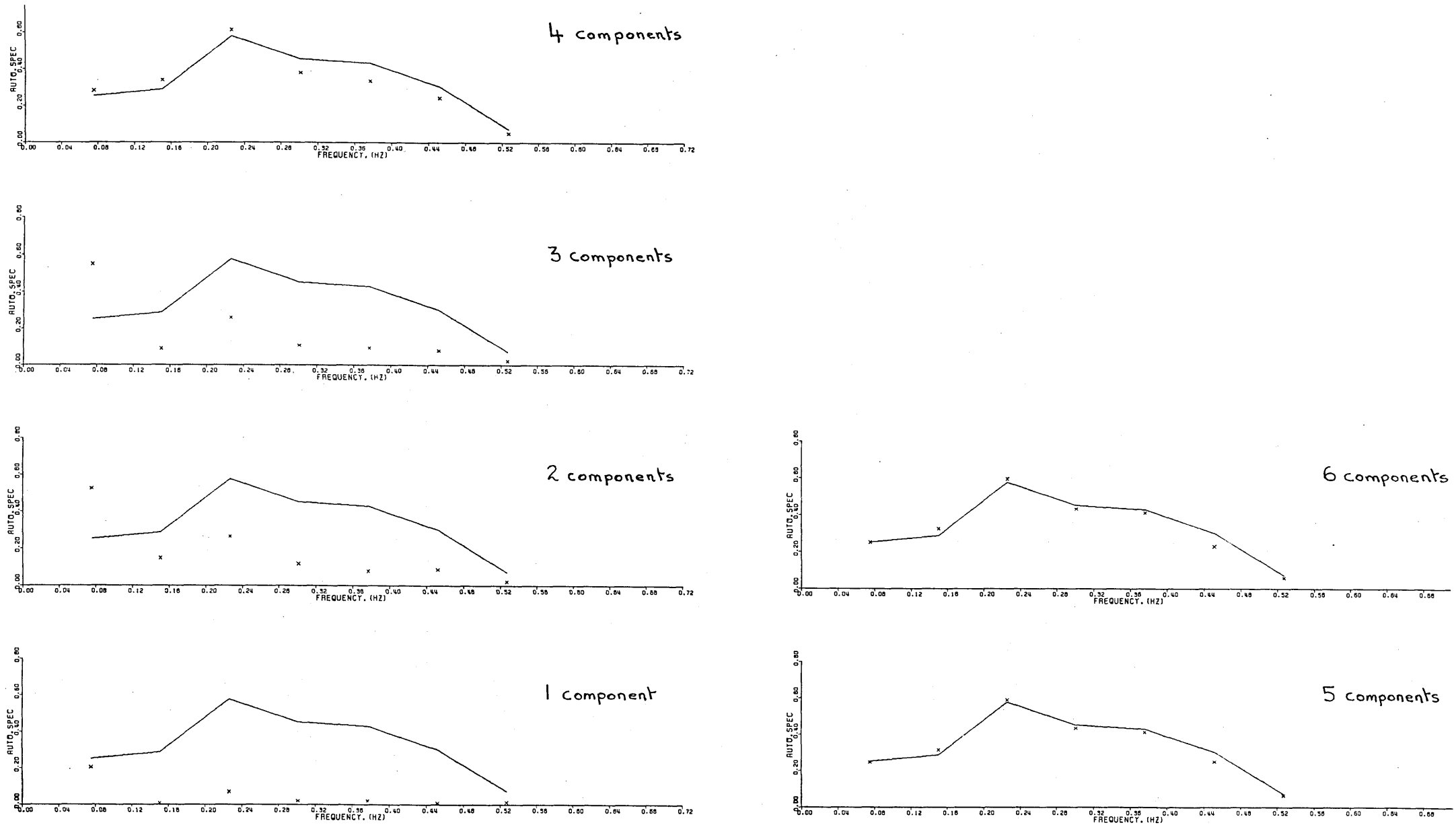

FIGURE 3-10 a) FREQUENCY-DOMAIN EQUATION-ERROR FITS
FOR DIFFERENT NOS. OF ORTHOGONAL COMPONENTS
(SINGULAR-VALUE DECOMPOSITION).
MODEL WITHOUT TIME DELAY.
PITCHING-MOMENT EQUATION. RUN R0201A

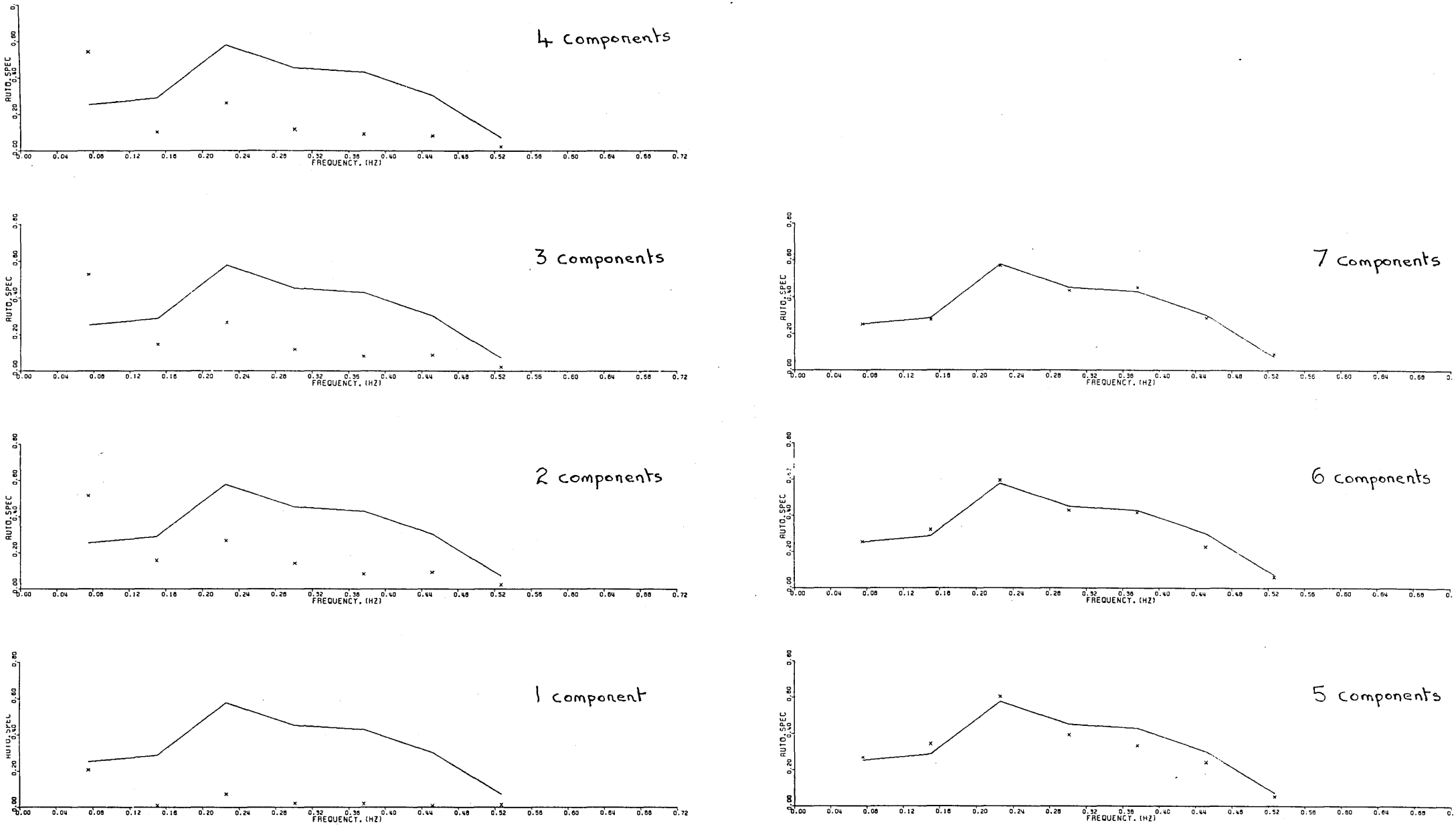

FIGURE 3-10 b) FREQUENCY-DOMAIN EQUATION-ERROR FITS
FOR DIFFERENT NOS. OF ORTHOGONAL COMPONENTS
(SINGULAR-VALUE DECOMPOSITION).
MODEL WITH TIME DELAY.
PITCHING-MOMENT EQUATION, RUN R0201A

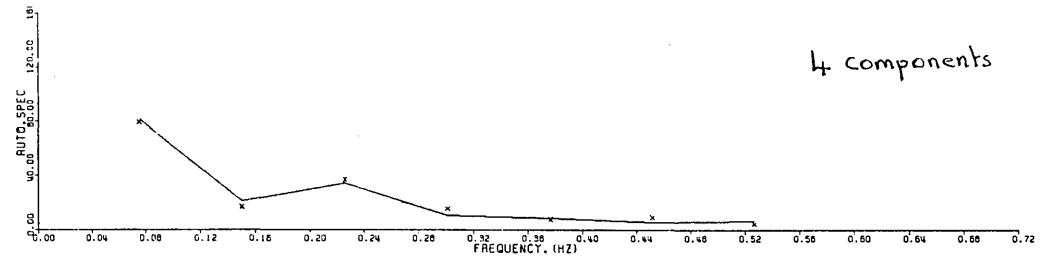

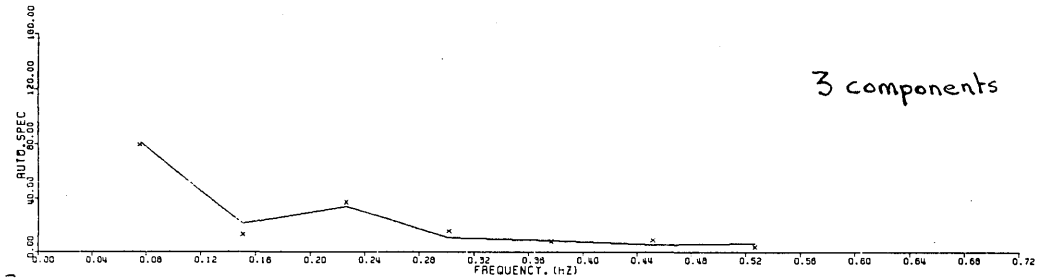

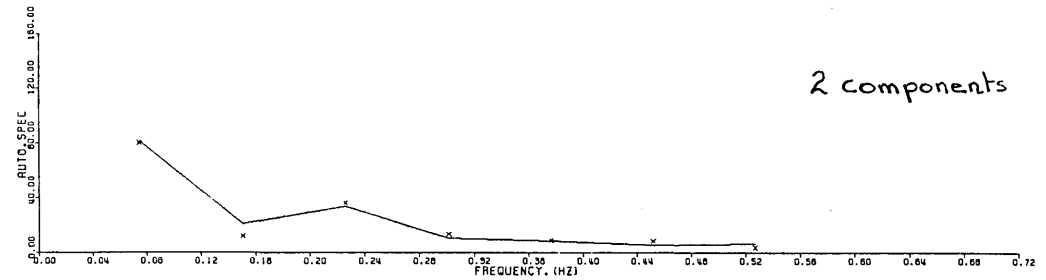

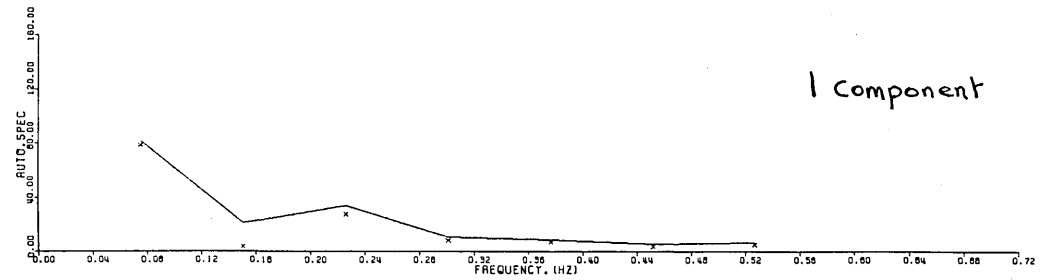

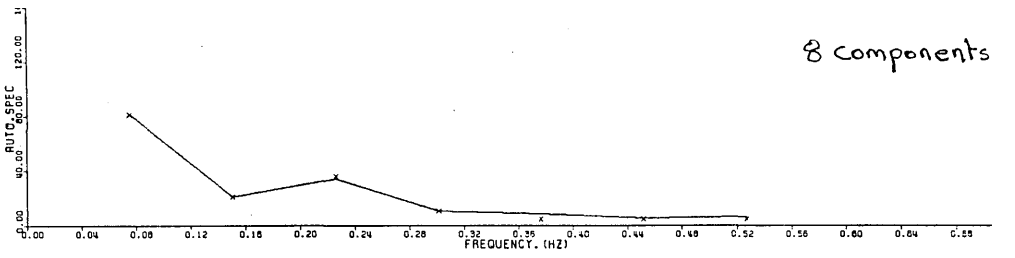

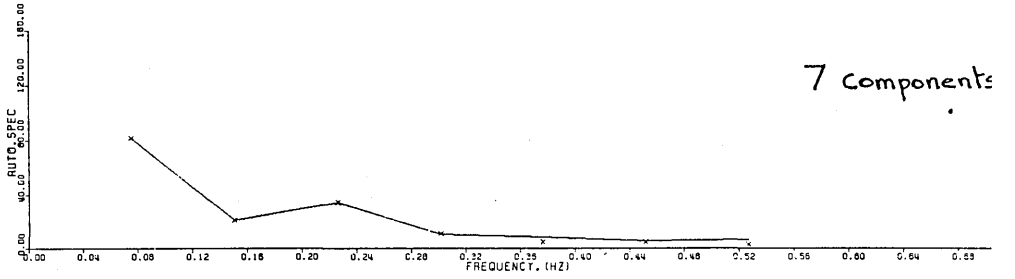

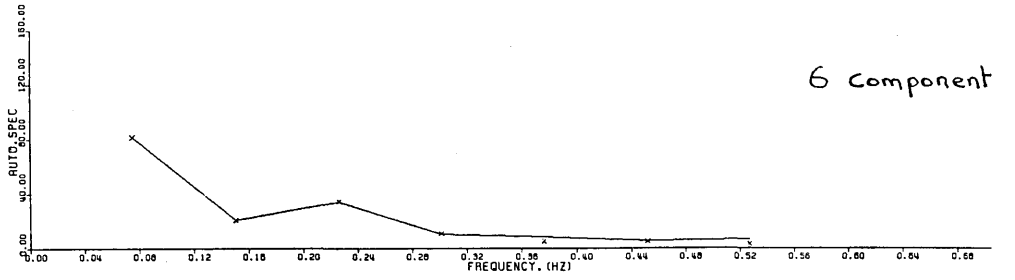

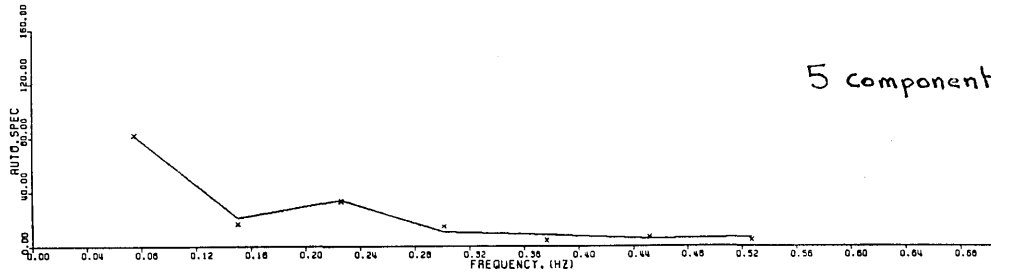

FIGURE 3-11 b) FREQUENCY-DOMAIN EQUATION-ERROR FITS
FOR DIFFERENT NOS. OF ORTHOGONAL COMPONENTS
(SINGULAR-VALUE DECOMPOSITION).
MODEL WITH TIME DELAY.
NORMAL-FORCE EQUATION. RUN R0201A

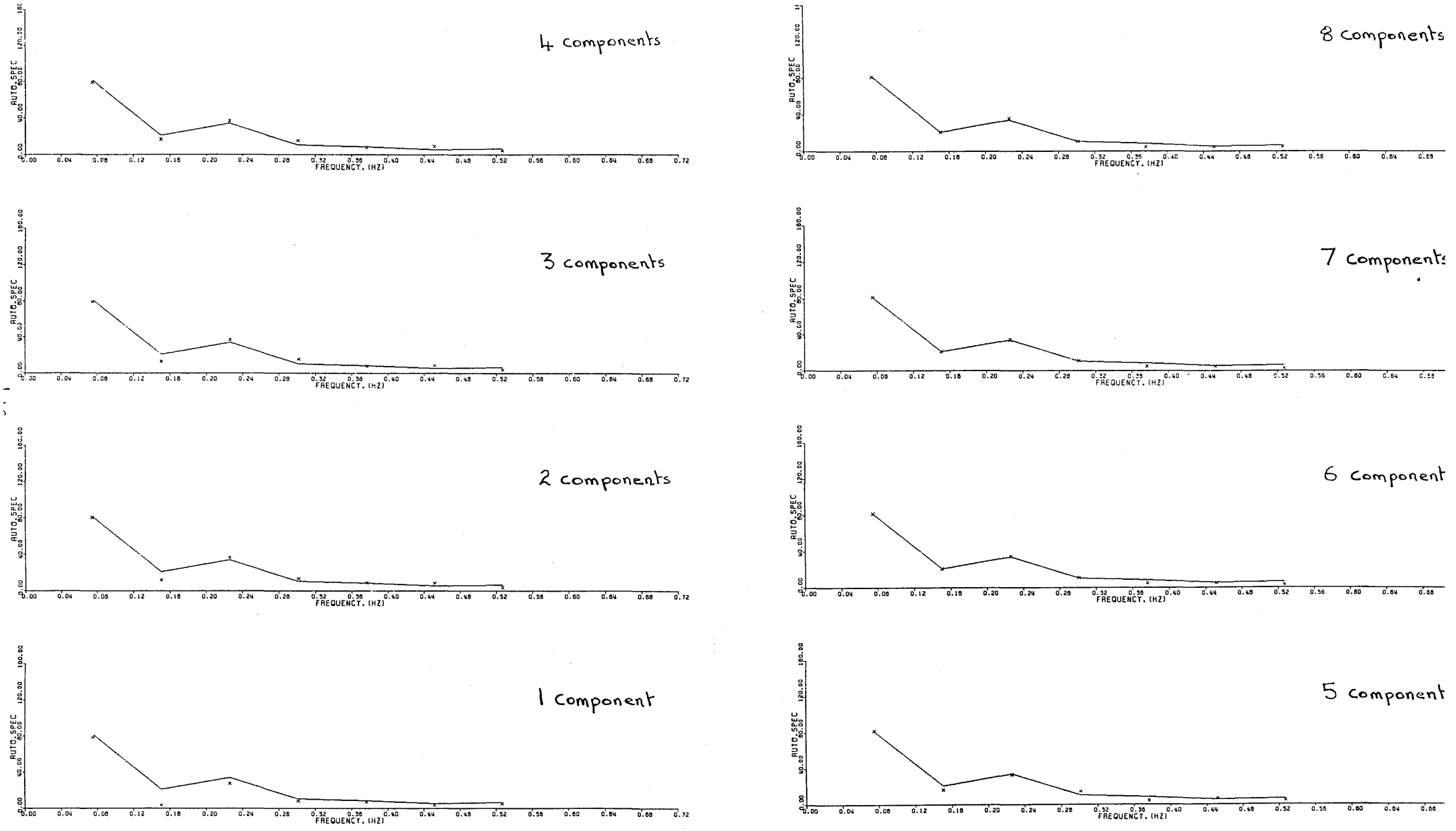

FIGURE 3-11 b) FREQUENCY-DOMAIN EQUATION-ERROR FITS
FOR DIFFERENT NOS. OF ORTHOGONAL COMPONENTS
(SINGULAR-VALUE DECOMPOSITION).
MODEL WITH TIME DELAY.

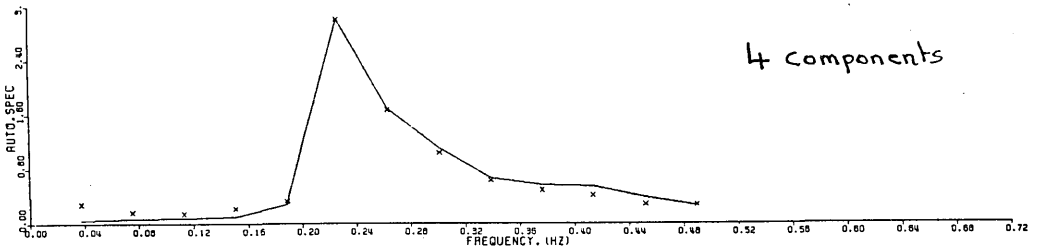

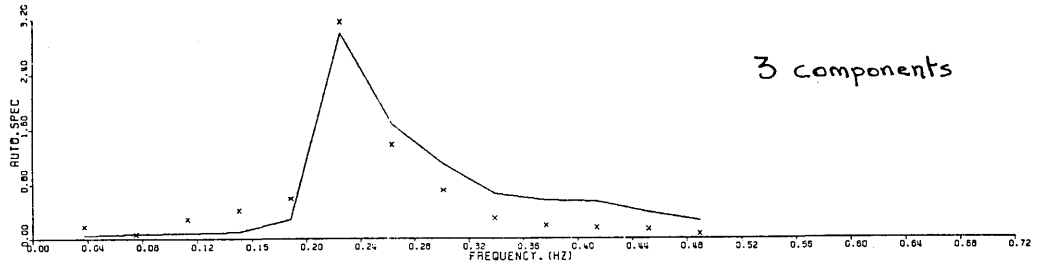

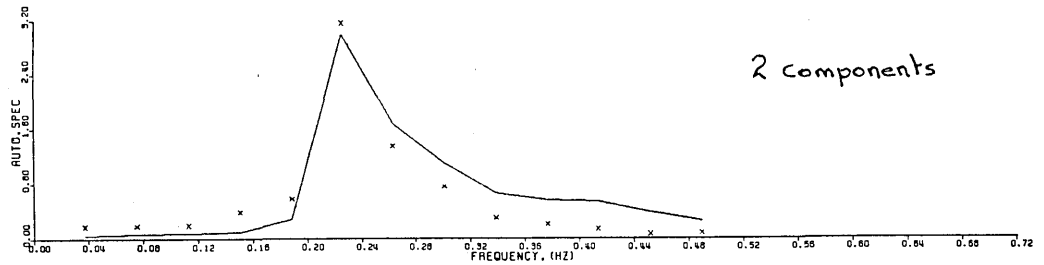

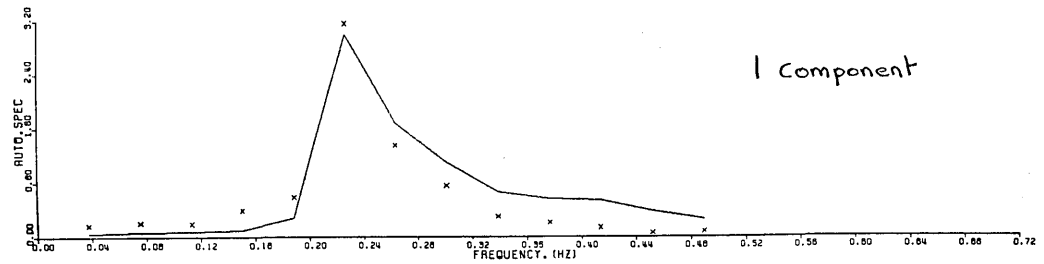

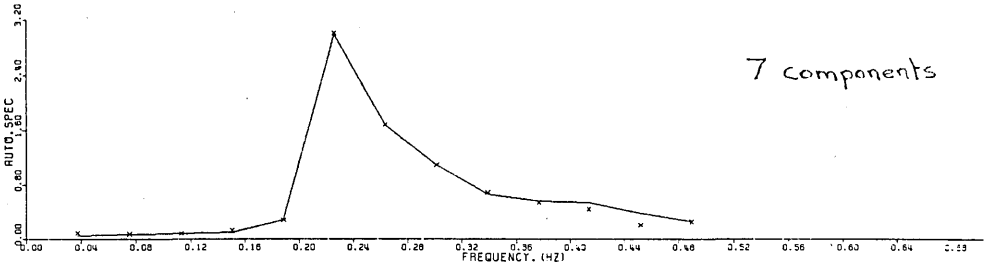

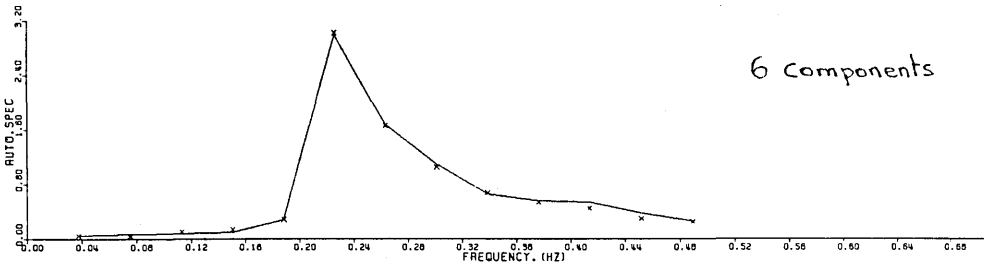

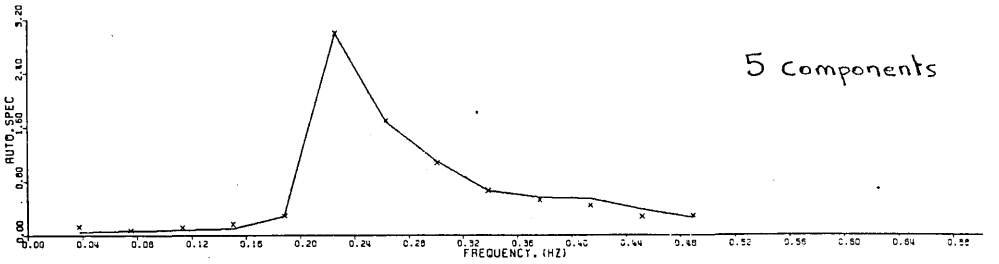

FIGURE 3-12 a) FREQUENCY-DOMAIN EQUATION-ERROR FITS
FOR DIFFERENT NOS. OF ORTHOGONAL COMPONENTS
(SINGULAR-VALUE DECOMPOSITION).
MODEL WITHOUT TIME DELAY.
YAWING-MOMENT EQUATION. RUN R0201A

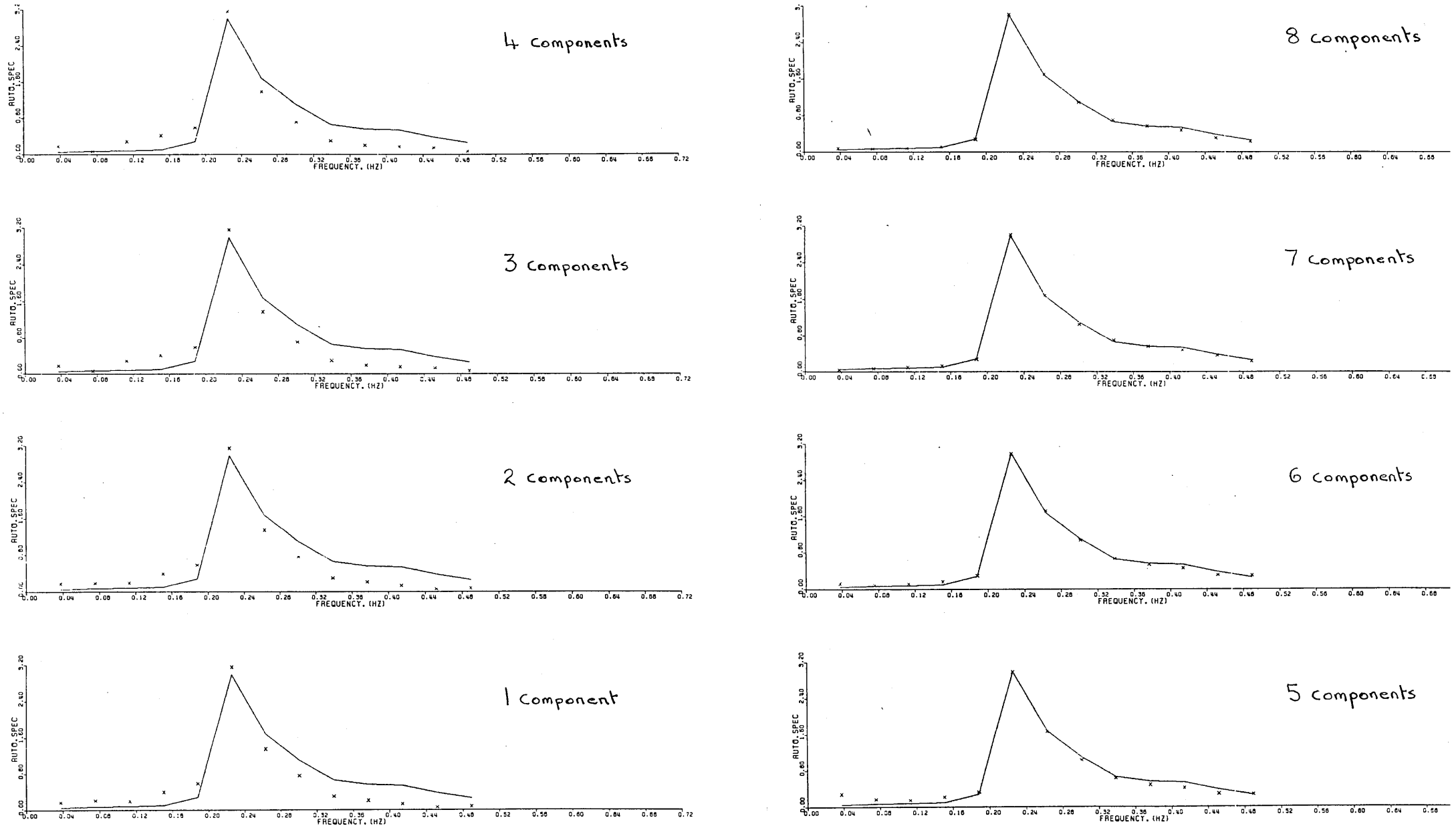

FIGURE 3-12 b) FREQUENCY-DOMAIN EQUATION-ERROR FITS
FOR DIFFERENT NOS. OF ORTHOGONAL COMPONENTS
(SINGULAR-VALUE DECOMPOSITION).
MODEL WITH TIME DELAY.
YAWING-MOMENT EQUATION. RUN R0201A

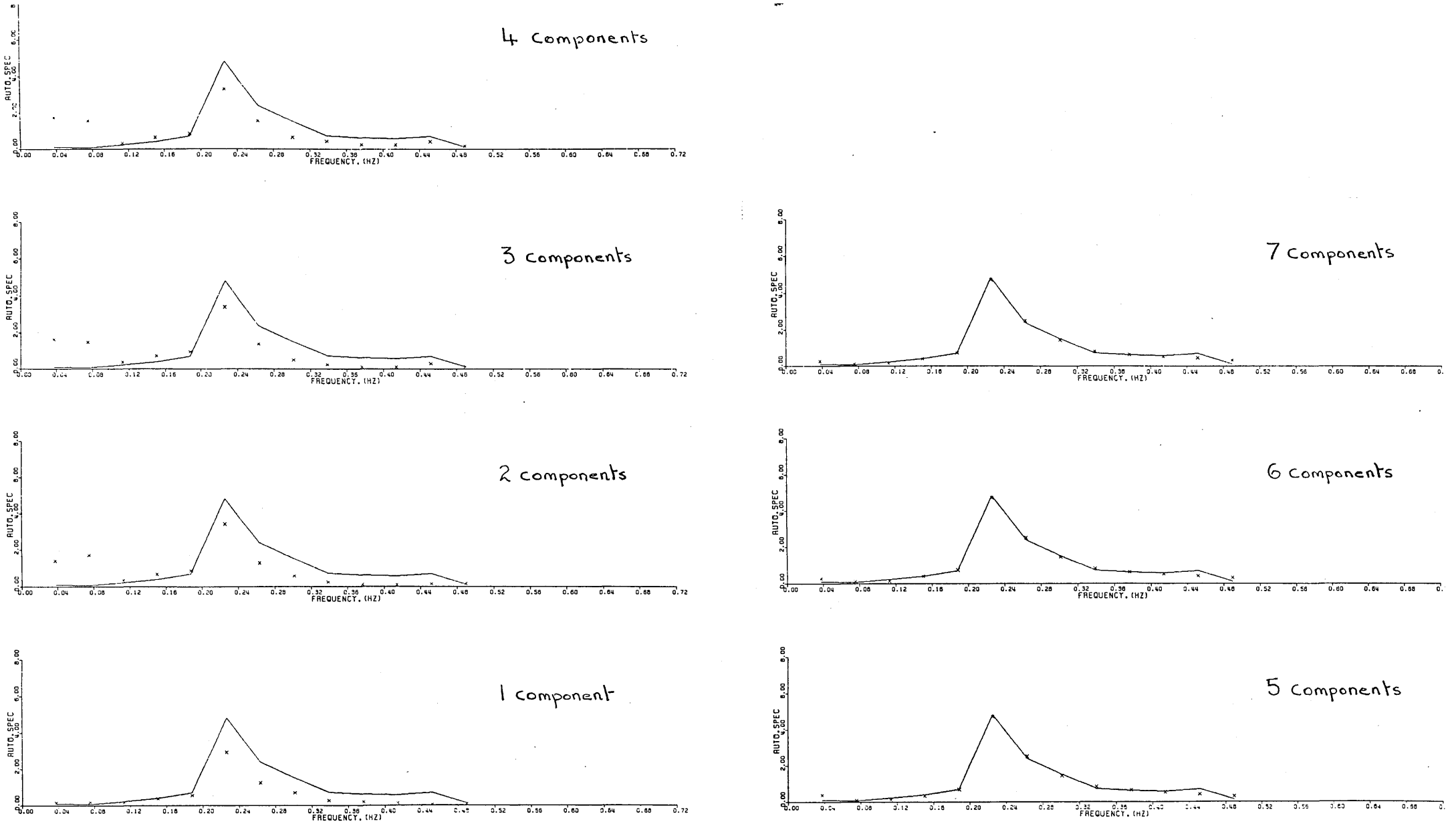

FIGURE 3-13 a) FREQUENCY-DOMAIN EQUATION-ERROR FITS
FOR DIFFERENT NOS. OF ORTHOGONAL COMPONENTS
(SINGULAR-VALUE DECOMPOSITION).
MODEL WITHOUT TIME DELAY.
ROLLING-MOMENT EQUATION. RUN R0201A

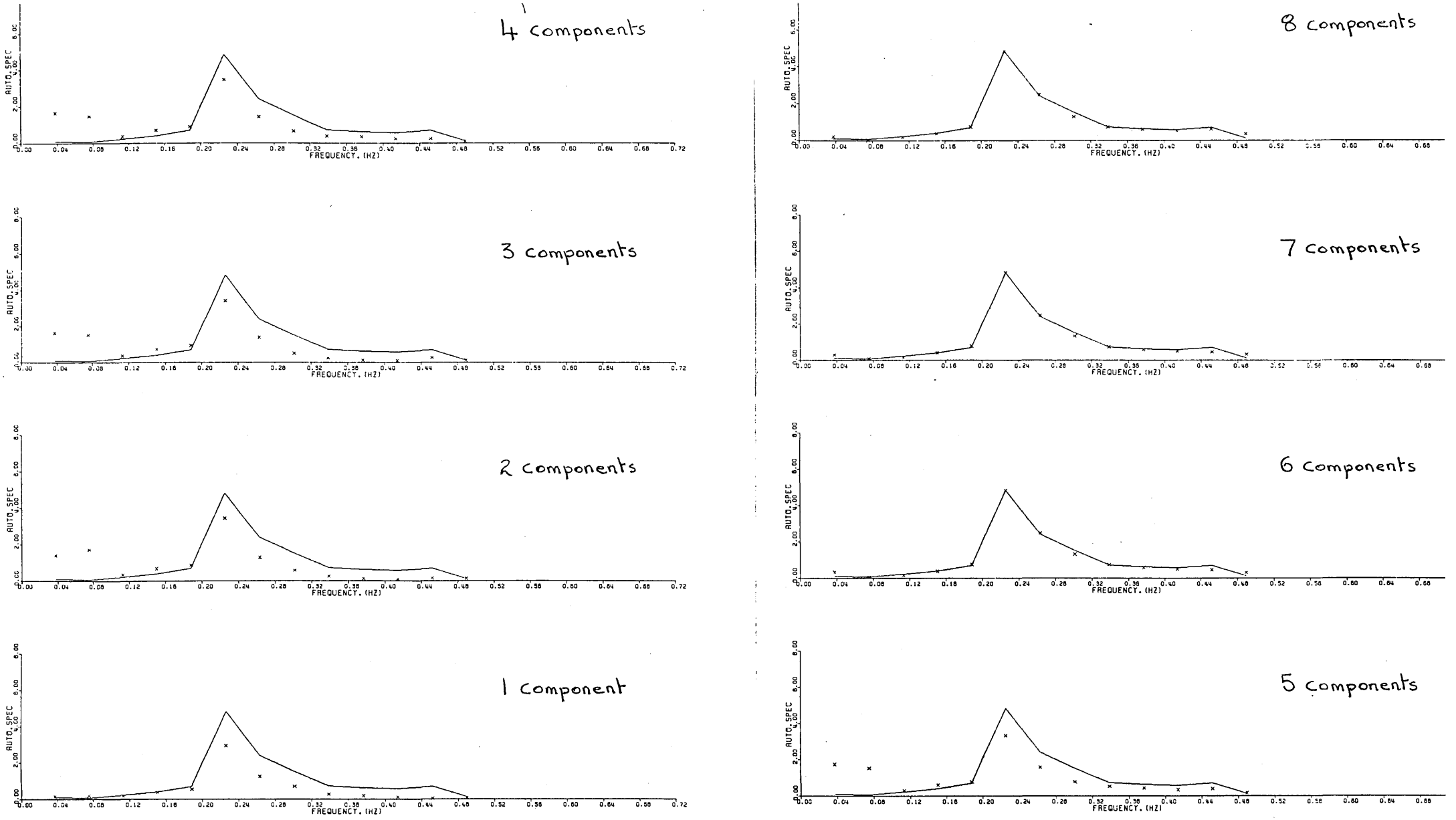

FIGURE 3-13 b) FREQUENCY-DOMAIN EQUATION-ERROR FITS
FOR DIFFERENT NOS. OF ORTHOGONAL COMPONENTS
(SINGULAR-VALUE DECOMPOSITION).
MODEL WITH TIME DELAY.
ROLLING-MOMENT EQUATION. RUN R0201A

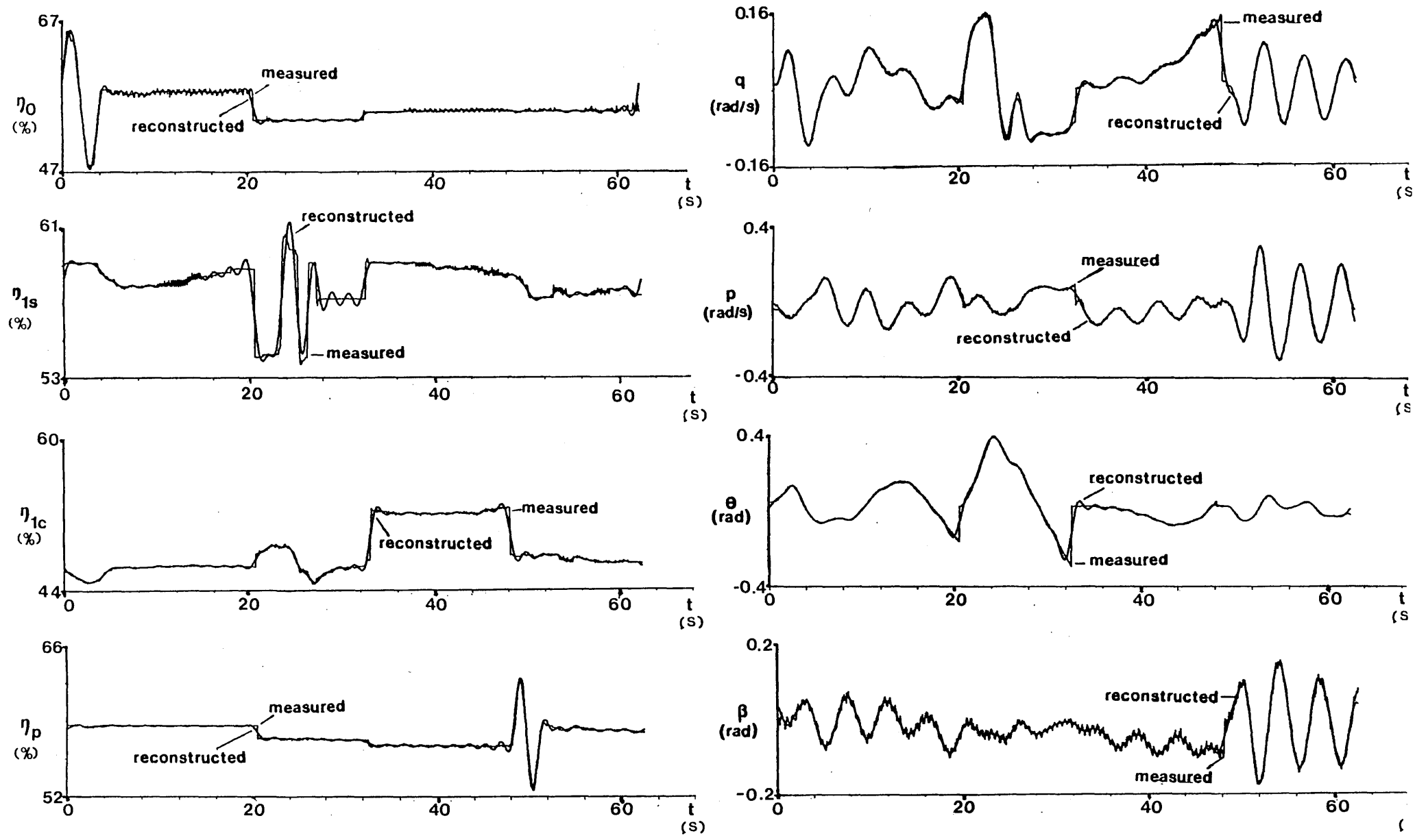

FIGURE 3-14 MULTIRUN TIME-DOMAIN RECORDS TOGETHER WITH LOW-FREQUENCY RECONSTRUCTIONS

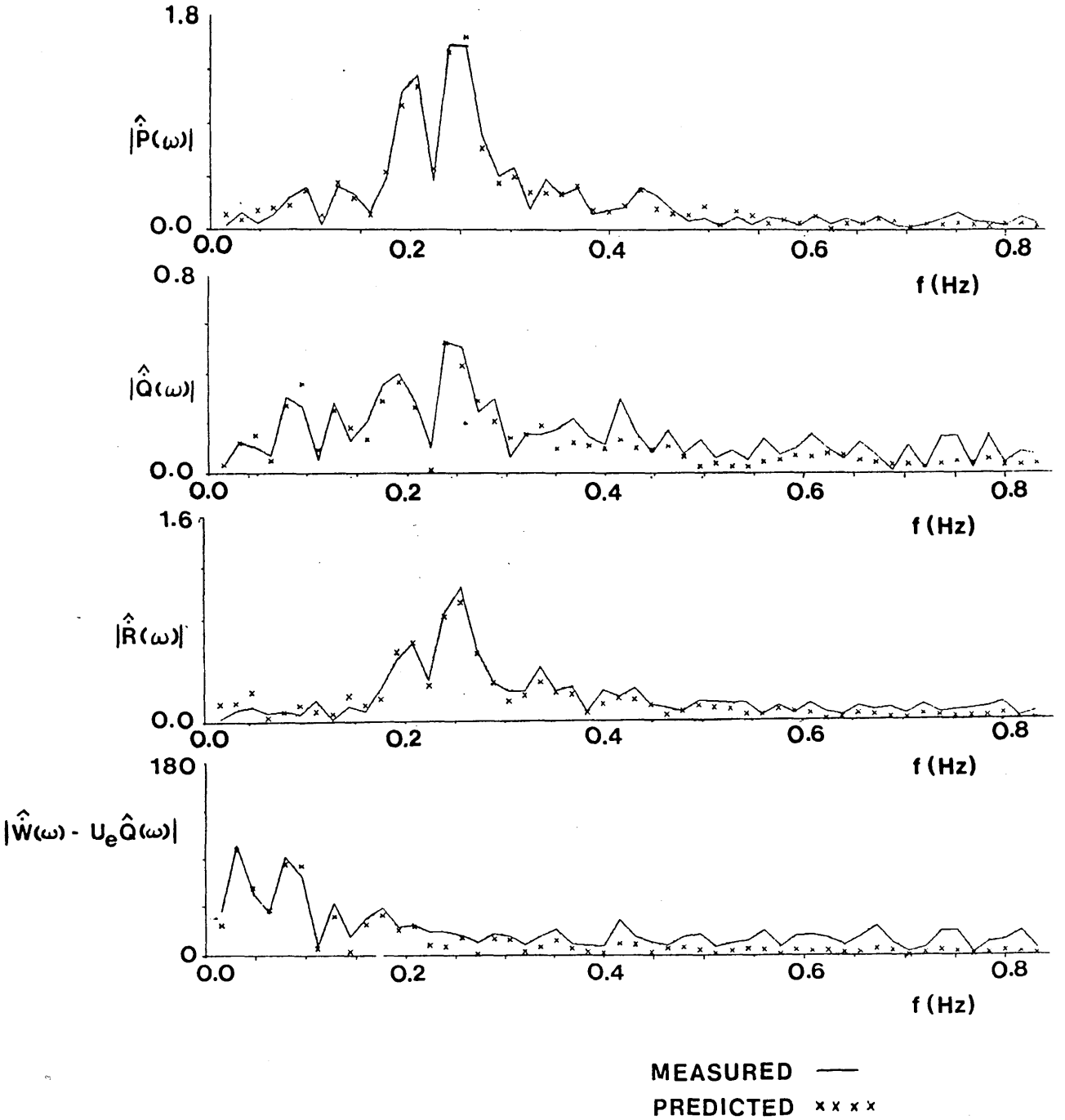

FIGURE 3-15 FREQUENCY-DOMAIN EQUATION-ERROR FITS
FOR MULTIRUN DATA SET

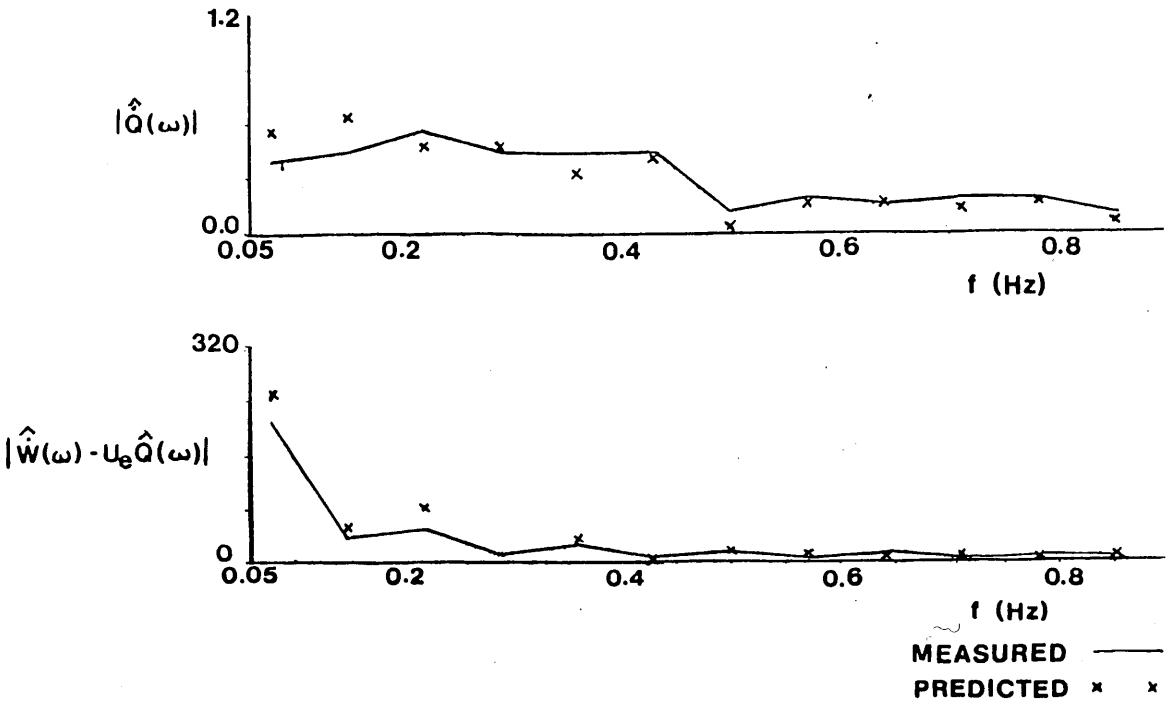

FIGURE 3-16 a) FREQUENCY-DOMAIN VERIFICATION.
MEASURED VALUES OBTAINED FROM RESPONSE TO LONGITUDINAL-CYCLIC 3211 INPUT. PREDICTED VALUES BASED ON MODEL IDENTIFIED FROM RESPONSE TO LONGITUDINAL-CYCLIC DOUBLET

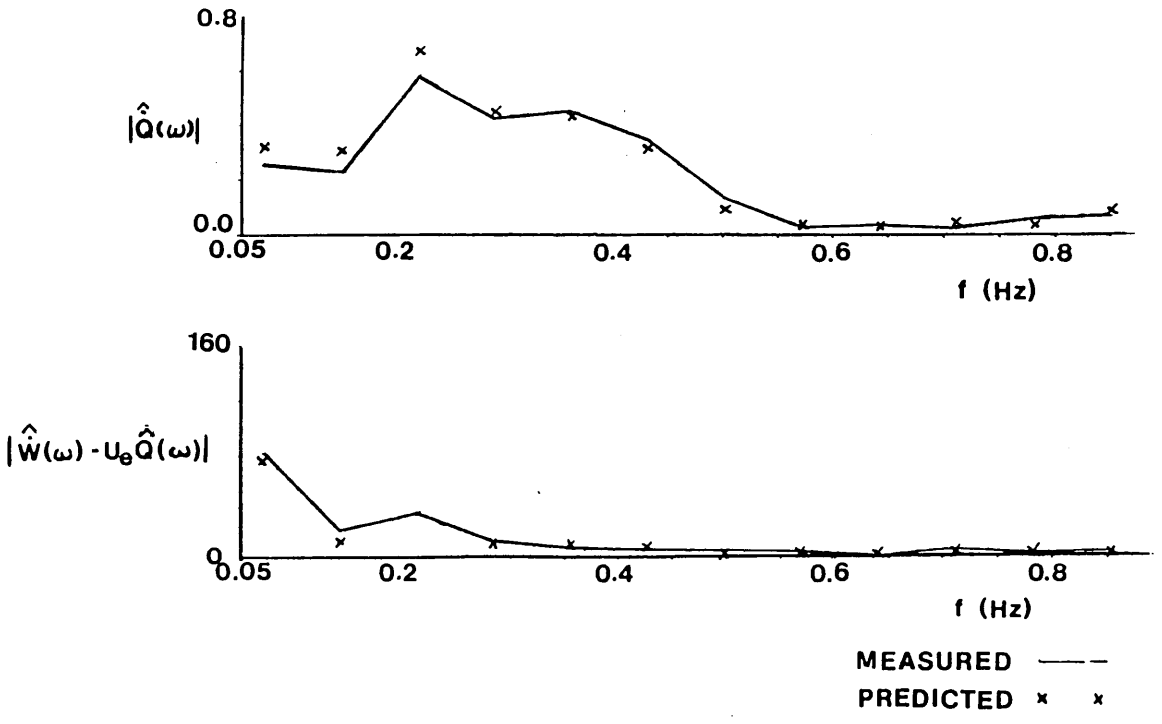

FIGURE 3-16 b) FREQUENCY-DOMAIN VERIFICATION.
MEASURED VALUES OBTAINED FROM RESPONSE TO LONGITUDINAL-CYCLIC DOUBLET. PREDICTED VALUES BASED ON MODEL IDENTIFIED FROM MULTIRUN DATA

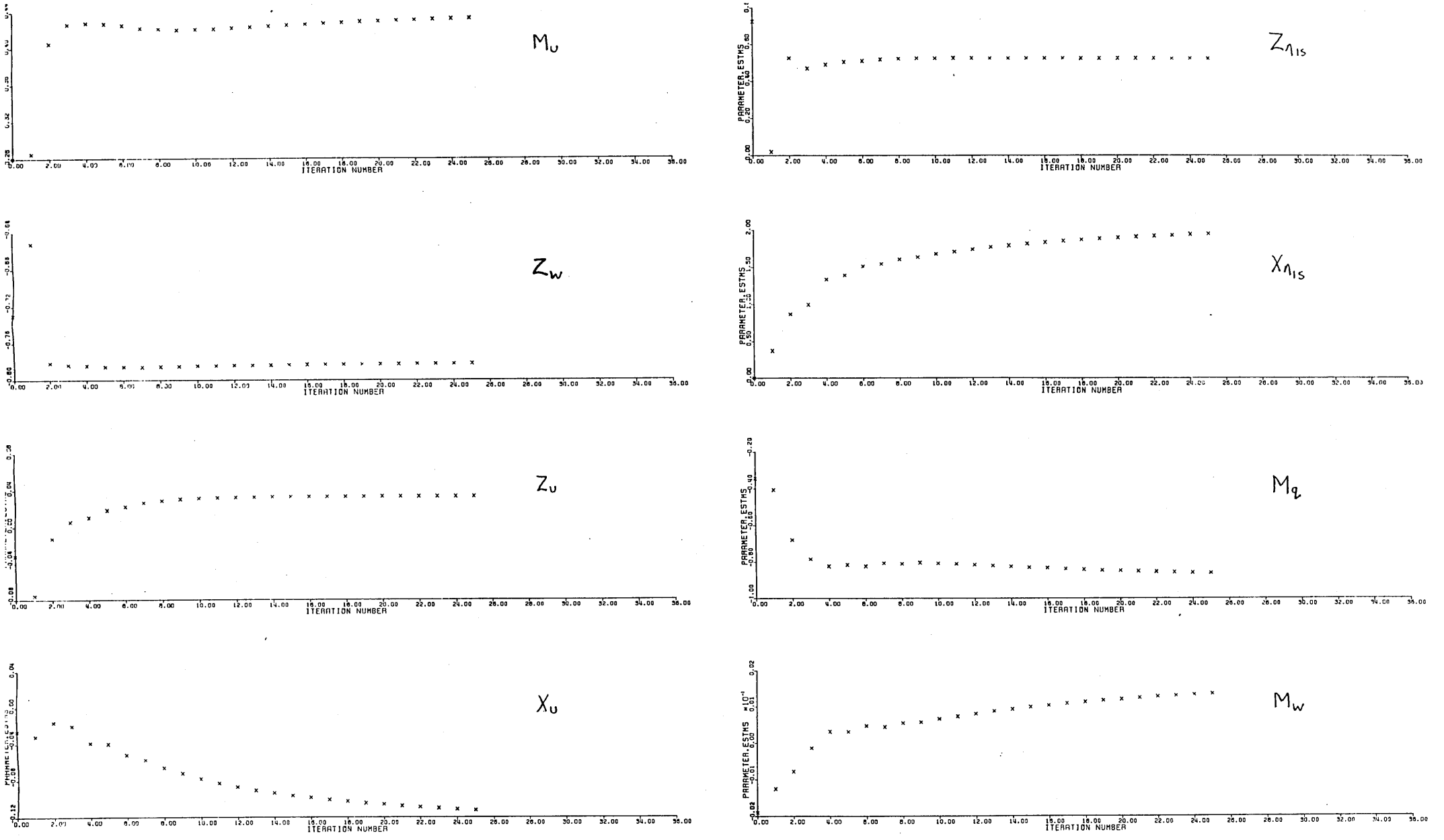

FIGURE 4-1 PARAMETER ESTIMATES AND COST-FUNCTION VALUE AS A FUNCTION OF ITERATION NUMBER. RUN R0201A

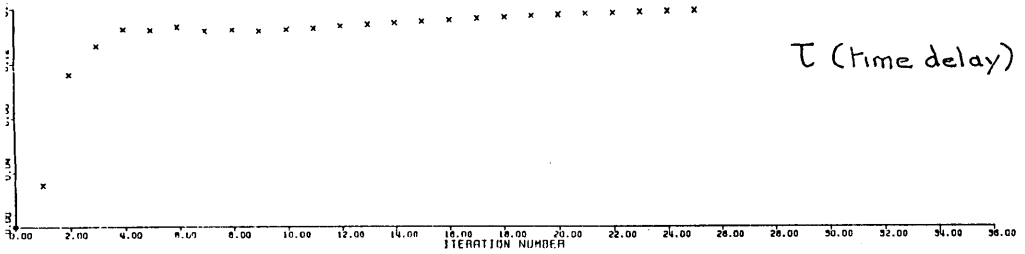

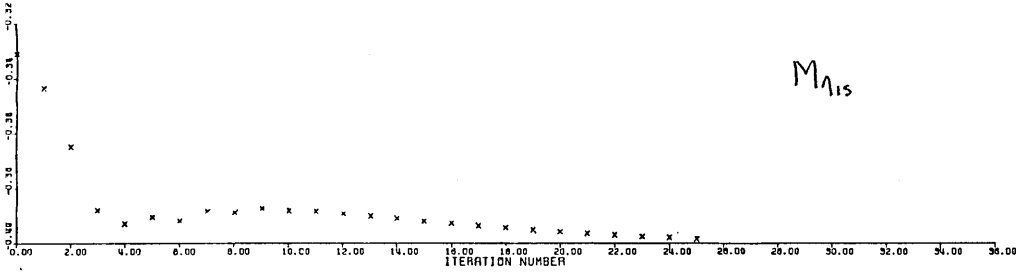

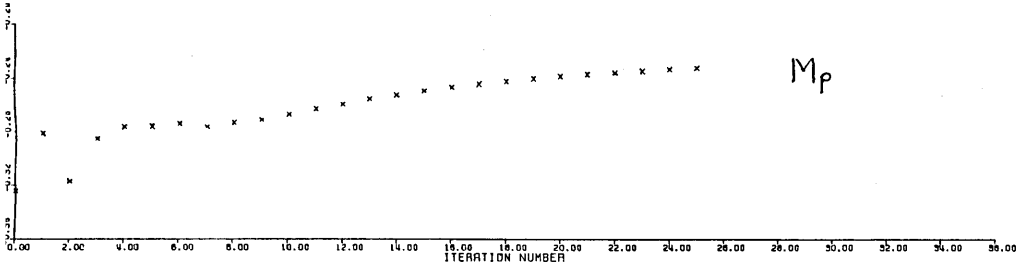

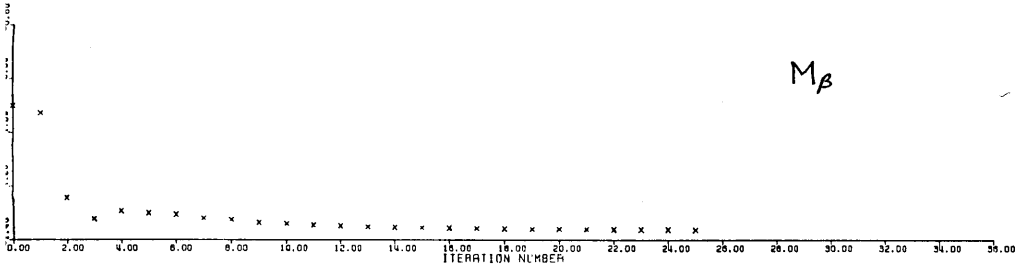

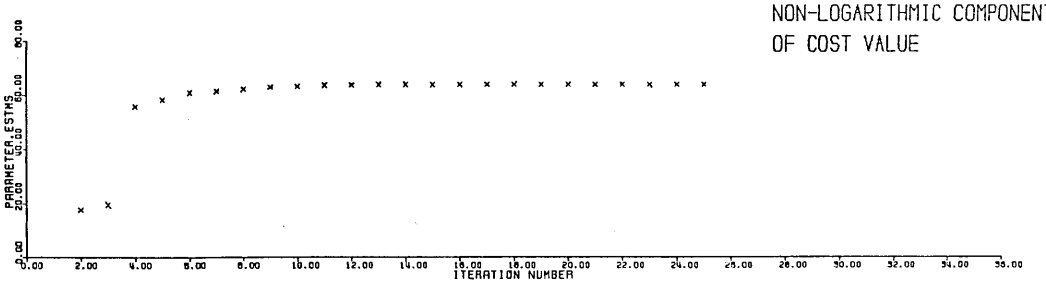

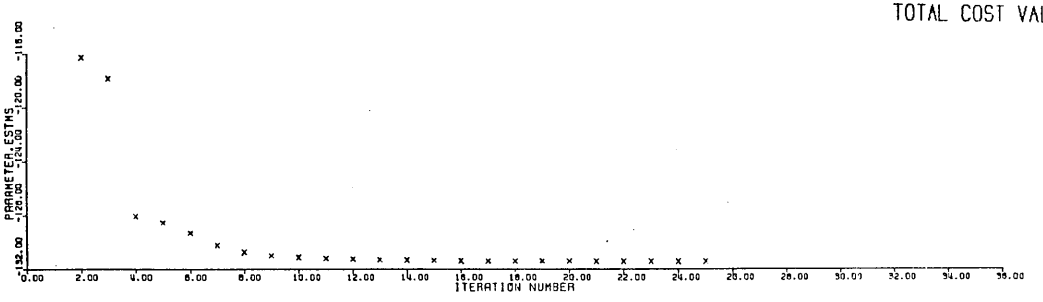

FIGURE 4-1 CONTD.

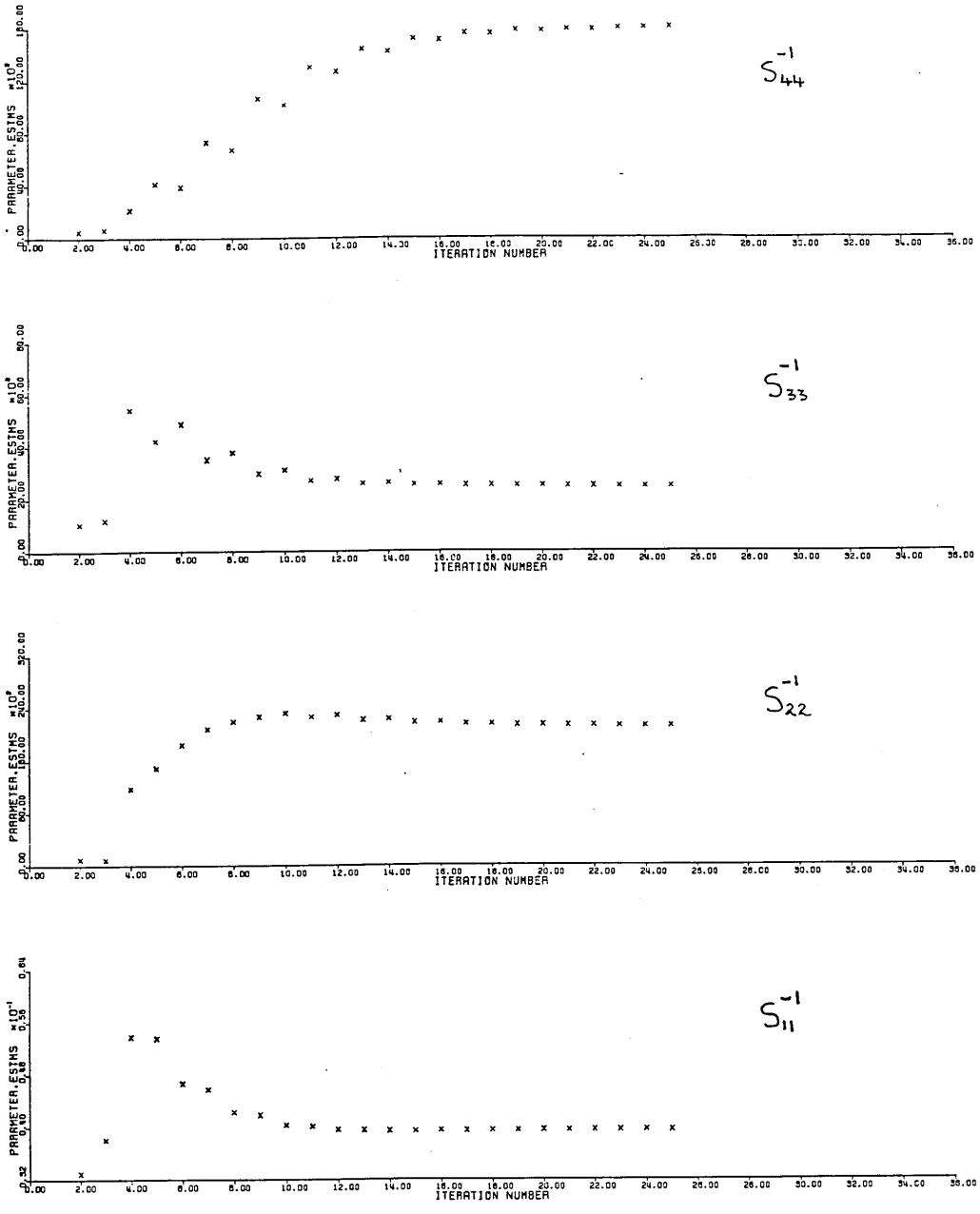

FIGURE 4-2 ESTIMATES OF THE DIAGONAL ELEMENTS OF INVERSE OF ERROR-COVARIANCE MATRIX AS A FUNCTION OF ITERATION NUMBER. RUN R0201A

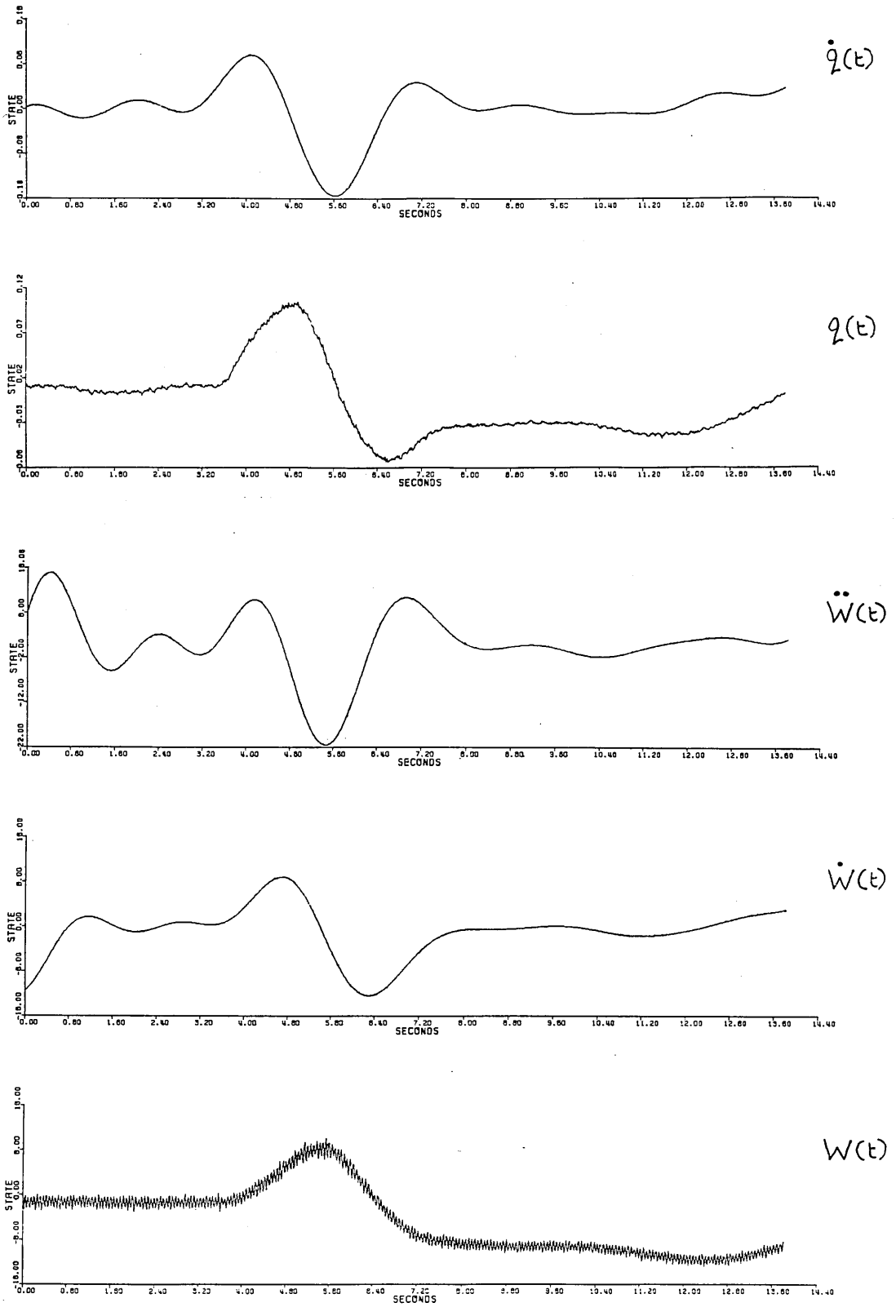

FIGURE 4-3 MEASURED SIGNALS FOR TRANSFER-FUNCTION EXAMPLE.
RUN R0201A

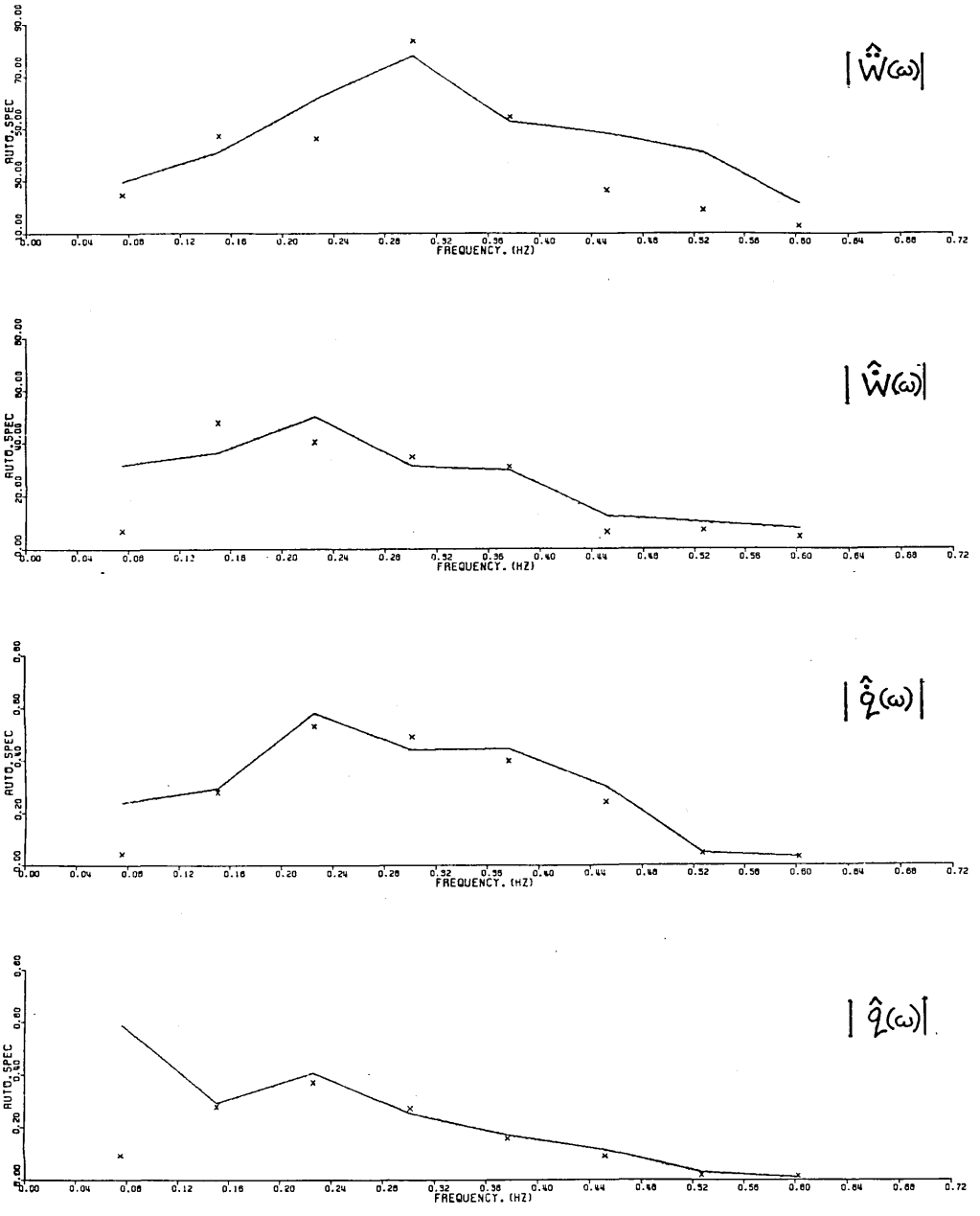

FIGURE 4-4 FREQUENCY-DOMAIN OUTPUT-ERROR FITS.
TRANSFER FUNCTION EXAMPLES. RUN R0201A

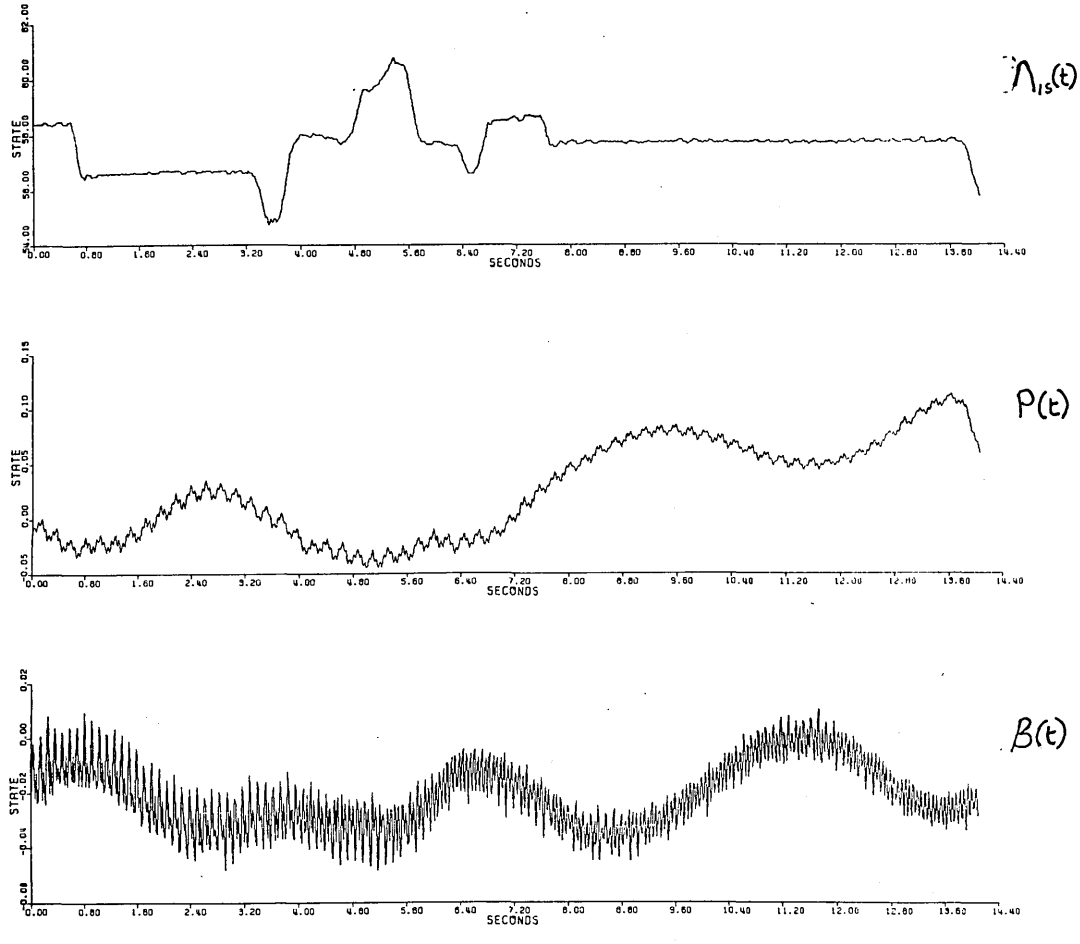

FIGURE 4-5 TIME HISTORIES OF THE LONGITUDINAL-CYLIC CONTROL
AND LATERAL PSEUDO CONTROL TERMS.
COMBINED DATA RUN: R0201A, R0501A

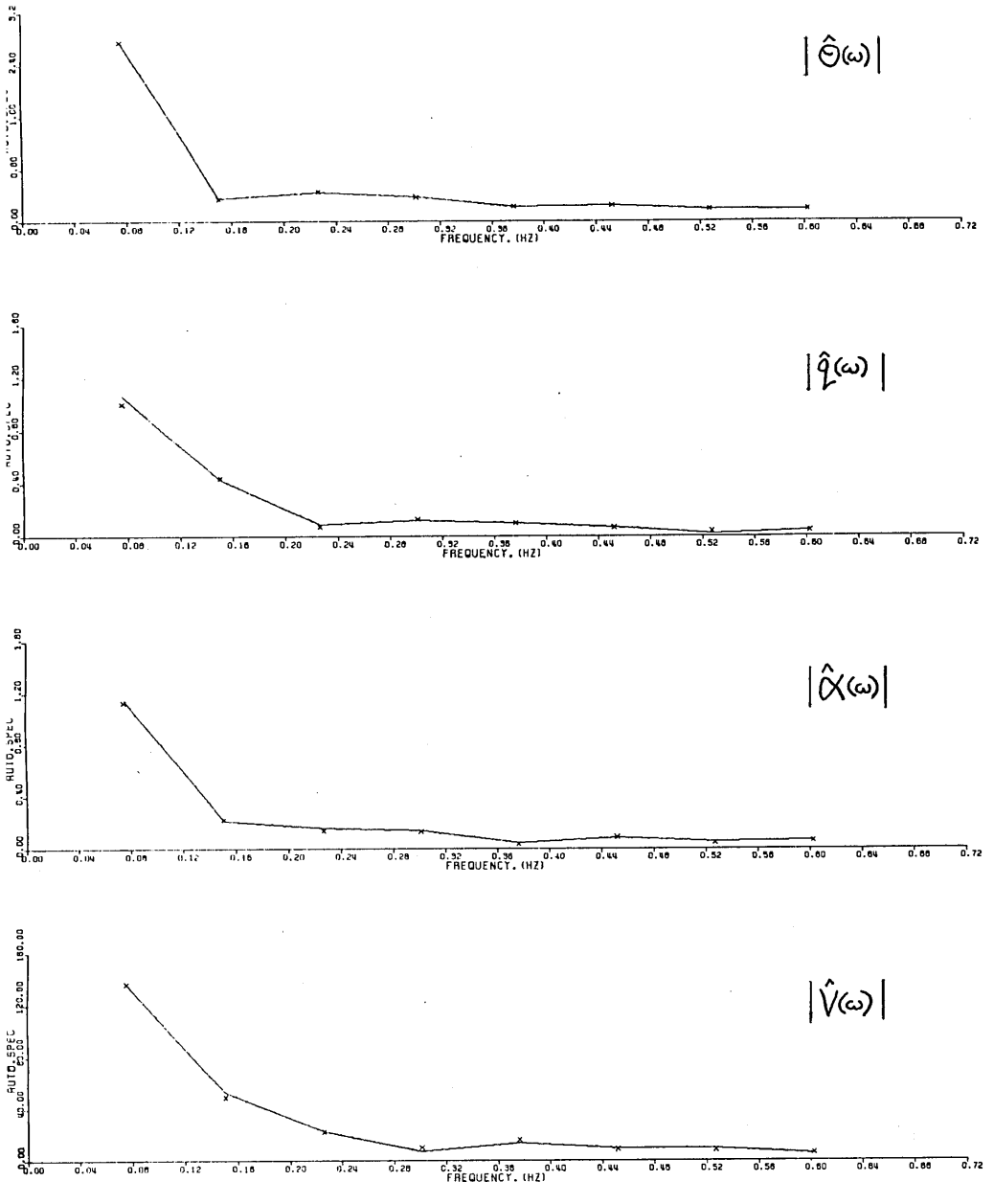

FIGURE 4-6 FREQUENCY-DOMAIN OUTPUT-ERROR FITS.
COMBINED DATA RUN: R0201A, R0501A

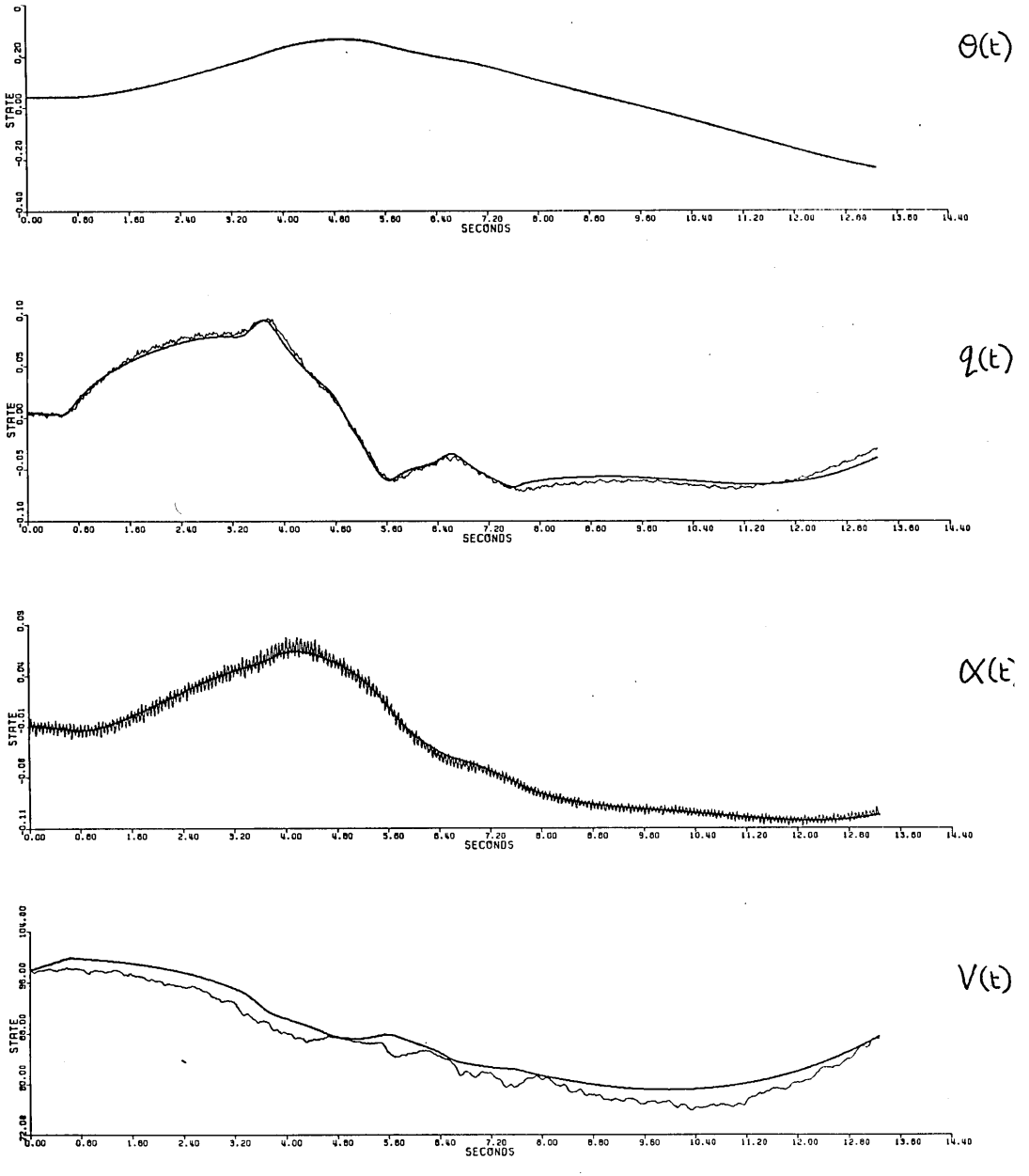

FIGURE 4-7 TIME-DOMAIN FITS.
COMBINED DATA RUN: R0201A, R0501A

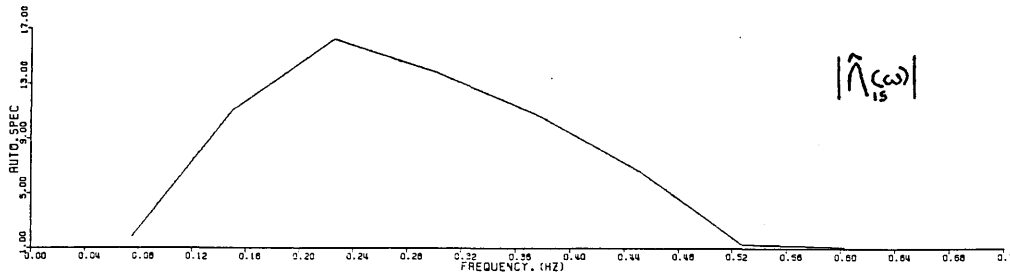

FIGURE 4-8 a) MAGNITUDE OF FFT's FOR DOUBLET INPUT

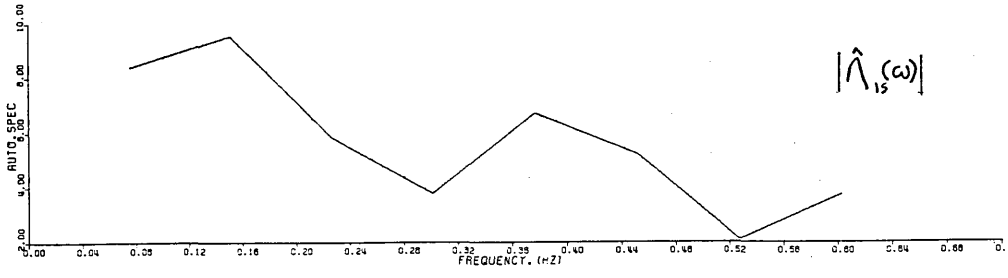

FIGURE 4-8 b) MAGNITUDE OF FFT's FOR THE EFFECTIVE INPUT. COMBINED DATA RUN (R0201A,R0501A)

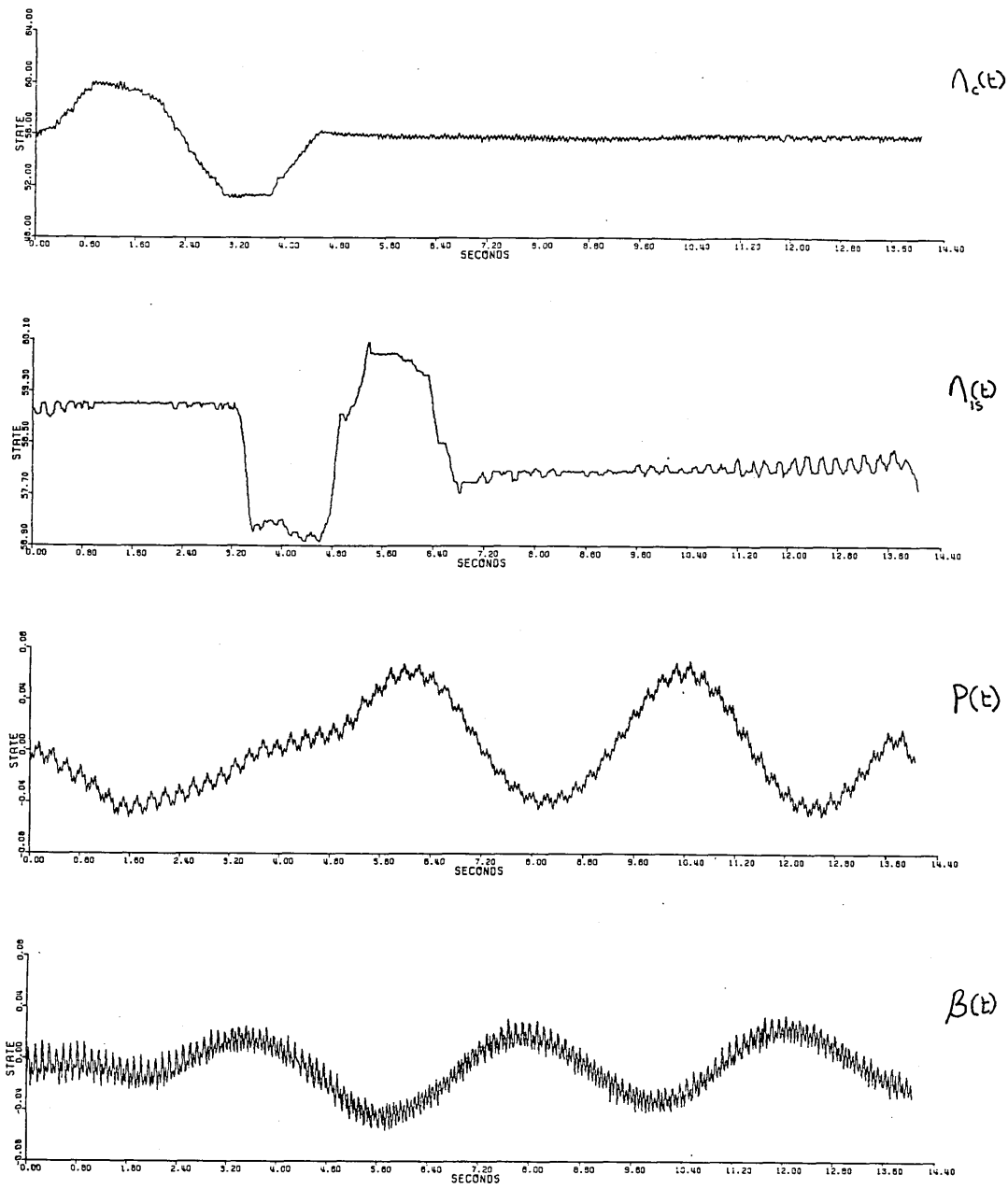

FIGURE 4-9 TIME HISTORIES OF CONTROLS AND LATERAL PSEUDO CONTROLS. MULTIRUN EXAMPLE: R0201A, R1501U

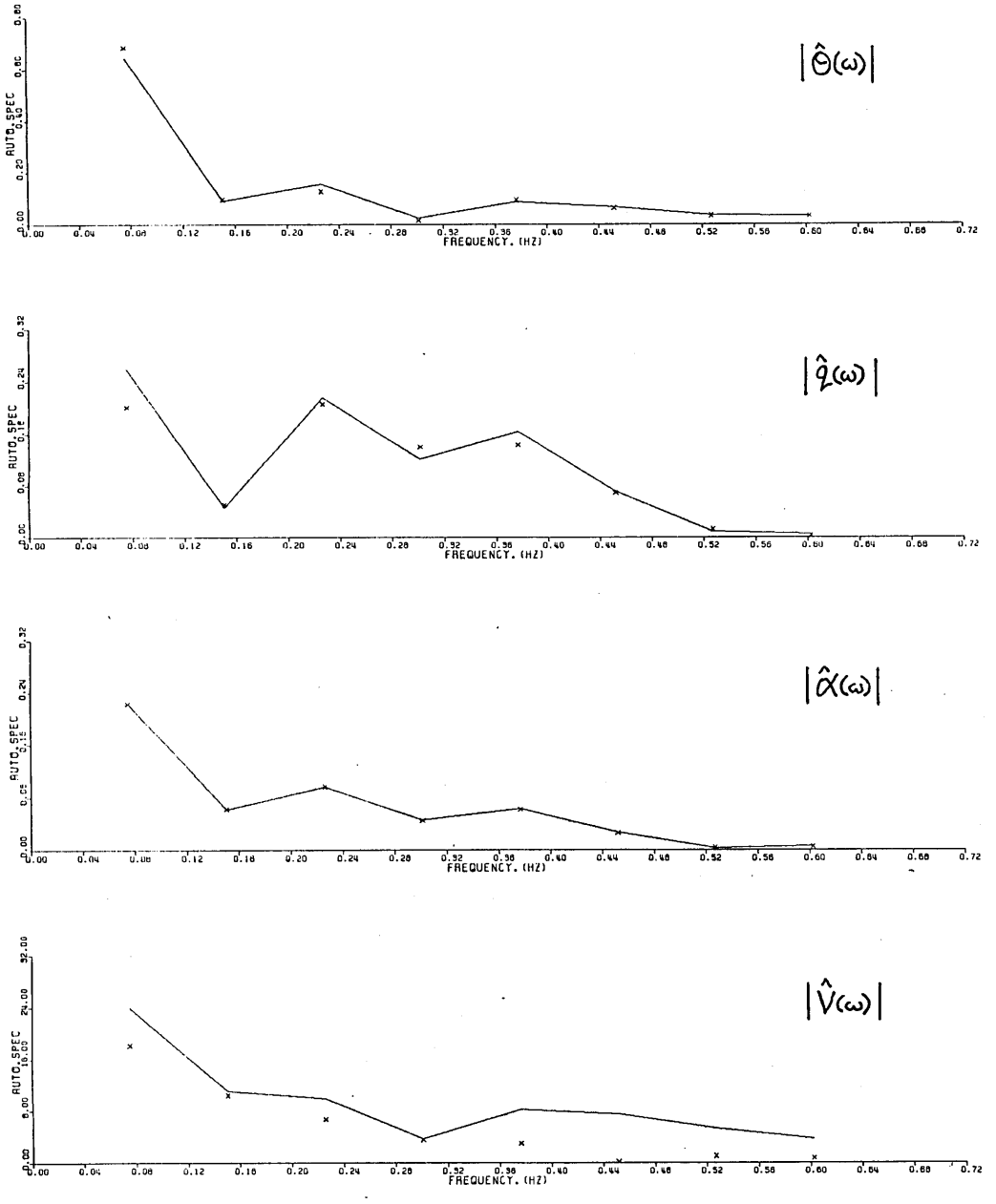

FIGURE 4-10 FREQUENCY-DOMAIN OUTPUT-ERROR FITS (RANK 13).
MULTIRUN EXAMPLE: R0201A, R1501U

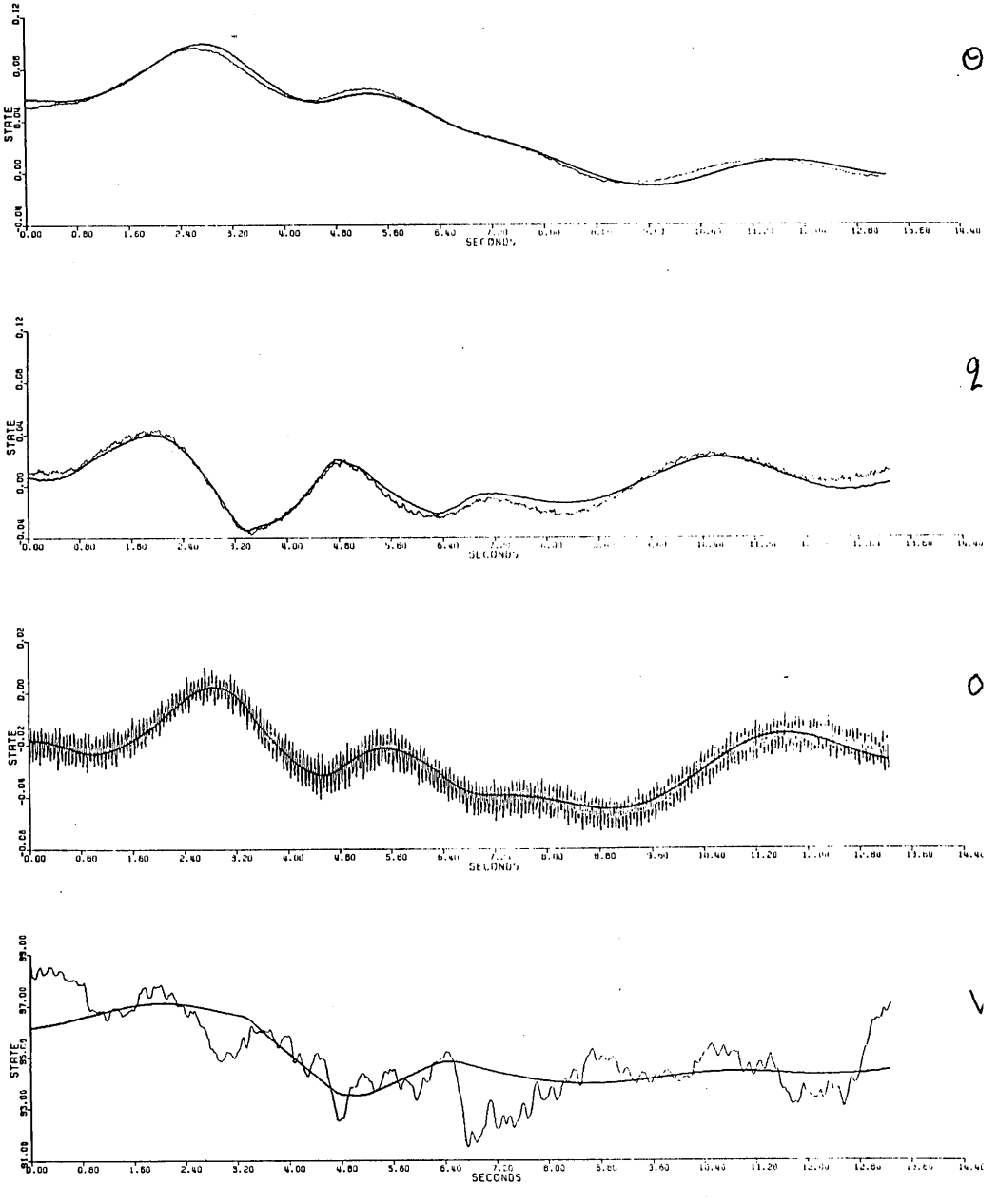

FIGURE 4-11 TIME-DOMAIN FITS (FOR RANK 13 ESTIMATES).
MULTIRUN EXAMPLE: R0201A, R1501U

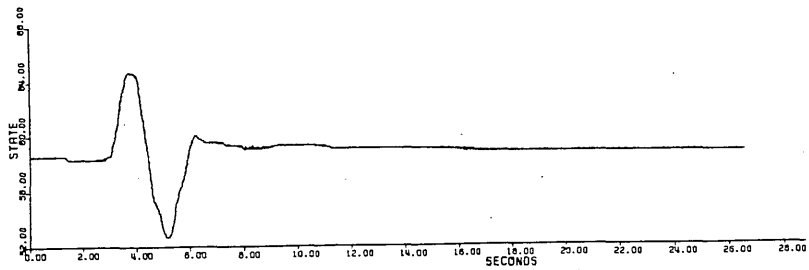

FIGURE 4-12 PEDAL DOUBLET INPUT. PUMA, 100 KNOTS, RUN R1201L.

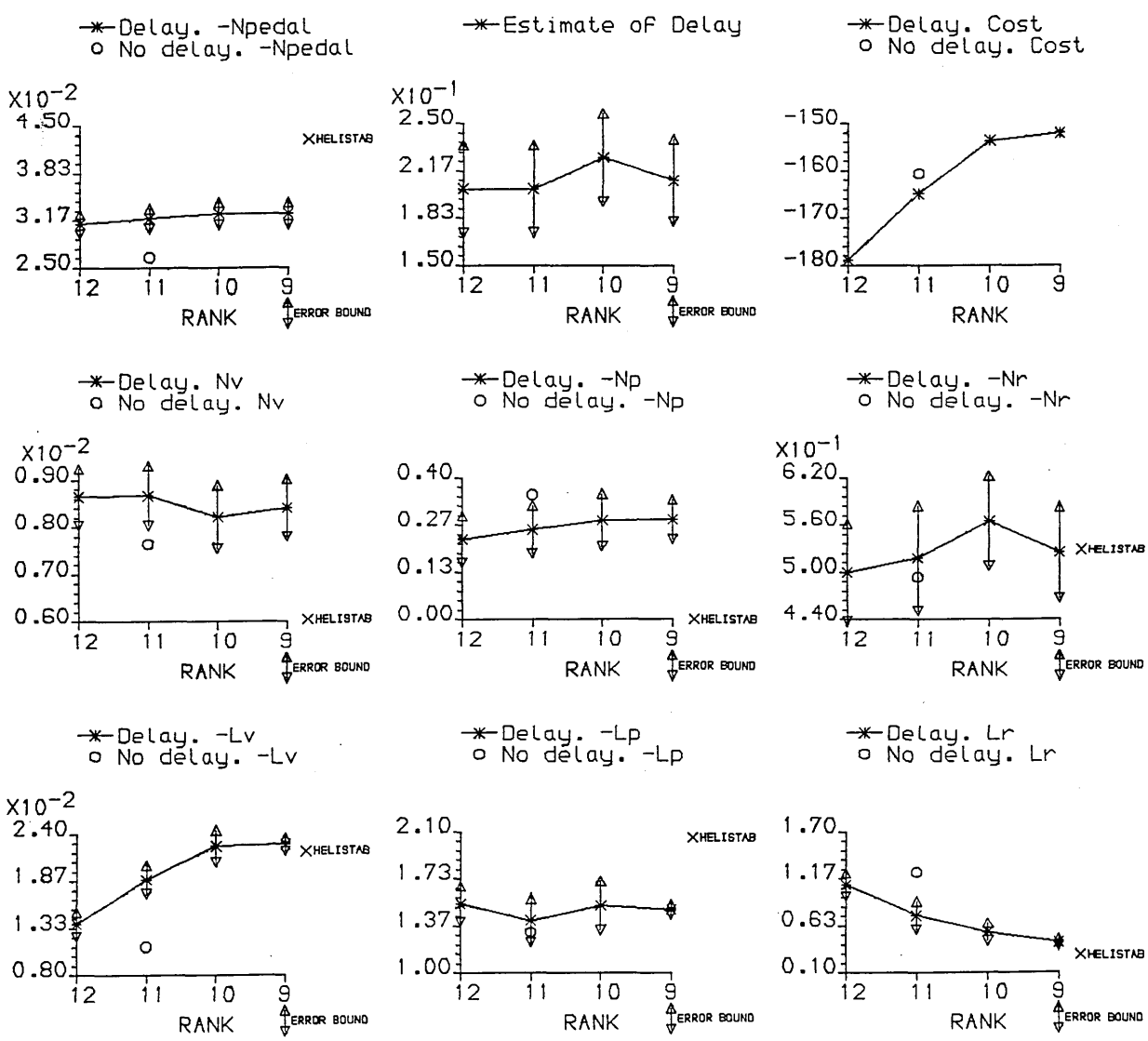

FIGURE 4-13 ESTIMATE VERSUS RANK OF INFORMATION MATRIX USED.
PUMA, 100 KNOTS, RUN R1201L

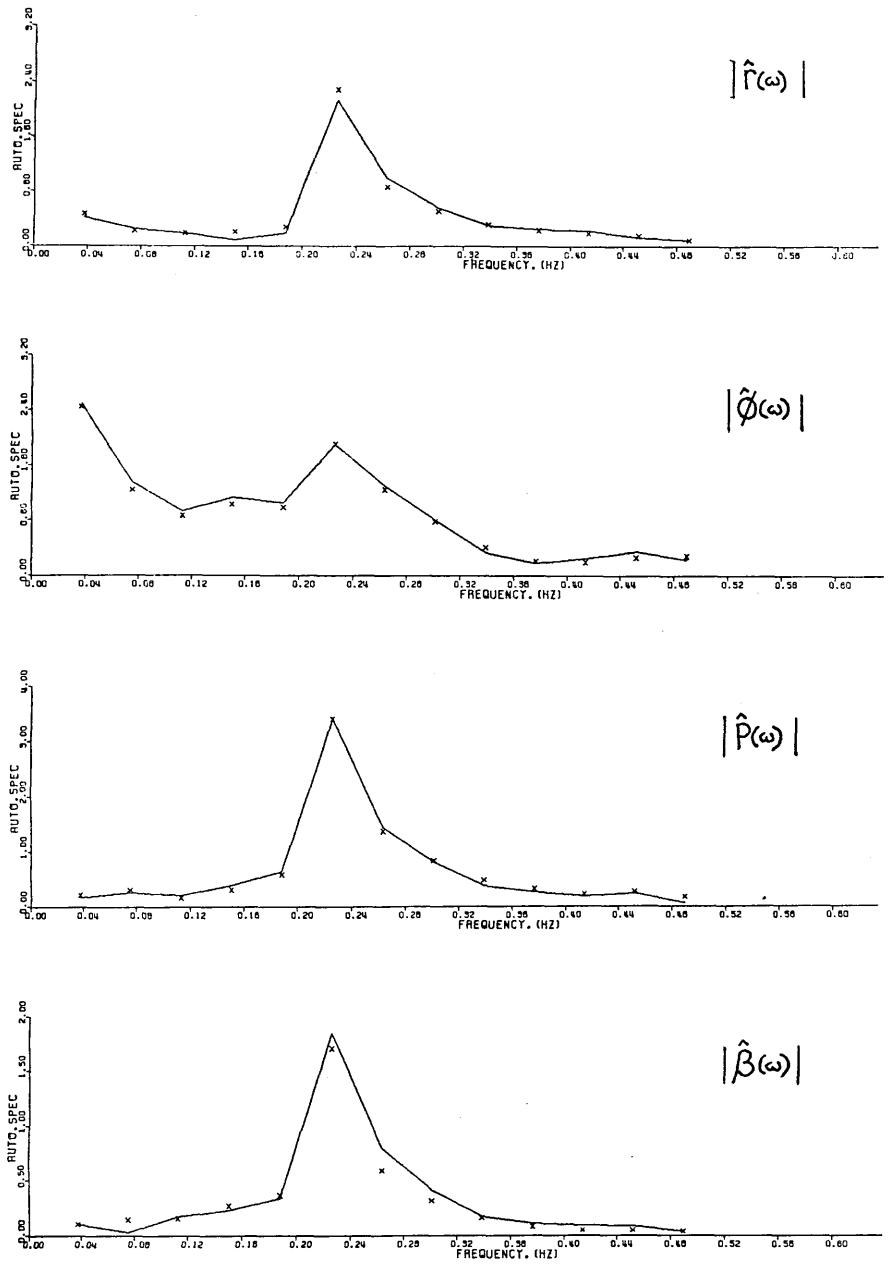

FIGURE 4-14 OUTPUT-ERROR FREQUENCY-DOMAIN FITS.
NO DELAY IN ESTIMATION MODEL.
PUMA, 100 KNOTS, RUN R1201L

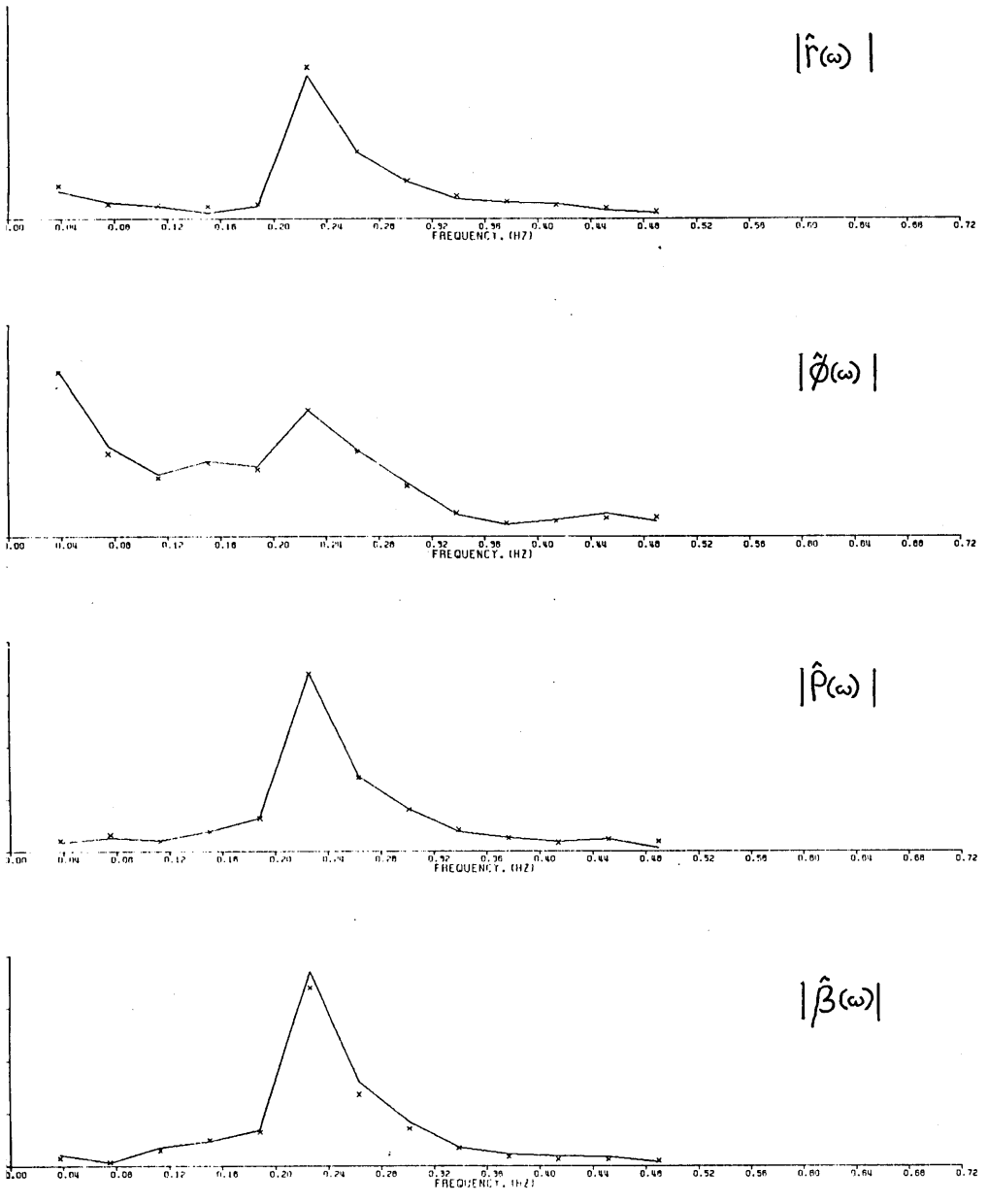

FIGURE 4-15 OUTPUT-ERROR FREQUENCY-DOMAIN FITS.
DELAY IN ESTIMATION MODEL.
PUMA, 100 KNOTS, RUN R1201L

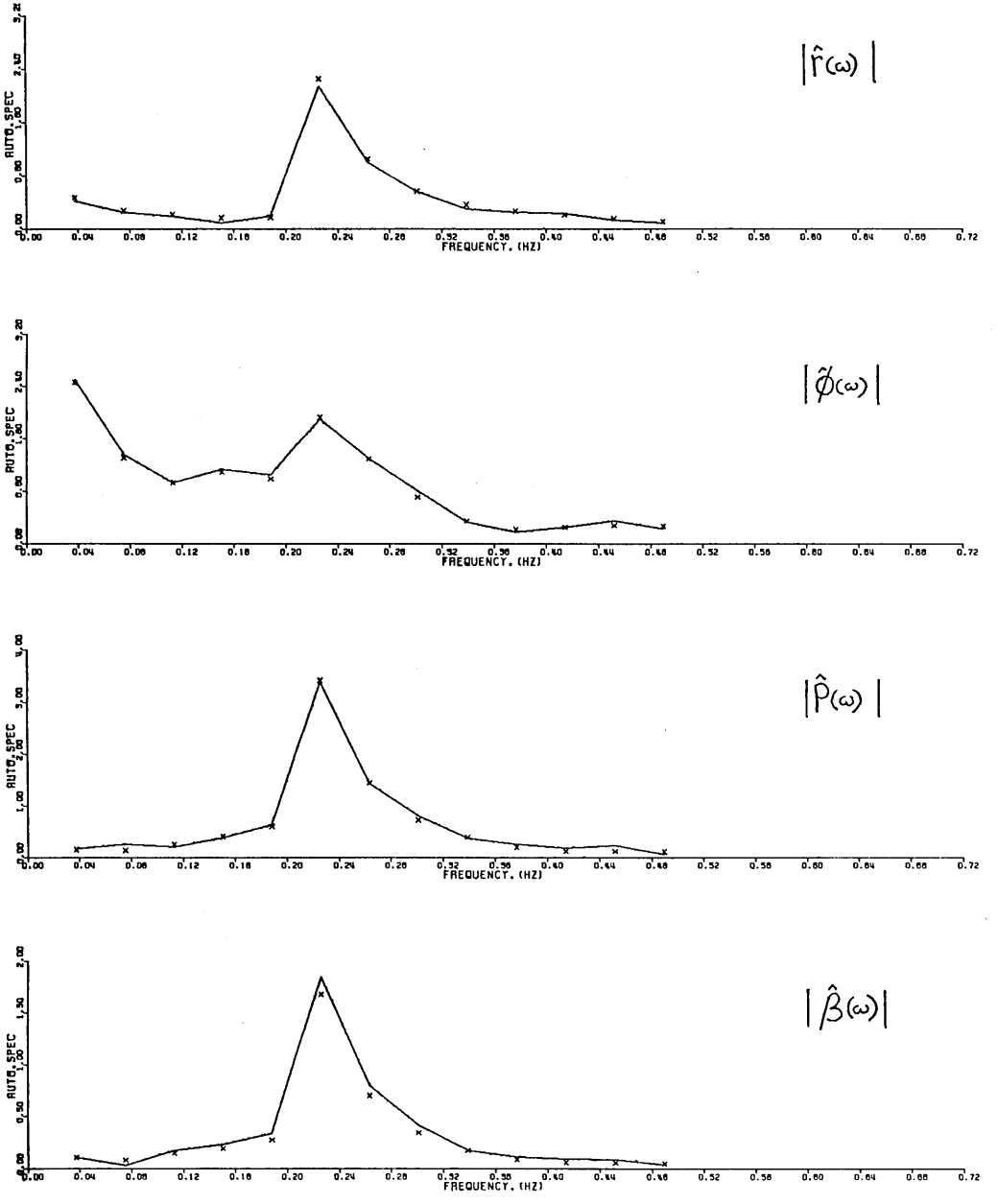

FIGURE 4-16 OUTPUT-ERROR FREQUENCY-DOMAIN FITS.
DELAY IN ESTIMATION MODEL, RANK-9 SOLUTION.
PUMA, 100 KNOTS, RUN R1201L

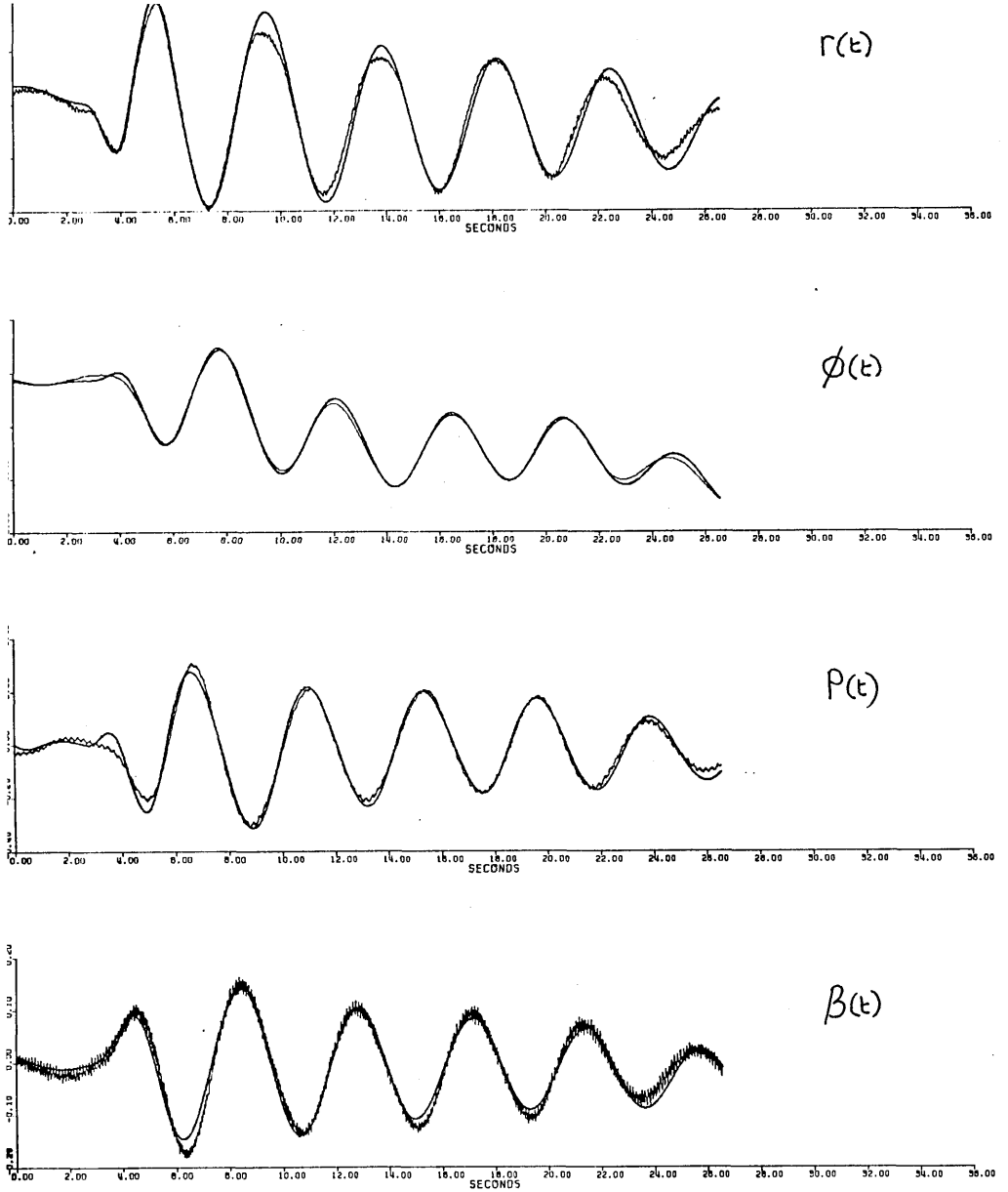

FIGURE 4-17 TIME-DOMAIN VERIFICATION.
NO DELAY IN ESTIMATION MODEL.
PUMA, 100 KNOTS, RUN R1201L

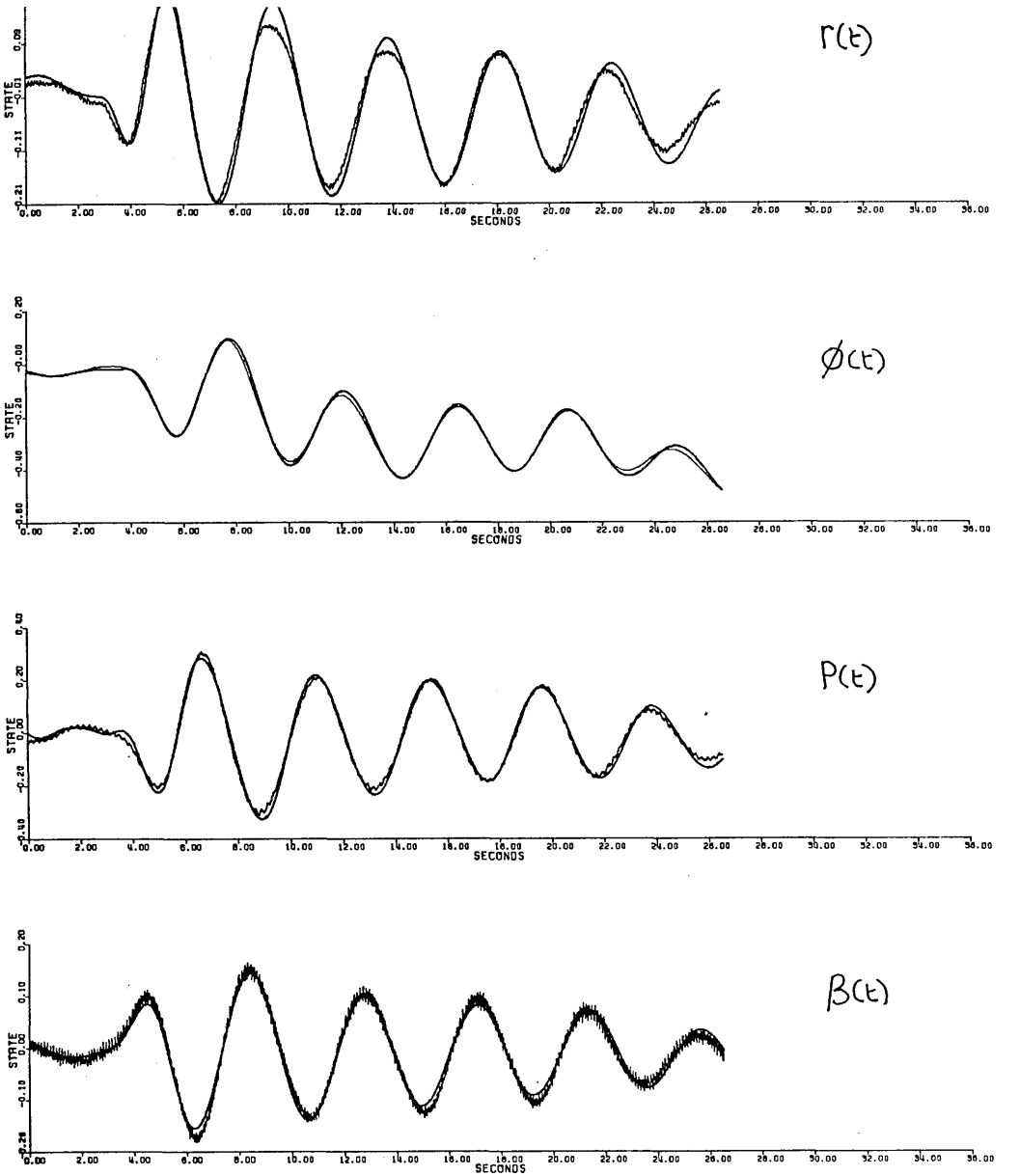

FIGURE 4-18 TIME-DOMAIN VERIFICATION.
DELAY IN ESTIMATION MODEL.
PUMA, 100 KNOTS, RUN R1201L

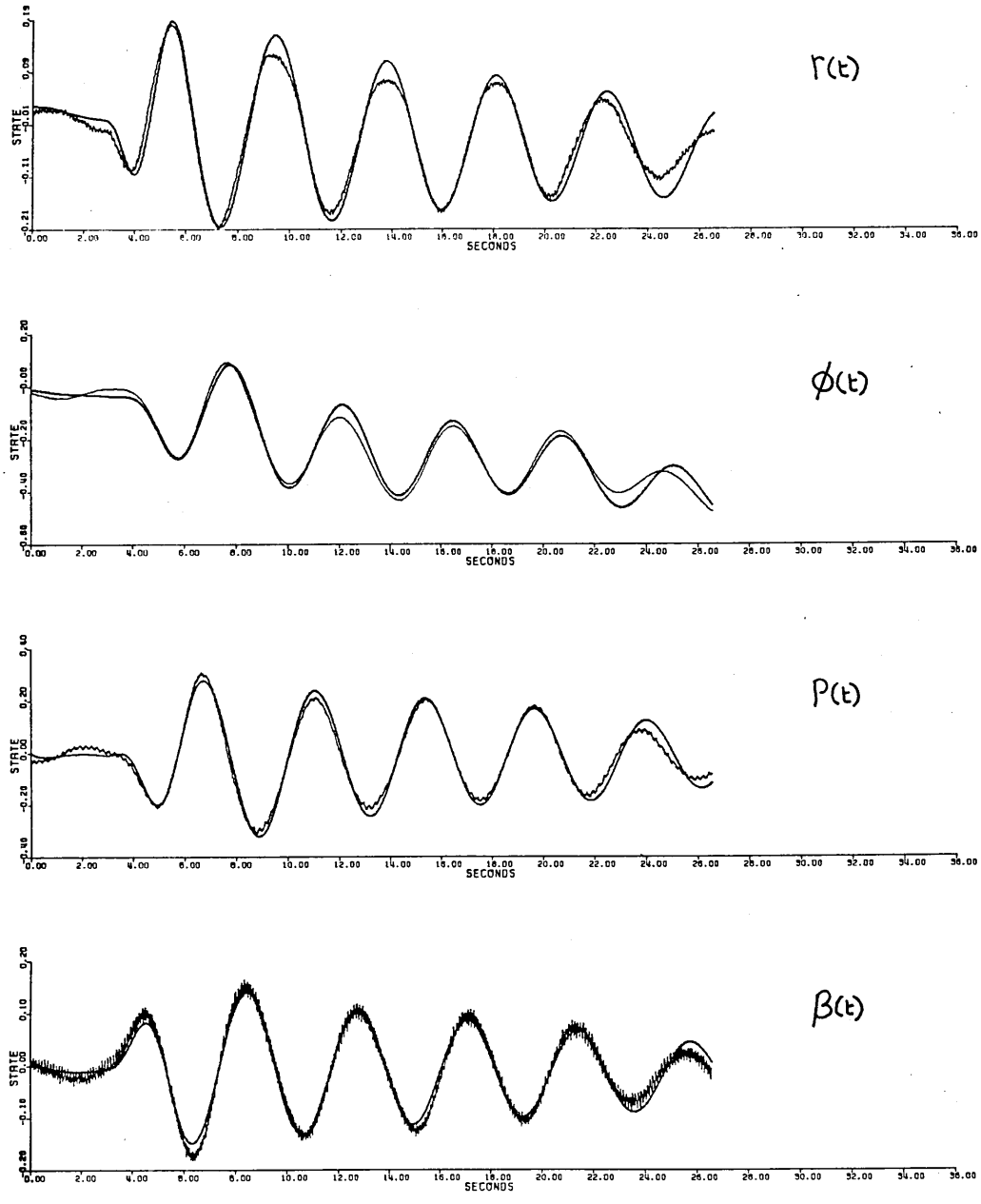

FIGURE 4-19 TIME-DOMAIN VERIFICATION.
DELAY IN ESTIMATION MODEL, RANK-9 SOLUTION.
PUMA, 100 KNOTS, RUN R1201L

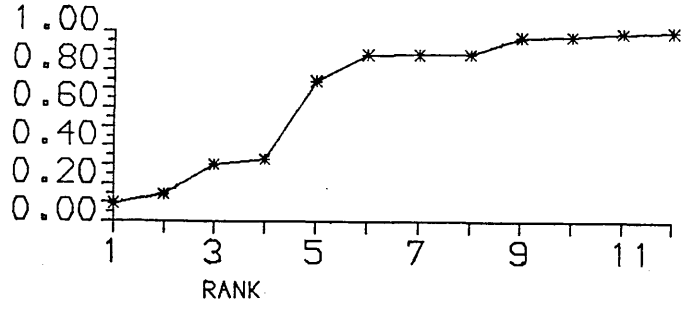

FIGURE 4-20 TYPICAL REDUCTION IN COST VALUE FOR USE OF INCREASING RANK OF INFORMATION MATRIX. NORMALISED WITH RESPECT TO FULL-RANK SOLUTION.

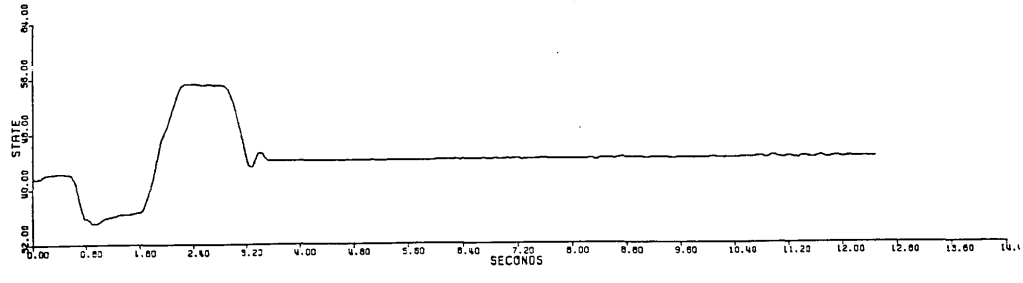

FIGURE 4-21 LATERAL-CYCLIC DOUBLET INPUT. PUMA, 60 KNOTS, RUN R2501R

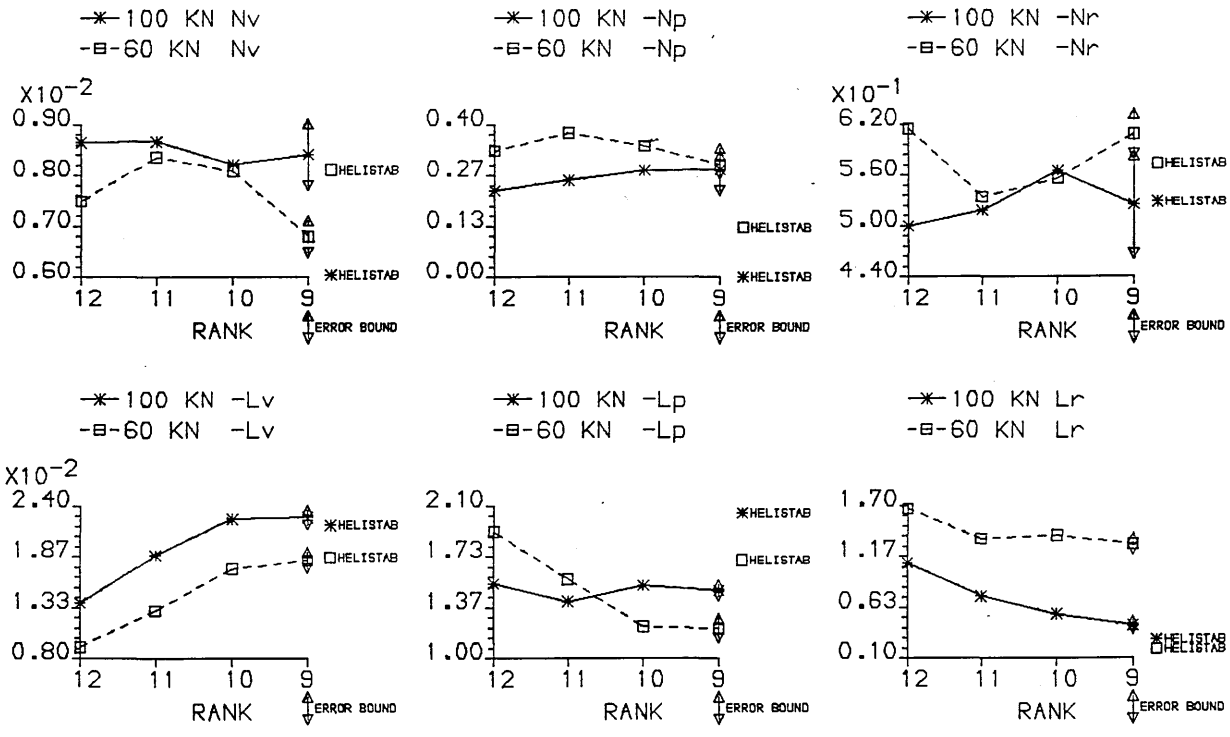

FIGURE 4-22 a) ESTIMATE VERSUS RANK OF INFORMATION MATRIX USED. PUMA, 60 KNOTS (LATERAL-CYCLIC RUN R2501R) & 100 KNOTS (PEDAL RUN R1201L) COMPARISONS

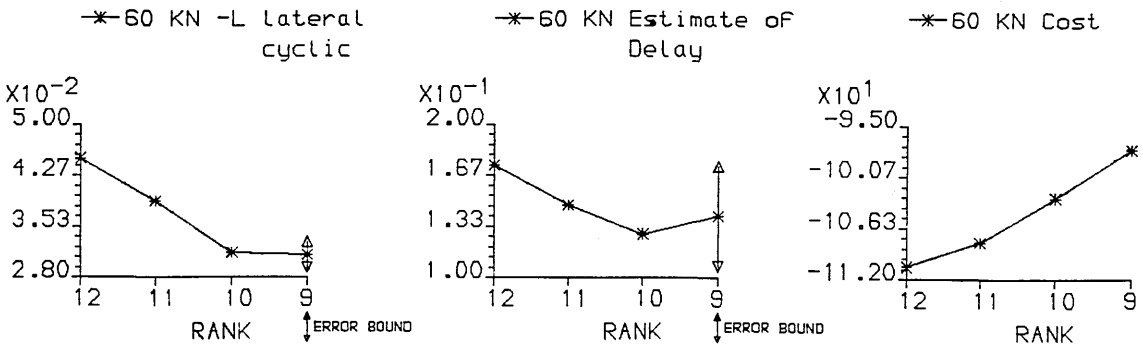

FIGURE 4-22 b) ESTIMATE VERSUS RANK OF INFORMATION MATRIX USED. PUMA, 60 KNOTS, RUN R2501R

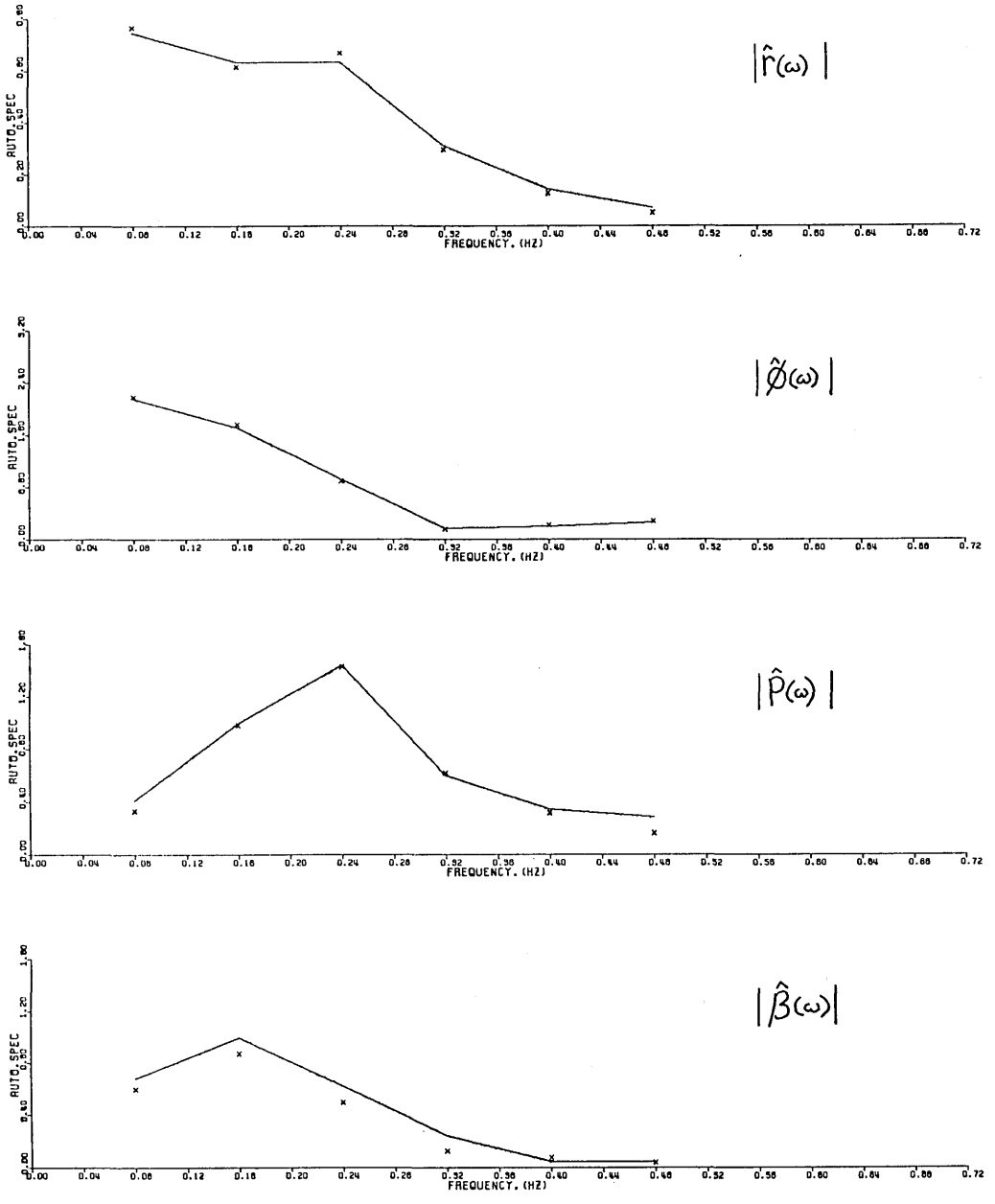

FIGURE 4-23 OUTPUT-ERROR FREQUENCY-DOMAIN FITS.
DELAY IN ESTIMATION MODEL, RANK-10 SOLUTION.
PUMA, 60 KNOTS, RUN R2501R

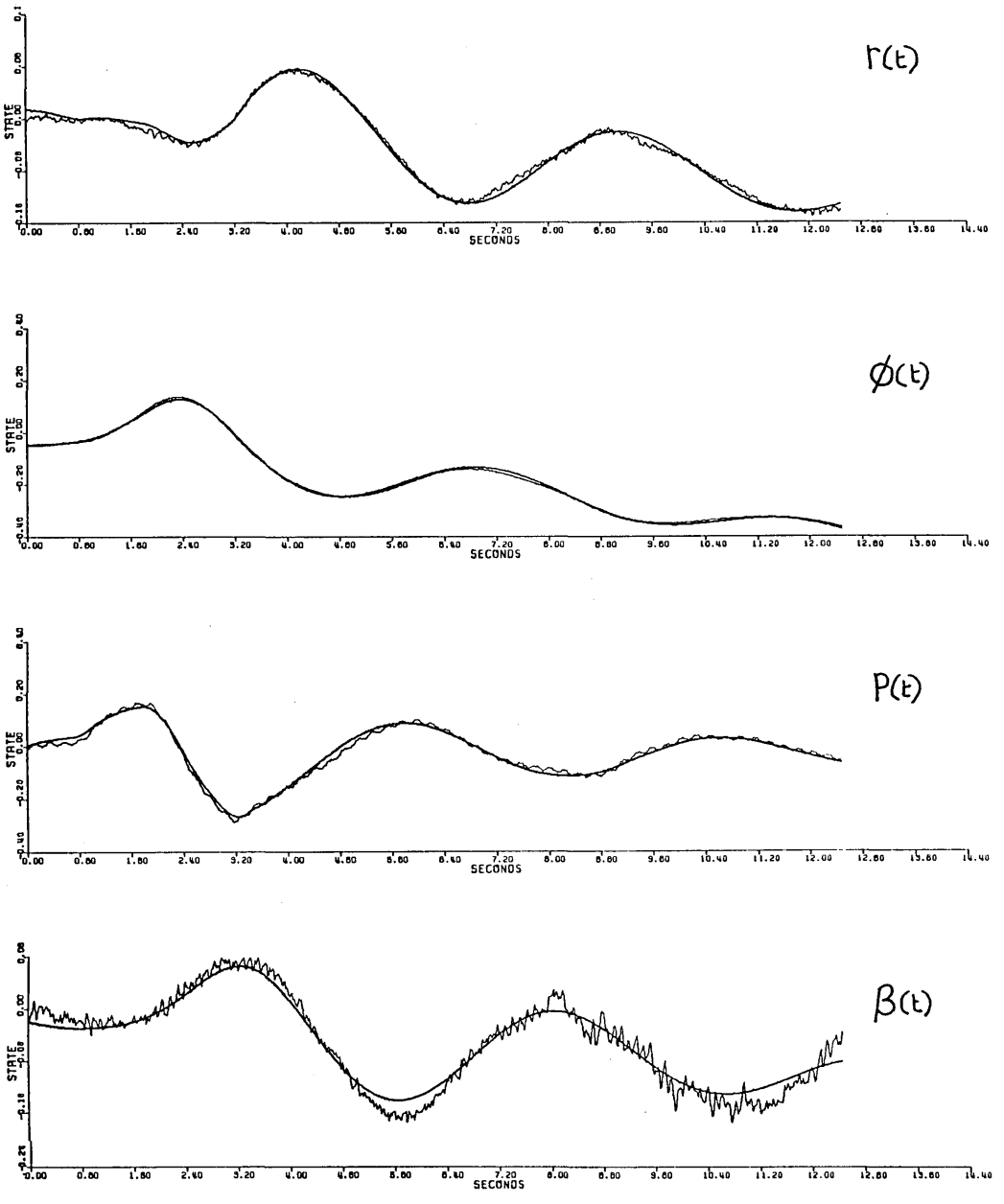

FIGURE 4-24 TIME-DOMAIN VERIFICATION.
DELAY IN ESTIMATION MODEL, RANK-10 SOLUTION.
PUMA, 60 KNOTS, RUN R2501R

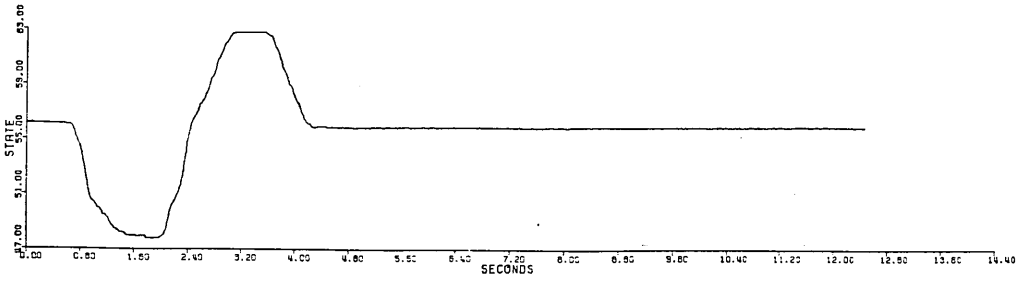

FIGURE 4-25 PEDAL DOUBLET INPUT.
PUMA, 60 KNOTS, RUN R3401R

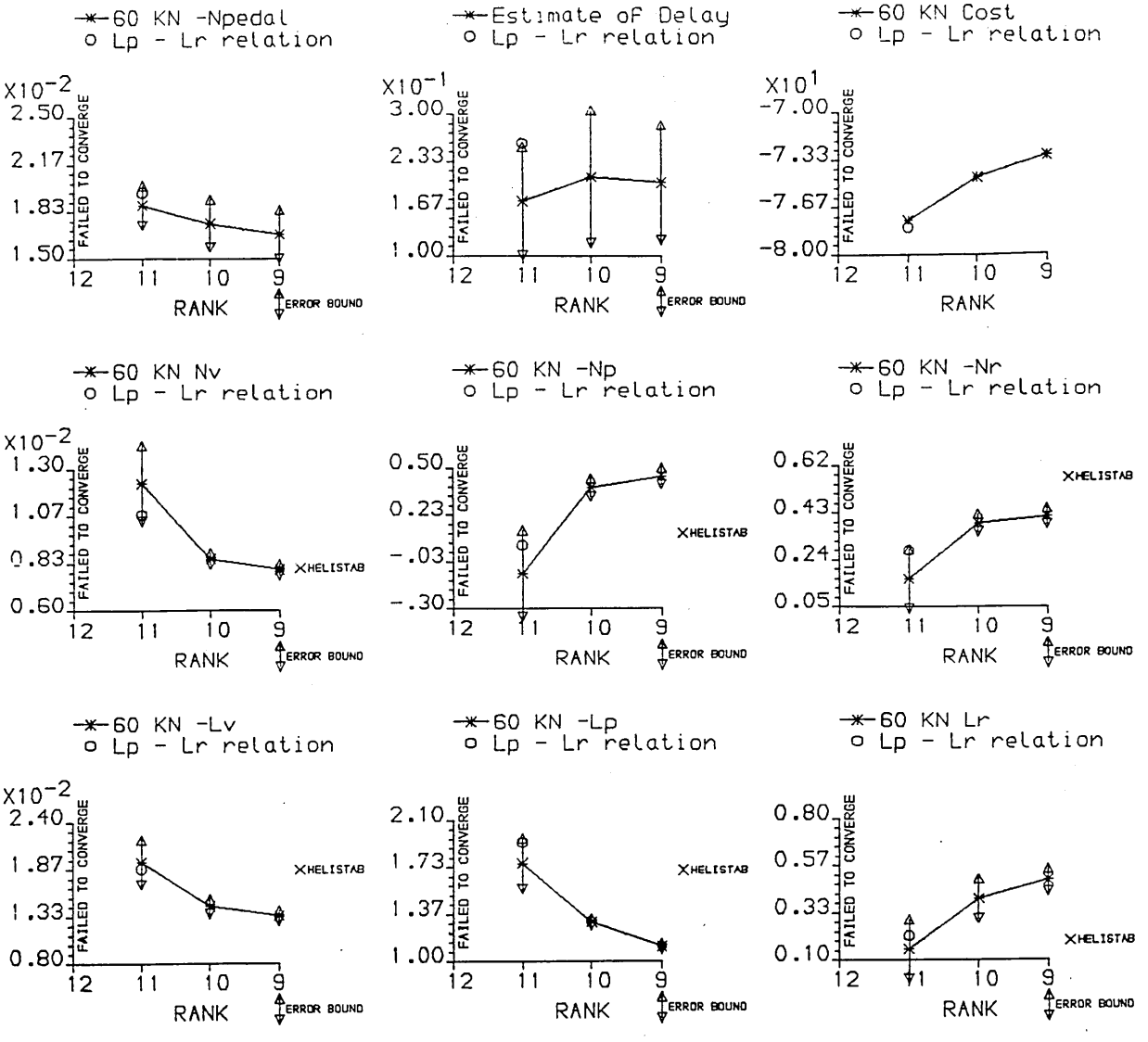

FIGURE 4-26 ESTIMATE VERSUS RANK OF INFORMATION MATRIX USED.
PUMA, 60 KNOTS, RUN R3401R

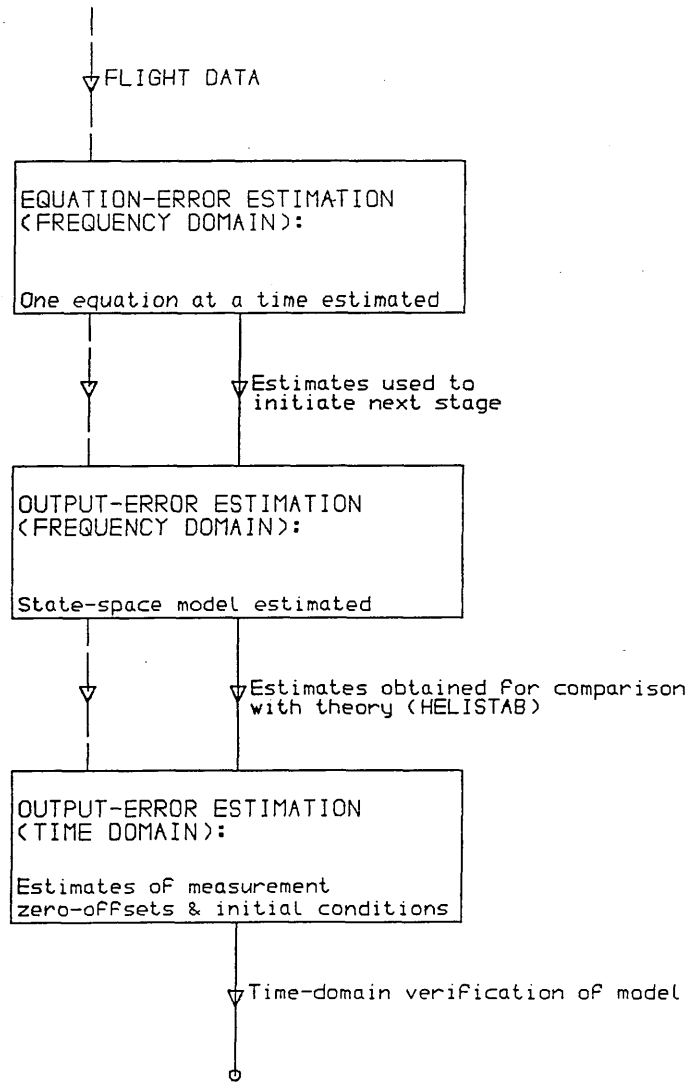

FIGURE 5-1 BASIC STAGES OF THE IDENTIFICATION METHODOLOGY

NOMENCLATURE

A	State matrix.
$\mathbf{A}, \mathbf{b}$	Matrices used to represent a linear system of equations.
$A_{FF}, A_{FR} \ldots B_F$	Partition matrices of the 9 DOF model relating fuselage and rotor effects.
$A_{11}, A_{12}, \ldots B_{22}$	Partitions of the six-degrees-of-freedom state and control matrices.
A_2, B_2, U_2	State matrix, control dispersion matrix, and control vector for steady-state Kalman-filter representation of the system.
a_{ij}, α_{ij}	True values and estimates of the state-space matrix (equation error).
$a_n, \bar{a}_n$	Coefficients and aliased coefficients of the Fourier-series expansion.
a_x, a_y, a_z	Components of acceleration.
$\underline{A}(\omega)$	Frequency-dependent matrix associated with the state matrix A, and used in the frequency-domain model representation developed for quantities of the form $[\check{\ }]$.
α	Line-search scalar parameter.
$\alpha_1, \alpha_2 \ldots \beta_1 . \beta_p$	Estimates of coefficients associated with various stages in the subset-regression procedure.
B	Control dispersion matrix.
B	Matrix with orthogonal columns used in singular-value decomposition.
B_w	(Approximate) Bandwidth of measurement noise.
$B_2(\omega)$	Frequency-dependent matrix relating to delays in the controls.
$\underset{\sim}{b}$	Vector of biases in measurements.
$\hat{b}_i$	Columns of matrix B used in singular-value decomposition.
b_{ij}, β_{ij}	True values and estimates of elements of the control dispersion matrix. (equation error).
$b_v, b_\beta \ldots b_r$	Constant biases in indicated measured quantities.
$\underline{B}$	Frequency-independent matrix associated with the control dispersion matrix B, and used with vector quantities of the form $[\check{\ }]$.
$\underline{B}(\omega)$	Frequency-dependent matrix associated with the matrix $B_2(\omega)$, and used with vector quantities of the form $[\check{\ }]$.
$\beta_0, \beta_{1c}, \beta_{1s}, \beta_d$	Coning, longitudinal and lateral-cyclic flapping, and differential coning multiblade flapping angles.
$\hat{\mathcal{E}}(\omega), \hat{\mathcal{S}}(\omega)$	Frequency-domain equation-error control terms used in the approximate estimation of time delays.
$\check{\underset{\sim}{\chi}}(\omega)$	Expected model-output vector (output-error method) in the form $[\check{\ }]$.
Cond ( )	Condition number of indicated matrix.
Cov ( )	Covariance matrix of indicated vector quantity.

$\underset{\sim}{\delta}^n$	Input vector containing higher-order terms of Taylor expansion.
$\mathrm{Diag}(\ )$	Diagonal matrix with indicated quantities in the leading diagonal.
$e(r), \hat{e}(r)$	Estimated equation-error residuals (time and frequency domain).
$\underset{\sim}{\varepsilon}$	Vector of equation errors.
$\eta_0, \eta_{1s}, \eta_{1c}, \eta_p$	Collective, longitudinal-cyclic, lateral-cyclic, and pedal control positions.
$E[\ ]$	Expected value of indicated quantity.
$\exp[\ ]$	Complex exponential.
$F_{est}(\omega)$, $F(\omega)$	Frequency-response values (estimated and predicted)
F_p	Partial-F statistic (or ratio)
F_{TOTAL}	Total-F statistic (or ratio)
$f(t)$; $f(m\Delta t)$, $f_q(m\Delta t)$	General function of time; discrete function of time and filtered form.
$\Delta F(\omega)$	Frequency-response errors.
$\mathcal{F}[\ ]$	Fourier transform operator (integral defined between infinite limits).
$\hat{\underset{\sim}{G}}(\omega_n)$, $\hat{\underset{\sim}{G}}_t(\omega_n)$	Correction terms for a non-periodic measurement window (frequency-dependent).
$\underset{\sim}{g}^K$	Gradient vector of the output-error cost function at the Kth iteration.
g	Acceleration due to gravity.
$\underset{\sim}{\gamma}$	Vector of true output-error model parameter values.
$\Delta\hat{\underset{\sim}{\gamma}}$	Update increment vector for model parameter values (output error).
$\Delta\underset{\sim}{\gamma}_t$	Update increment vector required to take estimates to the true model parameter values (output error).
$\underset{\sim}{\gamma}^K_{est}$, $\Delta\underset{\sim}{\gamma}^K$	Vector of output-error model parameter estimates and the vector of update increments at the Kth iteration.
γ	Set of output-error model parameters.
H	Measurement transition matrix (relating measured quantities to states in the model).
$H_2(\omega)$	Frequency-dependent matrix relating to delays in the measurements.
$\mathcal{H}$	Frequency-independent matrix associated with the measurement transition matrix H , and used with vector quantities of the form $[\ ^{\vee}]$.
$\mathcal{H}_2(\omega)$	Frequency-dependent matrix associated with the matrix $H_2(\omega)$, and used with vector quantities of the form $[\ ^{\vee}]$.
I	Identity matrix.

$J(\Theta)$	Equation-error cost function (time and frequency domain).
$J(Y,S)$	Frequency-domain output-error (maximum-likelihood) cost function.
$J_H(\Theta)$	Equation-error cost function (Hartley transform).
J_T	Time-domain output-error (maximum-likelihood) cost function.
j	Complex number such that $j^2 = -1$.
ΔJ	Change in cost-function value.
K	Matrix of Kalman gains.
$\underset{\sim}{K}$	Vector of trim constants for measurements.
$\underset{\sim}{K}_c, \underset{\sim}{K}_m$	Vectors of control and measurement zero offsets.
K_c, K_s	Coefficients of the equation-error control terms $\hat{C}(\omega)$ and $\hat{S}(\omega)$.
K_c	Set of control zero offsets.
K_m	Set of measurement zero offsets.
λ_i	Eigenvalues of indicated matrix.
$\log_e$	Natural logarithm.
$l_x^v, l_y^v \ldots l_z^\alpha$	Offsets (in body-fixed axes) of indicated measurement devices relative to the centre of gravity.
M^K	Output-error information matrix at the Kth iteration.
M_{true}	Output-error information matrix evaluated at the true parameter values.
$M_q, M_u \ldots$	Pitching-moment derivatives with respect to subscripted quantities.
μ, σ_N^2	Mean and variance of measurement noise.
N	Number of sampled points in time-domain record.
N	Number of data points used in equation-error identification.
N_i, D_K	Numerator and denominator transfer-function coefficients.
N_ω	Number of frequency-domain points used in output-error identification.
N_x	Number of states in the model for output-error identification.
$n_v, n_\beta, \ldots n_r$	Measurement noise terms in indicated quantities.
$\underset{\sim}{V}(n\Delta t), \hat{\underset{\sim}{V}}(\omega_K)$	Vectors of discrete Kalman-filter innovations; time domain (real-valued) and frequency domain (complex-valued).
ω, ω_n	Angular frequency and discrete values of angular frequency.
ω_F	Fundamental frequency.
ω_{sp}	Short-period mode natural frequency.

Λ	Diagonal matrix containing eigenvalues of the equation-error information matrix.
$O(\ )$	Quantities of the indicated order.
p	Number of unknown parameters to be estimated.
ψ_i	Rotor azimuth position.
$\underset{\sim}{\phi}$ $\underset{\sim}{\hat{\phi}}$	Vectors of true orthogonal parameter values and estimated orthogonal parameter values used in singular-value decomposition.
$\underset{\sim}{\hat{\phi}}(r)$	Vector whose first r elements equal those of $\underset{\sim}{\hat{\phi}}$, the remaining elements being zero.
$\hat{\phi}_i$	The ith element of $\underset{\sim}{\hat{\phi}}$.
Φ, D	Discrete versions of the state matrix A and control dispersion matrix B .
$\Delta\underset{\sim}{\phi}$	Orthogonal-update increment vector related to $\underset{\sim}{\hat{\phi}}$.
$\Delta\underset{\sim}{\phi}(r)$	Vector whose first r elements equal those of $\Delta\underset{\sim}{\hat{\phi}}$, the remaining elements being zero.
$P[a/b]$	Conditional probability (a conditioned on b).
q, p, r	Angular rates of pitch, roll and yaw.
$\underset{\sim}{q}(s)$, $\eta_{1s}(s)$	Laplace transforms of indicated quantities.
R	Time-domain error-covariance matrix.
R^2	Squared-correlation coefficient.
R_{at}	Theoretical ratio of parameter estimates.
r_{jy}	Partial-correlation coefficient used in subset regression procedure.
$R_e[\ ]$, $I_m[\ ]$	Real and imaginary parts of the complex-valued quantity [ ].
S, $S(\omega_i)$	Frequency-domain error-covariance matrix (frequency-independent and frequency-dependent versions).
S	Diagonal square matrix with singular values in the leading diagonal.
S^+	Matrix obtained from the inverse of S used in singular-value decomposition.
$S^2(\alpha_i)$	Variance of estimated coefficients obtained for the subset-regression procedure.
$S_{xy}(\omega)$, $S_{xx}(\omega)$	Cross and auto-spectral density functions.
$\underset{\sim}{S}$	Frequency-domain error-covariance matrix used with vector quantities of the form $[\ ^{v}]$.
s	Laplace operator.
s_i	Singular values.
$\underset{\sim}{S}$	Set of unknown parameters of error covariance matrix .
σ, σ^2	Standard deviation and variance of parameter estimate. (1).
σ^2, S^2	Equation-error variance of residuals (true and estimated values). (2).

T	Time length of measurement window.
T_θ	Transfer-function parameter.
t	Time.
Δt	Sampling interval.
$\hat{\underset{\sim}{\Theta}}_{IV}, \hat{\underset{\sim}{\Theta}}_{FR}$	Vector of parameter estimates relating to the instrumental variable technique and its frequency-domain equivalent.
Θ	Vector of true parameter values (equation error).
$\hat{\Theta}$	Vector of parameter estimates (equation error).
$\Theta, \phi, \Psi, \theta, \phi, \psi$	Euler pitch, roll, and yaw angles (and perturbations from trim).
τ	Time delay; time constant.
τ_θ, τ_{az}	Effective transfer-function time delays.
$\boldsymbol{\theta}$	Set of equation-error parameters.
$\boldsymbol{\tau}_c$	Set of time delays in the controls.
$\boldsymbol{\tau}_m$	Set of time delays in the measurements.
U	Matrix formed by closing together the eigenvectors of the system matrix. (1).
U	Matrix with orthogonal columns; used in singular-value decomposition. (2).
$\underset{\sim}{U}$	Control vector.
$\hat{\underset{\sim}{U}}_{LONG}, \underset{\sim}{U}_{LAT}$	Portions of the control vector relating to the longitudinal and lateral controls respectively.
U_L	Columns of the matrix U used in singular-value decomposition.
U_i	Eigenvectors of system matrix.
U, V, W	Aircraft translational velocity components (total values).
$\underset{\sim}{U}_{ef}$	Effective control input.
u, v, w	Aircraft translational velocity components (perturbations from trim).
V	Orthogonal matrix used in singular-value decomposition.
$\underset{\sim}{V}(t), \underset{\sim}{V}(i), \hat{\underset{\sim}{V}}(\omega), \hat{\underset{\sim}{V}}(i)$	Continuous and discrete measurement noise (time domain and frequency domain).
V_{sp}, β, α	Speed, flank angle and incidence angle.
V_i	The ith row of V .
$\underset{\sim}{W}(t), \hat{\underset{\sim}{W}}(\omega_K)$	Process noise vector (time and frequency domain).
$X, \hat{X}$	Matrix of independent-variable frequency (or time) response data arranged in columns (for equation-error method). The form of the matrix with a hat is used to indicate frequency-domain quantities when a distinction with time-domain quantities is required.
$\underset{\sim}{X}$	State vector.
$\underset{\sim}{X}(t), \underset{\sim}{U}(t), \underset{\sim}{Z}(t)$	State, control and output vectors (time domain).
$\hat{\underset{\sim}{X}}(\omega), \hat{\underset{\sim}{U}}(\omega), \hat{\underset{\sim}{Z}}(\omega)$	State, control and output vectors (frequency domain).
$\check{\underset{\sim}{X}}(\omega), \check{\underset{\sim}{U}}(\omega), \check{\underset{\sim}{Z}}(\omega)$	State, control and output vectors in the form $[\check{\ }]$.

$\underset{\sim}{X}(0)$	Vector of initial state conditions.
$\underset{\sim}{X}_{LONG}$, $\underset{\sim}{X}_{LAT}$	Partitions of the state vector relating to longitudinal and lateral states respectively.
$\underset{\sim}{X}_R$, $\underset{\sim}{X}_F$	Rotor state vector and fuselage state vector.
$\Delta\underset{\sim}{X}$, $\Delta\underset{\sim}{X}_{NAG}$	Vector associated with correction term for a non-periodic measurement window, and version for NAG definition of discrete Fourier transform.
X, Y, Z	Body-fixed axes components.
$X_i(r)$, $U_j(r)$, $\hat{X}_i(r)$ $\hat{U}_j(r)$	Independent variables relating to states and controls (equation error); time and frequency domain.
$\dot{X}_i(r)$, $\hat{\dot{X}}_i(r)$	Dependent variable relating to time derivative of state (equation error); time and frequency domain.
$X_j(r)$	Subset-regression independent variables.
$X_j^*(r)$	Subset-regression variables associated with $X_j(r)$.
X_u, X_w ..	Forward force derivatives.
$\mathbf{X}_0$	Set of initial state conditions.
ζ	Short-period mode damping
$\underset{\sim}{Y}$	Equation-error dependent variable (vector form).
$Y(r)$, $\hat{Y}(r)$	Equation-error dependent variable and model prediction (scalar form).
$Y^*(r)$	Subset-regression dependent variable constructed from residuals.
Y_v, Y_w ..	Lateral force derivatives.
Z'_{FR}	Complex-valued matrix used to illustrate the frequency-domain equivalence to the instrumental-variable technique.
Z_{FR}	Real-valued matrix associated with Z'_{FR} .
Z_{IV}	Instrumental-variable matrix.
$\underset{\sim}{Z}$	Model output vector.
$\underset{\sim}{Z}(\omega)$	Model output vector (output-error method) in the form $[\,^{v}\,]$.
$\hat{\underset{\sim}{Z}}(\omega_i/i-1)$	Expected value of $\hat{\underset{\sim}{Z}}(\omega_i)$ conditioned on the sets $\mathbf{Z}_{q-1}$ and Υ .
$\Delta\underset{\sim}{Z}$, $\Delta\underset{\sim}{Z}_{NAG}$	Vectors associated with the correction term for a non-periodic measurement window (relate to $\Delta\underset{\sim}{X}$ and $\Delta\underset{\sim}{X}_{NAG}$).
Z_u, Z_w ..	Normal force derivatives.
$\mathbf{Z}_q$	Set of measured frequency-domain values corresponding to the first q frequency values.
$[\,\dot{}\,]$	Derivative of [ ] with respect to time.
$\partial/\partial\Upsilon\,[\ ]$	Partial derivative of [ ] with respect to indicated quantity.
$[\ ]^{\#}$	Least-squares pseudo inverse of [ ].
$[\ ]^{-1}$	Inverse of [ ].
$[\ ]^{T}$	Transpose of [ ].
$[\ ]^{*}$	Transpose of complex conjugate of [ ].
$\|\ \|$	Magnitude of indicated quantity.
$\|\ \|$	Determinant of indicated quantity.
$[\,\hat{\cdot}\,]$	Fourier transform of the time derivative of [ ].

$[\ ]_m$	Measured value of [ ].
$[\ ]_{OFF}$	Offset term for [ ] combining trim constants and measurement biases.
$[\hat{\ }]$	Fourier transform of [ ] - unless otherwise defined separately.
$[\bar{\ }]$	Expected (or mean) value of [ ].
$\|\ \|$	Matrix and vector norm of indicated quantity.
$\triangleq$	Definition.
$[\ _]$	Integer value of indicated quantity (i.e. truncated not rounded).
$[\check{\ }_]$	Frequency-domain vector quantity relating to $[\hat{\ }]$ and obtained by stacking the real on top of the imaginary part of the otherwise complex-valued vector quantity.
$[\ ]_e$	Subscript e signifies trim values of indicated scalar quantities. e.g. θ_e.

Appendix 1 Linearised Equations of Aircraft Motion

The force, moment and kinematic equations of motion are given below:

Translational Motion

$$m\dot{U} = -m(Wq - Vr) + X(x) - mg\sin\theta \qquad \text{(A1.1)}$$

$$m\dot{V} = -m(Ur - Wp) + Y(x) + mg\cos\theta\sin\phi \qquad \text{(A1.2)}$$

$$m\dot{W} = -m(Vp - Uq) + Z(x) + mg\cos\theta\cos\phi \qquad \text{(A1.3)}$$

Rotational Motion

$$I_{xx}\dot{p} = (I_{yy} - I_{zz})qr + I_{xz}(\dot{r} + pq) + L(x) \qquad \text{(A1.4)}$$

$$I_{yy}\dot{q} = (I_{zz} - I_{xx})rp + I_{xz}(r^2 - p^2) + M(x) \qquad \text{(A1.5)}$$

$$I_{zz}\dot{r} = (I_{xx} - I_{yy})pq + I_{xz}(\dot{p} - qr) + N(x) \qquad \text{(A1.6)}$$

Kinematic Relations

$$\dot{\phi} = p + q\sin\phi\tan\theta + r\cos\phi\tan\theta \qquad \text{(A1.7)}$$

$$\dot{\theta} = q\cos\phi - r\sin\phi \qquad \text{(A1.8)}$$

$$\dot{\psi} = q\sin\phi\sec\theta + r\cos\phi\sec\theta \qquad \text{(A1.9)}$$

The equations are linearised about a reference trim state. The total value of states are represented by reference plus perturbed values (indicated by the subscript e). For example we have:

$$V = V_e + v \tag{A1.10}$$

The trim values of the angular rates p, q and r are zero:

$$p_e = q_e = r_e = 0 \tag{A1.11}$$

The external forces and moments are expressed as a Taylor expansion, for example:

$$X(x) = X_e + \frac{\partial X}{\partial u} u + \frac{\partial X}{\partial v} v + \dots \frac{\partial X}{\partial \eta_o} \eta_o + \dots \tag{A1.12}$$

Details of the working through of the linearisations of Equations (A1.1) to (A1.9) are provided by the current author in the reference BLAC003. The linearised equations of motion are represented below. (In relation to the linearised moment equations, no assumptions relating to the relative magnitudes of the moments and products of inertia are made, and the most general form of the rolling-moment and yawing-moment equations are presented).

$$\dot{u} = -(W_e q - V_e r) - g\theta \cos\Theta_e + X(x)/m \tag{A1.13}$$

$$\dot{V} = -(U_e r - W_e p) + g(\phi \cos\phi_e \cos\Theta_e - \Theta \sin\Theta_e \sin\phi_e) + Y(x)/m \tag{A1.14}$$

$$\dot{W} = -(V_e p - U_e q) - g(\Theta \cos\phi_e \sin\Theta_e + \phi \sin\phi_e \cos\Theta_e) + Z(x)/m \tag{A1.15}$$

$$I_{xx}\dot{p} = I_{xz}\dot{r} + L(x) \tag{A1.16}$$

$$I_{yy}\dot{q} = M(x) \tag{A1.17}$$

$$I_{zz}\dot{r} = I_{xz}\dot{p} + N(x) \tag{A1.18}$$

$$\dot{\phi} = p + q \sin\phi_e \tan\Theta_e + r \cos\phi_e \tan\Theta_e \tag{A1.19}$$

$$\dot{\Theta} = q \cos\phi_e - r \sin\phi_e \tag{A1.20}$$

$$\cos\Theta_e \dot{\Psi} = q \sin\phi_e + r \cos\phi_e \tag{A1.21}$$

The linearised equations of motion can be written in state-space form as:

$$\dot{\underset{\sim}{X}} = A\underset{\sim}{X} + B\underset{\sim}{U} \tag{A1.22}$$

where $\underset{\sim}{X} = (u, w, q, \Theta, v, p, \phi, r)^T$

$\underset{\sim}{U} = (\eta_0, \eta_{1s}, \eta_{1c}, \eta_p)^T$

The system matrix A and control dispersion matrix B follow from the linearised equations of motion given by Equations (A1.13) to (A1.21,) and are as follows:

$$A = \begin{bmatrix} X_u & X_w & X_q - W_e & X_\theta + C_1 & X_v & X_p & X_\phi & X_r + V_e \\ Z_u & Z_w & Z_q + U_e & Z_\theta + C_2 & Z_v & Z_p - V_e & Z_\phi + C_3 & Z_r \\ M_u & M_w & M_q & M_\theta & M_v & M_p & M_\phi & M_r \\ 0 & 0 & \cos\phi_e & 0 & 0 & 0 & 0 & -\sin\phi_e \\ Y_u & Y_w & Y_q & Y_\theta + C_4 & Y_v & Y_p + W_e & Y_\phi + C_5 & Y_r - U_e \\ L'_u & L'_w & L'_q & L'_\theta & L'_v & L'_p & L'_\phi & L'_r \\ 0 & 0 & C_5 & 0 & 0 & 1.0 & 0 & C_6 \\ N'_u & N'_w & N'_q & N'_\theta & N'_v & N'_p & N'_\phi & N'_r \end{bmatrix}$$

$$C_1 = -g\cos\theta_e \qquad C_2 = -g\cos\phi_e\sin\theta_e$$

$$C_3 = -g\sin\phi_e\cos\theta_e \qquad C_4 = -g\sin\theta_e\sin\phi_e$$

$$C_5 = \sin\phi_e\tan\theta_e \qquad C_6 = \cos\phi_e\tan\theta_e$$

$$B = \begin{bmatrix} X_{\eta_0} & X_{\eta_{1s}} & X_{\eta_{1c}} & X_{\eta_p} \\ Z_{\eta_0} & Z_{\eta_{1s}} & Z_{\eta_{1c}} & Z_{\eta_p} \\ M_{\eta_0} & M_{\eta_{1s}} & M_{\eta_{1c}} & M_{\eta_p} \\ 0 & 0 & 0 & 0 \\ Y_{\eta_0} & Y_{\eta_{1s}} & Y_{\eta_{1c}} & Y_{\eta_p} \\ L'_{\eta_0} & L'_{\eta_{1s}} & L'_{\eta_{1c}} & L'_{\eta_p} \\ 0 & 0 & 0 & 0 \\ N'_{\eta_0} & N'_{\eta_{1s}} & N'_{\eta_{1c}} & N'_{\eta_p} \end{bmatrix}$$

where, for a general subscript c, $L'_c = L_c + N_c$. Ixz/Izz and $N'_c = N_c + L_c$. Ixz/Ixx. The derivatives relating to the force equations (i.e. for a general subscript c, X_c, Y_c, and Z_c) are divided by the aircraft mass m. The pitching-moment derivatives are divided by Iyy, and the rolling-moment and yawing-moment derivatives are divided by Izz/(IzzIxx - Ixz^2) and Ixx/(IzzIxx - Ixz^2) respectively.

Appendix 2 Conditions for Unbiased Estimates from the Frequency-Domain Output-Error Method

The proof given below to show, in the absence of process (or model) noise, and for uncorrelated Graussian measurement noise, that unbiased parameter estimates are obtained using the output-error method, is in essence the same as that given in KLEI001; however, the proof is presented here for frequency-domain quantities and some additional explanation and development is provided. The same notation is used as in Chapter 4.

Consider Equation (4.2-44) giving the linearised approximatioon for elements of the Hessian matrix at the Kth iteration (defined by Equation (4.2-39). We can write:

$$M^K = \sum_{\omega} A^{K^T}(\omega)\, S^{-1} A^K(\omega) \tag{A2.1}$$

where $$A^K_{ij}(\omega) \triangleq \frac{\partial \check{\chi}_i(\omega)}{\partial \varphi_j} \tag{A2.2}$$

And similarly for the gradient vector $\underset{\sim}{g}^K$ (defined by Equation (4.2-40)) we can write, using Equation (4.2-42) and the definition given by (A2.2):

$$\underset{\sim}{g}^K = \sum_{\omega} A^{K^T}(\omega)\, S^{-1} [\underset{\sim}{\check{\chi}}(\omega) - \underset{\sim}{\check{z}}(\omega)] \tag{A2.3}$$

For the Gauss-Newton method, given in Equation (4.2-38), and using (A2.1) and (A2.3), we have:

$$\underset{\sim}{\zeta}_{est}^{K+1} - \underset{\sim}{\zeta}_{est}^{K} = \Delta\underset{\sim}{\zeta}_{est}^{K+1} = -M^{K^{-1}}\underset{\sim}{g}^{K} =$$

$$\left(\sum_{\omega} A^{K^T}(\omega) S^{-1} A^{K}(\omega)\right)^{-1} \left(\sum_{\omega} A^{K^T}(\omega) S^{-1} [\underset{\sim}{Z}(\omega) - \check{\underset{\sim}{\chi}}(\omega)]\right) \quad \text{(A2.4)}$$

The value of the output vector $\check{\underset{\sim}{\chi}}(\omega)$ at the Kth iteration is dependent upon the vector of parameter estimates $\underset{\sim}{\zeta}$ obtained, and indicating this fact in the notation, we can expand the true model output vector in a Taylor expansion about the output vector obtained at the kth iteration:

$$\check{\underset{\sim}{\chi}}(\omega, \underset{\sim}{\zeta}) = \check{\underset{\sim}{\chi}}(\omega, \underset{\sim}{\zeta}^{K} + \Delta\underset{\sim}{\zeta}_{t}) =$$

$$\check{\underset{\sim}{\chi}}(\omega, \underset{\sim}{\zeta}^{K}) + A^{K}(\omega)\Delta\underset{\sim}{\zeta}_{t} + \text{Second and higher-order terms.} \quad \text{(A2.5)}$$

where $\underset{\sim}{\zeta}$ is the true parameter vector, and $\Delta\underset{\sim}{\zeta}_{t}$ is the parameter increment required to move from the current parameter estimates to their true values. The measurements and the true model output vector are related (using Equation (4.2-25) and the definition (4.2-30)) by:

$$\check{\underset{\sim}{Z}}(\omega) = \check{\underset{\sim}{\chi}}(\omega, \zeta) + \check{\underset{\sim}{V}}(\omega) \quad \text{(A2.6)}$$

Hence, by using the first-order terms only in (A2.5), we can substitute into (A2.6) to obtain:

$$\check{\underset{\sim}{Z}}(\omega) - \check{\underset{\sim}{\chi}}(\omega, \underset{\sim}{\zeta}^{K}) \simeq A^{K}(\omega)\Delta\underset{\sim}{\zeta}_{t} + \check{\underset{\sim}{V}}(\omega) \quad \text{(A2.7)}$$

Now using the first-order approximation for the left-hand

side of (A2.7), we can substitute it into (A2.4), and obtain:

$$\Delta \underset{\sim}{Y}_{est}^{K+1} \doteq \Delta \underset{\sim}{Y}_t + M^{K^{-1}} \left(\sum_{\omega} A^{K^T}(\omega) S^{-1} \check{\underset{\sim}{V}}(\omega) \right) \qquad \text{(A2.8)}$$

where the expression for M^K is given by (A2.1) has been used. Rearranging (A2.8), and taking the expected value of both sides, we have to the first degree of approximation, that:

$$E[\Delta \underset{\sim}{Y}_{est}^{K+1} - \Delta \underset{\sim}{Y}_t] = \underset{\sim}{0} \qquad \text{(A2.9)}$$

when $E[\check{\underset{\sim}{V}}(\omega)] = 0$. This means, that to the first degree of approximation, the parameter estimates are unbiased. It is interesting to note that to obtain unbiased estimates is not dependent upon the value of the matrix S (except that it must be non-singular).

Parameter Covariance Matrix

By using (A2.8) an expression for the parameter covariance matirx can be obtained. The parameter covariance matrix is defined for estimates obtained after K + 1 iterations by:

$$\begin{aligned} Cov(\underset{\sim}{Y}_{est}^{K+1} - \underset{\sim}{Y}) &= Cov(\Delta \underset{\sim}{Y}_{est}^{K+1} - \Delta \underset{\sim}{Y}_t) \triangleq \\ & E[(\Delta \underset{\sim}{Y}_{est}^{K+1} - \Delta \underset{\sim}{Y}_t)(\Delta \underset{\sim}{Y}_{est}^{K+1} - \Delta \underset{\sim}{Y}_t)^T] = \\ & E[M^{K^{-1}} (\sum_{\omega_a} A^{K^T}(\omega_a) S^{-1} \check{\underset{\sim}{V}}(\omega_a)) (\sum_{\omega_b} \check{\underset{\sim}{V}}^T(\omega_b) S^{-1} A(\omega_b)) M^{K^{-1}}] \end{aligned} \qquad \text{(A2.10)}$$

where ω_a and ω_b are the frequency values relating to the separately defined summations. For frequency-domain noise terms that are uncorrelated (see Section 2.2.5), we can write the above as:

$$\mathrm{Cov}(\underset{\sim}{Y}_{est}^{K+1} - \underset{\sim}{Y}) =$$

$$M^{K^{-1}}\left(\sum_{\omega} A^{K^T}(\omega)\, S^{-1} E[\check{\underset{\sim}{V}}(\omega)\check{\underset{\sim}{V}}^T(\omega)]\, S^{-1} A^K(\omega)\right) M^{K^{-1}} \qquad \text{(A2.11)}$$

Equation (A2.11) becomes, when we use the expression for the error-covariance matrix given by Equation (4.2-37) and the expression for M^K given be (A2.1):

$$\mathrm{Cov}(\underset{\sim}{Y}_{est}^{K+1} - \underset{\sim}{Y}) = M^{K^{-1}} \qquad \text{(A2.12)}$$

That is, the parameter covariance matrix which specifies the error bounds on the parameter estimates, is given by the inverse of the information matrix used to obtain the estimates (assuming that the parameter values obtained are near to their true values, hence justifying the use of the first-order terms only in (A2.5)).

Appendix 3 The Line-Search Algorithm

The line-search algorithm which is presented here, and which is used in addition to the basic Gauss-Newton method, is the same as that presented in FOST002. The notation used here is the same as that in Section 4.2.2, and Appendix 2.

Consider the Gauss-Newton method which may be written, for the Kth iteration, as:

$$M^K \Delta \underset{\sim}{\zeta}_{est}^{K+1} = -\underset{\sim}{g}^K \tag{A3.1}$$

If we define the cost function at the (K+1)th iteration for a scalar multiple α of the update increment $\Delta \underset{\sim}{\zeta}^{K+1}$ as:

$$J(\alpha) \triangleq J(\underset{\sim}{\zeta}_{est}^{K} + \alpha \Delta \underset{\sim}{\zeta}_{est}^{K+1}) \tag{A3.2}$$

then with the line search we seek a value of α which minimises $J(\alpha)$. The steps of the line search algorithm are as follows:

1. Fit a quadratic through J(0) and J(1). The additional information requried is provided by J'(0), which is assumed to be negative. We have:

$$f = a\alpha^2 + b\alpha + c \tag{A3.3}$$

$$f' = 2a\alpha + b \tag{A3.4}$$

where $J(0) = c$, $J(1) = a+b+c$, and $J'(0) = \partial J/\partial \alpha$ evaluated at $\alpha = 0$. From (A3.2) we have

$$\partial J/\partial \alpha \Big|_{\alpha=0} = \partial J^T/\partial \underset{\sim}{\varsigma} \Big|_{\underset{\sim}{\varsigma}^K_{est}} \Delta \underset{\sim}{\varsigma}^{K+1}_{est} \qquad \text{(A3.5)}$$

2. Assume that the quadratic obtained in step (1) has a minimum at α_3. Set $\alpha_1 = 0$ and $\alpha_2 = 1$. From (A3.4) the minimum is given by:

$$\alpha_3 = -b/2a \qquad \text{(A3.6)}$$

where $a > 0$ for a minimum.

3. Re-order α_1, α_2, and α_3 so that $J(\alpha_1) \leqslant J(\alpha_2) \leqslant J(\alpha_3)$

4. Fit a quadratic $A\alpha^2 + B\alpha + C$ through the three points: α_1, α_2 and α_3 given in step (3). The minimum α^* is given by:

$$\alpha^* = -B/2A \qquad \text{(A3.7)}$$

where $A > 0$ for a minimum.

5. A series of tests are now carried out to see if α^* is to be accepted as the value of the line-search parameter. These are:

a) $|\alpha^* - \alpha_1| \leqslant$ TESTS(3)

b) Absolute value of the gradient of the line from $(\alpha_1, J(\alpha_1))$ is tested to see if it is small compared with $|\partial J/\partial\alpha|_{\alpha=0}|$, using:

gradient $\leqslant$ TESTS(4) $\cdot$ $|\partial J/\partial\alpha|_{\alpha=0}|$

c) If the limit on the number of cost evaluations permitted in the line search has been reached. This is determined by TESTS(5).

If either of tests a), b) or c) indicate that α^* should be accepted as the value of the line-search parameter for this iteration, then stop, otherwise proceed to step 6.

6. Evaluate $J(\alpha^*)$, and assuming that it is, at worst, smaller that $J(\alpha_3)$, set $\alpha_3 = \alpha^*$ and $J(\alpha_3) = J(\alpha^*)$ and go to step (3).

A number of alternative actions need to be taken if the assumptions made throughout the algorithm are not true. The following recommendations are taken from the original reference (FOST002). If at step (1), $\partial J/\partial\alpha|_{\alpha=0}$ is positive, then a possible solution is to use $\alpha=-1$, and proceed in the opposite direction. If at steps (2) and (4), no minimum exists for the quadratic, then to move in

a direction where the cost is decreasing, a worthwhile step is to go to $\alpha^* = 2\alpha_1 - \alpha_2$. If the assumption made at step (6) is not true, the line search is no longer reducing the cost, and it is advised to accept α_1 as the best α that can be found.

It is advisable to put limits on the range of the line search (specified by TESTS(6) and TESTS(7)) to avoid divergence through extrapolations when the parabola is very shallow, though the parameter TESTS(5) (shown in step (5)) also helps to prevent this.

The values of TESTS(8) and TESTS(9) indicate the iteration numbers between which the line search algorithm is used in addition to the basic Gauss-Newton method. The parameters TESTS(3) to TESTS(9) are values specified by the user.

Appendix 4 The Kalman Filter Algorithm

a. Discrete Kalman Filter Algorithm

System Model:

$$\underset{\sim}{X}(t_K) = \Phi \underset{\sim}{X}(t_{K-1}) + D\underset{\sim}{U}(t_{K-1}) + W(t_{K-1}) \tag{A4.1}$$

where $\underset{\sim}{W}(t_K) \sim N(\underset{\sim}{0}, Q)$ and t_K is discrete time.
Q is the process noise covariance matrix, assumed time-invariant.

Measurement Model:

$$\underset{\sim}{Z}(t_K) = H\underset{\sim}{X}(t_K) + \underset{\sim}{V}(t_K) \tag{A4.2}$$

where $\underset{\sim}{V}(t_K) \sim N(\underset{\sim}{0}, R)$
R is the measurement noise covariance matrix, assumed time-invariant.

Covariance Matrices:

$$P(t,-) \triangleq E[(\underset{\sim}{X}(t) - \bar{\underset{\sim}{X}}(t,-))(\underset{\sim}{X}(t) - \bar{\underset{\sim}{X}}(t,-))^T] \tag{A4.3}$$

$$P(t,+) \triangleq E[(\underset{\sim}{X}(t) - \bar{\underset{\sim}{X}}(t,+))(\underset{\sim}{X}(t) - \bar{\underset{\sim}{X}}(t,+))^T] \tag{A4.4}$$

where the bar $^-$ above a quantity indicates the expected (or mean) value; (t,-) indicates the value before the

measurements $\underset{\sim}{Z}(t)$ are received; and (t,+) indicates the value after the measurements $\underset{\sim}{Z}(t)$ are received.

1. Error - Covariance Extrapolation:

$$P(t_K,-) \triangleq \Phi P(t_{K-1},+)\Phi^T + Q \tag{A4.5}$$

2. Kalman Gain Matrix:

$$K(t_K) = P(t_K,-)H^T(HP(t_K,-)H^T + R)^{-1} \tag{A4.6}$$

3. State Estimate Extrapolation:

$$\bar{\underset{\sim}{X}}(t_K,-) = \Phi \bar{\underset{\sim}{X}}(t_{K-1},+) + D\underset{\sim}{U}(t_{K-1}) \tag{A4.7}$$

4. State Estimate Update:

$$\bar{\underset{\sim}{X}}(t_K,+) = \bar{\underset{\sim}{X}}(t_K,-) + K(t_K)(\underset{\sim}{Z}(t_K) - H\bar{\underset{\sim}{X}}(t_K,-)) \tag{A4.8}$$

5. Error Covariance Update:

$$P(t_K,+) = (I - K(t_K)H)P(t_K,-) \tag{A4.9}$$

Steady State Formulation

As $t_K \to \infty$, we have:

for (1) $$P(\infty,-) = \Phi P(\infty,+)\Phi^T + Q \tag{A4.10}$$

For (2) $K(\infty) = P(\infty,-)H^T(HP(\infty,-)H^T + R)^{-1}$ (A4.11)

For (5) $P(\infty,+) = (I - K(\infty)H)P(\infty,-)$ (A4.12)

Equations (A4.10), (A4.11) and (A4.12) constitute the steady-state Kalman filter equations discussed in Section 4.2.5 as constraints on the steady-state Kalman gain matrix $K(\infty)$.

b. Continuous Kalman Filter Algorithm

<u>System Model:</u>

$$\dot{\underset{\sim}{X}}(t) = A\underset{\sim}{X}(t) + B\underset{\sim}{U}(t) + \underset{\sim}{W}(t) \qquad \text{(A4.13)}$$

where $\underset{\sim}{W}(t) \sim N(\underset{\sim}{0}, Q)$ and t is continuous time

Q is the process noise spectral density matrix, assumed time invariant.

<u>Measurement Model:</u>

$$\underset{\sim}{Z}(t) = H\underset{\sim}{X}(t) + \underset{\sim}{V}(t) \qquad \text{(A4.14)}$$

where $\underset{\sim}{V}(t) \sim N(\underset{\sim}{0}, R)$

R is the measurement noise spectral density matrix, assumed time invariant.

1. Error Covariance Propagation:

$$\dot{P}(t) = AP(t) + P(t)A^T + Q \tag{A4.15}$$

2. Kalman Gain Matrix:

$$K(t) = P(t)H^T R^{-1} \tag{A4.16}$$

3. State Estimate:

$$\dot{\bar{\underset{\sim}{X}}}(t) = A\bar{\underset{\sim}{X}}(t) + K(t)(\underset{\approx}{Z}(t) - H\bar{X}(t)) \tag{A4.17}$$

It is assumed in both a) and b) that the process and measurement noise terms are uncorrelated. Also the initial state value and its uncertainty needs to be specified at the outset.

REFERENCES/BIBLIOGRAPHY

AGAR001. AGARD Lecture series No. 104: Parameter Identification Nov., 1979.

BAJP001. BAJPA1, A.C.; CALUS, I.M.; FAIRLEY, J.A.; Statistical Methods for Engineers and Scientists. John Wiley and Sons (publishers), 1978.

BATT001. BATTERSON, J.G.; KLEIN, V.; On the Identification of a Highly Augmented Airplane. 7H IFAC Symposium on Identification and System Parameter Estimation, York, 1985.

BEND001. BENDAT, J.S.; PIERSOL, A.G.; Engineering Application of Correlation and Spectral Analysis. John Wiley and Sons (publishers), 1980.

BLAC003. BLACK, C.G.. Helicopter Parameter Identification - The Foundation of a Frequency-Domain Approach. Glasgow University Aero Report 8602, Apr., 1986.

BLAC004. BLACK, C.G.. A Frequency-Domain Output-Error Method of Parameter Estimation: Development of Method and Computer Implementation. Glasgow University Aero Report 8603, Apr., 1986.

BLAC005. BLACK, C.G.; MURRAY-SMITH, D.J.; PADFIELD, G.D.. Experience with Frequency-Domain Methods in Helicopter System Identification. Paper no. 76, Twelfth European Rotorcraft Forum, Garmisch - Partenkirchen, Federal Republic of Germany, Sept., 1986.

BLAC006. BLACK, C.G.. User's Guide to some Frequency-Domain Identification programs. Glasgow University Aero Report (to be published).

BLAC007. BLACK, C.G.. Consideration of Trends in Stability and Control Derivatives from Helicopter System Identification. Paper no. 7.8, Thirteenth European Rotorcraft Forum, Arles, France, Sept., 1987.

BOOM001. BOOM V.D.. On the Relation between Weighted Least-squares Estimators and Instrumental Variable Estimators. 4th IFAC Symposium on Identification and System Parameter Estimation, Tbilisi, USSR, 1976.

BRAC001. BRACEWELL R.N.. Discrete Hartley Transform. Journal of the Optical Society of America, Volume 73, no. 12. Dec., 1983.

BUCK001. BUCKINGHAM S.L.. Digital Spectral Analysis: A Guide based on Experience with Aircraft

Vibrations. Royal Aircraft Establishment, Technical Report 81014, Feb., 1981.

CRAN001. CRANFIELD INSTITUTE OF TECHNOLOGY (Signal Processing and Applications Group). Basic Signal Processing (course notes), 1979.

DUVA001. DU VAL, R.W.; WANG. J.C.; DEMIROZ M.Y.; A Practical Approach to Rotorcraft Systems Identification. 39th AHS National Forum, St. Louis, May, 1983.

DORN001. DORNY, C.N.; A Vector Space Approach to Models and Optimization. Wiley-Interscience (publishers), 1975.

ETKI001. ETKIN, B.. Dynamics of Flight - Stability and Control (second edition). John Wiley and Sons (Publishers), 1982.

EVAN001. EVANS, R.J.; GOODWIN, G.C.; FEIK, R.A.; MARTIN, C.; LOZANO-LEAL, R.. Aircraft Flight Data Compatibility Checking Using Maximum Likelihood and Extended Kalman Filter Estimation. 7th IFAC Symposium on Identification and System Parameter Estimation, York, 1985.

FEIK002. FEIK, R.A.. Maximum Likelihood Program for Non-linear System Identification with Application to Aircraft Flight Data Compatibility Checking. Department of Defence Support, ARL-AERO-NOTE 411, Defence Science and Technology Organisation Aeronautical Research Laboratories, Melbourne, Victoria Commonwealth of Australia, July, 1982.

FOST001. FOSTER, G.W.. A Description of the Weighted Least-Squares Output-Error Method of Parameter Identification. Royal Aircraft Establishment, Technical Memo FS 215, Dec. 1978.

FOST002. FOSTER, G.W.. The Identification of Aircraft Stability and Control Parameters in Turbulence. Royal Aircraft Establishment, Technical Report 83025, Mar., 1983.

FOST003. FOSTER, G.W.. Identification of Hunter MK12 Longitudinal and Lateral Aerodynamic Stability and Control Derivatives. Royal Aircraft Establishment Technical Report 77009, 1977.

FUKH001. FU, K-H.; MARCHAND M.. Helicopter System Identification in the Frequency-Domain. Paper No. 96, Ninth European Rotorcraft Forum, Stresa, Italy, Sept. 1983.

GELB001. GELB, G. (EDITOR) Applied Optimal Estimation, The Analytic sciences Corporation. The M.I.T. press (publishers), 1974.

GILB001. GILBERT, N.E.; WILLIAMS M.J.. Preliminary Kinematic Consistency Checking of Helicopter Flight Data. Department of Defence Support, ARL-AERO-NOTE 414. Defence Science and Technology Organisation Aeronautical Research Laboratories, Melbourne, Victoria. Commonwealth of Australia, Jan., 1983.

GOLU001. GOLUB, G; KAHAN W.. Calculating the Singular Values and Pseudoinverse of a Matrix. Journal SIAM, Numerical Analysis, pp. 205-224, 1965.

GREIG001. GREIG, D.M. Optimisation. Longman Mathematical Texts (publishers), 1980.

GUPT002 GUPTA, N.K.; HALL, W. EARL JR.. Input Design for Identification of Aircraft Stability and Control Derivatives. NASA Contractor Report: NASA CR-2493, Feb., 1975.

HALL001 HALL W. EARL JR.; GUPTA, N.K; HANSEN, R.S. Rotorcraft System Identification Techniques for Handling Qualities and Stability and Control Evaluation. 34th Annual National Forum of the American Helicopter Society, Washington, D.C., May, 1978.

HALL002. HALL, W. EARL JR.; BOHN, J.G.; VINCENT, J.H.. Development of Advanced Techniques for Rotorcraft State Estimation and Parameter Identification. System Control, Inc., Palo Alto, California 94304. NASA Contractor Report NAS-14549, Au., 1980.

ILIF001. ILIFF, K.W.. Aircraft Identification Experience. Lecture No. 6, AGARD Lecture Series No. 104: Parameter Identification, Nov., 1979.

ISAA001 ISAACSON, E,; KELLER, H.B.. Analysis of Numerical Methods. John Wiley and Sons (publishers), 1966.

ISER001. ISERMANN, R.. Identification of Very Noisy Dynamic Processes Using Models with Few Parameters. 1st IFAC Symposium on Identification and System Parameter Estimation, The Hague/Delft, 1973.

JACO001. JACOBS, D. (EDITOR). Proceedings of the Conference on Applications of Numerical Software - Needs and Availability. Academic Press (publishers), 1978.

KALE001. KALETKA, J. Rotorcraft Identification Experience. Lecture No. 7, AGARD Lecture Series No. 104: Parameter Identification, Nov., 1979.

KALM001. KALMAN, R.E.. A New Approach to Linear Filtering and Prediction Problems. Journal of Basic Engineering, pp 35-45, March, 1960.

KERR001. KERR, T.H.. The Proper Computation of the Matrix Pseudoinverse and its impact on MVRO Filtering. IEEE Transactions on Aerospace and Electronic Systems. Vol AES-21, No 5, Sept., 1985.

KLEI001. KLEIN, V.. Identification Evaluation Methods. Lecture No.2, AGARD Lecture Series No. 104: Parameter Identification, Nov., 1979.

KLEI002. KLEIN, V.; BATTERSON, J.G.; MURPHY, P.C.. Determination of Airplane Model Structure from Flight Data by Using Modified Stepwise Regression. NASA Technical Paper 1916, Oct., 1981.

KLEI003. KLEIN, V.; BATTERSON, J.G.. Determination of Airplane Model Structure from Flight Data Using Splines and Stepwise Regression. NASA Technical Paper 2126, March 1983.

KLEI004. KLEIN, V.; KESKAR, D.A.. Frequency Domain Identification of a Linear System Using Maximum Likelihood Estimation. 5th IFAC Symposium on Identification and System Parameter Estimation, Hampton, U.S.A, 1979.

KLEI005. KLEIN, V.. Maximum Likelihood Method for Estimating Airplane Stability and Control Parameters from Flight Data in Frequency-Domain. NASA Technical Paper 1637, May, 1980.

KRAM001. KRAMER, N.J.T.A. - Systems Thinking - Concepts and Notions. Martinus Nijhoff Social Sciences Division, Leiden, 1977.

LEIT001. LEITH, D.. Optimal Test Inputs for Helicopter System Identification. University of Glasgow, Department of Electronics and Electrical Engineering. Report, July 1987.

MAIN001. MAINE, R.E.; ILIFF, K.W.. The Theory and Practice of Estimating the Accuracy of Dynamic Flight-Determined Coefficients. NASA Reference Publication 1077, July, 1981.

MAIN002. MAINE, R.E.; ILIFF, K.W.. Identification of Dynamic Systems. Theory and Formulation. NASA Reference Publication 1138, Feb., 1985.

MARC001. MARCHAND, M.. The Identification of Linear Multivariable Systems from Frequency Response Data. 3rd IFAC Symposium on Identification and System Parameter Estimation, 1973.

MARC002. MARCHAND, M; Fu, K-H.. Frequency Domain Parameter Estimation of Aeronautical Systems Without and With Time Delay. 7th IFAC Symposium on Identification and System Parameter Estimation. York, 1985.

MEHR001. MEHRA, R.K.. Identification of Stochastic Linear Dynamic Systems Using Kalman Filter Representation. AIAA Journal, Volume 9 Number 1, Jan., 1971.

MOLU001. MOLUSIS, J.A.. Helicopter Stability Derivative Extraction and Data Processing Using Kalman Filtering Techniques. 28th AHS National Forum, Washington, D.C., May, 1972.

MOLU002. MOLUSIS, J.A.. Helicopter Stability Derivative Extraction from Flight Data Using the Bayesian Approach to Optimisation. Journal of the AHS, July, 1973.

MOLU003. MOLUSIS, J.A.. Rotorcraft Derivative Extraction from Analytical Models and Flight Test Data. AGARD CP 172: Methods for Aircraft State and Parameter Identification, Nov., 1974.

MOOD001. MOOD, A.M.. Introduction to the Theory of Statistics. McGraw Hill Book Company (publishers), 1974.

MURD001. MURDOCH, D.C.. Linear Algebra. John Wiley and Sons (publishers), 1970.

MURR001. MURRAY-SMITH, D.J.. The Selection of Test Inputs for Helicopter Parameter Identification. (Report) Department of Electronics and Electrical Engineering, University of Glasgow, July, 1984.

MURR002. MURRAY-SMITH D.J.. Persistently Exciting Test Signals for Helicopter System Identification. (Report) Department of Electronics and Electrical Engineering, University of Glasgow, Aug., 1984.

NAGOO- NAG - Fortran Library Manual, Mark II; Volume 1: Contents - DO2J; Volume 2: D02K - EO2; Volume 3: E04, Volume 4: FO1-FO3; Volume 5: F04-G08.

NASH001. NASH, J.C.. Compact Numerical Methods for Computers: Linear Algebra and Function Minimisation. Adam Hilger Ltd., Bristol (publishers), 1979.

NELS001. NELSON, C.D.. A Vector Space Approach to Models and Optimization. John Wiley and Sons (publishers) 1975.

OTNE001. OTNES, R.K.; ENOCHSON, L.. Applied Time Series Analysis - Volume 1, Basic Techniques. John Wiley and Sons (publishers), 1978.

PADF002. PADFIELD, G.D., DU VAL, R.W.. Applications of System Identification Methods to the Prediction of Helicopter Stability, Control and Handling Characteristics. AHS/NASA Specialists' Meeting, Palo Alto, California, April, 1982.

PADF003. PADFIELD, G.D.. Longitudinal Trim, Stability and Response Calculations for Helicopters. Royal Aircraft Establishment, Tech. Memo (structures) 990, April, 1981.

PADF004. PADFIELD, G.D.. Flight Testing for Performance and Handling Qualities. Lecture No. 7, AGARD Lecture Series No. 139: Helicopter Aeromechanics.

PADF005. PADFIELD, G.D.; THORNE, R.; MURRAY-SMITH, D.J.; BLACK, C.G.; CALDWELL, A.. U.K. Research into System Identification for Helicopter Flight Mechanics. Paper No. 82, Eleventh European Rotorcraft Forum, London, Sept., 1985.

PADF006. PADFIELD G.D.. On the Use of Approximate Models in Helicopter Flight Mechanics. Vertica, Volume 5, pp 243 to 259, 1981.

PADF007. PADFIELD, G.D.. Integrated System Identification Methodology for Helicopter Flight Dynamics. Prepared for a Panel Session on "System Identification and its Application for Rotorcraft" of the 42nd Annual Forum of the American Helicopter Society, Washington, D.C., June, 1986.

PADF008. PADFIELD, G.D.. An Analysis of Helicopter Flight Mechanics: Part 2 - Theory for the Software Package HELISTAB, R.A.E. Technical Report (In preparation).

PADF009. PADFIELD, G.D.. A Theoretical Model of Helicopter Flight Mechanics for Application to Piloted Simulation. Royal Aircraft Establishment, Technical Report 81048, April, 1981.

PAP0001. PAPOULIS, A.. Signal Analysis, McGraw-Hill Book Company (publishers), 1984.

REID001. REID, G.E.A.. Validation of Kinematic Compatibility of Flight Data Using Parameter Estimation Methodology. Royal Aircraft Establishment Technical Report 81020, 1981.

ROSS001. ROSS, J.A.. Identification Experience in

Extreme Flight Conditions. Lecture Number 8, AGARD Lecture Series Number 104: Parameter Identification, Nov., 1979.

SCHO001. SCHOUKENS, J.; RENNEBOOG, J.. Modelling the Noise Influence on the Fourier Coefficients after a Discrete Fourier Transform. IEEE Transactions on Instrumentation and Measurement, Volume IM-35, pp 278-286, Sept., 1986.

SMIT001. SMITH, J.. An Analysis of Helicopter Flight Mechanics: Part 1 - User's Guide to the Software Package HELISTAB. Royal Aircraft Establishment Technical Memorandum FS(B) 569, 1984.

SODE001. SODERSTROM, T.. On Model Structure Testing in System Identification. INT. J. Control, Volume 26, Number 1, 1-18, 1977.

STEP001. STEPNER, D.E., MEHRA, R.K.. Maximum Likelihood Identification and Optimal Input Design for Identifying Aircraft Stability and Control Derivatives. NASA Contractor Report CR-2200, March, 1973.

STOE001. STOER, J.; BULIRSCH, R.. Introduction to Numerical Analysis. Springer-Verlag (publisher), 1980.

TOPP001. TOPPING, J.. Errors of Observation and their Treatment. Chapman and Hall (publishers), London, Fourth Edition, 1972.

TISC001. TISCHLER, M.B.; LEUNG J.G.M.; DUGAN, D.C.. Identification and Verification of Frequency-Domain Models for XV-15 Tilt-Rotor Aircraft Dynamics. Paper No. 75, Tenth European Rotorcraft Forum, The Hague, The Netherlands, Aug., 1984.

WALS001. WALSH, G.R.. Methods of Optimization. John Wiley and Sons (publishers), 1975.

WANG001. WANG, J.C.; De MIROZ, M.Y.; TALBOT, P.D.. Flight Test Planning and Parameter Extraction for Rotorcraft System Identification. AIAA/AHS/CASI/DGLR/IES/ITEA/SETP/SFTE 3rd Flight Testing Conference, Las Vegas, Nevada, U.S.A., April, 1986.

WYLI001. WYLIE, C.R.; BARRET, L.C. Advanced Engineering Mathematics, McGraw-Hill Book Company, 1985.

GLASGOW UNIVERSITY LIBRARY